World Journal of

Gastroenterology

Contents

Contents

ABOUT COVER

Editorial Board of *World Journal of Gastroenterology*, Yoichi Matsuo, MD, PhD, Professor, Department of Gastroenterological Surgery, Nagoya City University Graduate School of Medical Sciences, Kawasumi 1, Mizuho-cho, Mizuho-ku, Nagoya 4678601, Japan. matsuo@med.nagoya-cu.ac.jp

AIMS AND SCOPE

The primary aim of *World Journal of Gastroenterology* (*WJG*, *World J Gastroenterol*) is to provide scholars and readers from various fields of gastroenterology and hepatology with a platform to publish high-quality basic and clinical research articles and communicate their research findings online. *WJG* mainly publishes articles reporting research results and findings obtained in the field of gastroenterology and hepatology and covering a wide range of topics including gastroenterology, hepatology, gastrointestinal endoscopy, gastrointestinal surgery, gastrointestinal oncology, and pediatric gastroenterology.

INDEXING/ABSTRACTING

The *WJG* is now abstracted and indexed in Science Citation Index Expanded (SCIE, also known as SciSearch®), Current Contents/Clinical Medicine, Journal Citation Reports, Index Medicus, MEDLINE, PubMed, PubMed Central, Scopus, Reference Citation Analysis, China National Knowledge Infrastructure, China Science and Technology Journal Database, and Superstar Journals Database. The 2022 edition of Journal Citation Reports® cites the 2021 impact factor (IF) for *WJG* as 5.374; IF without journal self cites: 5.187; 5-year IF: 5.715; Journal Citation Indicator: 0.84; Ranking: 31 among 93 journals in gastroenterology and hepatology; and Quartile category: Q2. The *WJG*'s CiteScore for 2021 is 8.1 and Scopus CiteScore rank 2021: Gastroenterology is 18/149.

RESPONSIBLE EDITORS FOR THIS ISSUE

Production Editor: *Yi-Xuan Cai*; **Production Department Director:** *Xiang Li*; **Editorial Office Director:** *Jia-Ru Fan*.

REVIEW

Robotic, self-propelled, self-steerable, and disposable colonoscopes: Reality or pipe dream? A state of the art review

Conchubhair Winters, Venkataraman Subramanian, Pietro Valdastri

Conchubhair Winters, Venkataraman Subramanian, Leeds Institute of Medical Research, University of Leeds, St. James's University Hospital, Leeds LS9 7TF, United Kingdom

Pietro Valdastri, School of Electronic and Electrical Engineering, University of Leeds, Leeds LS2 9JT, United Kingdom

Corresponding author: Conchubhair Winters, MBChB, Doctor, Research Fellow, Leeds Institute of Medical Research, University of Leeds, St. James's University Hospital, Beckett Street, Leeds LS9 7TF, United Kingdom. c.r.winters@leeds.ac.uk

Abstract

Robotic colonoscopes could potentially provide a comfortable, less painful and safer alternative to standard colonoscopy. Recent exciting developments in this field are pushing the boundaries to what is possible in the future. This article provides a comprehensive review of the current work in robotic colonoscopes including self-propelled, steerable and disposable endoscopes that could be alternatives to standard colonoscopy. We discuss the advantages and disadvantages of these systems currently in development and highlight the technical readiness of each system to help the reader understand where and when such systems may be available for routine clinical use and get an idea of where and in which situation they can best be deployed.

Key Words: Robot-enhanced procedures; Colonoscopy; Endoscopy; Capsule endoscopy; Colorectal cancer; Colonic polyp

Core Tip: Colorectal cancer is a common cause of cancer related mortality. Detection and removal of precancerous polyps reduces the risk of colorectal cancer. Colonoscopy is the gold standard investigation for colorectal polyps and cancer but can be uncomfortable due to the mechanics of the procedure. Robotics has the potential to reduce the discomfort and improve the procedure for patients, while improving key performance indicators. Robotics can offer a more intuitive endoscopic appearance, using various methods to negotiate the colon to reduce discomfort. Robotics could lead to a more effective, better tolerated, safer, autonomous colonoscopy with minimal operator interaction.

INTRODUCTION

Colorectal cancer incidence

Colorectal cancer (CRC) is the third most diagnosed cancer and the second most common cause of cancer related mortality worldwide[1]. Many countries, particularly those with a high human development index (HDI), continue to see an increasing incidence[2]. Rapid increases in the incidence of CRC can be seen in countries transitioning from medium to high HDI[2]. Although CRC aetiology is heterogeneous, the majority are sporadic, and the increasing incidence has been attributed to the western lifestyle and increasing levels of obesity[3].

The majority of CRCs have a detectable precursor lesion, a colonic polyp, which can be present for many years before cancer develops[4]. Endoscopic resection of colonic polyps has been shown to reduce cancer related mortality by up to 53%[5]. More and more countries are utilising screening programmes to control the increasing incidence of CRC. Screening programmes vary in nature and often utilise faecal testing such as faecal immunochemical testing (FIT). However, colonoscopy remains the gold standard for diagnosing and removing colonic polyps. Colonoscopy is also utilised in many polyp, colitis, and hereditary CRC surveillance programmes[6-9].

Despite the recommendations for colonoscopy as a diagnostic, screening, or surveillance tool, it is often underutilised. Delays in colonoscopy following a positive FIT has been shown to increase the likelihood of finding advanced adenomas, CRC, and advanced CRC[10]. A meta-analysis looking at second evaluation after a positive faecal occult blood test found that only 72.5% underwent a second evaluation in the form of any lower gastrointestinal investigation[11]. Additionally, a recent international survey of FIT screening programmes found that only 79% of those with a positive FIT underwent a colonoscopy[12]. Studies from Lee *et al*[13] and Zorzi *et al*[14] suggest the risk of CRC related mortality is double in those with a positive FIT who refuse colonoscopy than those who undergo a colonoscopy [13,14].

The reason for a lack of follow-up investigation may be the decision of a healthcare worker, for example due to co-morbidity. However, approximately 10% of those with a positive faecal blood test that are not followed up are due to patient refusal to have a colonoscopy[15]. Alternative tests such as computed tomography colonography (CTC) and colon capsule are available, and their merits will be discussed in future sections. Several qualitative studies have been done exploring the barriers and facilitators to colonoscopy. Although the barriers are numerous, complex, and interrelated, previous bad experiences of colonoscopy and fear of pain or discomfort are commonly cited[15-17].

History of colonoscopy

The first descriptions of an endoscope came from Bozzini in 1805 which he called the Lichtleiter (light conductor)[18,19]. Several rigid endoscopes were subsequently invented, but it was over a century before Wolfe and Schindler developed the semi-rigid gastroscope which paved the way for our endoscopes of today[20]. The evolution of the modern endoscope gained speed in the 1950s when Hirschowitz and Curtiss developed the fibreoptic endoscope[21]. A flexible endoscope was developed in Japan to assess of the lower GI tract, the first colonoscope, and by the late 1960s Shinya introduced therapeutics by performing the first polypectomy[21,22]. The charged couple device (CCD) was developed and in the 1980s the videoendoscope was born. Since then, the optics have been the mainstay of research focus and endoscope advancements. We have ever evolving improvements in the optics such as high definition, magnification, and an increasing range of image enhancement virtual chromoendoscopy options. And although the technique by which we perform colonoscopy has been refined, reducing risk and discomfort, we still push and torque a semirigid tube from the distal end to advance around the colon. The introduction of electromagnetic guidance, such as ScopeGuide (ScopeGuide Endoscope Insertion Tube System, Olympus America, Inc., Allentown, PA), allowed further refinement of the technique. However, it was not until the 1990s, with advances in robotics, that the potential for a new way to perform colonoscopy was explored.

Robots in endoscopy

Following Food and Drug Administration (FDA) approval in 2000 of robotic surgical master-slave platforms such as da Vinci and Zeus, there has been an upsurge in interest in robotic endoscopic devices. Figure 1 shows the increasing number of robotic colonoscopy articles on PubMed[23]. Robotic colonoscopy has potential benefits over conventional colonoscopy (CC) for the patient as well as the endoscopist and service provider. Robotics in colonoscopy is not only limited to diagnostic procedures,
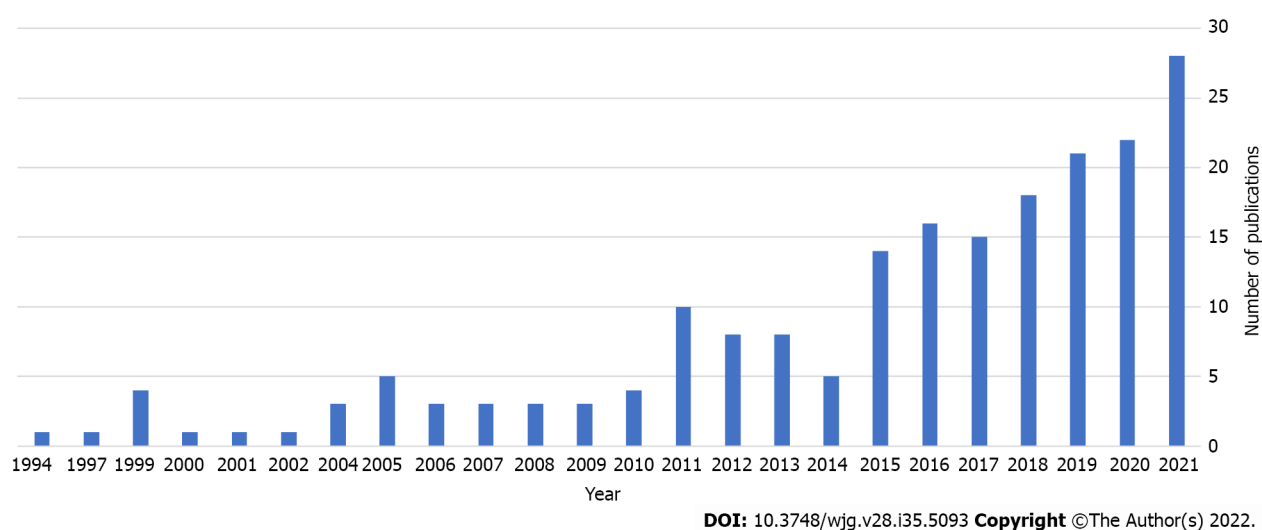
Figure 1 PubMed search for "robotic colonoscopy" showing the increasing number of papers over the last 3 decades[23].

the additional dexterity and triangulation offered by many robotic platforms has great potential in therapeutic procedures such as endoscopic submucosal dissection (ESD).

Recent advances in robotics and miniaturisation, as well as the evolving nature of artificial intelligence (AI) in endoscopy, make this the perfect time to explore robotic colonoscopy. The expanding use of surgical robotic platforms should make patients and endoscopists more accepting of these new technologies in endoscopy. The potential for teleoperated endoscopes to facilitate "medical distancing" is also a concept of increasing interest given the current severe acute respiratory syndrome coronavirus 2 global pandemic.

For robotics to be accepted in endoscopy they must not only offer the same role as CC, but more. The ideal robotic colonoscope should fulfil several criteria as listed in Table 1.

POTENTIAL BENEFITS OF ROBOTIC COLONOSCOPY OVER CC

Patients
Much work in robotic colonoscopy is aimed at delivering a less painful and lower risk endoscopic procedure by reducing the forces on the colonic mucosa and tethering structures. The principal method of reducing this discomfort is through altering the actuation method. Many devices have taken inspiration from nature through biomimicry, for example inchworm or snake like movements. Others use external actuation, such as magnets to pull the device through the colon. A lower discomfort procedure also offers the potential for less anaesthetic/sedative use, further lowering the risk of colonoscopy[24]. Miniaturisation, and particularly capsule endoscopy, have the potential to offer a less invasive, less embarrassing, and more convenient option for patients. Some devices may even be provided in a community setting, negating the need to travel to hospital. Although incomplete colonoscopy rates have improved over the last few decades, there remain a number of patients who require a second procedure. Robotics has the potential to reduce the number of failed procedures by improving caecal intubation rates (CIRs).

Endoscopists
Training in both the diagnostic and therapeutic aspects of colonoscopy take considerable time[25,26]. Robotics has the potential to make colonoscopy training easier through more intuitive controls, autonomous features and the increased dexterity offered by many platforms. Less loop formation and lower discomfort rates could translate into improved completion rates. The improvement in manoeuvrability could reduce polyp miss rates and potential post-colonoscopy CRCs. Robotics has the potential to 'democratise' colonoscopy, reducing the variability in polyp detection rates by improving the detection rates of less well performing endoscopists. Many platforms are aiming to improve the ergonomics of colonoscopy in an attempt to reduce fatigue and endoscopy related musculoskeletal injuries[27,28].

Service providers
Our forebearers in surgical robotics have yet to provide any clear answers as to the cost effectiveness of robotic procedures. The initial purchase costs are often high, but the cost benefit thereafter is unclear

Table 1 The features of the ideal robotic colonoscope

No.	Ideal robotic colonoscope features
1	Affordable
2	Acceptable to patients and endoscopists
3	More comfortable than conventional colonoscopy
4	Lower risk than conventional colonoscopy
5	Improved caecal intubation rate compared to conventional colonoscopy
6	Offer at least comparable mucosal visibility with the option of image enhancement (virtual chromoendoscopy)
7	Capable of taking biopsies and therapeutics such as polypectomy
8	Offer integration with artificial intelligence for polyp detection and characterisation
9	Ideally have autonomous features, such as self-navigation
10	Reduce the training time to achieve competence compared to conventional colonoscopy
11	Procedure times should be less than, but must not be significantly longer than, conventional colonoscopy
12	Have sustainability in mind in the manufacturing, reprocessing or disposal of the device

and variable between procedures[29-32]. The Endotics robotic colonoscope, discussed in detail later, claims to offer a cost neutral alternative to standard colonoscopy[33]. Although few robotic colonoscopes are at a technology readiness level (TRL) to perform health economics studies, we will aim to discuss several potential benefits to service providers.

Unsedated procedures offer cost and efficiency saving benefits through utilisation of less anaesthetic and recovery staff, as well as a quicker turnaround within the department. There is an increasing demand on endoscopy services caused by an aging population, increasing environmental and behavioural risk factors, and ever increasing screening and surveillance populations[34]. The addition of the recent pandemic associated service provision issues and enhanced infection control and prevention measures are stretching endoscopy departments to their limit[35]. The ideal robotic colonoscope to ease these pressures would require less staff and be quicker, pain-free, teleoperated, mobile and have therapeutic capabilities. A single use device would negate the cost associated with reprocessing, as well as potentially reducing cross contamination[36]. Improvements in sustainability may also be achieved using single use devices which reduce the need for carbon- and water-heavy reprocessing facilities.

AVAILABLE ALTERNATIVES TO COLONOSCOPY

Alternative procedures to assess the colon are required if a patient refuses or is unfit for a colonoscopy, or in the event of an incomplete colonoscopy. There are a number of alternatives to CC, most commonly CTC and colon capsule endoscopy (CCE). The advantages and limitations of these commonly used alternatives are shown in Table 2.

CTC, until the recent adoption of CCE, was the most commonly used alternative to colonoscopy. CTC has a similar sensitivity to colonoscopy for the detection of large (> 10 mm) polyps and CRC[37,38]. CTC is better tolerated than CC and over half of patients have an additional pathology detected on the scan [37,39]. However, approximately 30% of CTC patients require further investigation, often in the form of a colonoscopy to remove polyps[38]. CTC is significantly less sensitive than colonoscopy for detection of small polyps and flat lesions such as sessile serrated lesions[40].

CCE is better tolerated than CC[41]. A recent meta-analysis showed that when compared with CC, CCE had a sensitivity and specificity of 87% and 88% respectively, for detection of polyps ≥ 6 mm[42]. However, a large retrospective study by Benech *et al*[43], showed that 19% of CCEs had a missed advanced adenoma when they underwent a further procedure[43]. When comparing CTC to CCE, Spada *et al*[44] compared 100 patients with an incomplete colonoscopy and found a relative sensitivity of 2.0 in favour of CCE for identifying polyps ≥ 6 mm[44]. The recently published TOPAZ study also suggested CCE was superior to CTC for the detection of polyps ≥ 6 mm and non-inferior for polyps ≥ 10 mm[45]. However, some inherent biases and flaws in methodology of the TOPAZ study have been pointed out by Burr *et al*[46] which cast some doubt on the validity of these results[46]. A meta-analysis of CTC *vs* CCE in incomplete colonoscopies showed that CCE had superior diagnostic yields for all polyp sizes (37% *vs* 10%), but poorer completion rates (76% *vs* 98%)[47].

Magnetic resonance imaging techniques, magnetic resonance colonography (MRC), have also been evaluated as an alternative to CC. MRC has the benefits of being non-invasive and not carry the radiation risks associated with CTC. However, magnetic resonance imaging scanners can be claustro-

Table 2 Advantages and limitations of conventional colonoscopy alternatives

Procedure	Advantages	Limitations
Conventional colonoscopy	Extensive knowledge base and expertise already available, diagnostic and therapeutic capabilities. Gold standard	Bowel cleansing required, painful for some (sedative and analgesics often required), prolonged training period required, risk of perforation due to forces required
CT colonography [39,41,101]	Lower intensity bowel cleansing, shorter procedure, less discomfort (no sedation or analgesia needed), other intraabdominal pathology can be detected, lower risk of perforation, better patient tolerance	Low dose radiation used, lower sensitivity for small and flat polyps, no therapeutic capability, no direct mucosal visualisation, limited evidence of a benefit in CRC incidence or mortality
Wireless capsule colonoscopy	Minimally invasive, painless, better patient tolerability, low perforation risk	Aggressive bowel cleansing required, lower sensitivity than CC for polyps, no control of the capsule, no therapeutic capability, risk of capsule retention, limited battery life can cut out before complete colon visualisation

CRC: Colorectal cancer; CC: Conventional colonoscopy; CT: Computed tomography.

phobic for some and are very time consuming procedures. A meta-analysis in 2009 found the sensitivity of MRC for the detection of CRC was 100%, but was only 84% for polyps ≥ 10 mm[48]. A study in 30 lynch syndrome patients who underwent tandem MRC then colonoscopy, found that MRC was unable to detect any lesions under 10 mm, including one missed cancer[49]. Another study of MRC in asymptomatic individuals found MRC and colonoscopy had sensitivities of 78.4% and 97.3%, respectively, for polyps ≥ 6 mm[50]. Although some meta-analysis suggest MRC has a good sensitivity for the detection of CRC, other meta-analysis suggest the sensitivity for detection of all lesions could be as low as 75%[51].

CHALLENGES FOR ROBOTIC COLONOSCOPY

As technologies advance, many of the technical challenges to robotic colonoscopy are being resolved. The deformable, slick surface of the colon and it's many and varying orientations and bends make for a challenging environment and a multitude of solutions have been proposed by various research teams.

Locomotion
The first challenge for any robotic device is locomotion. Passive locomotion is adopted by most capsule endoscopes, in which the device passes through the gastrointestinal tract by natural peristalsis. However, the lack of control has the consequence of potentially missing lesions and rules out any therapeutic application.

Actively controlled robotic colonoscopes can be divided into internally and externally actuated devices. Internally actuated devices control propulsion by interacting directly with the surrounding environment by means of wheels, propellers, belts or bio-mimicked animal-like movements. Much inspiration for the locomotion of these devices has been taken from nature with many attempting to copy the movements of animals such as snakes, earthworms, or caterpillars, and some even mimicking the movement of micro cilia. These actuation principles are achieved using electromechanical or pneumatic mechanisms, or a combination of both. External actuation involved controlling the internal device by means of an external mechanism such as magnetic fields and field gradients. With external magnetic actuation comes the challenge of localisation of the endoscope within its environment.

Localisation
Localisation refers to the position and orientation (*i.e.*, pose) of the device. Localisation can be relative or absolute. Relative localisation is a well-developed technology and is implemented in a number of wireless capsule endoscopes (WCE) giving an estimated position with respect to the anatomy. Absolute localisation gives an accurate position and orientation. Several proposed solutions have been investigated in endoscopes including magnetic, ultrasound, radiofrequency and computer-vision technology. Many WCEs use radiofrequency localisation, current capsules have an error in position on average 38 mm and up to 100 mm[52]. Magnetic localisation is gaining increasing academic interest, and can be combined with magnetic actuation. Magnetic localisation can perform a 6 degrees of freedom (DOF) localisation with an average error in position and orientation under 5 mm and 6 mm, respectively[53].

Miniaturisation
Miniaturisation is a challenge for all robotic colonoscopes, but is of particular importance in capsule endoscopy. A capsule endoscope contains several components: External case, optical window, light emitting diode (LED), lens, image sensor, radio frequency transmitter, antenna, and a power source.

Powering a capsule endoscope to allow for the variable colonic transit times requires a battery sufficiently large and often means adjusting the frames *per* seconds, and ultimately sensitivity, to preserve battery life. All this must then fit within a safe size for transit through the GI tract. Most capsule endoscopes are 11 mm in diameter and up to 32 mm in length with a battery life now exceeding 10 h and often containing two cameras[34]. One proposed method to overcome the miniaturisation challenge is external actuation *via* magnetic coupling, reducing the size of the battery in capsules and the need for intricate mechanisms of locomotion. One such commercially available capsule endoscope which already takes advantage of magnetic coupling is the NaviCam (Ankon Technologies, Wuhan, Shanghai, China) for inspection of the upper gastrointestinal tract[54].

Patient tolerance
The goal for most robotic colonoscopes is to improve the patient experience. For most devices this takes the form of reducing discomfort and risk. Capsule endoscopes achieve this by causing no distortion to the GI tract during their passive transit. Actively controlled devices aim to traverse the colon retrograde while reducing distortion and pressure exerted, resulting in less pain. Potentially also reducing the risk of perforation associated with the forces often required to torque and push around the colon in CC. Various actuation methods aim to tackle this problem by rolling, walking, inching, slithering, or pulling with magnets along the colon.

Cost
Not many robotic colonoscopy devices have health economic studies assessing their financial impact. Even the colon capsule, which is now available as an alternative to CC in some health services such as the National Health Service in the United Kingdom, has yet to show any cost effectiveness benefit over CC[55].

Sustainability
Reprocessing presents a massive challenge in robotic colonoscopy due to the intricacy of some devices. Many researchers are pursuing the potential of single use devices. With over 18 million endoscopic procedure *per* year in the United States, endoscopy is the third highest generator of waste in healthcare. Endoscope reprocessing uses up to 100 L of water as well as the electricity, heat, disinfectants and detergents[56]. Single use endoscopes have the potential to avoid this carbon heavy process. Provided the disposal of the device does not incur a higher carbon footprint, single use robotic devices have the potential to present a greener option for colonoscopy.

Autonomy
Perhaps the most notable evidence of robotic autonomy in day-to-day life is in automotive vehicles which can park and even navigate with minimal external input. However, medical robotics is also seeing an evolution in autonomy. Standard colonoscopy is completely under the control of the endoscopist with no autonomy. The introduction of AI for polyp detection has moved endoscopy into the first level of autonomy by visually assisting the endoscopist. Robotic colonoscopes have the potential to push the levels of autonomy much further. Devices capable of autonomously navigating the colon are being researched. However, with such levels of autonomy come challenges such as ethical and legal considerations.

TRL

TRL assessment was introduced by NASA in the 1980 to replace the traditional research and development categories: Basic research, feasibility, development, and demonstration[57]. TRL provides an objective 9 stage assessment of how advanced a technology is towards adoption[58]. When discussing each device, we will attempt to give our objective assessment of the TRL of each device. The score assigned will range from 1 (basic principles of the technology observed and report) to 9 (proof of real-world successful use of the technology) as described in Table 3, and a score will be assigned to each device described alongside the device characteristics in Table 4.

ROBOTIC COLONOSCOPES

For the purpose of this review article a selection of the most advanced platforms will be discussed, dividing them into active flexible platforms, passive devices, robot assisted platforms and robotic platforms with therapeutic applications. A table offering additional detail on the devices, as well as several more devices, is available in Supplementary Table 1.

Table 3 Technology readiness levels as applicable to robotic colonoscopy[57,102,103]

TRL	Definition	Supporting information relevant to robotic colonoscopy
1	Basic principles observed and reported	Published research on the core principals of the technology
2	Technology concept and/or application formulated	Moving from principals to applied research with potential applications speculated
3	Analytical and experimental proof of concept	Active research and development proving the concept within a laboratory setting. Benchtop testing
4	Component validation in laboratory environment	Proof of concept and safety in an *ex-vivo* animal colon
5	Component/system validation in a relevant environment	*In-vivo* animal testing with an aim at providing relevant evidence for human testing or FDA approval
6	High fidelity alpha protype demonstration in a relevant environment	Clinical trials assessing feasibility and safety in small number of humans
7	Beta prototype demonstrated in a relevant environment	Clinical safety and effectiveness trials. Determination of risks and adverse events. Final design validation
8	Completed system and qualified to relevant requirement/standards through testing and demonstration	FDA or equivalent approval
9	Actual system proven through successful operation	Device being marked with post-market studies proving real world operational capability

Adopted from United States Department of Defense Technology Readiness Assessment (TRA) Guidance document, and the supporting evidence required from the United States Department of Defense Technology Readiness Assessment (TRA) Desk book. TRL: Technology readiness level; FDA: Food and Drug Administration.

Table 4 Active flexible colonoscopy platforms with technology readiness level

Device name (manufacturer)	Latest study	Outcomes	TRL
Aer-O-Scope-*GI View Ltd., Ramat Gan, Israel*[21, 59-61,63,64]	2016: Human tandem study, 58 CRC screening patients. CIR: 98.2%. CIT: 11 min. 87.5% of polyps detected. No PREMs	CE marked and FDA approved. Balloon propulsion model no longer manufactured	8
ColonoSight-*Stryker GI Ltd., Haifa, Israel*[65,66]	2008: Human study on 178 participants. CIR 90%. CIT: 11.2 min. No PREMs	FDA approved. No longer manufactured	8
Consis medical-*Beer'Sheva, Israel*[21,67]	None available	No regulatory approvals	3
Endoculus-*Department of Mechanical Engineering & Division of Gastroenterology, University of Colorado, United States*[20]	2020: *In-vivo* and *ex-vivo* porcine colon in one. Unable to traverse an *in-vivo* colon, but capable of negotiating an *ex-vivo* porcine colon	No regulatory approvals	4
ENDOO robotic colonoscope-*Endoo Project, Pisa, Italy*[87-89]	2020: *Ex-vivo* porcine colon human simulator study	No regulatory approvals	4
Endotics-*ERA Endoscopy SRL, Peccioli, Italy*[69-74]	2020**:** Learning curve study of 57 participants. CIR and CIT improved to 100% and 22 min following a learning block. PREMs: Mild or no discomfort in most	CE marked and FDA approved. Commercially available in Europe and Japan	8
Invendoscope-*Invendo Medical GmbH, Weinheim, Germany (acquired by Ambu A/S, Copenhagen, Denmark in 2017)*[21,77-79]	2018: Human study on 40 participants using the SC210 model. CIR 95%. CIT 14.2 min. No PREMs on this study, but previous studies reported lower pain scores than CC	CE marked and FDA approved. No longer manufactured	8
Magnetic Flexible Endoscope-*STORM lab, Leeds, United Kingdom & Nashville, TN, United States*[4, 53,85,86,104]	2020: *In-vivo* porcine study. Clinical trial due 2022	No regulatory approvals	5

TRL: Technology readiness level; CIR: Caecal intubation rate; CIT: Caecal intubation time; FDA: Food and Drug Administration; CRC: Colorectal cancer; CC: Conventional colonoscopy; CE: Capsule endoscopy.

Active flexible colonoscopy platforms

Aer-O-Scope: The Aer-O-Scope (GI View Ltd., Ramat Gan, Israel) is a single use flexible colonoscope that uses a CO_2 propulsion system to self-advance through the colon. With a 200° field of view offered by two cameras it aims to offer better visibility behind folds while reducing discomfort. The device works by inflating two polyurethane balloons (Figure 2), the first balloon is inflated at the rectum to create a seal, a second balloon which pulsates and has a hydrophilic coating to reduce friction is inflated proximal to the first. Using the seal between the balloons, CO_2 is inflated, and the pneumatic force
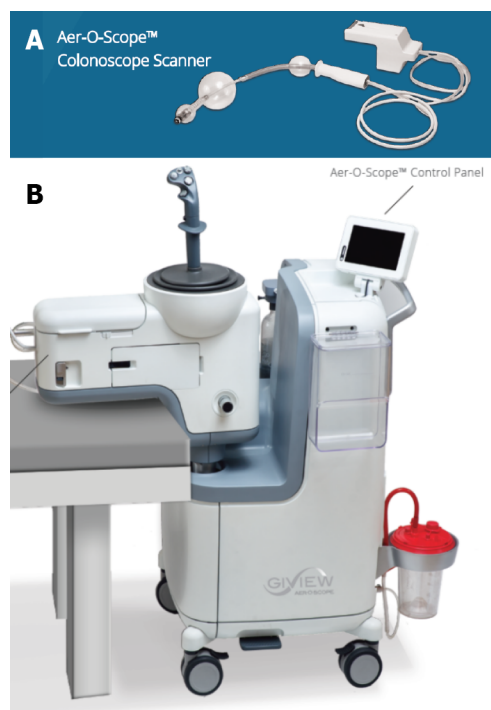
Figure 2 Aer-O-Scope (GI View Ltd., Ramat Gan, Israel). A: Single use colonoscope scanner; B: Workstation. Citation: Images supplied directly by the manufacturer with email detailing permission to use attached as a text file.

propels the proximal balloon forward. To protect the colon, the system controls the pressure so it does not exceed 60 mbar[59]. The most recent version of the device is equipped with two working channels to allow therapeutics[21]. Tip control is achieved using a hand-held controller. Once in the caecum, the pressures are reversed to propel the proximal balloon back towards the rectum while maintaining colonic distension for visibility.

Safety of this novel propulsion method was first demonstrated in 20 pigs in 2006 were only minor petechiae and no adverse events were noted[60]. That study was quickly followed by a clinical trial in the same year on 12 healthy young adults[61]. In this study 10 out of 12 procedures were completed to the caecum with the other two stopping at the hepatic flexure. In both these cases CC was also unable to progress beyond the hepatic flexure due to redundant colon in one and pain in the other. Caecal intubation occurred in an average of 14 min for the 10 completed. Two subjects requested analgesia, while the other 10 had a non-sedated procedure. Mild localised submucosal petechial lesions, thought to be related to balloon friction, were noted on 4 of the follow-up conventional colonoscopies. No other clinically significant adverse events were reported.

A further prospective, non-randomised clinic trial was published in 2016 on 58 CRC screening patients who underwent tandem colonoscopies with the Aer-O-Scope followed by CC[59]. Caecal intubation was achieved in 98.2% (94.4% in the training cohort and 100% in the study cohort). The Aer-O-Scope detected 87.5% of the polyps found by CC, and 100% of those ≥ 5 mm. Caecal intubation was achieved in a mean of 11 min. No mucosal damage or adverse events were reported. Patients were sedated and no patient related experience measures have been reported on.

A prospective clinical trial using the Aer-O-Scope completed recruitment on clinicaltrial.gov in November 2021 but the results have not yet been published at the time of writing and are likely to be for a newer model of the colonoscope[62]. The Aer-O-Scope is CE marked and received FDA approval in 2016[63]. GI View Ltd no longer produce the self-propelled version of the Aer-O-Scope, instead opting to use the technology on a new version which is a single use robotic colonoscope without the balloon self-propulsion[64].

Following correspondence with GI View Ltd, they felt the advances in colonoscopy technique, with improved CIRs and within shorter times, limited the need for a self-propelled device. Instead, they are choosing to concentrate on a single use colonoscope with a larger lens aimed at improved polyp detection, while maintaining similar controls to reduce the need for new training.

ColonoSight: ColonoSight (Stryker GI Ltd., Haifa, Israel) is a self-advancing system composed of a reusable colonoscope (EndoSight) covered by a single use plastic sleeve (ColonoSleeve). The Colono-Sleeve is a multi-lumen sheath that is inflated with air and progressively unfolds to propel the device through the colonic lumen. The IntraPull force that insufflates the air for propulsion is controlled using a foot pedal. The other controls resemble those of a standard colonoscope using a wheel and pully angulation control system. Push, pull and torque can also be used, similar to standard colonoscopy. On

reaching the caecum, air insufflation is directed toward the tip, insufflating and reversing the pressure. A CCD camera with an LED is used to capture image, eliminating the need for fibre optics. The device contains a working channel for therapeutic tools. The outer surface, tip and channels of the endoscope are single use, therefore negating the need for reprocessing of the reusable EndoSight component[65].

Shike *et al*[65] describe that the operation and safety of the instrument was first tested on animals (12 pigs and 7 sheep) with a mean progression into the colon of 80 cm. *In-vitro* dye and culture studies as well as *in-vivo* culture testing confirmed the integrity of the disposable sleeve to protect against bacterial transfer. A clinical trial published in 2008 included 178 participants achieved a 90% CIR in a mean caecal intubation time (CIT) of 11.2 min. The CIR in the final 50 participants was 94%, suggesting a possible learning curve effect. 40 participants underwent polypectomy, with biopsies and argon plasma coagulation was also performed. No immediate complications were noted, and no complications were reported at a two week follow-up telephone call. Participants received intravenous sedation and no patient experience measures are reported on. Physicians reported the IntraPull helped progress the device[65]. The ColonoSight Model 510B received FDA approval in 2004[66]. Stryker GI Ltd acquired Sightline Technologies Ltd, the original manufacturer, in 2006 and the device is no longer manufactured. The reason for discontinuation is not clear, but Stryker GI Ltd have focused on laparoscopic endoscopic equipment rather than colonoscopes, so they may not have had the infrastructure to market a new colonoscope or they may have chosen to integrate the technology into laparoscopic equipment.

Consis medical: Consis medical (Beer'Sheva, Israel) have developed a semi-disposable, single use colonoscope that self-propels along the colon by means of an inverted sleeve pressurised with water. The head of the device can be removed and sterilised at the end of the procedure, with the sleeve cartridge being disposable[67]. The reusable head contains a camera, light source, steering system and water/air nozzle. Human colon simulation and animal tests were due to take place in 2018 but no published results are yet available[21].

Endoculus: Endoculus (University of Colorado, United States) is a multi-DOF fixed tether single use robotic capsule endoscope. Locomotion is *via* two independently controlled motor drives with micropillared treads, offering 2-DOF skid steering. *Via* a fixed tether the Endoculus contains channels for insufflation and irrigation, and a working channel for introduction of endoscopic instruments. The tip of the capsule contains a complementary metal-oxide-semiconductor (CMOS) camera and an adjustable LED. The fixed tether is narrow in diameter and very flexible, however the motorised tip is larger than a standard colonoscope at 6.0 cm × 3.0 cm × 2.3 cm. The research team feel the device could be made smaller with advanced manufacturing techniques[68].

In-vivo testing was carried out in a porcine colon. The device was inserted manually to 10 cm but was then unable to negotiate the sigmoid colon. The research team postulated that this was due to friction from the narrow sigmoid colon in a pig on the non-tread sides of the device. *Ex-vivo* testing on a porcine colon was subsequently conducted on a 40 cm mid colon section. The Endoculus was capable of negotiating the *ex-vivo* colon at speeds up to 40 mm/s both in an insufflated 6 cm diameter colon and also in a collapsed lumen[68].

Endotics: Endotics (ERA Endoscopy SRL, Peccioli, Italy) is an FDA and CE marked biomimicking colonoscope on sale in Europe and Japan[69]. The electropneumatic system uses proximal and distal clamps to attach to the colon wall and in a semi-autonomous process of extension and retraction of the shaft between the clamps it progresses along the colon in an inchworm fashion. Image is captured *via* an integrated CMOS camera lit by an LED light source. The device has a 3 mm working channel, insufflation and suction, and is single use. A 180° steerable head is controlled using a handheld control unit[70].

In-vitro studies reported in 2009 showed the Endotics E-worm system reduced the pressure on sensors around a pig colon by 90% compared to CC. An *in-vivo* animal study showed no complication of the clamping system at follow-up colonoscopy 7 d later[71]. In a pilot tandem study of 40 patients in 2009 the Endotics system only managed to achieve a CIR of 27.5% with mean CIT of 57 minutes, compared to a CIR of 82.5% for CC. The patient experience for the Endotics system was reported to be much better with average pain and discomfort scores of 0.9 and 1.1 out of 10, compared to 6.9 and 6.8 for CC[71].

A second tandem human study on 71 participants was published by Tumino *et al*[72] in 2010 aimed at assessing the Endotics ability to detect polyps. The CIR was 81.6% for the Endotics system and 94.3% for CC, with mean CIT 45.1 (± 18.5) min compared to 23.7 (± 7.2) min, respectively. None of the participants required sedation for the Endotics procedure, with 14/71 asking for sedation during the subsequent CC procedure. The Endotics system showed a sensitivity of 93.3% for the detection of polyps, detecting 14/15 polyps seen on CC. 6/71 (8.4%) of participants reported mild adverse events (nausea, headache, abdominal pain and discomfort) which the authors say, due to the tandem nature of the study, couldn't be distinguished from bowel cleansing or CC related adverse events[72].

A retrospective analysis of 5 years of Endotics examination in a single centre in Italy reported on 102 procedures performed due to incomplete CC. The Endotics system was able to complete a colonoscopy

in 95/102 (93.1%) of these patients. Mean CIT was 51 (± 22.5) min[73]. A learning curve study from Trecca *et al*[74] in 2020 presents two blocks of 27 and 28 participants. The CIR improved from 92.7% to 100% and the CIT from 55 to 22 min between the first and second block. The polyp detection rate and adenoma detection rate was 40% and 26.7%, respectively. The procedure was reported as mild or no distress in most cases with 92.7% willing to have a repeat Endotics procedure[74].

Endotics have performed a health economics study comparing Endotic robotic colonoscopy to standard colonoscopy in the Italian healthcare system and found the robotic colonoscopy to be comparable in price to standard colonoscopy, €441.25 *vs* €426.25, respectively[33].

Invendoscope

The Invendoscope (Invendo Medical GmbH, Weinheim, Germany) has a number of models with several CE and FDA approvals[75,76]. The single use computer-assisted device is propelled through the colon by an inverted sleeve driven by 8 wheels (Figure 3). The wheels grip the inside of the inverted sleeve to move forward and backwards. Control is *via* a handheld joystick. The tip of the colonoscope is robotically assisted and can be defected up to 180°, is equipped with three LEDs and a CMOS vision chip with an 114° field of view. Standard colonoscope functions such as insufflation, suction and irrigation are available, as well as a 3.2 mm working channel.

Animal testing using the SC20 model on the *in-vivo* small bowel of 5 pigs showed the device could be inserted through 3 small bowel loops and there was no mucosal damage found on microscopic pathological examination[77]. In a clinical trial of the SC40 model published in 2008, using two varying length prototypes in 34 participants, CIRs of 79% and 90% were achieved. CITs were 26 min and 20 min. The shorter of the two prototypes had a lower CIR, longer procedure time and more pain and bloating. Five cases had to be excluded due to instrument defects. Two of the failures to achieve caecal intubation were due to pain. Overall, the participants gave a mean acceptance rating of 1.96 (range 1-6). No immediate or delayed complications were reported[77].

A clinical trial on the Invendo SC20 model published by Groth *et al*[78] in 2011 found a CIR of 98.4% in 61 volunteers. Median CIT was 15 min and only 3/61 (4.9%) requested sedation. There were 32 polypectomies and no device-related complications reported. Water instillation was used in half of the cases to aid progression. Endoscope malfunctions were experienced in 2 cases. Post-procedure pain and discomfort scores were 1.6 and 2.3 out of 6, respectively[78].

Invendo Medical GmbH was acquired by Ambu in 2017 and the SC40 inverted sleeve wheel driven prototype has been replaced by the SC200 and then the SC210 which are manually inserted single use devices utilising robotic tip controls[21].

Only a conference abstract could be found on the Invendo SC210 model. In this clinical trial 40 participants underwent colonoscopy with the SC210, CIR was 95% with a median CIT of 14.2 min. Most patients (35/40) received propofol sedation. Twelve patients had polypectomies performed. There were 3 complaints of abdominal pain post-procedure and one self-limiting haemorrhage from the sigmoid colon, but no major complications[79].

The SC210 model no longer has any robotic locomotion, with the only robotics left being tip deflection, making it predominantly a single use colonoscope. Since the acquisition by Ambu, the Invendoscope is no longer on the market. Following correspondence with Ambu, the long scope length (220 cm) required for the self-propelled version made it difficult to control looping. Physicians also reportedly found it difficult to transition to the robotic tip control of the SC210 so Ambu have decided to focus on conventional control mechanisms.

Robotic capsule colonoscope

A European FP6 project called "Versatile Endoscopic Capsule for GI TumOr Recognition and therapy" (VECTOR project) was tasked to explore magnetic capsule endoscopy from 2006 to 2011. One of the outputs of the project was a magnetically controlled capsule for colonoscopy. A 13.5 mm × 29.5 mm endoscopic capsule containing 6 LEDs and a CCD camera capable of 550 × 582 pixel resolution and a 120° field of view was designed. The capsule also contained 3 permanent magnets and a triaxial magnetic sensor to monitor the magnetic link. Power and transmission to and from the capsule was achieved *via* a 2 mm cable. The capsule was controlled using an external permanent magnet fixed to a robotic arm end effector which was found to offer more precision than manual control[80]. The robotic arm has 6 DOF and an additional 7th DOF was added at the end effector-magnet connection. The capsule trajectory is controlled by means of controlling the robotic arm and the magnetic attraction between the external and internal magnets pulls the capsule along the colon. The initial version of the device was not able to insufflate the colon, so a Foley catheter had to be passed rectally to insufflate[81].

A benchtop study of the magnetic capsule colonoscope was undertaken, including 11 endoscopist and 11 trainees, who performed the robotic capsule colonoscopy and CC on an *ex-vivo* porcine colon used to simulate a human colon. All 22 participants were able to complete the procedure using both the robotic capsule and conventional colonoscope. Pins inserted in the phantom colon were found with a mean accuracy of 80.9% (± 11.0%) in the robotic capsule procedures and 85.8% (± 9.9%) in the CC procedures[81].
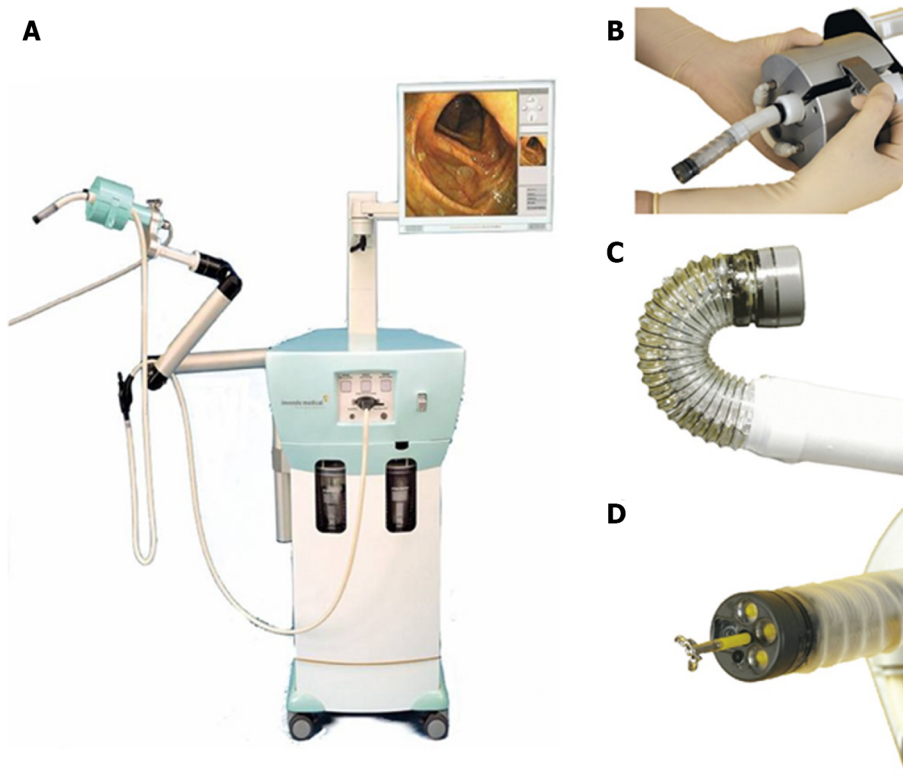
Figure 3 Invendoscope SC20 (Invendo Medical GmbH, Weinheim, Germany). A: Workstation; B: Drive unit; C: Deflectable tip; D: Working channel.
Citation: Groth S, Rex DK, Rösch T, Hoepffner N. High cecal intubation rates with a new computer-assisted colonoscope: a feasibility study. *Am J Gastroenterol*
2011; 106: 1075-1080. Copyright© The Authors 2020. Published by Creative Commons Attribution-NonCommercial-No Derivative Works 3.0 License.

The next prototype from the same team of researchers, named the Magnetic Air Capsule, included a soft multi-lumen tether to allow insufflation, washing, suctioning, lens cleaning and a working channel for passing therapeutic tools. *Ex-vivo* testing on a porcine colon within a human phantom model was undertaken using 12 participants and all participants were able to complete an 85 cm phantom colonoscopy, with 85% (± 11%) of the beads found. *In-vivo* porcine testing proved the device was capable of traversing an average distance of 800 (± 40) mm in an average of 900 (± 195) seconds[82].

The VECTOR project team were also able to explore several other aspects of robotic colonoscope design. Experiments exploring the human robot interface were conducted and teleoperated (remote control) was found to be more reliable than a human/robot cooperative haptic control using a torque/force sensor[83].

Following on from the VECTOR project, some of the research team have gone on to develop the technologies further in the ENDOO magnetic colonoscope and the magnetic flexible endoscope (MFE).

MFE

The MFE research team (STORM lab, Leeds, United Kingdom and Nashville, TN, United States) has developed the soft tether capsule colonoscope technology further (Figure 4). Advancements in the localisation and real time pose estimation allow closed loop control of the endoscope. Closed loop control allows the user to steer the endoscope based on what they see from the video feed rather than controlling movement of the robotic arm and attempting to translate that into the movement desired of the endoscope tip[53,84]. Further developments have allowed the capsule to levitate in the colon lumen rather than skimming along the mucosal surface. Autonomous navigation and autonomous retroflexion have been demonstrated in porcine studies[4,85]. Laboratory based learning curve studies and task load assessments suggest a quicker learning curve than with CC and a lower perceived workload[86]. *In-vivo* porcine studies have not demonstrated any safety concerns and even novice user were able to navigate the device 85 cm into a pig colon[84]. The platform is currently undergoing final pre-clinical steps in preparation for first-in-human trials.

ENDOO

The ENDOO project (Pisa, Italy) was a European H2020 project between 2015 and 2019 that also designed a magnetically actuated soft tether robot. A permanent magnet in the capsular tip of the endoscope is pulled through the colon using closed loop interaction with an external permanent magnet on an industrial anthropomorphic robotic arm[87,88]. The capsular tip has two 1080p CMOS cameras to allow stereoscopic, 3-dimensional, views. Four LEDs offer white light illumination, and 4 ultraviolet
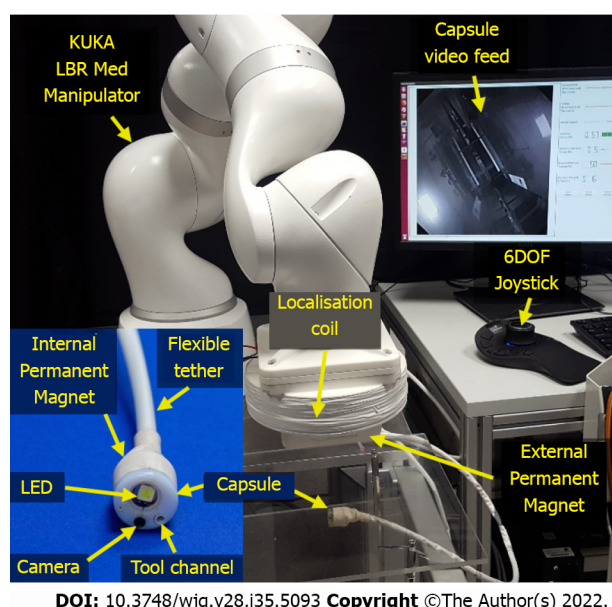
Figure 4 Magnetic flexible endoscope (STORM lab, Leeds, United Kingdom and Nashville, TN, United States).

LEDs allow narrow band imaging. The 160 cm soft tether carries 4 channels, including a 3.7 mm working channel, providing suction, irrigation, lens cleaning and insufflation. The soft tether also integrates nylon cables to allow variable stiffness of the shaft.

Ex-vivo testing using a porcine colon in a human abdomen simulator compared key functionalities, forces generated, simulated polyp detection and usability when compared to CC in 10 expert endoscopists and 5 trainees. The forces generated by the robotic colonoscope were significantly less than those generated by CC, with cumulative interaction forces of 16.5N for CC and 1.67N for the robotic colonoscope. The robotic colonoscope was able to complete the procedure 67% of the time with a comparable polyp detection rate to CC[89].

PASSIVE COLONOSCOPY

Passive colonoscopes are capsule devices designed to assess the colon with movement through the gastrointestinal tract passively *via* natural peristalsis. There is now a commercially available colon capsule endoscope, the Pillcam™ COLON2 (Given Imaging, Yokneam Illit, Israel). Researchers have also been exploring the addition of further robotics within capsular devices in an attempt to overcome some of their disadvantages. Advances in miniaturisation, image capture and batteries have allowed researchers the space within the small confines of a safe capsule size to add further robotics. A full review of these devices is beyond the scope of this review but have been done in detail by Manfredi[90] and Slawinski *et al*[91].

ROBOT ASSISTED FLEXIBLE ENDOSCOPY PLATFORMS

The previously described robotic platforms aim to provide an alternative to CC. However, some researchers have been developing platforms to assist with some of the challenges of performing CC by adapting the current colonoscope. Adding robotic controls to existing endoscopes could improve the ergonomics and assist with the difficult learning curve associated with colonoscopy.

The Endodrive (ECE Medical Products, Erlangen, Germany) is a platform using a rotating engine and foot pedal to control shaft insertion. Rotation and tip control is still required[92]. Rozeboom *et al*[93] present a robotic-assisted flexible colonoscope that uses an add-on to the handle of the colonoscope that convert the wheel control mechanism into a robotic joystick control. CIR using Rozeboom's device was 68%[93]. Robotic steering and automated lumen centralisation (RS-ALC, Enschede, Netherlands) is another platform which uses joystick control of an add-on to the endoscope handle with the addition of lumen centralisation software. A study of novices and experts on a colon simulation model found that novices had a faster CIT and polyp detection rate with the RS-ALC than CC. The opposite was found of experts, who found CC better[94]. The master–slave endoscopic operation robot (EOR; Kyushu Institute of Technology, Kitakyushu, Japan) which is in its third iteration, added on therapeutic tools. The EOR version 3 uses a rotary motor, rotating handle, torque sensor and mini joystick which allows haptic

feedback and 4 axis movement. An *ex-vivo* colon phantom study using 8 endoscopists performed 48 colonoscopies with a CIR of 100% and CIT of 118.5 (± 89.4) seconds[69].

ROBOTIC FLEXIBLE ENDOSCOPES WITH THERAPEUTIC APPLICATIONS

Advances in the therapeutic capabilities of gastrointestinal endoscopy and the evolution of natural orifice transluminal endoscopy (NOTES) have led researchers to look to robotics to enhance the dexterity offered by our endoscopes. A number of systems have been developed that claim to offer greater triangulation, dexterity and DOF to improve our ability to perform procedures such as ESD, third space endoscopy and NOTES. Examples include Endoluminal Assistant for Surgical Endoscopy (EASE; KARL STORZ/IRCAD, Strasbourg, France) (Figure 5), K-FLEX (EasyEndo Surgical, Daejeon, Korea) and the MASTER (EndoMASTER Pte, Singapore)[95-97]. A detailed review of these devices is beyond the scope of this review article but has been done by Lim[98].

CONCLUSION

Endoscopy is an expanding speciality with colonoscopy demand rising by at least 5% *per* year[99,100]. Yet a significant number of people decline to undergo colonoscopy due to several factors including pain and previous bad experiences[16,17]. Robotics has the potential to provide an alternative to CC. However, the ideal robotic platform must be affordable; versatile and capable of performing precise movements while maintaining patient comfort. The potential for robotics to improve the dexterity of an endoscope in the ever-expanding field of therapeutic endoscopy is also worth consideration and likely to be something we will see in the future. Researchers developing new medical devices must keep sustainability in mind. And with a global pandemic in the forefronts of everyone's minds, the potential for robotics to provide a 'medically distanced' procedure will be appealing to many.

AI has not been covered in this review article but is likely to be integrated in robotic colonoscopes. AI in endoscopy has many facets, including image assistance for lesion detection or characterisation, but also integrates closely with robotics in the form of autonomous movement/navigation. Although for many this seems like science fiction and not yet requiring discussion, the technology is available. The MFE device can autonomously navigate a pig colon.

However, advances in AI and increasingly autonomous tasks introduce a number a challenges. Regulatory, ethical and legal uncertainty is likely to take time to overcome, hindering commercialisation. Integration is therefore likely to be slow, with a gradual increase in the autonomy of devices despite the technology being available for further autonomy.

The technology to allow a completely autonomous colonoscopy, including diagnostics, with an endoscopist only required on a supervisory capacity is not so far away. Autonomous robotic colonoscopy has the potential to increased capacity with fewer operators required to perform more procedures. Endoscopists could potentially be trained much quicker. Robotics has the potential to raise the standard of procedures, democratising colonoscopy, thus reducing post-colonoscopy CRCs, reducing complications and improving the colonoscopy experience for patients.

Some of the devices discussed have reached TRLs of 8 and gained FDA or CE marking, however few have yet been adopted enough to perform post-marketing studies or health economics studies. Although, the Endotics health economics study has shown promising result, health economics studies in other areas of robotic healthcare, such as surgery, have been fraught with conflicting results.

Several of the discussed robotic colonoscopes have been modified, removing some of the robotics and opting to pursue the single use colonoscope market. It is probable that the improvements in endoscopy technique have put off commercialisation for the purpose of improved caecal intubation. However, much of the need for these devices is to improve patient experience, which now seems to be the focus of many research teams. What may seem like more intuitive controls will still be different to the standard endoscope controls experienced endoscopists have grown used to. Resistance to change is going to be a challenge for all new devices.

These technologies are often expensive initially, but the cost should not be confused with the potential cost effectiveness of a test which is more acceptable, with the subsequent reduction in morbidity and mortality. Technological advances are happening at an exponential rate and although none of the device to date have challenged the dominance of CC, it is probable that one will in the very near future.
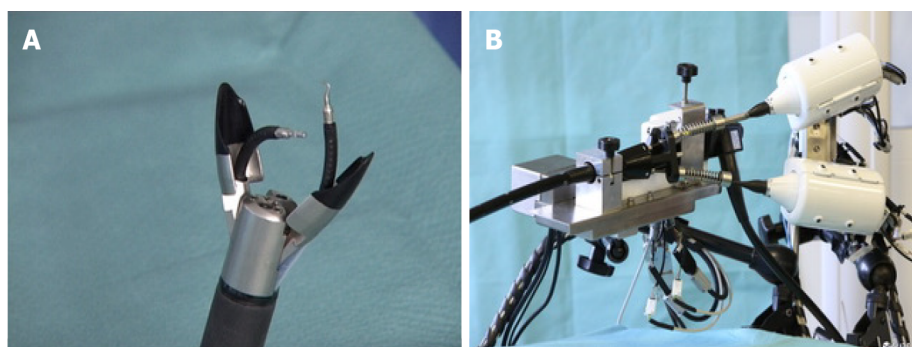
Figure 5 Endoluminal assistant for surgical endoscopy (EASE; KARL STORZ/IRCAD, Strasbourg, France). A: Flexible tip with antagonistic tendons with tools attached; B: Slave unit. Citation: Permission for use and images provided directly by the lab who developed the device. Email confirmation attached as a text file.

FOOTNOTES

REFERENCES

1   **Sung H**, Ferlay J, Siegel RL, Laversanne M, Soerjomataram I, Jemal A, Bray F. Global Cancer Statistics 2020: GLOBOCAN Estimates of Incidence and Mortality Worldwide for 36 Cancers in 185 Countries. *CA Cancer J Clin* 2021; **71**: 209-249 [PMID: 33538338 DOI: 10.3322/caac.21660]
2   **Arnold M**, Sierra MS, Laversanne M, Soerjomataram I, Jemal A, Bray F. Global patterns and trends in colorectal cancer incidence and mortality. *Gut* 2017; **66**: 683-691 [PMID: 26818619 DOI: 10.1136/gutjnl-2015-310912]
3   **Keum N**, Giovannucci E. Global burden of colorectal cancer: emerging trends, risk factors and prevention strategies. *Nat Rev Gastroenterol Hepatol* 2019; **16**: 713-732 [PMID: 31455888 DOI: 10.1038/s41575-019-0189-8]
4   **Slawinski PR**, Taddese AZ, Musto KB, Sarker S, Valdastri P, Obstein KL. Autonomously Controlled Magnetic Flexible Endoscope for Colon Exploration. *Gastroenterology* 2018; **154**: 1577-1579.e1 [PMID: 29530377 DOI: 10.1053/j.gastro.2018.02.037]
5   **Medical Technologies Innovation and Knowledge Centre**.   The Medical Technologies Innovation and Knowledge Centre. [cited 10 April 2022]. Available from: https://medical-technologies.co.uk/
6   **Lamb CA**, Kennedy NA, Raine T, Hendy PA, Smith PJ, Limdi JK, Hayee B, Lomer MCE, Parkes GC, Selinger C, Barrett KJ, Davies RJ, Bennett C, Gittens S, Dunlop MG, Faiz O, Fraser A, Garrick V, Johnston PD, Parkes M, Sanderson J, Terry H; IBD guidelines eDelphi consensus group, Gaya DR, Iqbal TH, Taylor SA, Smith M, Brookes M, Hansen R, Hawthorne AB. British Society of Gastroenterology consensus guidelines on the management of inflammatory bowel disease in adults. *Gut* 2019; **68**: s1-s106 [PMID: 31562236 DOI: 10.1136/gutjnl-2019-318484]
7   **Monahan KJ**, Bradshaw N, Dolwani S, Desouza B, Dunlop MG, East JE, Ilyas M, Kaur A, Lalloo F, Latchford A, Rutter

MD, Tomlinson I, Thomas HJW, Hill J; Hereditary CRC guidelines eDelphi consensus group. Guidelines for the management of hereditary colorectal cancer from the British Society of Gastroenterology (BSG)/Association of Coloproctology of Great Britain and Ireland (ACPGBI)/United Kingdom Cancer Genetics Group (UKCGG). *Gut* 2020; **69**: 411-444 [PMID: 31780574 DOI: 10.1136/gutjnl-2019-319915]

8   **Rutter MD**, East J, Rees CJ, Cripps N, Docherty J, Dolwani S, Kaye PV, Monahan KJ, Novelli MR, Plumb A, Saunders BP, Thomas-Gibson S, Tolan DJM, Whyte S, Bonnington S, Scope A, Wong R, Hibbert B, Marsh J, Moores B, Cross A, Sharp L. British Society of Gastroenterology/Association of Coloproctology of Great Britain and Ireland/Public Health England post-polypectomy and post-colorectal cancer resection surveillance guidelines. *Gut* 2020; **69**: 201-223 [PMID: 31776230 DOI: 10.1136/gutjnl-2019-319858]

9   **Hassan C**, Antonelli G, Dumonceau JM, Regula J, Bretthauer M, Chaussade S, Dekker E, Ferlitsch M, Gimeno-Garcia A, Jover R, Kalager M, Pellisé M, Pox C, Ricciardiello L, Rutter M, Helsingen LM, Bleijenberg A, Senore C, van Hooft JE, Dinis-Ribeiro M, Quintero E. Post-polypectomy colonoscopy surveillance: European Society of Gastrointestinal Endoscopy (ESGE) Guideline - Update 2020. *Endoscopy* 2020; **52**: 687-700 [PMID: 32572858 DOI: 10.1055/a-1185-3109]

10   **Mutneja HR**, Bhurwal A, Arora S, Vohra I, Attar BM. A delay in colonoscopy after positive fecal tests leads to higher incidence of colorectal cancer: A systematic review and meta-analysis. *J Gastroenterol Hepatol* 2021; **36**: 1479-1486 [PMID: 33351959 DOI: 10.1111/jgh.15381]

11   **Gingold-Belfer R**, Leibovitzh H, Boltin D, Issa N, Tsadok Perets T, Dickman R, Niv Y. The compliance rate for the second diagnostic evaluation after a positive fecal occult blood test: A systematic review and meta-analysis. *United European Gastroenterol J* 2019; **7**: 424-448 [PMID: 31019712 DOI: 10.1177/2050640619828185]

12   **Selby K**, Senore C, Wong M, May FP, Gupta S, Liang PS. Interventions to ensure follow-up of positive fecal immunochemical tests: An international survey of screening programs. *J Med Screen* 2021; **28**: 51-53 [PMID: 32054392 DOI: 10.1177/0969141320904977]

13   **Lee YC**, Li-Sheng Chen S, Ming-Fang Yen A, Yueh-Hsia Chiu S, Ching-Yuan Fann J, Chuang SL, Chiang TH, Chou CK, Chiu HM, Wu MS, Wu CY, Chia SL, Chiou ST, Chen HH. Association Between Colorectal Cancer Mortality and Gradient Fecal Hemoglobin Concentration in Colonoscopy Noncompliers. *J Natl Cancer Inst* 2017; **109** [PMID: 28376228 DOI: 10.1093/jnci/djw269]

14   **Zorzi M**, Battagello J, Selby K, Capodaglio G, Baracco S, Rizzato S, Chinellato E, Guzzinati S, Rugge M. Non-compliance with colonoscopy after a positive faecal immunochemical test doubles the risk of dying from colorectal cancer. *Gut* 2022; **71**: 561-567 [PMID: 33789965 DOI: 10.1136/gutjnl-2020-322192]

15   **Dalton ARH**. Incomplete diagnostic follow-up after a positive colorectal cancer screening test: a systematic review. *J Public Health (Oxf)* 2018; **40**: e46-e58 [PMID: 28069989 DOI: 10.1093/pubmed/fdw147]

16   **Kerrison RS**, Sheik-Mohamud D, McBride E, Whitaker KL, Rees C, Duffy S, von Wagner C. Patient barriers and facilitators of colonoscopy use: A rapid systematic review and thematic synthesis of the qualitative literature. *Prev Med* 2021; **145**: 106413 [PMID: 33412167 DOI: 10.1016/j.ypmed.2020.106413]

17   **Kerrison RS**, Travis E, Dobson C, Whitaker KL, Rees CJ, Duffy SW, von Wagner C. Barriers and facilitators to colonoscopy following fecal immunochemical test screening for colorectal cancer: A key informant interview study. *Patient Educ Couns* 2022; **105**: 1652-1662 [PMID: 34607734 DOI: 10.1016/j.pec.2021.09.022]

18   **Meester RG**, Doubeni CA, Zauber AG, Goede SL, Levin TR, Corley DA, Jemal A, Lansdorp-Vogelaar I. Public health impact of achieving 80% colorectal cancer screening rates in the United States by 2018. *Cancer* 2015; **121**: 2281-2285 [PMID: 25763558 DOI: 10.1002/cncr.29336]

19   **Ramai D**, Zakhia K, Etienne D, Reddy M. Philipp Bozzini (1773-1809): The earliest description of endoscopy. *J Med Biogr* 2018; **26**: 137-141 [PMID: 29405817 DOI: 10.1177/0967772018755587]

20   **Visconti TAC**, Otoch JP, Artifon ELA. Robotic endoscopy. A review of the literature. *Acta Cir Bras* 2020; **35**: e202000206 [PMID: 32348403 DOI: 10.1590/s0102-865020200020000006]

21   **Ciuti G**, Skonieczna-Żydecka K, Marlicz W, Iacovacci V, Liu H, Stoyanov D, Arezzo A, Chiurazzi M, Toth E, Thorlacius H, Dario P, Koulaouzidis A. Frontiers of Robotic Colonoscopy: A Comprehensive Review of Robotic Colonoscopes and Technologies. *J Clin Med* 2020; **9** [PMID: 32486374 DOI: 10.3390/jcm9061648]

22   **Holme Ø**, Løberg M, Kalager M, Bretthauer M, Hernán MA, Aas E, Eide TJ, Skovlund E, Lekven J, Schneede J, Tveit KM, Vatn M, Ursin G, Hoff G; NORCCAP Study Group†. Long-Term Effectiveness of Sigmoidoscopy Screening on Colorectal Cancer Incidence and Mortality in Women and Men: A Randomized Trial. *Ann Intern Med* 2018; **168**: 775-782 [PMID: 29710125 DOI: 10.7326/M17-1441]

23   **PubMed**. PubMed search "Robotic Colonoscopy". National Library of Medicine; 2021. [cited 10 January 2022]. Available from: https://pubmed.ncbi.nlm.nih.gov/

24   **Wernli KJ**, Brenner AT, Rutter CM, Inadomi JM. Risks Associated With Anesthesia Services During Colonoscopy. *Gastroenterology* 2016; **150**: 888-94; quiz e18 [PMID: 26709032 DOI: 10.1053/j.gastro.2015.12.018]

25   **Maida M**, Alrubaiy L, Bokun T, Bruns T, Castro V, China L, Conroy G, Trabulo D, Van Steenkiste C, Voermans RP, Burisch J, Ianiro G. Current challenges and future needs of clinical and endoscopic training in gastroenterology: a European survey. *Endosc Int Open* 2020; **8**: E525-E533 [PMID: 32258375 DOI: 10.1055/a-1093-0877]

26   **Siau K**, Anderson JT, Valori R, Feeney M, Hawkes ND, Johnson G, McKaig BC, Pullan RD, Hodson J, Wells C, Thomas-Gibson S, Haycock AV, Beales ILP, Broughton R, Dunckley P; Joint Advisory Group on Gastrointestinal Endoscopy (JAG). Certification of UK gastrointestinal endoscopists and variations between trainee specialties: results from the JETS e-portfolio. *Endosc Int Open* 2019; **7**: E551-E560 [PMID: 30957005 DOI: 10.1055/a-0839-4476]

27   **Shergill AK**, Harris Adamson C. Failure of an engineered system: The gastrointestinal endoscope. *Tech Gastrointest Endosc* 2019; **21**: 116-123 [DOI: 10.1016/j.tgie.2019.02.001]

28   **Yung DE**, Banfi T, Ciuti G, Arezzo A, Dario P, Koulaouzidis A. Musculoskeletal injuries in gastrointestinal endoscopists: a systematic review. *Expert Rev Gastroenterol Hepatol* 2017; **11**: 939-947 [PMID: 28705042 DOI: 10.1080/17474124.2017.1356225]

29   **Merola G**, Sciuto A, Pirozzi F, Andreuccetti J, Pignata G, Corcione F, Milone M, De Palma GD, Castaldo R, Pecchia L,

Ceccarelli G, Bracale U. Is robotic right colectomy economically sustainable? *Surg Endosc* 2020; **34**: 4041-4047 [PMID: 31617088 DOI: 10.1007/s00464-019-07193-z]

30   **Gomolin A**, Gotlieb W, Lau S, Salvador S, Racovitan F, Abitbol J. Mandate to evaluate robotic surgery implementation: a 12-year retrospective analysis of impact and future implications. *J Robot Surg* 2022; **16**: 783-788 [PMID: 34741713 DOI: 10.1007/s11701-021-01327-z]

31   **Partelli S**, Ricci C, Cinelli L, Montorsi RM, Ingaldi C, Andreasi V, Crippa S, Alberici L, Casadei R, Falconi M. Evaluation of cost-effectiveness among open, laparoscopic and robotic distal pancreatectomy: A systematic review and meta-analysis. *Am J Surg* 2021; **222**: 513-520 [PMID: 33853724 DOI: 10.1016/j.amjsurg.2021.03.066]

32   **Lundin ES**, Carlsson P, Wodlin NB, Nilsson L, Kjölhede P. Cost-effectiveness of robotic hysterectomy *vs* abdominal hysterectomy in early endometrial cancer. *Int J Gynecol Cancer* 2020; **30**: 1719-1725 [PMID: 32863275 DOI: 10.1136/ijgc-2020-001611]

33   **Sicuro R**, Tumino E, Lambiase C, Mamone D.   Robotic Colonoscopy: Comparative Analysis of Costs Compared to Painless Conventional Colonoscopy. 2020 Preprint. Available from: Research Square [DOI: 10.21203/rs.3.rs-104356/v1]

34   **Shenbagaraj L**, Thomas-Gibson S, Stebbing J, Broughton R, Dron M, Johnston D, Shaw T, Haboubi HN, Green JT. Endoscopy in 2017: a national survey of practice in the UK. *Frontline Gastroenterol* 2019; **10**: 7-15 [PMID: 30651952 DOI: 10.1136/flgastro-2018-100970]

35   **Calderwood AH**, Calderwood MS, Williams JL, Dominitz JA. Impact of the COVID-19 Pandemic on Utilization of EGD and Colonoscopy in the United States: An Analysis of the GIQuIC Registry. *Tech Innov Gastrointest Endosc* 2021; **23**: 313-321 [PMID: 34345871 DOI: 10.1016/j.tige.2021.07.003]

36   **Larsen S**, Kalloo A, Hutfless S. The hidden cost of colonoscopy including cost of reprocessing and infection rate: the implications for disposable colonoscopes. *Gut* 2020; **69**: 197-200 [PMID: 31413166 DOI: 10.1136/gutjnl-2019-319108]

37   **Halligan S**, Dadswell E, Wooldrage K, Wardle J, von Wagner C, Lilford R, Yao GL, Zhu S, Atkin W. Computed tomographic colonography compared with colonoscopy or barium enema for diagnosis of colorectal cancer in older symptomatic patients: two multicentre randomised trials with economic evaluation (the SIGGAR trials). *Health Technol Assess* 2015; **19**: 1-134 [PMID: 26198205 DOI: 10.3310/hta19540]

38   **Atkin W**, Dadswell E, Wooldrage K, Kralj-Hans I, von Wagner C, Edwards R, Yao G, Kay C, Burling D, Faiz O, Teare J, Lilford RJ, Morton D, Wardle J, Halligan S; SIGGAR investigators. Computed tomographic colonography versus colonoscopy for investigation of patients with symptoms suggestive of colorectal cancer (SIGGAR): a multicentre randomised trial. *Lancet* 2013; **381**: 1194-1202 [PMID: 23414650 DOI: 10.1016/S0140-6736(12)62186-2]

39   **Halligan S**, Wooldrage K, Dadswell E, Shah U, Kralj-Hans I, von Wagner C, Faiz O, Teare J, Edwards R, Kay C, Yao G, Lilford RJ, Morton D, Wardle J, Atkin W; SIGGAR Investigators. Identification of Extracolonic Pathologies by Computed Tomographic Colonography in Colorectal Cancer Symptomatic Patients. *Gastroenterology* 2015; **149**: 89-101.e5 [PMID: 25796362 DOI: 10.1053/j.gastro.2015.03.011]

40   **IJspeert JE**, Tutein Nolthenius CJ, Kuipers EJ, van Leerdam ME, Nio CY, Thomeer MG, Biermann K, van de Vijver MJ, Dekker E, Stoker J. CT-Colonography vs. Colonoscopy for Detection of High-Risk Sessile Serrated Polyps. *Am J Gastroenterol* 2016; **111**: 516-522 [PMID: 27021193 DOI: 10.1038/ajg.2016.58]

41   **Ghanouni A**, Halligan S, Plumb A, Boone D, Wardle J, von Wagner C. Non- or full-laxative CT colonography vs. endoscopic tests for colorectal cancer screening: a randomised survey comparing public perceptions and intentions to undergo testing. *Eur Radiol* 2014; **24**: 1477-1486 [PMID: 24817084 DOI: 10.1007/s00330-014-3187-9]

42   **Kjølhede T**, Ølholm AM, Kaalby L, Kidholm K, Qvist N, Baatrup G. Diagnostic accuracy of capsule endoscopy compared with colonoscopy for polyp detection: systematic review and meta-analyses. *Endoscopy* 2021; **53**: 713-721 [PMID: 32858753 DOI: 10.1055/a-1249-3938]

43   **Benech N**, Vinet O, Gaudin JL, Benamouzig R, Dray X, Ponchon T, Galmiche JP, Sacher-Huvelin S, Samaha E, Saurin JC; ONECC Study Group. Colon capsule endoscopy in clinical practice: lessons from a national 5-year observational prospective cohort. *Endosc Int Open* 2021; **9**: E1542-E1548 [PMID: 34540548 DOI: 10.1055/a-1526-0923]

44   **Spada C**, Hassan C, Barbaro B, Iafrate F, Cesaro P, Petruzziello L, Minelli Grazioli L, Senore C, Brizi G, Costamagna I, Alvaro G, Iannitti M, Salsano M, Ciolina M, Laghi A, Bonomo L, Costamagna G. Colon capsule *vs* CT colonography in patients with incomplete colonoscopy: a prospective, comparative trial. *Gut* 2015; **64**: 272-281 [PMID: 24964317 DOI: 10.1136/gutjnl-2013-306550]

45   **Cash BD**, Fleisher MR, Fern S, Rajan E, Haithcock R, Kastenberg DM, Pound D, Papageorgiou NP, Fernández-Urién I, Schmelkin IJ, Rex DK. Multicentre, prospective, randomised study comparing the diagnostic yield of colon capsule endoscopy *vs* CT colonography in a screening population (the TOPAZ study). *Gut* 2021; **70**: 2115-2122 [PMID: 33443017 DOI: 10.1136/gutjnl-2020-322578]

46   **Burr NE**, Plumb A, Sood R, Rembacken B, Tolan DJM. CT colonography remains an important test for colorectal cancer. *Gut* 2022; **71**: 217-218 [PMID: 33753420 DOI: 10.1136/gutjnl-2021-324399]

47   **Deding U**, Kaalby L, Bøggild H, Plantener E, Wollesen MK, Kobaek-Larsen M, Hansen SJ, Baatrup G. Colon Capsule Endoscopy vs. CT Colonography Following Incomplete Colonoscopy: A Systematic Review with Meta-Analysis. *Cancers (Basel)* 2020; **12** [PMID: 33202936 DOI: 10.3390/cancers12113367]

48   **Zijta FM**, Bipat S, Stoker J. Magnetic resonance (MR) colonography in the detection of colorectal lesions: a systematic review of prospective studies. *Eur Radiol* 2010; **20**: 1031-1046 [PMID: 19936754 DOI: 10.1007/s00330-009-1663-4]

49   **Lim EJ**, Leung C, Pitman A, Stella DL, Brown G, Slattery M, Marion K, Macrae F. Magnetic resonance colonography for colorectal cancer screening in patients with Lynch syndrome gene mutation. *Fam Cancer* 2010; **9**: 555-561 [PMID: 20495877 DOI: 10.1007/s10689-010-9350-9]

50   **Graser A**, Melzer A, Lindner E, Nagel D, Herrmann K, Stieber P, Schirra J, Mansmann U, Reiser MF, Göke B, Kolligs FT. Magnetic resonance colonography for the detection of colorectal neoplasia in asymptomatic adults. *Gastroenterology* 2013; **144**: 743-750.e2 [PMID: 23415805 DOI: 10.1053/j.gastro.2012.12.041]

51   **Gao Y**, Wang J, Lv H, Xue Y, Jia R, Liu G, Bai W, Wu Y, Zhang L, Yang J. Diagnostic value of magnetic resonance and computed tomography colonography for the diagnosis of colorectal cancer: A systematic review and meta-analysis. *Medicine (Baltimore)* 2019; **98**: e17187 [PMID: 31574825 DOI: 10.1097/MD.0000000000017187]

52   **Bianchi F**, Masaracchia A, Shojaei Barjuei E, Menciassi A, Arezzo A, Koulaouzidis A, Stoyanov D, Dario P, Ciuti G. Localization strategies for robotic endoscopic capsules: a review. *Expert Rev Med Devices* 2019; **16**: 381-403 [PMID: 31056968 DOI: 10.1080/17434440.2019.1608182]

53   **Taddese AZ**, Slawinski PR, Pirotta M, De Momi E, Obstein KL, Valdastri P. Enhanced Real-Time Pose Estimation for Closed-Loop Robotic Manipulation of Magnetically Actuated Capsule Endoscopes. *Int J Rob Res* 2018; **37**: 890-911 [PMID: 30150847 DOI: 10.1177/0278364918779132]

54   **Dupont PE**, Nelson BJ, Goldfarb M, Hannaford B, Menciassi A, O'Malley MK, Simaan N, Valdastri P, Yang GZ. A decade retrospective of medical robotics research from 2010 to 2020. *Sci Robot* 2021; **6**: eabi8017 [PMID: 34757801 DOI: 10.1126/scirobotics.abi8017]

55   **England PH**.   Bowel Cancer Screening: Programme Overview. 2019. [cited 10 April 2022]. Available from: https://www.gov.uk/guidance/bowel-cancer-screening-programme-overview

56   **Siau K**, Hayee BH, Gayam S. Endoscopy's Current Carbon Footprint. *Tech Innov Gastrointest Endosc* 2021; **23**: 344-352 [DOI: 10.1016/j.tige.2021.06.005]

57   **Tapia-Siles SC**, Coleman S, Cuschieri A. Current state of micro-robots/devices as substitutes for screening colonoscopy: assessment based on technology readiness levels. *Surg Endosc* 2016; **30**: 404-413 [PMID: 26092000 DOI: 10.1007/s00464-015-4263-1]

58   **Taherdoost H**. A review of technology acceptance and adoption models and theories. *Procedia Manuf* 2018; **22**: 960-967

59   **Gluck N**, Melhem A, Halpern Z, Mergener K, Santo E. A novel self-propelled disposable colonoscope is effective for colonoscopy in humans (with video). *Gastrointest Endosc* 2016; **83**: 998-1004.e1 [PMID: 26391735 DOI: 10.1016/j.gie.2015.08.083]

60   **Pfeffer J**, Grinshpon R, Rex D, Levin B, Rösch T, Arber N, Halpern Z. The Aer-O-Scope: proof of the concept of a pneumatic, skill-independent, self-propelling, self-navigating colonoscope in a pig model. *Endoscopy* 2006; **38**: 144-148 [PMID: 16479421 DOI: 10.1055/s-2006-925089]

61   **Vucelic B**, Rex D, Pulanic R, Pfefer J, Hrstic I, Levin B, Halpern Z, Arber N. The aer-o-scope: proof of concept of a pneumatic, skill-independent, self-propelling, self-navigating colonoscope. *Gastroenterology* 2006; **130**: 672-677 [PMID: 16530508 DOI: 10.1053/j.gastro.2005.12.018]

62   **View G**.   Validation of Aer-O-Scope Colonoscope System Cecal Intubation. ClinicalTrials.gov: U.S. National Library of Medicine; 2019. [cited 8 April 2022]. Available from: https://clinicaltrials.gov/ct2/show/NCT03949777?cond=aer-o-scope&draw=2&rank=1

63   **Federal Drug Administration**.   Aer-O-Scope FDA approval. Department of Health & Human Services 30th June 2016. [cited 8 April 2022]. Available from: https://www.gao.gov/products/gao-16-729r

64   **View G**.   Aer-O-Scope. GI View. [cited 8 April 2022]. Available from: https://www.giview.com/

65   **Shike M**, Fireman Z, Eliakim R, Segol O, Sloyer A, Cohen LB, Goldfarb-Albak S, Repici A. Sightline ColonoSight system for a disposable, power-assisted, non-fiber-optic colonoscopy (with video). *Gastrointest Endosc* 2008; **68**: 701-710 [PMID: 18501356 DOI: 10.1016/j.gie.2007.12.062]

66   **Federal Drug Administration**.   Colonsight FDA approval. Department of Health & Human Services 24th November 2003. [cited 8 April 2022]. Available from: https://www.fda.gov/

67   **Medical C**.   Consis Medical. Consis-medical; 2018 [updated 2018]. [cited 8 April 2022]. Available from: http://consis-medical.com/

68   **Formosa GA**, Prendergast JM, Edmundowicz SA, Rentschler ME. Novel Optimization-Based Design and Surgical Evaluation of a Treaded Robotic Capsule Colonoscope. *IEEE Transact Robot* 2020; **36**: 545-552 [DOI: 10.1109/tro.2019.2949466]

69   **Kume K**, Sakai N, Goto T. Development of a novel endoscopic manipulation system: the Endoscopic Operation Robot ver.3. *Endoscopy* 2015; **47**: 815-819 [PMID: 25910062 DOI: 10.1055/s-0034-1391973]

70   **Boškoski I**, Orlandini B, Papparella LG, Matteo MV, De Siena M, Pontecorvi V, Costamagna G. Robotics and Artificial Intelligence in Gastrointestinal Endoscopy: Updated Review of the Literature and State of the Art. *Curr Robot Rep* 2021; **2**: 43-54 [DOI: 10.1007/s43154-020-00040-3]

71   **Cosentino F**, Tumino E, Passoni GR, Morandi E, Capria A. Functional evaluation of the endotics system, a new disposable self-propelled robotic colonoscope: *in vitro* tests and clinical trial. *Int J Artif Organs* 2009; **32**: 517-527 [PMID: 19844894 DOI: 10.1177/039139880903200806]

72   **Tumino E**, Sacco R, Bertini M, Bertoni M, Parisi G, Capria A. Endotics system *vs* colonoscopy for the detection of polyps. *World J Gastroenterol* 2010; **16**: 5452-5456 [PMID: 21086563 DOI: 10.3748/wjg.v16.i43.5452]

73   **Tumino E**, Parisi G, Bertoni M, Bertini M, Metrangolo S, Ierardi E, Cervelli R, Bresci G, Sacco R. Use of robotic colonoscopy in patients with previous incomplete colonoscopy. *Eur Rev Med Pharmacol Sci* 2017; **21**: 819-826 [PMID: 28272700]

74   **Trecca A**, Catalano F, Bella A, Borghini R. Robotic colonoscopy: efficacy, tolerability and safety. Preliminary clinical results from a pilot study. *Surg Endosc* 2020; **34**: 1442-1450 [PMID: 31932942 DOI: 10.1007/s00464-019-07332-6]

75   **Federal Drug Administration**.   Invendoscope E210 FDA approval. Public Health Service 27 September 2017. [cited 8 April 2022]. Available from: https://www.fda.gov/

76   **Federal Drug Administration**.   Invendoscope E200 FDA approval. Public Health Service: Department of Health & Human Services 15 July 2016. [cited 8 April 2022]. Available from: https://www.docin.com/p-1892232862.html

77   **Rösch T**, Adler A, Pohl H, Wettschureck E, Koch M, Wiedenmann B, Hoepffner N. A motor-driven single-use colonoscope controlled with a hand-held device: a feasibility study in volunteers. *Gastrointest Endosc* 2008; **67**: 1139-1146 [PMID: 18355823 DOI: 10.1016/j.gie.2007.10.065]

78   **Groth S**, Rex DK, Rösch T, Hoepffner N. High cecal intubation rates with a new computer-assisted colonoscope: a feasibility study. *Am J Gastroenterol* 2011; **106**: 1075-1080 [PMID: 21386833 DOI: 10.1038/ajg.2011.52]

79   **Straulino F**, Genthner A, Kiesslich R, Eickhoff A. Sa1938 Colonoscopy with the sterile single use endoscope INVENDOSCOPE SC210. *Gastrointest Endosc* 2018; **87** [DOI: 10.1016/j.gie.2018.04.459]

80   **Ciuti G**, Donlin R, Valdastri P, Arezzo A, Menciassi A, Morino M, Dario P. Robotic *vs* manual control in magnetic

steering of an endoscopic capsule. *Endoscopy* 2010; **42**: 148-152 [PMID: 20017088 DOI: 10.1055/s-0029-1243808]

81 **Arezzo A**, Menciassi A, Valdastri P, Ciuti G, Lucarini G, Salerno M, Di Natali C, Verra M, Dario P, Morino M. Experimental assessment of a novel robotically-driven endoscopic capsule compared to traditional colonoscopy. *Dig Liver Dis* 2013; **45**: 657-662 [PMID: 23453360 DOI: 10.1016/j.dld.2013.01.025]

82 **Valdastri P**, Ciuti G, Verbeni A, Menciassi A, Dario P, Arezzo A, Morino M. Magnetic air capsule robotic system: proof of concept of a novel approach for painless colonoscopy. *Surg Endosc* 2012; **26**: 1238-1246 [PMID: 22179445 DOI: 10.1007/s00464-011-2054-x]

83 **Salerno GCM**, Lucarini G, Valdastri P, Arezzo A, Menciassi A, Morino M, Dario P. A Comparative Evaluation of Control Interfaces for a Robotic-Aided Endoscopic Capsule Platform. *IEEE Trans Robot* 2012; **28**: 534-538 [DOI: 10.1109/TRO.2011.2177173]

84 **Martin JW**, Scaglioni B, Norton JC, Subramanian V, Arezzo A, Obstein KL, Valdastri P. Enabling the future of colonoscopy with intelligent and autonomous magnetic manipulation. *Nat Mach Intell* 2020; **2**: 595-606 [PMID: 33089071 DOI: 10.1038/s42256-020-00231-9]

85 **Pittiglio G**, Barducci L, Martin JW, Norton JC, Avizzano CA, Obstein KL, Valdastri P. Magnetic Levitation for Soft-Tethered Capsule Colonoscopy Actuated With a Single Permanent Magnet: A Dynamic Control Approach. *IEEE Robot Autom Lett* 2019; **4**: 1224-1231 [PMID: 31304240 DOI: 10.1109/LRA.2019.2894907]

86 **Mamunes AP**, Campisano F, Martin J, Scaglioni B, Mazomenos E, Valdastri P, Obstein KL. Magnetic flexible endoscope for colonoscopy: an initial learning curve analysis. *Endosc Int Open* 2021; **9**: E171-E180 [PMID: 33532555 DOI: 10.1055/a-1314-9860]

87 **Bianchi F**, Ciuti G, Koulaouzidis A, Arezzo A, Stoyanov D, Schostek S, Oddo CM, Menciassi A, Dario P. An innovative robotic platform for magnetically-driven painless colonoscopy. *Ann Transl Med* 2017; **5**: 421 [PMID: 29201873 DOI: 10.21037/atm.2017.09.15]

88 **Endoo Project**. Endoo EU Project; 2020. [cited 8 April 2022]. Available from: http://www.endoo-project.eu/

89 **Verra M**, Firrincieli A, Chiurazzi M, Mariani A, Lo Secco G, Forcignanò E, Koulaouzidis A, Menciassi A, Dario P, Ciuti G, Arezzo A. Robotic-Assisted Colonoscopy Platform with a Magnetically-Actuated Soft-Tethered Capsule. *Cancers (Basel)* 2020; **12** [PMID: 32887238 DOI: 10.3390/cancers12092485]

90 **Manfredi L**. Endorobots for Colonoscopy: Design Challenges and Available Technologies. *Front Robot AI* 2021; **8**: 705454 [PMID: 34336938 DOI: 10.3389/frobt.2021.705454]

91 **Slawinski PR**, Obstein KL, Valdastri P. Capsule endoscopy of the future: What's on the horizon? *World J Gastroenterol* 2015; **21**: 10528-10541 [PMID: 26457013 DOI: 10.3748/wjg.v21.i37.10528]

92 **Endoskopie EC**. Endodrive systems workstation. www.ece-medical-systems.com: Ece medical systems. [cited 8 April 2022]. Available from: http://www.endodrive.de/

93 **Rozeboom ED**, Bastiaansen BA, de Vries ES, Dekker E, Fockens PA, Broeders IA. Robotic-assisted flexible colonoscopy: preliminary safety and efficiency in humans. *Gastrointest Endosc* 2016; **83**: 1267-1271 [PMID: 26551732 DOI: 10.1016/j.gie.2015.10.046]

94 **Pullens HJ**, van der Stap N, Rozeboom ED, Schwartz MP, van der Heijden F, van Oijen MG, Siersema PD, Broeders IA. Colonoscopy with robotic steering and automated lumen centralization: a feasibility study in a colon model. *Endoscopy* 2016; **48**: 286-290 [PMID: 26126158 DOI: 10.1055/s-0034-1392550]

95 **Mascagni P**, Lim SG, Fiorillo C, Zanne P, Nageotte F, Zorn L, Perretta S, de Mathelin M, Marescaux J, Dallemagne B. Democratizing Endoscopic Submucosal Dissection: Single-Operator Fully Robotic Colorectal Endoscopic Submucosal Dissection in a Pig Model. *Gastroenterology* 2019; **156**: 1569-1571.e2 [PMID: 30768985 DOI: 10.1053/j.gastro.2018.12.046]

96 **Hwang M**, Kwon DS. K-FLEX: A flexible robotic platform for scar-free endoscopic surgery. *Int J Med Robot* 2020; **16**: e2078 [PMID: 31945797 DOI: 10.1002/rcs.2078]

97 **Lomanto D**, Wijerathne S, Ho LK, Phee LS. Flexible endoscopic robot. *Minim Invasive Ther Allied Technol* 2015; **24**: 37-44 [PMID: 25627436 DOI: 10.3109/13645706.2014.996163]

98 **Lim SG**. The development of robotic flexible endoscopic platforms. *Inter J Gastrointest Interven* 2020; **9**: 9-12 [DOI: 10.18528/ijgii190022]

99 **Comas M**, Mendivil J, Andreu M, Hernández C, Castells X. Long-Term Prediction of the Demand of Colonoscopies Generated by a Population-Based Colorectal Cancer Screening Program. *PLoS One* 2016; **11**: e0164666 [PMID: 27732635 DOI: 10.1371/journal.pone.0164666]

100 **Ravindran S**, Bassett P, Shaw T, Dron M, Broughton R, Johnston D, Healey CJ, Green J, Ashrafian H, Darzi A, Coleman M, Thomas-Gibson S. National census of UK endoscopy services in 2019. *Frontline Gastroenterol* 2021; **12**: 451-460 [PMID: 34712462 DOI: 10.1136/flgastro-2020-101538]

101 **Lauby-Secretan B**, Vilahur N, Bianchini F, Guha N, Straif K; International Agency for Research on Cancer Handbook Working Group. The IARC Perspective on Colorectal Cancer Screening. *N Engl J Med* 2018; **378**: 1734-1740 [PMID: 29580179 DOI: 10.1056/NEJMsr1714643]

102 **Director RD**. Technology Readiness Assessment (TRA) Deskbook. US Department of Defense, 2009

103 **Engineering ASoDfRa**. Technology Readiness Assessment (TRA) Guidance. US Department of Defense, 2011

104 **Slawinski PR**, Taddese AZ, Musto KB, Obstein KL, Valdastri P. Autonomous Retroflexion of a Magnetic Flexible Endoscope. *IEEE Robot Autom Lett* 2017; **2**: 1352-1359 [PMID: 28289703 DOI: 10.1109/LRA.2017.2668459]

Noncoding RNAs as additional mediators of epigenetic regulation in nonalcoholic fatty liver disease

Mohamed Zaiou

Mohamed Zaiou, Institut Jean Lamour, UMR CNRS 7198, CNRS, University of Lorraine, Nancy 54011, France

Corresponding author: Mohamed Zaiou, PhD, Professor, Institut Jean Lamour, UMR CNRS 7198, CNRS, University of Lorraine, 2 allée André Guinier, BP 50840, Nancy 54011, France. mohamed.zaiou@univ-lorraine.fr

Abstract

Nonalcoholic fatty liver disease (NAFLD) has emerged as the most common cause of chronic liver disorder worldwide. It represents a spectrum that includes a continuum of different clinical entities ranging from simple steatosis to non-alcoholic steatohepatitis, which can evolve to cirrhosis and in some cases to hepatocellular carcinoma, ultimately leading to liver failure. The pathogenesis of NAFLD and the mechanisms underlying its progression to more pathological stages are not completely understood. Besides genetic factors, evidence indicates that epigenetic mechanisms occurring in response to environmental stimuli also contribute to the disease risk. Noncoding RNAs (ncRNAs), including microRNAs, long noncoding RNAs, and circular RNAs, are one of the epigenetic factors that play key regulatory roles in the development of NAFLD. As the field of ncRNAs is rapidly evolving, the present review aims to explore the current state of knowledge on the roles of these RNA species in the pathogenesis of NAFLD, highlight relevant mechanisms by which some ncRNAs can modulate regulatory networks implicated in NAFLD, and discuss key challenges and future directions facing current research in the hopes of developing ncRNAs as next-generation non-invasive diagnostics and therapies in NAFLD and subsequent progression to hepatocellular carcinoma.

Key Words: MicroRNAs; Nonalcoholic fatty liver disease; Steatohepatitis; Noncoding RNAs; Circular RNAs; Biomarker

Core Tip: Nonalcoholic fatty liver disease (NAFLD) covers a spectrum of hepatic pathologies, ranging from simple steatosis to nonalcoholic steatohepatitis, all of which can evolve to cirrhosis and in some cases to hepatocellular carcinoma. There are now indications that noncoding RNAs (ncRNAs), a component of epigenetic mechanisms, contribute to the pathogenesis of NAFLD and may serve as potential prognostic and diagnostic biomarkers. However, little is known about the role of these RNA species in NAFLD and its progressive forms. This paper discusses the current state of research on the role of most clinically relevant ncRNAs in the pathogenesis of NAFLD.

INTRODUCTION

Nonalcoholic fatty liver disease (NAFLD) has emerged as a liver disorder with an increasing prevalence but unclear etiology. The disease covers a wide spectrum of histologic lesions, ranging from simple steatosis to its subtype, nonalcoholic steatohepatitis (NASH), which is characterized by inflammation and hepatocyte injury. Over several years, NASH can progress to more serious disease stages, such as cirrhosis and hepatocellular carcinoma (HCC)[1]. Based on the close association between hepatic steatosis and metabolic dysregulation, international consensus guidelines recommended the renaming of NAFLD to metabolic-associated fatty liver disease[2,3]. The prevalence of NAFLD depends on race and ethnicity. In the United Sates, the estimated prevalence of NAFLD was reported to be about 32%[4]. However, estimates are likely higher in other populations that are currently witnessing the rapid rise in the incidence of type 2 diabetes mellitus (T2DM), obesity, metabolic and insulin resistance syndrome, and dyslipidemia rates[5,6].

NAFLD is sometimes called the "silent killer", because most patients with the condition are typically asymptomatic in the early stages until the liver is severely damaged. The unsuspected disease condition is often found incidentally when liver enzyme levels, such as alanine aminotransferase, are elevated in routine laboratory work-up or hepatic steatosis appears on imaging for reasons other than liver symptoms or signs. Currently, liver biopsy remains the gold standard method for NAFLD diagnosis and degree of liver injury evaluation[7]. Computed tomography scans and ultrasound can also be performed as part of the standard evaluation of NAFLD. However, these methods have a number of limitations, including invasiveness, low sensitivity, sampling variability, and inaccurate diagnosis[8,9]. The American Association for the Study of Liver Diseases has identified uncertainties about these diagnostic tools, which represent a barrier to the effective treatment of patients with NAFLD[10]. Thus, there is increased recognition of the need to develop non-invasive biomarkers that have the ability to identify simple steatosis from NASH patients who are at high risk of progression to cirrhosis and HCC conditions.

Many concepts important to understanding the pathogenesis of NAFLD have arisen. The traditional view of this complex disease suggests that an interplay between genetic and triggering and/or modifying environmental events is the fundamental basis for disease initiation and development[11,12]. Over the last several years, a growing body of functional evidence has pointed towards a central role of epigenetic factors in fatty liver diseases, including NAFLD. Epigenetics was redefined multiple times and Cavalli and Heard described it as "the study of molecules and mechanisms that can perpetuate alternative gene activity states in the context of the same DNA sequence"[13]. Epigenetic machinery could be another layer that orchestrates gene expression and provides a molecular link between genetic and environment effects on NAFLD. Thus, the integration of epigenetic information may represent another opportunity to tackle the complexity of NAFLD and identify new predictive biomarkers and potential therapeutic targets of this disease. Indeed, recent advancements in the emerging field of epigenetics have revealed that epigenetic mechanisms and associated systems may regulate many aspects of the pathogenesis of NAFLD[3,14]. Unlike genetic alterations, epigenetic alterations can be mostly heritable and reversible. Thus, further discoveries in the field could enable the development of epigenetic tools that can be used not only to complement current strategies for early disease diagnosis and optimal individualized patient risk stratification but also to improve therapy.

To date, the most studied epigenetic mechanisms include DNA methylation, histone modifications, and noncoding RNA (ncRNA)-based regulation. While certain epigenetic mechanisms underlying DNA and chromatin modifications in NAFLD were addressed elsewhere[15,16], only relevant studies shedding light on the roles played by ncRNAs' machinery will be reviewed next.

EMERGING ROLE OF NCRNAS IN THE PATHOGENESIS OF NAFLD

For decades, only the portion of the genome that is transcribed into mRNA (approximately 2%) was the central focus of basic science and medical research. The remaining 98% was simply believed non-functional and referred to as "junk DNA" or "dark matter"[17]. Due to advances in high-throughput sequencing technologies enabling more in-depth genomic and transcriptomic analyses, the Encyclopedia of DNA Elements project revealed that up to 80% of the human genome is transcribed, generating a multitude of functional transcripts commonly referred to as ncRNAs[18,19]. The biological significance of these nonprotein coding transcripts is now becoming evident, with many ncRNAs found to have epigenetic activity and substantial roles in regulating diverse cellular processes. Indeed, they can affect gene expression by interacting with the transcriptional apparatus, and regulating chromatin structure and RNA processing mechanisms[20]. There is also proof that interaction and crosstalk between different species of ncRNA groups can create complicated and intertwined networks that can affect gene expression[21]. Regulatory ncRNAs mainly consist of microRNAs (miRNAs) (< 30 nucleotides), long noncoding RNAs (lncRNAs) (≥ 200 nucleotides)[19], and circular RNAs (circRNAs). Due to their stability and easy detection in biological fluids, ncRNAs are continuously investigated as promising diagnostic and therapeutic tools in metabolic diseases. A growing body of literature indicates that ncRNAs are abundantly expressed in the liver and their altered expression patterns are associated with various types of liver diseases including NAFLD[22,23]. Moreover, ncRNAs reveal significant differences in expression according to the severity of NAFLD and histological features[24]. In the next sections, the role of miRNAs, lncRNAs, and circRNAs will be discussed, to better improve our understanding of their appealing potential as biomarkers for early NAFLD/NASH staging and therapeutic targets.

miRNAs in NAFLD

miRNAs are small, highly conserved short single-stranded ncRNAs (approximately 18-22 nucleotides in length) with epigenetic functions able to transcriptionally regulate gene expression of other RNAs notably mRNAs[25]. They are transcribed in the cell nucleus and transported to the cytoplasm, where they are processed into mature miRNAs[26]. With respect to their function, miRNAs primarily regulate gene expression by promoting mRNA degradation or repressing their translation. They serve as master regulators that control the expression of thousands of coding and noncoding genes. Prior research suggests that more than 60% of human coding genes are potential targets of miRNAs[27]. Mounting evidence reveals that dysregulation in miRNAs' expression is associated with molecular processes of various forms of metabolic and liver diseases, including NAFLD conditions[3,28-30]. Indeed, several differentially expressed miRNAs play key roles in the development of NAFLD in animal models and humans[30-33], essentially through the regulation of several pathogenic processes including altered lipid and glucose metabolism, insulin resistance, and inflammation pathways[34,35]. Because miRNAs are stably detected in biofluids and can circulate within microvesicles, exosomes, or apoptotic bodies, or bound to RNA-binding proteins, interest in studying these molecules has increased tremendously. Additionally, considerable research has demonstrated that these RNA species may offer new insights into disease biology, and their easy profiling in the serum has raised enthusiasm about their potential use in clinical practice as biomarkers for early diagnosis and clinical monitoring of NAFLD progression [36,37]. While a plethora of miRNAs are associated with fatty liver diseases, only those shown to be repeatedly involved in different stages of NAFLD will be discussed next.

miR-21

There is evidence that miR-21-mediated regulation may play an important role in the pathogenesis of several types of liver diseases[38]. Dysregulated miR-21 expression has been reported in animal models of steatohepatitis and human NASH. Specifically, the levels of circulating miR-21 and its expression in the liver are heavily elevated in both NAFLD patients and mouse models[39-41]. Likewise, circulating miR-21 Levels are significantly increased in patients suffering from NASH compared to NAFL and healthy controls[42]. Other studies have shown that inhibiting miR-21 can alleviate steatosis by activating peroxisome proliferator-activated receptor alpha (PPARα)[40,43]. In support of these findings, another report indicated that hepatocyte-specific knockout (KO) of miR-21 in mice improved high-fat diet (HFD)-induced steatosis through upregulation of multiple miR-21-targeted pathways governing lipid metabolism[44]. Similarly, miR-21 abrogation along with obeticholic acid treatment significantly reduced NASH in mice[45].

Moreover, miR-21 plays a key role in hepatic lipid metabolism by promoting hepatic lipid accumulation *via* its interaction with several proteins including sterol regulatory element binding protein (SREBP1)[46] and 3-hydroxy-3-methylglutaryl-co-enzyme A reductase (HMGCR)[47]. Additionally, miR-21 can target phosphatase and tensin homolog, which prevents hepatic steatosis[48], and PPARα expression, which induces inflammation and fibrosis progression and activates lipid oxidation in NAFLD[40]. Other investigations have revealed that miR-21 can inactivate the Wnt/β-catenin signaling pathway by targeting low-density lipoprotein (LDL) receptor-related protein 6, thereby aggravating lipid accumulation and inflammation[49]. Mechanistic studies have also demonstrated that miR-21

promotes hepatic insulin resistance and steatosis in diet-induced obese mice through the regulation of several key transcription factors, such as forkhead box protein O1, insulin-induced gene 2, signal transducer and activator of transcription 3, and hepatocyte nuclear factor 4-alpha (HNF4-α)[44]. Together, these studies clearly show that miR-21 plays an essential role in key transitions of NAFLD pathogenesis. Such findings hold the potential to develop miR-21 as a reliable serum biomarker to identify patients "at risk" for NASH.

miR-29a

The miR-29 family of miRNAs consists of miR-29a, miR-29b, and miR-29c members[50], and are mainly expressed in hepatocytes and hepatic stellate cells (HSCs)[51,52]. A body of evidence suggests that miR-29a is significantly associated with diagnostic relevance of NAFLD[31,53], NASH[54] and liver fibrosis [54,55], as well as aggressiveness and prognosis of HCC[31]. López-Riera *et al*[56] identified circulating miR-29a as one of the potential biomarkers that could predict drug-induced NAFLD in humans. Yang *et al*[57] found that serum miR-29a levels were significantly lower in NAFLD patients compared to controls. Furthermore, another study revealed that miR-29a disrupts DNA methyltransferase 3β (DNMT3β) to improve diet-induced NASH in mice. Mattis *et al*[58] used a mouse model to demonstrate that miR-29a protects hepatocytes from steatosis by repressing lipoprotein lipase in hepatocytes. Moreover, miR-29a inhibits glycogen synthase kinase 3 beta to repress sirtuin 1 (SIRT1)-mediated mitochondrial biogenesis and improve methionine–choline-deficient diet-induced NASH in mice[59]. Roderburg *et al*[52] reported that miR-29 family members are downregulated in mouse models of liver fibrosis and in human fibrotic livers. A recent study indicated that miR-29a plays a regulatory role in NAFLD by improving HFD-induced steatohepatitis and liver fibrosis through the suppression of cluster of differentiation 36 (CD36)[31]. Together, these findings highlight the potential of miR-29a-targeted therapy for the treatment of NAFLD and its advanced stages.

miR-33a/miR33b

In humans, the miR-33 family comprises two members, miR-33a and miR-33b (miR-33a/b), which are co-transcribed with the sterol regulatory element-binding protein 2 (SREBP2) and 1 respectively, and their main targets are SREBP and SREBP2 and ATP-binding cassette subfamily A member 1 (ABCA1). miR-33a/b is implicated in fatty liver disease and plays key roles in lipid metabolism and transport by targeting a number of genes involved in cholesterol homeostasis and insulin signaling pathways[60,61]. In mice, there is only one miR-33 isoform, which is an ortholog form of human miR-33a[60].

In addition, expression levels of miR-33 are increased in the liver tissues of patients with NAFLD[62]. Circulating miR-33a is associated with steatosis and inflammation in patients with NAFLD after liver transplantation and can serve as an independent predictor of these pathological conditions[63]. The expression of hepatic miR-33a/miR-144 is increased in NASH patients with morbid obesity[64]. A further study in mice also demonstrated that miR-33 can regulate hepatic lipogenesis signaling and may serve as a potential circulating biomarker of NAFLD[65].

From a therapeutic perspective, several studies have demonstrated that treatment with anti-miR-33 therapeutic agents can significantly reduce plaque burden in mouse models of atherosclerosis and offer promise for treating cardiovascular disease[66-68]. However, a previously published clinical trial indicated that increased expression of miR-33a in the liver is associated with steatohepatitis in morbidly obese humans and metabolic dysfunction[64]. In line with this, long-term therapeutic silencing of miR-33 in mice leads to the development of adverse outcomes, including hypertriglyceridemia and hepatic steatosis[69,70]. miR-33 KO mice exposed to HFD developed marked worsening of obesity and liver steatosis *via* targeting SREBP1[71]. Recently, Price *et al*[61] provided additional evidence that genetic loss of miR-33 results in an increase in food intake and promotes obesity and insulin resistance. Thus, further research is needed to fully understand the role of miR-33a/b in NAFLD, which may provide new insights into the physiopathology of various forms of this disease.

miR-34a

The miR-34 family comprises three members: miR-34a, miR-34b, and miR-34c. miR-34a expression levels are increased both in the liver and serum of patients with NAFLD and NASH compared to healthy controls and are positively correlated with total cholesterol (TC) and triglyceride (TG) levels[72, 73]. miR-34 regulates many transcription factors, such as HNF4-α, SIRT1, and p53, which are involved in lipid metabolism, cholesterol synthesis, and fatty acid b-oxidation[72,74]. In addition, Xu *et al*[73] demonstrated that miR-34a inhibits hepatic very LDL secretion by promoting steatosis through interaction with HNF4-α in patients with NASH and mice fed HFD. miR-34a regulates steatosis by directly targeting PPARα expression in NAFLD[75]. Recently, another study demonstrated that the miR-34a/SIRT1/AMPK pathway is involved in mitochondrial dysfunction in a mouse NASH model[76]. Higher circulating levels of miR-34a have been seen in patients with NAFLD and NASH and mice fed HFD[73,77]. An association of miR-34a and miR-122 with dyslipidemia among patients with NAFLD has also been reported[78], and both miRNAs could be useful biomarkers in children with obesity and NAFLD[79]. Finally, in a meta-analysis study, miR-34a, miR-122, and miR-192 were identified as potential diagnostic markers to segregate NAFL from NASH[32]. Here, miR-34 showed the best

diagnostic accuracy for discriminating NASH *vs* NAFLD.

miR-122

miR-122 is the most abundant and extensively studied hepatic miRNA representing about 70% of the total miRNA in the liver[80]. Current evidence indicates that miR-122 plays an essential role in different aspects of liver function as well as in the epigenetic modulation of several genes linked to chronic hepatic pathology[72,80,81]. miR-122 is involved in the regulation of lipid and cholesterol metabolism. Animal experiments have revealed that inhibition of miR-122 results in a decrease of hepatic fatty acid and cholesterol synthesis rate, reduction in plasma cholesterol levels, enhanced liver fatty acid oxidation, and protection of HFD-fed mice from hepatic steatosis[82,83]. Further investigations have reported that miR-122 targets specific genes of cholesterol biosynthesis, such as *HMGCR,* microsomal TG transfer protein, 3-hydroxy-3-methylglutaryl-coenzyme A (CoA) synthase 1, fatty acid synthase, and acetyl-CoA carboxylase[33,82,83], suggesting a role in the pathogenesis of NAFLD.

Excessive accumulation of TG in the cytoplasm of hepatocytes is a hallmark of NAFLD. Genetic deletion of miR-122 Locus in mice results in TG accumulation in the liver and hepatic steatosis that progresses to NASH, fibrosis, and HCC[81,84], whereas restoration of miR-122a expression reduces disease symptoms and tumorigenesis[84]. Consistent with the results from animal investigations, reduced expression of miR-122 is observed in hepatic tissues of NASH patients compared to that in simple steatosis and healthy controls[72,80]. Interestingly, changes in miRNA expression profiles were observed at various stages of NAFLD, including simple fatty liver, NASH, and liver fibrosis to HCC. In this respect, a study reported that in NAFLD patients, the hepatic miR-122 Levels were lower in patients with mild steatosis compared to those with severe steatosis, while hepatic and serum miR-122 Levels were significantly higher in patients with mild fibrosis than in those with severe fibrosis[74].

Conversely, elevated serum levels of miR-122 have been found in patients with NAFLD patients compared to controls, and these levels are positively correlated with disease severity[85,86]. These data are in line with reports demonstrating that circulating levels of miR-122 are positively associated with fatty liver disease, T2DM, obesity, and atherosclerosis[80,87,88]. Additionally, NASH patients exhibit increased levels of miR-122 in the serum[80] and decreased hepatic expression of this RNA[72]. Although studies have consistently demonstrated that miR-122 expression differs between hepatocytes and blood, mechanisms underlying such an inverse correlation are certainly complex and need further attention. Attempts have been made to explain the observed difference in expression between the two tissues. The elevated levels of circulating miR-122 could be attributed to its secretion *via* liver exosomes. In agreement with this, Gallo *et al*[89] reported that miR-122 is localized in abundance to secreted liver exosomes. However, it must be acknowledged that the dynamic of miRNAs expression, secretion, and transport is complex and the contribution of other tissues such as adipose tissue to the pool of miR-122 Levels must not be ruled out.

miR-155

miR-155 is a multifunctional miRNA known to regulate numerous fundamental processes such as immunity, inflammation, lipid metabolism, and cancer[90,91]. Several studies have reported that miR-155 is one of the biologically most relevant miRNAs in several liver diseases including NAFLD[92,93]. In this respect, a study by Wang *et al*[94] demonstrated that the level of miR-155 is decreased in liver tissue and peripheral blood of NAFLD patients compared with healthy controls. Other studies indicated that miR-155 activity was also decreased in patients with NAFLD, which could be attributed to the adipogenic transcription factors CCAAT/enhancer binding protein (C/EBP)-α, C/EBP-β, PPAR-γ and LXRα[94,95]. On the other hand, miR-155-deficient mice fed a HFD developed increased hepatic steatosis compared to controls[94], while conditionally liver-specific overexpression of miR-155 reduced serum and hepatic levels of TC, TG, and high-density lipoprotein, and alleviated NAFLD[93]. These results suggest that miR-155 has a protective role in NAFLD and its pathological conditions. However, conflicting study results have somewhat dimmed the promise of using this miRNA to prevent NAFLD. For instance, miR-155 KO mice fed a methionine-choline-deficient diet showed a decrease in steatosis along with a reduction in the expression of genes involved in fatty acid metabolism and fibrosis, but not liver injury or inflammation[95]. Upon ingestion of a diet high in fat, high in cholesterol, and high in sucrose, miR-155 KO mice displayed less liver injury, decreased steatosis, and attenuation in fibrosis compared to control mice[96]. The ambiguous miR-155 roles suggest that this transcript may exert pleiotropic functions depending on the etiology and disease context. Another scenario is that miR-155-containing exosomes or miR-155-containing microvesicles released from cells into the surrounding tissue could contribute to the observed differences in results. As an example, adipose tissue-derived miR-155 upregulated by HFD was shown to induce hepatic insulin resistance in murine models[97]. Thus, further studies are warranted to clarify the contradictory results and determine the role of miR-155 in intracellular lipid accumulation and NAFLD development and progression.

miR-192

miR-192 is highly expressed in quiescent HSCs. Overexpression of miR-192 significantly suppresses the activity of these cells by reducing the proliferation and migratory potential of primary mouse HSCs[98].

A previous study found that circulating miR-192 is differentially expressed in NAFLD patients and even identified a miRNA panel (hsa-miR-122-5p, hsa-miR-1290, hsa-miR-27b-3p, and hsa-miR-192-5p) with high diagnostic accuracy for this disease[99]. Another study indicated that serum levels of miR-192-5p were significantly elevated in NAFLD patients and positively associated with hepatic inflammatory activity score and disease progression[100]. Recently, Wang *et al*[101] observed that miR-34a, miR-122, and miR-192 represent suitable biomarkers to distinguish NAFLD and NASH severity. Another study found that in NASH patients levels of miR-192 were elevated in serum, while decreased in the liver[80]. Similar to miR-122, miR-192 was increased in NASH serum compared with steatosis and downregulated in NASH liver, both in human and animal models, suggesting that these miRNAs are released from hepatocytes during pathophysiological states associated with cell membrane impairment[42,100]. A recent meta-analysis identified several miRNAs as potential biomarkers of NAFLD and NASH, including miR-34a, miR-122, and miR-192[32]. Together, these findings suggest that circulating miRNA-192 Levels may represent a potential noninvasive diagnostic biomarker and therapeutic target for the different stages of NAFLD.

miR-375

miR-375 is highly expressed in pancreatic islets and considered to be an essential regulator of glucose homeostasis and insulin secretion[102]. miR-122, miR-192, and miR-375 are significantly upregulated in NAFLD patients compared to controls[80]. miR-375 is involved in the pathogenesis of NAFLD and its inhibition suppresses the production of inflammatory cytokines tumor necrosis factor-alpha as well as interluekin-6, increased the expression of adiponectin, and suppressed lipid accumulation in palmitate (PA)-induced HepG2 cells[103]. These preliminary data suggest that miR-375 as well as the above discussed miRNAs (Table 1) could be promising targets for the prevention and progression of NAFLD.

LncRNAs in NAFLD pathogenesis

LncRNAs are relatively long RNA transcripts (> 200 nucleotides) that lack coding potential[104]. They are regulatory molecules transcribed from intergenic, exonic, or the distal protein-coding regions by RNA polymerase II and capped at the 5'-end and polyadenylated at the 3'-end[104]. Regarding their functions, there are subsets of lncRNAs that act as guides by binding to proteins and directing their localization, providing dynamic scaffolds providing a central platform for the transient assembly of multiple proteins and RNAs[105] and decoys that bind targeted proteins or miRNAs to limit their availability and function by acting as a molecular sink[106]. However, other functions related to these RNA species may arise as research in the field rapidly progresses. Over the last decade, dysregulation of lncRNAs has been linked to the pathophysiology of various human diseases, such as cancer, diabetes, and cardiovascular diseases[107]. In the context of NAFLD, some reports have noted that lncRNA expression patterns are dysregulated, suggesting that these molecules may represent potential drivers of NAFLD biology and have utility as clinical biomarkers. However, the role of lncRNAs in the development and progression of NAFLD still remains relatively unexplored. Herein, we provide a scientific update on lncRNAs relevant to NAFLD and its stages.

H19 LncRNA

The lncRNA H19 (H19) is a transcription product of the *H19* gene and represents one of the first discovered lncRNAs. H19 predominantly acts to affect miRNAs stability in different physiological and pathological conditions[108]. In recent years, H19 has attracted great attention in the research of liver diseases due to its aberrant expression and extensive involvement in several hepatic metabolic processes [109]. In this respect, existing evidence has shown that overexpression of H19 results in hepatic metabolic reprogramming and exacerbates diet-induced fatty liver[110]. In agreement with this, Liu *et al* [111] reported that expression of H19 induces hepatic steatosis by activating both the lipogenic transcription factor MLX interacting protein-like and the mammalian target of rapamycin complex 1 signaling pathways. In animal models, knockdown of H19 inhibited steatosis and alleviated hepatic lipogenesis by directly regulating the miR-130a/PPARγ axis in NAFLD[112]. However, further studies would be useful for determining the precise contribution of H19 to the pathogenesis of NAFLD.

Blnc1

Brown fat lncRNA 1 (Blnc1) is implicated in the regulation of adipocyte differentiation and function [113] and may serve as a regulator of triacylglycerol biosynthesis. Recently, Zhao *et al*[114] reported that hepatic Blnc1 expression was strongly linked to activation of lipogenesis in mouse models of obesity and NAFLD, whereas its liver-specific inactivation abrogated HFD-induced hepatic steatosis and insulin resistance, and protected mice from diet-induced NASH pathogenesis. Conversely, overexpression of Blnc1 in epididymal white fat tissue improved whole body insulin sensitivity, partially attenuated systemic dyslipidemia and glucose metabolism, and markedly protected against diet-induced obesity hepatic steatosis, probably *via* enhancement of mitochondrial biogenesis and function in white fat[115]. Overall, these results suggest that Blnc1 has different regulatory mechanisms and distinct functions in the liver and white adipose tissue.

Table 1 Selected microRNAs shown to be highly involved in the pathogenesis of nonalcoholic fatty liver disease

miRNA	Circulation level	Tissue expression	Main functional and pathophysiological impacts	Ref.
miR-21	↑	↑	Promotes lipogenesis	[38-40,42, 44]
			Involved in NASH, fibrosis, and HCC	
			Targets several metabolic and inflammatory signaling pathways related to the pathogenesis of NAFLD	
miR-29a	↑	↓	Highly connected with the diagnostic relevance of NAFLD, NASH, and HCC	[31,53,52, 58]
			Modulates oxidative stress and inflammation in the context of NAFLD	
miR-33a/b	↑	↑	Involved in lipid metabolism, glucose homeostasis and hepatic lipogenesis	[61-63, 65]
			Associated with steatosis and inflammation in patients with NAFLD/NASH	
miR-34a	↑	↑	Regulates lipoprotein metabolism and promotes liver steatosis	[72,73,75]
			Involved in NAFLD/NASH	
			Correlates with the severity of hepatic inflammatory activity	
			Can serve as a biomarker to distinguish NAFLD from NASH patients	
miR-122	↑	↓	Modulates several genes linked to chronic hepatic pathology and lipid metabolism	[74,82-84]
			Promotes hepatic steatosis	
			Serum miR-122 correlates positively with markers of NAFLD severity as well as with NASH	
miR-155	↑	↑	Regulates key cellular events in NAFLD/NASH	[96,97]
			Promotes insulin resistance	
miR-192	↑	↓	Significantly elevated in NAFLD patients and positively associated with hepatic inflammatory activity score and disease progression	[32,80, 100]
			Increased in serum from NASH patients compared with steatosis	
			Could be a potential biomarker of NAFLD and NASH	
miR-375	↑	↑	Involved in the pathogenesis of NAFLD/NASH/fibrosis	[80,102]
			Key regulator of glucose homeostasis and insulin secretion	

HCC: Hepatocellular carcinoma; miRNAs: MicroRNAs; NAFLD: Nonalcoholic fatty liver disease; NASH: Nonalcoholic steatohepatitis.

lncHR1

The lncRNA HCV regulated 1 (lncHR1) was recently identified as a novel human-specific lncRNA that has an effect on lipid metabolism. A study by Li *et al*[116] reported that in an HFD mouse model, overexpression of lncHR1 inhibited fatty acid synthase and lowered oleic acid-induced hepatic cell TG and lipid droplets' accumulation by inhibiting *SREBP1c* gene expression. These findings are relevant to NAFLD since dyslipidemia in patients with NAFLD is atherogenic in nature and it is characterized by increased levels of serum TG. Furthermore, elevated TG levels in the circulation are associated with metabolic syndrome and cardiovascular disease[117].

Metastasis-associated lung adenocarcinoma transcript 1

Metastasis-associated lung adenocarcinoma transcript 1 (MALAT1) is one of the highly conserved lncRNAs shown to play a significant role in many diseases, including cancer, diabetes, and insulin resistance. A previous study showed that excess PA increases MALAT1 expression, activated SREBP1c and induced intracellular lipid accumulation in hepatocytes, whereas inhibition of MALAT1 expression decreased nuclear SREBP1c level and lipid accumulation both *in vitro* and *in vivo*[118]. Further analysis by these authors revealed that the reduction of MALAT1 in the liver improved insulin sensitivity in ob/ob mice. They concluded that MALAT1 may promote hepatic steatosis and insulin resistance by increasing nuclear SREBP1c protein stability in hepatocytes[118]. Furthermore, results from lncRNA profiling in the liver biopsies of NAFLD patients demonstrated the potential of MALAT1 as a regulator of liver inflammation and fibrosis and insulin resistance by targeting the C-X-C motif chemokine ligand 5[119]. Consistent with these observations, another study found that MALAT1 expression was significantly increased in NASH patients compared to NAFLD individuals with simple steatosis and controls[120]. Previous studies have reported that MALAT is overexpressed in both HCC cell lines and clinical tissue samples[121,122], providing additional evidence that this lncRNA could be used as a

biomarker of liver damage and HCC development.

Nuclear enriched abundant transcript 1

Nuclear enriched abundant transcript 1 (NEAT1) is a nuclear lncRNA involved in various liver diseases [123]. It is involved in adipogenesis processes, including lipolysis, lipid uptake, and LDL oxidation. A recent study indicated that the NEAT1 and mTOR signaling pathway proteins were increased in NAFLD *in vitro* and *in vivo* while downregulation of NEAT1 alleviated NAFLD *via* the mTOR/S6K1 signaling pathway in rat model[124]. Additionally, NEAT1 plays an important role in the activation of estrogen receptor alpha to regulate water-glycerol transporter (AQP7)-mediated hepatic steatosis[125]. Chen *et al*[126] found that NEAT1 promotes steatosis by sponging miR-146a-5p, subsequently increasing the expression of Rho-kinase1 (ROCK1) and significantly inducing the AMPK/SREBP pathway. Silencing of NEAT1 alleviated fibrosis and inflammatory responses by regulating the miR-506/GLI3 axis in an NAFLD cellular model[127]. A recent study indicated that NEAT1 and paternally expressed gene 3 were highly expressed in the liver and HSCs from NASH mice and silencing of NEAT1 effectively reduced the fibrotic characteristics of HSCs in the setting of NASH[128]. These results corroborate previous findings by Leti *et al*[119] indicating that NEAT1 is upregulated in the fibrosis of NASH patients compared to controls. Together, these studies highlight the potential value of NEAT1 for aiding in the prognosis and diagnosis of NASH.

Ultra-conserved element

Ultra-conserved element (UC372) is a lncRNA associated with impaired homeostasis of lipid metabolism and may play a role in the pathogenesis of NAFLD. UC372 is upregulated in a murine model of T2DM (db/db mice), HFD-fed mice, and NAFLD patients, indicating a role in liver steatosis and fatty liver[129]. Mechanistically, UC372 may drive hepatic steatosis through binding to pri-miR-195/pri-miR-4668, thus preventing miR-195/miR-4668 from regulating the expression of target genes associated with lipid synthesis and uptake, including acetyl-CoA carboxylase, fatty acid synthase, stearoyl-CoA desaturase 1, and lipid uptake-related genes such as CD36[129]. These preliminary results suggest that UC372 may be a promising target for therapies combating hepatic steatosis.

Maternally expressed gene 3

Maternally expressed gene 3 (MEG3), also known as gene trap locus 2, is another lncRNA that plays a regulatory role in the carcinogenesis and progression of several types of cancer. MEG3 is also suspected to be involved in the pathogenesis of NAFLD. In this respect, an early study reported that expression of hepatic MEG3 was consistently decreased in the chemokine (C-C motif) ligand 4 (CCl4)-induced mouse progressive liver fibrosis model compared to normal tissues, and HSCs may be one of the main sources of the MEG3 Levels present in CCl4-treated livers[130]. The same study revealed that MEG3 was also downregulated in human liver fibrotic tissues compared with control liver tissues. In line with this these studies, Huang *et al*[131] showed that the downregulation of MEG3 in *in vitro* and *in vivo* models of NAFLD is negatively correlated with lipogenesis-related genes, and that overexpression of MEG3 alleviates lipid overaccumulation in HepG2 cells. The downregulation of MEG3 in two models of NAFLD (free fatty acid-challenged primary hepatocytes and HFD-induced mouse) was also indicated in a more recent study by Zou *et al*[132].

In contradiction with these results, hepatic MEG3 Levels are significantly increased in liver fibrosis and NASH cirrhosis in human patients[133]. Similarly, MEG3 was shown to be one of the most differentially expressed lncRNAs in the vascular endothelium in diet-induced obese mice, and its expression was elevated in human nonalcoholic fatty livers and NASH livers, whereas its knockdown potentiated obesity-induced insulin resistance and impaired glucose homeostasis[134]. These conflicting results underline the complexity of MEG regulation, and further studies are required to clarify the biological significance of MEG3 and its potential role MEG3 either as a biomarker or a therapeutic target for NAFLD.

Highly upregulated in liver cancer

The lncRNA highly upregulated in liver cancer (HULC) was the first identified lncRNA specifically overexpressed in HCC. HULC, a functionally important lncRNA, promotes HCC growth, metastasis and drug resistance[135]. HULC expression was found to be increased in the liver tissue of NAFLD rats [136]. Inhibition of this lncRNA improves hepatic fibrosis and lipid deposition and decreases hepatocyte apoptosis in rats with NAFLD *via* inhibition of the mitogen-activated protein kinase signaling pathway in liver tissue[136]. Interestingly, the antidiabetic drug metformin was also reported to decrease HULC by inhibiting the expression of specificity protein 1 transcription factor in liver cancer cells[137]. Indeed, metformin was shown to improve insulin resistance and hyperinsulinemia and increase insulin sensitivity. This drug is now recommended and has proven to be effective for the treatment of NAFLD [138]. Collectively, these findings suggest that HULC could be a promising target for NAFLD diagnosis, staging, and therapy.

Homeobox transcript antisense intergenic RNA

Homeobox (HOX) transcript antisense intergenic RNA (HOTAIR) is a lncRNA that resides on a boundary of the HOXC locus on chromosome 12q13.13. HOTAIR is increased in different forms of cancers and involved in diverse cellular functions. In NAFLD, free fatty acid treatment promotes TG accumulation in HepG2 cells, significantly induces HOTAIR expression and inhibits phosphatase and tensin homolog expression[139]. A recent study reported that HOTAIR was activated in NAFLD, and HOTAIR knockdown significantly inhibited the development of NAFLD *via* mediation of miR-130b-3p/ROCK1/AMPK axis, further suggesting a target for NAFLD[140]. HOTAIR shows several oncogenic functions in HCC and its expression levels are increased in liver fibrosis, which causes acceleration of carcinogenesis in hepatitis B virus-infected patients[141]. Other investigations have reported that HOTAIR can serve as a competing endogenous RNA to sponge miR-29b and then repress DNMT3b, which contributes to hepatic fibrosis[141].

Fatty liver-related lncRNA 2

The lncRNA fatty liver-related lncRNA 2 (FLRL2) is located in the intronic region of the aryl hydrocarbon receptor nuclear translocator-like (*Arntl*) gene, and *Arntl* is predicted as a cis target of FLRL2. FLRL2 was identified as a potential key molecule in the pathogenesis of NAFLD. This nuclear-localized lncRNA is downregulated in the NAFLD mouse model, suggesting a role in the pathogenesis of this disease[142]. Further mechanistic studies have demonstrated that overexpression of FLRL2 alleviates NAFLD through activation of the Arntl-SIRTA pathway, inhibits lipogenesis, and reduces hepatic steatosis in HFD mice[143]. These results render FLRL2 another promising therapeutic candidate for the treatment of NAFLD and its complications. Finally, the above-discussed lncRNAs with their potential functions in NAFLD are also summarized in Table 2.

circRNAs in NAFLD

As their name implies, circRNAs are single-stranded covalently closed RNA species formed through back-splicing. Distinct characteristics of circRNAs, such as high stability, evolutionary conservation among species, exonuclease resistance, and existence in body fluids endow this class of RNAs with numerous potential functions ranging from miRNA and protein sponges to gene transcriptional regulators and protein/peptide translators. Moreover, circRNAs are dysregulated in numerous pathological conditions and may potentially serve as novel diagnostic biomarkers and therapeutic targets.

Although there is increasing evidence linking circRNAs to the pathogenesis of metabolic diseases, studies centered on the investigation of circRNAs in NAFLD were only recently conducted[144-146]. Data from recent literature suggest that circRNAs are involved in several fundamental processes governing the onset and progression of NAFLD and display aberrant expression[147]. For instance, a circRNA_0046367 was decreased in HFD-induced hepatic steatosis[148]. Subsequently, the authors of this study demonstrated that normalization of circRNA_0046367 Levels prevents lipid peroxidation and mitochondrial dysfunction in steatosis through miR-34a sponging and PPARα downregulation. In a further analysis, the same research laboratory identified an additional circRNA: circRNA_0046366, whose expression was also diminished during free fatty acid-induced hepatocellular steatosis in high fat-treated HepG2 cells[149]. In HepG2 cells with hepatic steatosis induced by high-fat stimulation, circRNA_021412 was associated with hepatic steatosis *via* the circRNA_021412/miR-1972/LPIN1axis [150]. circRNA microarrays analysis in an HFD mouse model revealed that circScd1 expression was significantly decreased in NAFLD tissues compared to that in controls. Consistent with this, knockdown of circScd1 promoted hepatosteatosis through the regulation of the Janus kinase 2 and signal transducer and activator of transcription 5 signaling pathway[151]. In an *in vitro* model of NAFLD, Hsa_circ_0048179 was shown to attenuate free fatty acid-induced steatosis *via* Hsa_circ_0048179/miR-188-3p/glutathione peroxidase 4 signaling[152]. circRNA profiling in a NASH mouse model identified circRNA_29981 as the circRNA most significantly differentially expressed in this setting[153].

More recently, Jin *et al*[147] indicated that the circRNA_002581-miR-122-CPEB1 axis aggravates NASH partially through autophagy suppression, while silencing of circRNA_002581 significantly attenuated lipid droplet accumulation, eliminated liver damage in both mouse and cellular models of NASH. Chen *et al*[154] indicated that silencing of circ_0071410 alleviates hepatic stellate activation, a key step of liver cirrhosis. HSCs are the primary cell type responsible for liver fibrosis. In the CCl4-induced mouse model of liver fibrosis, mmu_circ_34116 was able to inhibit HSCs activation[155]. In a mouse model of NAFLD, Chen *et al*[156] found that circ_0057558 can promote NAFLD by regulating ROCK1/AMPK signaling through targeting miR-206. Interestingly, a novel mitochondrial genome-encoded circRNA termed mitochondrial steatohepatitis-associated circRNA ATP5B regulator (SCAR) was identified recently[157]. The latter study found SCAR to be significantly downregulated in liver fibroblasts from patients with NASH. Additionally, the overexpression of SCAR inhibited mitochondrial reactive oxygen species output and fibroblast activation *via* shutting down mitochondrial permeability transition pore. More importantly, *in vivo* targeting of SCAR alleviated HFD-induced cirrhosis and insulin resistance implying that circRNA SCAR may serve as a therapeutic target for NASH[157].

Table 2 Relevant dysregulated long noncoding RNAs associated with alterations in liver metabolism and nonalcoholic fatty liver disease

lncRNA	Expression	Main functional and pathophysiological effects	Ref.
MALAT1	↑	Promotes cell proliferation, migration, and invasion in several different human cancers including HCC	[119-122]
		Promotes hepatic steatosis and insulin resistance	
		Hepatic MALAT1 levels are higher in NASH patients with fibrosis	
		Promotes NAFLD progression and increase with the severity of the disease	
NEAT1	↑	Promotes adipogenesis, lipogenesis, and lipid absorption	[124,126,127]
		Modulates fibrosis and inflammatory responses	
		Silencing NEAT1 alleviated fibrosis and inflammatory in a NAFLD cellular model	
MEG3	↓	Involved in lipid metabolism and glucose homeostasis	[131-134]
		Correlates with steatosis and inflammation (NASH) in patients with NAFLD	
HULC	↑	Promotes HCC growth and metastasis	[135,136]
		Promotes NAFLD development	
		Metformin decreases HULC expression	
HOTAIR	↑	Activates lipid accumulation in hepatocytes and promotes hepatic steatosis development	[139-141]
		Expression profile is significantly increased in oleic acid-induced steatosis and during the development of HFD-induced NAFLD	
		Accelerates liver fibrosis and carcinogenesis	
FLRL2	↓	Decreases endoplasmic reticulum stress and liver inflammation	[143]
		Alleviates NAFLD and steatosis in mouse model	

FLR2: Fatty liver-related lncRNA 2; H19: H19 imprinted maternally expressed transcript; HCC: Hepatocellular carcinoma; HFD: High-fat diet; HOTAIR: HOX transcript antisense RNA; MALAT1: Metastasis-associated lung adenocarcinoma transcript 1; lncRNAs: Long noncoding RNAs; MEG3: Maternally expressed 3; NAFLD: Nonalcoholic fatty liver disease; NASH: Nonalcoholic steatohepatitis; NEAT1: Nuclear paraspeckle assembly transcript 1; HULC: Hepatocellular carcinoma upregulated long noncoding RNA.

Together, these findings suggest that certain circRNAs, including those summarized in Table 3, are likely to contribute to NAFLD phenotype, which makes them attractive targets for the development of diagnostic and interventional pharmacology. However, circRNA data are still lacking functional evidence and their underlying mechanisms are still awaiting elucidation. Nevertheless, further carefully designed prospective studies to emphasize and validate the potential use of circRNAs as NAFLD biomarkers are expected to yield new insights into the pathogenesis of this disease state.

CONCLUSION

The findings from the above research clearly indicate that alterations in miRNA, circRNA and lncRNA expression play critical roles in cellular physiology and many diseases, including NAFLD and cancer. Thus, these ncRNA subsets are promising non-invasive biomarkers for the diagnosis and stratification of patients with NAFLD and could inform future personalized treatments designed for this condition. Even though the concept is promising and optimism is high, there is a consensus that research in the field still has limitations and technical challenges. (1) Sustained research efforts in the ncRNAs field have aimed to develop biomarkers to support the diagnostic process in patients with NAFLD. Unfortunately, most of the studies were carried out in subjects who already display patterns of worsening symptoms and are seeking medical care. To overcome this challenge, an alternative option would be to investigate the status of ncRNAs in the general population, which may assess the risk and capture early stages of disease initiation and evolution. This strategy could help achieve early diagnosis in individuals at risk for NAFLD but yet asymptomatic, and determine whether the overserved aberration in ncRNA

Table 3 Relevant dysregulated circular RNAs associated with alterations in liver metabolism and nonalcoholic fatty liver disease

circRNA	Expression level	Main functional and pathophysiological effects	Ref.
circRNA_0046367	↑	Inhibits hepatic steatosis by preventing hepatotoxicity of lipid peroxidation	[148]
circRNA_0046366	↑	Inhibits hepatic steatosis through miR-34a/PPARα	[149]
circRNA_021412	↑	Associated with hepatic steatosis	[150]
circScd1	↓	Affects steatosis on NAFLD *via* JAK2/STAT5 signaling pathways	[151]
hsa_circ_0048179	↓	Attenuates free fatty acid-induceded steatosis by sponging of miR-188-3p *in vitro*	[152]
mmu_circRNA_29981	↑	Regulatory role in NASH mousee model	[153]
Circ_0057558	↑	Involved in lipogenesis	[156]
		Promotes nonalcoholic fatty liver disease by sponging miR-206	
SCAR	↓	Correlates with steatosis-to-NASH progression	[157]
		In vivo, targeting circRNA SCAR alleviates HFD-induced cirrhosis and insulin resistance	

circRNAs: Circular RNAs; HCC: Hepatocellular carcinoma; HFD: High-fat diet; JAK2: Janus Kinase 2; NAFLD: Nonalcoholic fatty liver disease; NASH: Nonalcoholic steatohepatitis; PPARα: Peroxisome proliferator-activated receptor α; STAT5: Signal transducer and activator of transcription 5.

expression is the trigger or it is just a consequence of other causes such as those associated with lipid metabolism disorder, inflammation and immune system; (2) The role of ncRNAs as mediators of cell and organ crosstalk as well as their impact on different signaling pathways involved in NAFLD pathogenesis are not fully understood. It is now recognized that some ncRNAs are present in the extracellular environment and may be involved in pathophysiological condition. They may act to affect their targets either in an autocrine or paracrine fashion. Hence, special attention should be drawn to further research addressing the role of ncRNAs and their carriers (extracellular vesicles) in mediating potential inter-organ crosstalk in NAFLD condition, and the dynamic interaction of ncRNAs with metabolism cell signaling pathways. While these strategies may seem difficult to carry out and complete, they can be a starting point for increasing our knowledge on the role of circulating ncRNAs in organ crosstalk and may represent an opportunity to better understand how they affect metabolic homeostasis to drive the onset and progression of NAFLD and related pathological conditions; and (3) From a clinical perspective, approaches based on an individual ncRNA targeting or overexpression are what researchers are shooting for. However, each ncRNA has highly redundant roles and multiple functions. Indeed, a previous study revealed that a miRNA can affect a phenotype not only through a simple regulatory process, but *via* multiple targets redundantly and often incoherently, and such a complex regulation is difficult to assemble and control[158]. Indeed, it is becoming evident that it is difficult to diagnose a multifactorial disease such as NAFLD using a single ncRNA. Attempts were conducted to use a combination of serum circulating ncRNAs. Understanding the ncRNA-ncRNA crosstalk and their intricate interplay with different genetic and other epigenetic regulators including DNA methylation, chromatin remodeling, and components of the transcriptional and posttranscriptional machineries to regulate gene networks involved in NAFLD could certainly expand our knowledge on the molecular mechanisms driving this disease. This approach can also lead to a breakdown into NAFLD subtypes which would add resolution and inform about the regulation of molecular processes involved in each stage of the disease by specific ncRNAs.

To sum up, this review highlights the evidence for potential subsets of ncRNAs that are associated with NAFLD and its pathological conditions. The findings from various human and animal studies clearly suggest that dysregulation in ncRNA profiles are critical factors in the initiation and progression of fatty liver diseases, including NAFLD. This may be an appealing argument to further explore the mystery of these RNA molecules and consider their clinical application as biomarkers/therapeutics in the prevention and treatment of NAFLD and its progressive forms.

FOOTNOTES

REFERENCES

1 **Baffy G**, Brunt EM, Caldwell SH. Hepatocellular carcinoma in non-alcoholic fatty liver disease: an emerging menace. *J Hepatol* 2012; **56**: 1384-1391 [PMID: 22326465 DOI: 10.1016/j.jhep.2011.10.027]

2 **Eslam M**, Sanyal AJ, George J; International Consensus Panel. MAFLD: A Consensus-Driven Proposed Nomenclature for Metabolic Associated Fatty Liver Disease. *Gastroenterology* 2020; **158**: 1999-2014.e1 [PMID: 32044314 DOI: 10.1053/j.gastro.2019.11.312]

3 **Eslam M**, Valenti L, Romeo S. Genetics and epigenetics of NAFLD and NASH: Clinical impact. *J Hepatol* 2018; **68**: 268-279 [PMID: 29122391 DOI: 10.1016/j.jhep.2017.09.003]

4 **Zou B**, Yeo YH, Nguyen VH, Cheung R, Ingelsson E, Nguyen MH. Prevalence, characteristics and mortality outcomes of obese, nonobese and lean NAFLD in the United States, 1999-2016. *J Intern Med* 2020; **288**: 139-151 [PMID: 32319718 DOI: 10.1111/joim.13069]

5 **Leite NC**, Salles GF, Araujo AL, Villela-Nogueira CA, Cardoso CR. Prevalence and associated factors of non-alcoholic fatty liver disease in patients with type-2 diabetes mellitus. *Liver Int* 2009; **29**: 113-119 [PMID: 18384521 DOI: 10.1111/j.1478-3231.2008.01718.x]

6 **Subichin M**, Clanton J, Makuszewski M, Bohon A, Zografakis JG, Dan A. Liver disease in the morbidly obese: a review of 1000 consecutive patients undergoing weight loss surgery. *Surg Obes Relat Dis* 2015; **11**: 137-141 [PMID: 25701959 DOI: 10.1016/j.soard.2014.06.015]

7 **Hardy T**, Oakley F, Anstee QM, Day CP. Nonalcoholic Fatty Liver Disease: Pathogenesis and Disease Spectrum. *Annu Rev Pathol* 2016; **11**: 451-496 [PMID: 26980160 DOI: 10.1146/annurev-pathol-012615-044224]

8 **Rinella ME**. Nonalcoholic fatty liver disease: a systematic review. *JAMA* 2015; **313**: 2263-2273 [PMID: 26057287 DOI: 10.1001/jama.2015.5370]

9 **Mazhar K**. The Future of Nonalcoholic Fatty Liver Disease Treatment. *Med Clin North Am* 2019; **103**: 57-69 [PMID: 30466676 DOI: 10.1016/j.mcna.2018.08.005]

10 **Younossi Z**, Tacke F, Arrese M, Chander Sharma B, Mostafa I, Bugianesi E, Wai-Sun Wong V, Yilmaz Y, George J, Fan J, Vos MB. Global Perspectives on Nonalcoholic Fatty Liver Disease and Nonalcoholic Steatohepatitis. *Hepatology* 2019; **69**: 2672-2682 [PMID: 30179269 DOI: 10.1002/hep.30251]

11 **Angulo P**. Nonalcoholic fatty liver disease. *N Engl J Med* 2002; **346**: 1221-1231 [PMID: 11961152 DOI: 10.1056/NEJMra011775]

12 **Anstee QM**, Daly AK, Day CP. Genetics of alcoholic and nonalcoholic fatty liver disease. *Semin Liver Dis* 2011; **31**: 128-146 [PMID: 21538280 DOI: 10.1055/s-0031-1276643]

13 **Cavalli G**, Heard E. Advances in epigenetics link genetics to the environment and disease. *Nature* 2019; **571**: 489-499 [PMID: 31341302 DOI: 10.1038/s41586-019-1411-0]

14 **Choudhary NS**, Duseja A. Genetic and epigenetic disease modifiers: non-alcoholic fatty liver disease (NAFLD) and alcoholic liver disease (ALD). *Transl Gastroenterol Hepatol* 2021; **6**: 2 [PMID: 33409397 DOI: 10.21037/tgh.2019.09.06]

15 **Pirola CJ**, Sookoian S. Epigenetics factors in nonalcoholic fatty liver disease. *Expert Rev Gastroenterol Hepatol* 2022; **16**: 521-536 [PMID: 32476509 DOI: 10.1080/17474124.2020.1765772]

16 **Zaiou M**, Amrani R, Rihn B, Hajri T. Dietary Patterns Influence Target Gene Expression through Emerging Epigenetic Mechanisms in Nonalcoholic Fatty Liver Disease. *Biomedicines* 2021; **9** [PMID: 34572442 DOI: 10.3390/biomedicines9091256]

17 **Mattick JS**, Makunin IV. Non-coding RNA. *Hum Mol Genet* 2006; **15** Spec No 1: R17-R29 [PMID: 16651366 DOI: 10.1093/hmg/ddl046]

18 **ENCODE Project Consortium**. An integrated encyclopedia of DNA elements in the human genome. *Nature* 2012; **489**: 57-74 [PMID: 22955616 DOI: 10.1038/nature11247]

19 **Djebali S**, Davis CA, Merkel A, Dobin A, Lassmann T, Mortazavi A, Tanzer A, Lagarde J, Lin W, Schlesinger F, Xue C, Marinov GK, Khatun J, Williams BA, Zaleski C, Rozowsky J, Röder M, Kokocinski F, Abdelhamid RF, Alioto T, Antoshechkin I, Baer MT, Bar NS, Batut P, Bell K, Bell I, Chakrabortty S, Chen X, Chrast J, Curado J, Derrien T, Drenkow J, Dumais E, Dumais J, Duttagupta R, Falconnet E, Fastuca M, Fejes-Toth K, Ferreira P, Foissac S, Fullwood MJ, Gao H, Gonzalez D, Gordon A, Gunawardena H, Howald C, Jha S, Johnson R, Kapranov P, King B, Kingswood C, Luo OJ, Park E, Persaud K, Preall JB, Ribeca P, Risk B, Robyr D, Sammeth M, Schaffer L, See LH, Shahab A, Skancke J, Suzuki AM, Takahashi H, Tilgner H, Trout D, Walters N, Wang H, Wrobel J, Yu Y, Ruan X, Hayashizaki Y, Harrow J, Gerstein M, Hubbard T, Reymond A, Antonarakis SE, Hannon G, Giddings MC, Ruan Y, Wold B, Carninci P, Guigó R,

Gingeras TR. Landscape of transcription in human cells. *Nature* 2012; **489**: 101-108 [PMID: 22955620 DOI: 10.1038/nature11233]

20   **Adams BD**, Parsons C, Walker L, Zhang WC, Slack FJ. Targeting noncoding RNAs in disease. *J Clin Invest* 2017; **127**: 761-771 [PMID: 28248199 DOI: 10.1172/JCI84424]

21   **Yamamura S**, Imai-Sumida M, Tanaka Y, Dahiya R. Interaction and cross-talk between non-coding RNAs. *Cell Mol Life Sci* 2018; **75**: 467-484 [PMID: 28840253 DOI: 10.1007/s00018-017-2626-6]

22   **Ganguly N**, Chakrabarti S. Role of long noncoding RNAs and related epigenetic mechanisms in liver fibrosis (Review). *Int J Mol Med* 2021; **47** [PMID: 33495817 DOI: 10.3892/ijmm.2021.4856]

23   **Khalifa O**, Errafii K, Al-Akl NS, Arredouani A. Noncoding RNAs in Nonalcoholic Fatty Liver Disease: Potential Diagnosis and Prognosis Biomarkers. *Dis Markers* 2020; **2020**: 8822859 [PMID: 33133304 DOI: 10.1155/2020/8822859]

24   **Gim JA**, Bang SM, Lee YS, Lee Y, Yim SY, Jung YK, Kim H, Kim BH, Kim JH, Seo YS, Yim HJ, Yeon JE, Um SH, Byun KS. Evaluation of the severity of nonalcoholic fatty liver disease through analysis of serum exosomal miRNA expression. *PLoS One* 2021; **16**: e0255822 [PMID: 34358264 DOI: 10.1371/journal.pone.0255822]

25   **Szabo G**, Csak T. Role of MicroRNAs in NAFLD/NASH. *Dig Dis Sci* 2016; **61**: 1314-1324 [PMID: 26769057 DOI: 10.1007/s10620-015-4002-4]

26   **O'Brien J**, Hayder H, Zayed Y, Peng C. Overview of MicroRNA Biogenesis, Mechanisms of Actions, and Circulation. *Front Endocrinol (Lausanne)* 2018; **9**: 402 [PMID: 30123182 DOI: 10.3389/fendo.2018.00402]

27   **Friedman RC**, Farh KK, Burge CB, Bartel DP. Most mammalian mRNAs are conserved targets of microRNAs. *Genome Res* 2009; **19**: 92-105 [PMID: 18955434 DOI: 10.1101/gr.082701.108]

28   **Mahmoudi A**, Butler AE, Jamialahmadi T, Sahebkar A. The role of exosomal miRNA in nonalcoholic fatty liver disease. *J Cell Physiol* 2022; **237**: 2078-2094 [PMID: 35137416 DOI: 10.1002/jcp.30699]

29   **Ji C**, Guo X. The clinical potential of circulating microRNAs in obesity. *Nat Rev Endocrinol* 2019; **15**: 731-743 [PMID: 31611648 DOI: 10.1038/s41574-019-0260-0]

30   **Hajri T**, Zaiou M, Fungwe TV, Ouguerram K, Besong S. Epigenetic Regulation of Peroxisome Proliferator-Activated Receptor Gamma Mediates High-Fat Diet-Induced Non-Alcoholic Fatty Liver Disease. *Cells* 2021; **10** [PMID: 34072832 DOI: 10.3390/cells10061355]

31   **Lin HY**, Yang YL, Wang PW, Wang FS, Huang YH. The Emerging Role of MicroRNAs in NAFLD: Highlight of MicroRNA-29a in Modulating Oxidative Stress, Inflammation, and Beyond. *Cells* 2020; **9** [PMID: 32331364 DOI: 10.3390/cells9041041]

32   **Liu CH**, Ampuero J, Gil-Gómez A, Montero-Vallejo R, Rojas Á, Muñoz-Hernández R, Gallego-Durán R, Romero-Gómez M. miRNAs in patients with non-alcoholic fatty liver disease: A systematic review and meta-analysis. *J Hepatol* 2018; **69**: 1335-1348 [PMID: 30142428 DOI: 10.1016/j.jhep.2018.08.008]

33   **Gjorgjieva M**, Sobolewski C, Dolicka D, Correia de Sousa M, Foti M. miRNAs and NAFLD: from pathophysiology to therapy. *Gut* 2019; **68**: 2065-2079 [PMID: 31300518 DOI: 10.1136/gutjnl-2018-318146]

34   **Arner P**, Kulyté A. MicroRNA regulatory networks in human adipose tissue and obesity. *Nat Rev Endocrinol* 2015; **11**: 276-288 [PMID: 25732520 DOI: 10.1038/nrendo.2015.25]

35   **Sobolewski C**, Calo N, Portius D, Foti M. MicroRNAs in fatty liver disease. *Semin Liver Dis* 2015; **35**: 12-25 [PMID: 25632931 DOI: 10.1055/s-0034-1397345]

36   **Dongiovanni P**, Meroni M, Longo M, Fargion S, Fracanzani AL. miRNA Signature in NAFLD: A Turning Point for a Non-Invasive Diagnosis. *Int J Mol Sci* 2018; **19** [PMID: 30544653 DOI: 10.3390/ijms19123966]

37   **Arrese M**, Eguchi A, Feldstein AE. Circulating microRNAs: emerging biomarkers of liver disease. *Semin Liver Dis* 2015; **35**: 43-54 [PMID: 25632934 DOI: 10.1055/s-0034-1397348]

38   **Zhang T**, Yang Z, Kusumanchi P, Han S, Liangpunsakul S. Critical Role of microRNA-21 in the Pathogenesis of Liver Diseases. *Front Med (Lausanne)* 2020; **7**: 7 [PMID: 32083086 DOI: 10.3389/fmed.2020.00007]

39   **Dattaroy D**, Pourhoseini S, Das S, Alhasson F, Seth RK, Nagarkatti M, Michelotti GA, Diehl AM, Chatterjee S. Micro-RNA 21 inhibition of SMAD7 enhances fibrogenesis *via* leptin-mediated NADPH oxidase in experimental and human nonalcoholic steatohepatitis. *Am J Physiol Gastrointest Liver Physiol* 2015; **308**: G298-G312 [PMID: 25501551 DOI: 10.1152/ajpgi.00346.2014]

40   **Loyer X**, Paradis V, Hénique C, Vion AC, Colnot N, Guerin CL, Devue C, On S, Scetbun J, Romain M, Paul JL, Rothenberg ME, Marcellin P, Durand F, Bedossa P, Prip-Buus C, Baugé E, Staels B, Boulanger CM, Tedgui A, Rautou PE. Liver microRNA-21 is overexpressed in non-alcoholic steatohepatitis and contributes to the disease in experimental models by inhibiting PPARα expression. *Gut* 2016; **65**: 1882-1894 [PMID: 26338827 DOI: 10.1136/gutjnl-2014-308883]

41   **Pillai SS**, Lakhani HV, Zehra M, Wang J, Dilip A, Puri N, O'Hanlon K, Sodhi K. Predicting Nonalcoholic Fatty Liver Disease through a Panel of Plasma Biomarkers and MicroRNAs in Female West Virginia Population. *Int J Mol Sci* 2020; **21** [PMID: 32933141 DOI: 10.3390/ijms21186698]

42   **Becker PP**, Rau M, Schmitt J, Malsch C, Hammer C, Bantel H, Müllhaupt B, Geier A. Performance of Serum microRNAs -122, -192 and -21 as Biomarkers in Patients with Non-Alcoholic Steatohepatitis. *PLoS One* 2015; **10**: e0142661 [PMID: 26565986 DOI: 10.1371/journal.pone.0142661]

43   **Pawlak M**, Lefebvre P, Staels B. Molecular mechanism of PPARα action and its impact on lipid metabolism, inflammation and fibrosis in non-alcoholic fatty liver disease. *J Hepatol* 2015; **62**: 720-733 [PMID: 25450203 DOI: 10.1016/j.jhep.2014.10.039]

44   **Calo N**, Ramadori P, Sobolewski C, Romero Y, Maeder C, Fournier M, Rantakari P, Zhang FP, Poutanen M, Dufour JF, Humar B, Nef S, Foti M. Stress-activated *miR-21/miR-21** in hepatocytes promotes lipid and glucose metabolic disorders associated with high-fat diet consumption. *Gut* 2016; **65**: 1871-1881 [PMID: 27222533 DOI: 10.1136/gutjnl-2015-310822]

45   **Rodrigues PM**, Afonso MB, Simão AL, Carvalho CC, Trindade A, Duarte A, Borralho PM, Machado MV, Cortez-Pinto H, Rodrigues CM, Castro RE. miR-21 ablation and obeticholic acid ameliorate nonalcoholic steatohepatitis in mice. *Cell Death Dis* 2017; **8**: e2748 [PMID: 28406477 DOI: 10.1038/cddis.2017.172]

46   **Wu H**, Ng R, Chen X, Steer CJ, Song G. MicroRNA-21 is a potential link between non-alcoholic fatty liver disease and

hepatocellular carcinoma *via* modulation of the HBP1-p53-Srebp1c pathway. *Gut* 2016; **65**: 1850-1860 [PMID: 26282675 DOI: 10.1136/gutjnl-2014-308430]

47   **Sun C**, Huang F, Liu X, Xiao X, Yang M, Hu G, Liu H, Liao L. miR-21 regulates triglyceride and cholesterol metabolism in non-alcoholic fatty liver disease by targeting HMGCR. *Int J Mol Med* 2015; **35**: 847-853 [PMID: 25605429 DOI: 10.3892/ijmm.2015.2076]

48   **Meng F**, Henson R, Wehbe-Janek H, Ghoshal K, Jacob ST, Patel T. MicroRNA-21 regulates expression of the PTEN tumor suppressor gene in human hepatocellular cancer. *Gastroenterology* 2007; **133**: 647-658 [PMID: 17681183 DOI: 10.1053/j.gastro.2007.05.022]

49   **Wang XM**, Wang XY, Huang YM, Chen X, Lü MH, Shi L, Li CP. Role and mechanisms of action of microRNA21 as regards the regulation of the WNT/βcatenin signaling pathway in the pathogenesis of nonalcoholic fatty liver disease. *Int J Mol Med* 2019; **44**: 2201-2212 [PMID: 31638173 DOI: 10.3892/ijmm.2019.4375]

50   **Zhao W**, Cheng L, Quek C, Bellingham SA, Hill AF. Novel miR-29b target regulation patterns are revealed in two different cell lines. *Sci Rep* 2019; **9**: 17449 [PMID: 31767948 DOI: 10.1038/s41598-019-53868-x]

51   **Kriegel AJ**, Liu Y, Fang Y, Ding X, Liang M. The miR-29 family: genomics, cell biology, and relevance to renal and cardiovascular injury. *Physiol Genomics* 2012; **44**: 237-244 [PMID: 22214600 DOI: 10.1152/physiolgenomics.00141.2011]

52   **Roderburg C**, Urban GW, Bettermann K, Vucur M, Zimmermann H, Schmidt S, Janssen J, Koppe C, Knolle P, Castoldi M, Tacke F, Trautwein C, Luedde T. Micro-RNA profiling reveals a role for miR-29 in human and murine liver fibrosis. *Hepatology* 2011; **53**: 209-218 [PMID: 20890893 DOI: 10.1002/hep.23922]

53   **Jampoka K**, Muangpaisarn P, Khongnomnan K, Treeprasertsuk S, Tangkijvanich P, Payungporn S. Serum miR-29a and miR-122 as Potential Biomarkers for Non-Alcoholic Fatty Liver Disease (NAFLD). *Microrna* 2018; **7**: 215-222 [PMID: 29848284 DOI: 10.2174/2211536607666180531093302]

54   **Huang C**, Zheng JM, Cheng Q, Yu KK, Ling QX, Chen MQ, Li N. Serum microRNA-29 levels correlate with disease progression in patients with chronic hepatitis B virus infection. *J Dig Dis* 2014; **15**: 614-621 [PMID: 25138057 DOI: 10.1111/1751-2980.12185]

55   **Lambrecht J**, Verhulst S, Reynaert H, van Grunsven LA. The miRFIB-Score: A Serological miRNA-Based Scoring Algorithm for the Diagnosis of Significant Liver Fibrosis. *Cells* 2019; **8** [PMID: 31470644 DOI: 10.3390/cells8091003]

56   **López-Riera M**, Conde I, Tolosa L, Zaragoza Á, Castell JV, Gómez-Lechón MJ, Jover R. New microRNA Biomarkers for Drug-Induced Steatosis and Their Potential to Predict the Contribution of Drugs to Non-alcoholic Fatty Liver Disease. *Front Pharmacol* 2017; **8**: 3 [PMID: 28179883 DOI: 10.3389/fphar.2017.00003]

57   **Yang YL**, Kuo HC, Wang FS, Huang YH. MicroRNA-29a Disrupts DNMT3b to Ameliorate Diet-Induced Non-Alcoholic Steatohepatitis in Mice. *Int J Mol Sci* 2019; **20** [PMID: 30917489 DOI: 10.3390/ijms20061499]

58   **Mattis AN**, Song G, Hitchner K, Kim RY, Lee AY, Sharma AD, Malato Y, McManus MT, Esau CC, Koller E, Koliwad S, Lim LP, Maher JJ, Raffai RL, Willenbring H. A screen in mice uncovers repression of lipoprotein lipase by microRNA-29a as a mechanism for lipid distribution away from the liver. *Hepatology* 2015; **61**: 141-152 [PMID: 25131933 DOI: 10.1002/hep.27379]

59   **Yang YL**, Wang PW, Wang FS, Lin HY, Huang YH. miR-29a Modulates GSK3β/SIRT1-Linked Mitochondrial Proteostatic Stress to Ameliorate Mouse Non-Alcoholic Steatohepatitis. *Int J Mol Sci* 2020; **21** [PMID: 32961796 DOI: 10.3390/ijms21186884]

60   **Najafi-Shoushtari SH**, Kristo F, Li Y, Shioda T, Cohen DE, Gerszten RE, Näär AM. MicroRNA-33 and the SREBP host genes cooperate to control cholesterol homeostasis. *Science* 2010; **328**: 1566-1569 [PMID: 20466882 DOI: 10.1126/science.1189123]

61   **Price NL**, Singh AK, Rotllan N, Goedeke L, Wing A, Canfrán-Duque A, Diaz-Ruiz A, Araldi E, Baldán Á, Camporez JP, Suárez Y, Rodeheffer MS, Shulman GI, de Cabo R, Fernández-Hernando C. Genetic Ablation of miR-33 Increases Food Intake, Enhances Adipose Tissue Expansion, and Promotes Obesity and Insulin Resistance. *Cell Rep* 2018; **22**: 2133-2145 [PMID: 29466739 DOI: 10.1016/j.celrep.2018.01.074]

62   **Lendvai G**, Jármay K, Karácsony G, Halász T, Kovalszky I, Baghy K, Wittmann T, Schaff Z, Kiss A. Elevated miR-33a and miR-224 in steatotic chronic hepatitis C liver biopsies. *World J Gastroenterol* 2014; **20**: 15343-15350 [PMID: 25386083 DOI: 10.3748/wjg.v20.i41.15343]

63   **Erhartova D**, Cahova M, Dankova H, Heczkova M, Mikova I, Sticova E, Spicak J, Seda O, Trunecka P. Serum miR-33a is associated with steatosis and inflammation in patients with non-alcoholic fatty liver disease after liver transplantation. *PLoS One* 2019; **14**: e0224820 [PMID: 31703079 DOI: 10.1371/journal.pone.0224820]

64   **Vega-Badillo J**, Gutiérrez-Vidal R, Hernández-Pérez HA, Villamil-Ramírez H, León-Mimila P, Sánchez-Muñoz F, Morán-Ramos S, Larrieta-Carrasco E, Fernández-Silva I, Méndez-Sánchez N, Tovar AR, Campos-Pérez F, Villarreal-Molina T, Hernández-Pando R, Aguilar-Salinas CA, Canizales-Quinteros S. Hepatic miR-33a/miR-144 and their target gene ABCA1 are associated with steatohepatitis in morbidly obese subjects. *Liver Int* 2016; **36**: 1383-1391 [PMID: 26945479 DOI: 10.1111/liv.13109]

65   **Pan JH**, Cha H, Tang J, Lee S, Lee SH, Le B, Redding MC, Kim S, Batish M, Kong BC, Lee JH, Kim JK. The role of microRNA-33 as a key regulator in hepatic lipogenesis signaling and a potential serological biomarker for NAFLD with excessive dietary fructose consumption in C57BL/6N mice. *Food Funct* 2021; **12**: 656-667 [PMID: 33404569 DOI: 10.1039/d0fo02286a]

66   **Rayner KJ**, Esau CC, Hussain FN, McDaniel AL, Marshall SM, van Gils JM, Ray TD, Sheedy FJ, Goedeke L, Liu X, Khatsenko OG, Kaimal V, Lees CJ, Fernandez-Hernando C, Fisher EA, Temel RE, Moore KJ. Inhibition of miR-33a/b in non-human primates raises plasma HDL and lowers VLDL triglycerides. *Nature* 2011; **478**: 404-407 [PMID: 22012398 DOI: 10.1038/nature10486]

67   **Rotllan N**, Ramírez CM, Aryal B, Esau CC, Fernández-Hernando C. Therapeutic silencing of microRNA-33 inhibits the progression of atherosclerosis in Ldlr-/- mice--brief report. *Arterioscler Thromb Vasc Biol* 2013; **33**: 1973-1977 [PMID: 23702658 DOI: 10.1161/ATVBAHA.113.301732]

68   **Karunakaran D**, Richards L, Geoffrion M, Barrette D, Gotfrit RJ, Harper ME, Rayner KJ. Therapeutic Inhibition of miR-

33 Promotes Fatty Acid Oxidation but Does Not Ameliorate Metabolic Dysfunction in Diet-Induced Obesity. *Arterioscler Thromb Vasc Biol* 2015; **35**: 2536-2543 [PMID: 26427794 DOI: 10.1161/ATVBAHA.115.306404]

69 **Goedeke L**, Salerno A, Ramírez CM, Guo L, Allen RM, Yin X, Langley SR, Esau C, Wanschel A, Fisher EA, Suárez Y, Baldán A, Mayr M, Fernández-Hernando C. Long-term therapeutic silencing of miR-33 increases circulating triglyceride levels and hepatic lipid accumulation in mice. *EMBO Mol Med* 2014; **6**: 1133-1141 [PMID: 25038053 DOI: 10.15252/emmm.201404046]

70 **Allen RM**, Marquart TJ, Jesse JJ, Baldán A. Control of very low-density lipoprotein secretion by N-ethylmaleimide-sensitive factor and miR-33. *Circ Res* 2014; **115**: 10-22 [PMID: 24753547 DOI: 10.1161/CIRCRESAHA.115.303100]

71 **Horie T**, Nishino T, Baba O, Kuwabara Y, Nakao T, Nishiga M, Usami S, Izuhara M, Sowa N, Yahagi N, Shimano H, Matsumura S, Inoue K, Marusawa H, Nakamura T, Hasegawa K, Kume N, Yokode M, Kita T, Kimura T, Ono K. MicroRNA-33 regulates sterol regulatory element-binding protein 1 expression in mice. *Nat Commun* 2013; **4**: 2883 [PMID: 24300912 DOI: 10.1038/ncomms3883]

72 **Cheung O**, Puri P, Eicken C, Contos MJ, Mirshahi F, Maher JW, Kellum JM, Min H, Luketic VA, Sanyal AJ. Nonalcoholic steatohepatitis is associated with altered hepatic MicroRNA expression. *Hepatology* 2008; **48**: 1810-1820 [PMID: 19030170 DOI: 10.1002/hep.22569]

73 **Xu Y**, Zalzala M, Xu J, Li Y, Yin L, Zhang Y. A metabolic stress-inducible miR-34a-HNF4α pathway regulates lipid and lipoprotein metabolism. *Nat Commun* 2015; **6**: 7466 [PMID: 26100857 DOI: 10.1038/ncomms8466]

74 **Miyaaki H**, Ichikawa T, Kamo Y, Taura N, Honda T, Shibata H, Milazzo M, Fornari F, Gramantieri L, Bolondi L, Nakao K. Significance of serum and hepatic microRNA-122 levels in patients with non-alcoholic fatty liver disease. *Liver Int* 2014; **34**: e302-e307 [PMID: 24313922 DOI: 10.1111/liv.12429]

75 **Ding J**, Li M, Wan X, Jin X, Chen S, Yu C, Li Y. Effect of miR-34a in regulating steatosis by targeting PPARα expression in nonalcoholic fatty liver disease. *Sci Rep* 2015; **5**: 13729 [PMID: 26330104 DOI: 10.1038/srep13729]

76 **Simão AL**, Afonso MB, Rodrigues PM, Gama-Carvalho M, Machado MV, Cortez-Pinto H, Rodrigues CMP, Castro RE. Skeletal muscle miR-34a/SIRT1:AMPK axis is activated in experimental and human non-alcoholic steatohepatitis. *J Mol Med (Berl)* 2019; **97**: 1113-1126 [PMID: 31139863 DOI: 10.1007/s00109-019-01796-8]

77 **Ezaz G**, Trivedi HD, Connelly MA, Filozof C, Howard K, L Parrish M, Kim M, Herman MA, Nasser I, Afdhal NH, Jiang ZG, Lai M. Differential Associations of Circulating MicroRNAs With Pathogenic Factors in NAFLD. *Hepatol Commun* 2020; **4**: 670-680 [PMID: 32363318 DOI: 10.1002/hep4.1501]

78 **Salvoza NC**, Klinzing DC, Gopez-Cervantes J, Baclig MO. Association of Circulating Serum miR-34a and miR-122 with Dyslipidemia among Patients with Non-Alcoholic Fatty Liver Disease. *PLoS One* 2016; **11**: e0153497 [PMID: 27077736 DOI: 10.1371/journal.pone.0153497]

79 **Oses M**, Margareto Sanchez J, Portillo MP, Aguilera CM, Labayen I. Circulating miRNAs as Biomarkers of Obesity and Obesity-Associated Comorbidities in Children and Adolescents: A Systematic Review. *Nutrients* 2019; **11** [PMID: 31783635 DOI: 10.3390/nu11122890]

80 **Pirola CJ**, Fernández Gianotti T, Castaño GO, Mallardi P, San Martino J, Mora Gonzalez Lopez Ledesma M, Flichman D, Mirshahi F, Sanyal AJ, Sookoian S. Circulating microRNA signature in non-alcoholic fatty liver disease: from serum non-coding RNAs to liver histology and disease pathogenesis. *Gut* 2015; **64**: 800-812 [PMID: 24973316 DOI: 10.1136/gutjnl-2014-306996]

81 **Hsu SH**, Wang B, Kota J, Yu J, Costinean S, Kutay H, Yu L, Bai S, La Perle K, Chivukula RR, Mao H, Wei M, Clark KR, Mendell JR, Caligiuri MA, Jacob ST, Mendell JT, Ghoshal K. Essential metabolic, anti-inflammatory, and anti-tumorigenic functions of miR-122 in liver. *J Clin Invest* 2012; **122**: 2871-2883 [PMID: 22820288 DOI: 10.1172/JCI63539]

82 **Krützfeldt J**, Rajewsky N, Braich R, Rajeev KG, Tuschl T, Manoharan M, Stoffel M. Silencing of microRNAs in vivo with 'antagomirs'. *Nature* 2005; **438**: 685-689 [PMID: 16258535 DOI: 10.1038/nature04303]

83 **Esau C**, Davis S, Murray SF, Yu XX, Pandey SK, Pear M, Watts L, Booten SL, Graham M, McKay R, Subramaniam A, Propp S, Lollo BA, Freier S, Bennett CF, Bhanot S, Monia BP. miR-122 regulation of lipid metabolism revealed by in vivo antisense targeting. *Cell Metab* 2006; **3**: 87-98 [PMID: 16459310 DOI: 10.1016/j.cmet.2006.01.005]

84 **Tsai WC**, Hsu SD, Hsu CS, Lai TC, Chen SJ, Shen R, Huang Y, Chen HC, Lee CH, Tsai TF, Hsu MT, Wu JC, Huang HD, Shiao MS, Hsiao M, Tsou AP. MicroRNA-122 plays a critical role in liver homeostasis and hepatocarcinogenesis. *J Clin Invest* 2012; **122**: 2884-2897 [PMID: 22820290 DOI: 10.1172/JCI63455]

85 **Cermelli S**, Ruggieri A, Marrero JA, Ioannou GN, Beretta L. Circulating microRNAs in patients with chronic hepatitis C and non-alcoholic fatty liver disease. *PLoS One* 2011; **6**: e23937 [PMID: 21886843 DOI: 10.1371/journal.pone.0023937]

86 **Pirola CJ**, Gianotti TF, Castaño GO, Sookoian S. Circulating MicroRNA-122 signature in nonalcoholic fatty liver disease and cardiovascular disease: a new endocrine system in metabolic syndrome. *Hepatology* 2013; **57**: 2545-2547 [PMID: 23111985 DOI: 10.1002/hep.26116]

87 **Jones A**, Danielson KM, Benton MC, Ziegler O, Shah R, Stubbs RS, Das S, Macartney-Coxson D. miRNA Signatures of Insulin Resistance in Obesity. *Obesity (Silver Spring)* 2017; **25**: 1734-1744 [PMID: 28834285 DOI: 10.1002/oby.21950]

88 **Willeit P**, Skroblin P, Moschen AR, Yin X, Kaudewitz D, Zampetaki A, Barwari T, Whitehead M, Ramírez CM, Goedeke L, Rotllan N, Bonora E, Hughes AD, Santer P, Fernández-Hernando C, Tilg H, Willeit J, Kiechl S, Mayr M. Circulating MicroRNA-122 Is Associated With the Risk of New-Onset Metabolic Syndrome and Type 2 Diabetes. *Diabetes* 2017; **66**: 347-357 [PMID: 27899485 DOI: 10.2337/db16-0731]

89 **Gallo A**, Tandon M, Alevizos I, Illei GG. The majority of microRNAs detectable in serum and saliva is concentrated in exosomes. *PLoS One* 2012; **7**: e30679 [PMID: 22427800 DOI: 10.1371/journal.pone.0030679]

90 **Chen Y**, Siegel F, Kipschull S, Haas B, Fröhlich H, Meister G, Pfeifer A. miR-155 regulates differentiation of brown and beige adipocytes *via* a bistable circuit. *Nat Commun* 2013; **4**: 1769 [PMID: 23612310 DOI: 10.1038/ncomms2742]

91 **Chen JQ**, Papp G, Szodoray P, Zeher M. The role of microRNAs in the pathogenesis of autoimmune diseases. *Autoimmun Rev* 2016; **15**: 1171-1180 [PMID: 27639156 DOI: 10.1016/j.autrev.2016.09.003]

92 **Miller AM**, Gilchrist DS, Nijjar J, Araldi E, Ramirez CM, Lavery CA, Fernández-Hernando C, McInnes IB, Kurowska-Stolarska M. MiR-155 has a protective role in the development of non-alcoholic hepatosteatosis in mice. *PLoS One* 2013;

8: e72324 [PMID: 23991091 DOI: 10.1371/journal.pone.0072324]

93   **Lin X**, Jia J, Du T, Li W, Wang X, Wei J, Lin X, Zeng H, Yao L, Chen X, Zhuang J, Weng J, Liu Y, Lin J, Wu Q, Wang W, Yao K, Xu K, Xiao D. Overexpression of miR-155 in the liver of transgenic mice alters the expression profiling of hepatic genes associated with lipid metabolism. *PLoS One* 2015; **10**: e0118417 [PMID: 25799309 DOI: 10.1371/journal.pone.0118417]

94   **Wang L**, Zhang N, Wang Z, Ai DM, Cao ZY, Pan HP. Decreased MiR-155 Level in the Peripheral Blood of Non-Alcoholic Fatty Liver Disease Patients may Serve as a Biomarker and may Influence LXR Activity. *Cell Physiol Biochem* 2016; **39**: 2239-2248 [PMID: 27832630 DOI: 10.1159/000447917]

95   **Csak T**, Bala S, Lippai D, Kodys K, Catalano D, Iracheta-Vellve A, Szabo G. MicroRNA-155 Deficiency Attenuates Liver Steatosis and Fibrosis without Reducing Inflammation in a Mouse Model of Steatohepatitis. *PLoS One* 2015; **10**: e0129251 [PMID: 26042593 DOI: 10.1371/journal.pone.0129251]

96   **Bala S**, Ganz M, Babuta M, Zhuang Y, Csak T, Calenda CD, Szabo G. Steatosis, inflammasome upregulation, and fibrosis are attenuated in miR-155 deficient mice in a high fat-cholesterol-sugar diet-induced model of NASH. *Lab Invest* 2021; **101**: 1540-1549 [PMID: 34453120 DOI: 10.1038/s41374-021-00626-1]

97   **Ying W**, Riopel M, Bandyopadhyay G, Dong Y, Birmingham A, Seo JB, Ofrecio JM, Wollam J, Hernandez-Carretero A, Fu W, Li P, Olefsky JM. Adipose Tissue Macrophage-Derived Exosomal miRNAs Can Modulate In Vivo and In Vitro Insulin Sensitivity. *Cell* 2017; **171**: 372-384.e12 [PMID: 28942920 DOI: 10.1016/j.cell.2017.08.035]

98   **Coll M**, El Taghdouini A, Perea L, Mannaerts I, Vila-Casadesús M, Blaya D, Rodrigo-Torres D, Affò S, Morales-Ibanez O, Graupera I, Lozano JJ, Najimi M, Sokal E, Lambrecht J, Ginès P, van Grunsven LA, Sancho-Bru P. Integrative miRNA and Gene Expression Profiling Analysis of Human Quiescent Hepatic Stellate Cells. *Sci Rep* 2015; **5**: 11549 [PMID: 26096707 DOI: 10.1038/srep11549]

99   **Tan Y**, Ge G, Pan T, Wen D, Gan J. A pilot study of serum microRNAs panel as potential biomarkers for diagnosis of nonalcoholic fatty liver disease. *PLoS One* 2014; **9**: e105192 [PMID: 25141008 DOI: 10.1371/journal.pone.0105192]

100   **Liu XL**, Pan Q, Cao HX, Xin FZ, Zhao ZH, Yang RX, Zeng J, Zhou H, Fan JG. Lipotoxic Hepatocyte-Derived Exosomal MicroRNA 192-5p Activates Macrophages Through Rictor/Akt/Forkhead Box Transcription Factor O1 Signaling in Nonalcoholic Fatty Liver Disease. *Hepatology* 2020; **72**: 454-469 [PMID: 31782176 DOI: 10.1002/hep.31050]

101   **Wang X**, He Y, Mackowiak B, Gao B. MicroRNAs as regulators, biomarkers and therapeutic targets in liver diseases. *Gut* 2021; **70**: 784-795 [PMID: 33127832 DOI: 10.1136/gutjnl-2020-322526]

102   **Dumortier O**, Fabris G, Pisani DF, Casamento V, Gautier N, Hinault C, Lebrun P, Duranton C, Tauc M, Dalle S, Kerr-Conte J, Pattou F, Prentki M, Van Obberghen E. microRNA-375 regulates glucose metabolism-related signaling for insulin secretion. *J Endocrinol* 2020; **244**: 189-200 [PMID: 31697642 DOI: 10.1530/JOE-19-0180]

103   **Lei L**, Zhou C, Yang X, Li L. Down-regulation of microRNA-375 regulates adipokines and inhibits inflammatory cytokines by targeting AdipoR2 in non-alcoholic fatty liver disease. *Clin Exp Pharmacol Physiol* 2018; **45**: 819-831 [PMID: 29569260 DOI: 10.1111/1440-1681.12940]

104   **Quinn JJ**, Chang HY. Unique features of long non-coding RNA biogenesis and function. *Nat Rev Genet* 2016; **17**: 47-62 [PMID: 26666209 DOI: 10.1038/nrg.2015.10]

105   **Tsai MC**, Manor O, Wan Y, Mosammaparast N, Wang JK, Lan F, Shi Y, Segal E, Chang HY. Long noncoding RNA as modular scaffold of histone modification complexes. *Science* 2010; **329**: 689-693 [PMID: 20616235 DOI: 10.1126/science.1192002]

106   **Wang KC**, Chang HY. Molecular mechanisms of long noncoding RNAs. *Mol Cell* 2011; **43**: 904-914 [PMID: 21925379 DOI: 10.1016/j.molcel.2011.08.018]

107   **Huarte M**. The emerging role of lncRNAs in cancer. *Nat Med* 2015; **21**: 1253-1261 [PMID: 26540387 DOI: 10.1038/nm.3981]

108   **Giovarelli M**, Bucci G, Ramos A, Bordo D, Wilusz CJ, Chen CY, Puppo M, Briata P, Gherzi R. H19 long noncoding RNA controls the mRNA decay promoting function of KSRP. *Proc Natl Acad Sci U S A* 2014; **111**: E5023-E5028 [PMID: 25385579 DOI: 10.1073/pnas.1415098111]

109   **Li X**, Liu R. Long non-coding RNA H19 in the liver-gut axis: A diagnostic marker and therapeutic target for liver diseases. *Exp Mol Pathol* 2020; **115**: 104472 [PMID: 32454104 DOI: 10.1016/j.yexmp.2020.104472]

110   **Liu C**, Yang Z, Wu J, Zhang L, Lee S, Shin DJ, Tran M, Wang L. Long noncoding RNA H19 interacts with polypyrimidine tract-binding protein 1 to reprogram hepatic lipid homeostasis. *Hepatology* 2018; **67**: 1768-1783 [PMID: 29140550 DOI: 10.1002/hep.29654]

111   **Liu J**, Tang T, Wang GD, Liu B. LncRNA-H19 promotes hepatic lipogenesis by directly regulating miR-130a/PPARγ axis in non-alcoholic fatty liver disease. *Biosci Rep* 2019; **39** [PMID: 31064820 DOI: 10.1042/BSR20181722]

112   **Wang H**, Cao Y, Shu L, Zhu Y, Peng Q, Ran L, Wu J, Luo Y, Zuo G, Luo J, Zhou L, Shi Q, Weng Y, Huang A, He TC, Fan J. Long non-coding RNA (lncRNA) H19 induces hepatic steatosis through activating MLXIPL and mTORC1 networks in hepatocytes. *J Cell Mol Med* 2020; **24**: 1399-1412 [PMID: 31809000 DOI: 10.1111/jcmm.14818]

113   **Zhao XY**, Li S, Wang GX, Yu Q, Lin JD. A long noncoding RNA transcriptional regulatory circuit drives thermogenic adipocyte differentiation. *Mol Cell* 2014; **55**: 372-382 [PMID: 25002143 DOI: 10.1016/j.molcel.2014.06.004]

114   **Zhao XY**, Xiong X, Liu T, Mi L, Peng X, Rui C, Guo L, Li S, Li X, Lin JD. Long noncoding RNA licensing of obesity-linked hepatic lipogenesis and NAFLD pathogenesis. *Nat Commun* 2018; **9**: 2986 [PMID: 30061575 DOI: 10.1038/s41467-018-05383-2]

115   **Tang S**, Zhu W, Zheng F, Gui W, Zhang W, Lin X, Li H. The Long Noncoding RNA Blnc1 Protects Against Diet-Induced Obesity by Promoting Mitochondrial Function in White Fat. *Diabetes Metab Syndr Obes* 2020; **13**: 1189-1201 [PMID: 32368112 DOI: 10.2147/DMSO.S248692]

116   **Li D**, Cheng M, Niu Y, Chi X, Liu X, Fan J, Fan H, Chang Y, Yang W. Identification of a novel human long non-coding RNA that regulates hepatic lipid metabolism by inhibiting SREBP-1c. *Int J Biol Sci* 2017; **13**: 349-357 [PMID: 28367099 DOI: 10.7150/ijbs.16635]

117   **Hegele RA**. Plasma lipoproteins: genetic influences and clinical implications. *Nat Rev Genet* 2009; **10**: 109-121 [PMID: 19139765 DOI: 10.1038/nrg2481]

118   **Yan C**, Chen J, Chen N. Long noncoding RNA MALAT1 promotes hepatic steatosis and insulin resistance by increasing nuclear SREBP-1c protein stability. *Sci Rep* 2016; **6**: 22640 [PMID: 26935028 DOI: 10.1038/srep22640]

119   **Leti F**, Legendre C, Still CD, Chu X, Petrick A, Gerhard GS, DiStefano JK. Altered expression of MALAT1 lncRNA in nonalcoholic steatohepatitis fibrosis regulates CXCL5 in hepatic stellate cells. *Transl Res* 2017; **190**: 25-39.e21 [PMID: 28993096 DOI: 10.1016/j.trsl.2017.09.001]

120   **Sookoian S**, Flichman D, Garaycoechea ME, San Martino J, Castaño GO, Pirola CJ. Metastasis-associated lung adenocarcinoma transcript 1 as a common molecular driver in the pathogenesis of nonalcoholic steatohepatitis and chronic immune-mediated liver damage. *Hepatol Commun* 2018; **2**: 654-665 [PMID: 29881817 DOI: 10.1002/hep4.1184]

121   **Lai MC**, Yang Z, Zhou L, Zhu QQ, Xie HY, Zhang F, Wu LM, Chen LM, Zheng SS. Long non-coding RNA MALAT-1 overexpression predicts tumor recurrence of hepatocellular carcinoma after liver transplantation. *Med Oncol* 2012; **29**: 1810-1816 [PMID: 21678027 DOI: 10.1007/s12032-011-0004-z]

122   **Konishi H**, Ichikawa D, Yamamoto Y, Arita T, Shoda K, Hiramoto H, Hamada J, Itoh H, Fujita Y, Komatsu S, Shiozaki A, Ikoma H, Ochiai T, Otsuji E. Plasma level of metastasis-associated lung adenocarcinoma transcript 1 is associated with liver damage and predicts development of hepatocellular carcinoma. *Cancer Sci* 2016; **107**: 149-154 [PMID: 26614531 DOI: 10.1111/cas.12854]

123   **Bu FT**, Wang A, Zhu Y, You HM, Zhang YF, Meng XM, Huang C, Li J. LncRNA NEAT1: Shedding light on mechanisms and opportunities in liver diseases. *Liver Int* 2020; **40**: 2612-2626 [PMID: 32745314 DOI: 10.1111/liv.14629]

124   **Wang X**. Down-regulation of lncRNA-NEAT1 alleviated the non-alcoholic fatty liver disease *via* mTOR/S6K1 signaling pathway. *J Cell Biochem* 2018; **119**: 1567-1574 [PMID: 28771824 DOI: 10.1002/jcb.26317]

125   **Fu X**, Zhu J, Zhang L, Shu J. Long non-coding RNA NEAT1 promotes steatosis *via* enhancement of estrogen receptor alpha-mediated AQP7 expression in HepG2 cells. *Artif Cells Nanomed Biotechnol* 2019; **47**: 1782-1787 [PMID: 31062612 DOI: 10.1080/21691401.2019.1604536]

126   **Chen X**, Tan XR, Li SJ, Zhang XX. LncRNA NEAT1 promotes hepatic lipid accumulation *via* regulating miR-146a-5p/ROCK1 in nonalcoholic fatty liver disease. *Life Sci* 2019; **235**: 116829 [PMID: 31484042 DOI: 10.1016/j.lfs.2019.116829]

127   **Jin SS**, Lin XF, Zheng JZ, Wang Q, Guan HQ. lncRNA NEAT1 regulates fibrosis and inflammatory response induced by nonalcoholic fatty liver by regulating miR-506/GLI3. *Eur Cytokine Netw* 2019; **30**: 98-106 [PMID: 31957704 DOI: 10.1684/ecn.2019.0432]

128   **Zhang Z**, Wen H, Peng B, Weng J, Zeng F. Downregulated microRNA-129-5p by Long Non-coding RNA NEAT1 Upregulates PEG3 Expression to Aggravate Non-alcoholic Steatohepatitis. *Front Genet* 2020; **11**: 563265 [PMID: 33574830 DOI: 10.3389/fgene.2020.563265]

129   **Guo J**, Fang W, Sun L, Lu Y, Dou L, Huang X, Tang W, Yu L, Li J. Ultraconserved element uc.372 drives hepatic lipid accumulation by suppressing miR-195/miR4668 maturation. *Nat Commun* 2018; **9**: 612 [PMID: 29426937 DOI: 10.1038/s41467-018-03072-8]

130   **He Y**, Wu YT, Huang C, Meng XM, Ma TT, Wu BM, Xu FY, Zhang L, Lv XW, Li J. Inhibitory effects of long noncoding RNA MEG3 on hepatic stellate cells activation and liver fibrogenesis. *Biochim Biophys Acta* 2014; **1842**: 2204-2215 [PMID: 25201080 DOI: 10.1016/j.bbadis.2014.08.015]

131   **Huang P**, Huang FZ, Liu HZ, Zhang TY, Yang MS, Sun CZ. LncRNA MEG3 functions as a ceRNA in regulating hepatic lipogenesis by competitively binding to miR-21 with LRP6. *Metabolism* 2019; **94**: 1-8 [PMID: 30711569 DOI: 10.1016/j.metabol.2019.01.018]

132   **Zou D**, Liu L, Zeng Y, Wang H, Dai D, Xu M. LncRNA MEG3 up-regulates SIRT6 by ubiquitinating EZH2 and alleviates nonalcoholic fatty liver disease. *Cell Death Discov* 2022; **8**: 103 [PMID: 35256601 DOI: 10.1038/s41420-022-00889-7]

133   **Zhang L**, Yang Z, Trottier J, Barbier O, Wang L. Long noncoding RNA MEG3 induces cholestatic liver injury by interaction with PTBP1 to facilitate shp mRNA decay. *Hepatology* 2017; **65**: 604-615 [PMID: 27770549 DOI: 10.1002/hep.28882]

134   **Cheng X**, Shihabudeen Haider Ali MS, Moran M, Viana MP, Schlichte SL, Zimmerman MC, Khalimonchuk O, Feinberg MW, Sun X. Long non-coding RNA Meg3 deficiency impairs glucose homeostasis and insulin signaling by inducing cellular senescence of hepatic endothelium in obesity. *Redox Biol* 2021; **40**: 101863 [PMID: 33508742 DOI: 10.1016/j.redox.2021.101863]

135   **Panzitt K**, Tschernatsch MM, Guelly C, Moustafa T, Stradner M, Strohmaier HM, Buck CR, Denk H, Schroeder R, Trauner M, Zatloukal K. Characterization of HULC, a novel gene with striking up-regulation in hepatocellular carcinoma, as noncoding RNA. *Gastroenterology* 2007; **132**: 330-342 [PMID: 17241883 DOI: 10.1053/j.gastro.2006.08.026]

136   **Shen X**, Guo H, Xu J, Wang J. Inhibition of lncRNA HULC improves hepatic fibrosis and hepatocyte apoptosis by inhibiting the MAPK signaling pathway in rats with nonalcoholic fatty liver disease. *J Cell Physiol* 2019; **234**: 18169-18179 [PMID: 30908654 DOI: 10.1002/jcp.28450]

137   **Gandhy SU**, Imanirad P, Jin UH, Nair V, Hedrick E, Cheng Y, Corton JC, Kim K, Safe S. Specificity protein (Sp) transcription factors and metformin regulate expression of the long non-coding RNA HULC. *Oncotarget* 2015; **6**: 26359-26372 [PMID: 26317792 DOI: 10.18632/oncotarget.4560]

138   **Feng W**, Gao C, Bi Y, Wu M, Li P, Shen S, Chen W, Yin T, Zhu D. Randomized trial comparing the effects of gliclazide, liraglutide, and metformin on diabetes with non-alcoholic fatty liver disease. *J Diabetes* 2017; **9**: 800-809 [PMID: 28332301 DOI: 10.1111/1753-0407.12555]

139   **Li P**, Chen X, Lin M, Huang D. Up-regulated HOTAIR induced by fatty acids inhibits PTEN expression and increases triglycerides accumulation in HepG2 cells. *Food Nutr Res* 2017; **61**: 1412794 [DOI: 10.1080/16546628.2017.1412794]

140   **Guo B**, Cheng Y, Yao L, Zhang J, Lu J, Qi H, Chen H. LncRNA HOTAIR regulates the lipid accumulation in non-alcoholic fatty liver disease *via* miR-130b-3p/ROCK1 axis. *Cell Signal* 2022; **90**: 110190 [PMID: 34774989 DOI: 10.1016/j.cellsig.2021.110190]

141   **Yu F**, Chen B, Dong P, Zheng J. HOTAIR Epigenetically Modulates PTEN Expression *via* MicroRNA-29b: A Novel

Mechanism in Regulation of Liver Fibrosis. *Mol Ther* 2017; **25**: 205-217 [PMID: 28129115 DOI: 10.1016/j.ymthe.2016.10.015]

142   **Chen Y**, Huang H, Xu C, Yu C, Li Y. Long Non-Coding RNA Profiling in a Non-Alcoholic Fatty Liver Disease Rodent Model: New Insight into Pathogenesis. *Int J Mol Sci* 2017; **18** [PMID: 28275212 DOI: 10.3390/ijms18010021]

143   **Chen Y**, Chen X, Gao J, Xu C, Xu P, Li Y, Zhu Y, Yu C. Long noncoding RNA FLRL2 alleviated nonalcoholic fatty liver disease through Arntl-Sirt1 pathway. *FASEB J* 2019; **33**: 11411-11419 [PMID: 31311301 DOI: 10.1096/fj.201900643RRR]

144   **Wu YL**, Li HF, Chen HH, Lin H. Emergent Roles of Circular RNAs in Metabolism and Metabolic Disorders. *Int J Mol Sci* 2022; **23** [PMID: 35162956 DOI: 10.3390/ijms23031032]

145   **Zaiou M**. The Emerging Role and Promise of Circular RNAs in Obesity and Related Metabolic Disorders. *Cells* 2020; **9** [PMID: 32560220 DOI: 10.3390/cells9061473]

146   **Xu ZX**, Li JZ, Li Q, Xu MY, Li HY. CircRNA608-microRNA222-PINK1 axis regulates the mitophagy of hepatic stellate cells in NASH related fibrosis. *Biochem Biophys Res Commun* 2022; **610**: 35-42 [PMID: 35436629 DOI: 10.1016/j.bbrc.2022.04.008]

147   **Jin X**, Gao J, Zheng R, Yu M, Ren Y, Yan T, Huang Y, Li Y. Antagonizing circRNA_002581-miR-122-CPEB1 axis alleviates NASH through restoring PTEN-AMPK-mTOR pathway regulated autophagy. *Cell Death Dis* 2020; **11**: 123 [PMID: 32054840 DOI: 10.1038/s41419-020-2293-7]

148   **Guo XY**, Chen JN, Sun F, Wang YQ, Pan Q, Fan JG. circRNA_0046367 Prevents Hepatoxicity of Lipid Peroxidation: An Inhibitory Role against Hepatic Steatosis. *Oxid Med Cell Longev* 2017; **2017**: 3960197 [PMID: 29018509 DOI: 10.1155/2017/3960197]

149   **Guo XY**, Sun F, Chen JN, Wang YQ, Pan Q, Fan JG. circRNA_0046366 inhibits hepatocellular steatosis by normalization of PPAR signaling. *World J Gastroenterol* 2018; **24**: 323-337 [PMID: 29391755 DOI: 10.3748/wjg.v24.i3.323]

150   **Guo XY**, He CX, Wang YQ, Sun C, Li GM, Su Q, Pan Q, Fan JG. Circular RNA Profiling and Bioinformatic Modeling Identify Its Regulatory Role in Hepatic Steatosis. *Biomed Res Int* 2017; **2017**: 5936171 [PMID: 28717649 DOI: 10.1155/2017/5936171]

151   **Li P**, Shan K, Liu Y, Zhang Y, Xu L. CircScd1 Promotes Fatty Liver Disease *via* the Janus Kinase 2/Signal Transducer and Activator of Transcription 5 Pathway. *Dig Dis Sci* 2019; **64**: 113-122 [PMID: 30259280 DOI: 10.1007/s10620-018-5290-2]

152   **Yang W**, Zhao J, Zhao Y, Li W, Zhao L, Ren Y, Ou R, Xu Y. Hsa_circ_0048179 attenuates free fatty acid-induced steatosis *via* hsa_circ_0048179/miR-188-3p/GPX4 signaling. *Aging (Albany NY)* 2020; **12**: 23996-24008 [PMID: 33221744 DOI: 10.18632/aging.104081]

153   **Ou Q**, Zhao Y, Zhou J, Wu X. Comprehensive circular RNA expression profiles in a mouse model of nonalcoholic steatohepatitis. *Mol Med Rep* 2019; **19**: 2636-2648 [PMID: 30720095 DOI: 10.3892/mmr.2019.9935]

154   **Chen Y**, Yuan B, Wu Z, Dong Y, Zhang L, Zeng Z. Microarray profiling of circular RNAs and the potential regulatory role of hsa_circ_0071410 in the activated human hepatic stellate cell induced by irradiation. *Gene* 2017; **629**: 35-42 [PMID: 28774651 DOI: 10.1016/j.gene.2017.07.078]

155   **Zhou Y**, Lv X, Qu H, Zhao K, Fu L, Zhu L, Ye G, Guo J. Preliminary screening and functional analysis of circular RNAs associated with hepatic stellate cell activation. *Gene* 2018; **677**: 317-323 [PMID: 30118889 DOI: 10.1016/j.gene.2018.08.052]

156   **Chen X**, Tan QQ, Tan XR, Li SJ, Zhang XX. Circ_0057558 promotes nonalcoholic fatty liver disease by regulating ROCK1/AMPK signaling through targeting miR-206. *Cell Death Dis* 2021; **12**: 809 [PMID: 34446693 DOI: 10.1038/s41419-021-04090-z]

157   **Zhao Q**, Liu J, Deng H, Ma R, Liao JY, Liang H, Hu J, Li J, Guo Z, Cai J, Xu X, Gao Z, Su S. Targeting Mitochondria-Located circRNA SCAR Alleviates NASH *via* Reducing mROS Output. *Cell* 2020; **183**: 76-93.e22 [PMID: 32931733 DOI: 10.1016/j.cell.2020.08.009]

158   **Liufu Z**, Zhao Y, Guo L, Miao G, Xiao J, Lyu Y, Chen Y, Shi S, Tang T, Wu CI. Redundant and incoherent regulations of multiple phenotypes suggest microRNAs' role in stability control. *Genome Res* 2017; **27**: 1665-1673 [PMID: 28904014 DOI: 10.1101/gr.222505.117]

Combination strategies for pharmacologic treatment of non-alcoholic steatohepatitis

Jaspreet Suri, Sebastian Borja, Joseph K Lim

Jaspreet Suri, Department of Gastroenterology, Norwalk Hospital, Norwalk, CT 06856, United States

Sebastian Borja, Department of Internal Medicine, Norwalk Hospital, Norwalk, CT 06850, United States

Joseph K Lim, Section of Digestive Diseases, Yale University School of Medicine, New Haven, CT 06520, United States

Corresponding author: Joseph K Lim, MD, Professor, Section of Digestive Diseases, Yale University School of Medicine, Yale Liver Center, 333 Cedar Street, LMP 1080, New Haven, CT 06520, United States. joseph.lim@yale.edu

Abstract

Non-alcoholic steatohepatitis (NASH) is defined as hepatic steatosis, inflammation, and hepatocyte injury with or without fibrosis. It has emerged as the second leading indication for liver transplantation with a rising death rate in the non-transplantable population. While there are many drugs in evaluation, currently no approved therapies are on the market for this condition. Given this importance, the Food and Drug Administration has provided formal guidance regarding drug development for stopping or reversing NASH or NASH associated fibrosis. The complex pathogenesis of NASH and its bidirectional relationship with metabolic syndrome has highlighted multiple drugs of interest that address metabolic, inflammatory, and fibrotic factors. A few promising liver specific targets include farnesoid X receptor agonists and peroxisome proliferator-activated receptor agonists. Previously studied drug classes such as glucagon-like peptide-1 analogs or sodium/glucose transport protein 2 inhibitors have also demonstrated ability to improve hepatic steatosis. Here we discuss current rationale, scientific work, and preliminary data in combining multiple drugs for the purposes of a multimodal attack on the pathogenesis of NASH. We highlight multiple Phase 2 and Phase 3 studies that demonstrate the potential to achieve a response rate higher than previously assessed monotherapies for this condition. Ultimately, one of these combination strategies may rise above in its safety and efficacy to become a part of a standardized approach to NASH.

Key Words: Non-alcoholic steatohepatitis; Fatty liver; Combination treatment; Drug therapy; Pharmacologic treatment; Clinical trials

Core Tip: Multimodal combination approaches targeting two or more molecular pathways contributing to steatohepatitis and liver fibrosis are needed to augment efficacy of novel investigational drug regimens to achieve non-alcoholic steatohepatiti (NASH) resolution and NASH fibrosis improvement.
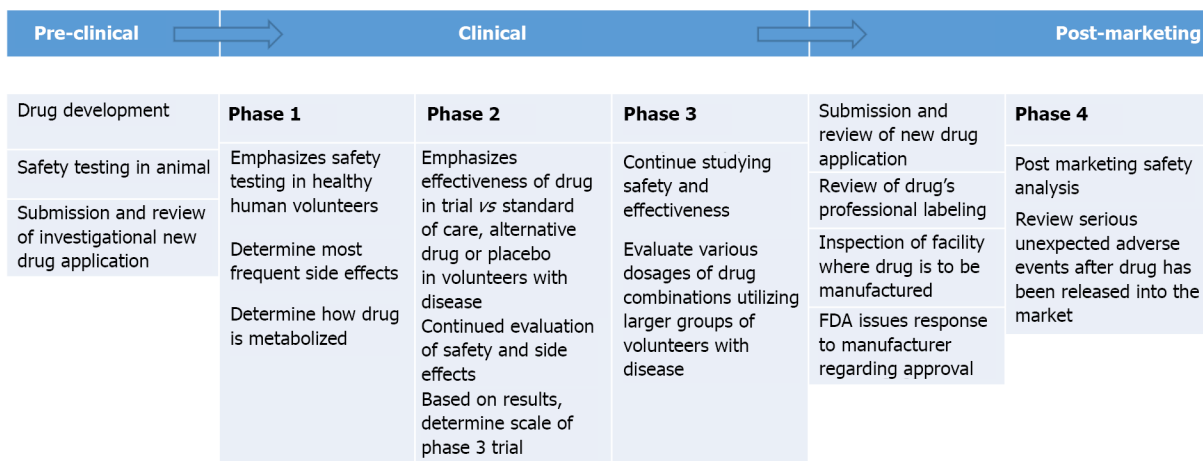
INTRODUCTION

Non-alcoholic steatohepatitis (NASH) is defined as the presence of ≥ 5% hepatic steatosis and inflammation with hepatocyte injury with or without fibrosis. Non-alcoholic fatty liver disease (NAFLD) represents a spectrum of pathology encompassing hepatic steatosis, steatohepatitis (NASH), and liver fibrosis, and poses a significant challenge to the medical community as there are currently no Food and Drug Administration (FDA) approved therapies available on the market. The definition of NAFLD includes the lack of secondary causes of hepatic steatosis such as alcohol consumption, steatogenic medication or hereditary liver disease. With NAFLD-associated death rates on the rise and NASH emerging as the second most common indication for liver transplantation, there has been heightened urgency to target various disease pathways in NASH development with the hopes of controlling the global impact of this disease[1,2]. With this rising importance, the FDA has published formal guidance regarding drug development aimed at stopping or reversing NASH and NASH fibrosis. The current drug development pipeline contains many mono-therapeutic options which address a wide range of metabolic, inflammatory, and fibrosis target pathways associated with NASH pathogenesis.

The pathophysiology of NASH is based on a bidirectional relationship between type 2 diabetes mellitus (T2DM), hypertension, obesity and dyslipidemia–or metabolic syndrome. This relationship contributes to excess free fatty acids generated from lipolysis and de novo lipogenesis in the liver, which creates lipotoxic species which induce oxidative stress, inflammasome activation, and fibrinogenesis[3] . Liver specific targets aimed at decreasing histologic inflammation or fibrosis such as farnesoid X receptor (FXR) agonists or peroxisome proliferator-activated receptor (PPAR) agonists are currently being evaluated for the treatment of NASH. These are in addition to drug classes such as glucagon-like peptide-1 (GLP-1) agonists and sodium/glucose transport protein 2 inhibitors that were initially approved for treatment of diabetes but have demonstrated the ability to decrease liver fat content[4,5]. While individually these agents have shown promise in early trials, there has been growing interest in pursuing a multimodal combination approach targeting two or more molecular targets/pathways responsible for NASH and NASH-associated liver fibrosis, particularly in context of modest effects of single agent strategies on histologic endpoints, with fewer than 50% of patients achieving either NASH resolution of fibrosis improvement of one stage or greater[6]. Therefore, this mini review will succinctly summarize the current efforts to examine combination strategies of drugs which may further augment therapeutic response in patients with NASH.

FDA APPROVAL PATHWAY

The FDA generally has two pathways for drug approval. The traditional pathway focuses on clinical benefit endpoints (*i.e.*, morbidity and mortality) and requires long term data. A brief review is provided in Figure 1. The accelerated approval pathway is intended to expedite the process for serious medical conditions with unmet needs. This pathway relies on short term surrogate markers that would reliably predict long term clinical outcomes to support drug approval. To inform clinical trial design for investigational drugs under evaluation for NASH, industry guidance was issued by the FDA in 2018 with a focus on patients with non-cirrhotic NASH with stage 2-3 liver fibrosis[7]. Although histologic endpoints were reinforced as required for assessment of surrogate endpoints for NASH and liver fibrosis, the agency encouraged the development and validation of noninvasive biomarkers in clinical trials to accelerate drug development. NASH was defined as a NAFLD activity score (NAS) greater than or equal to 4 with at least 1 point each in inflammation and ballooning degeneration, plus a NASH Clinical Research Network fibrosis score greater than stage 1 fibrosis but less than stage 4 for enrollment in these trials. Lastly, the primary regulatory endpoints required to support accelerated approval include: (1) NASH resolution on histology (NAS less than 4 with individual components scores of 0 for

Pre-clinical	Clinical				Post-marketing
Drug development	**Phase 1**	**Phase 2**	**Phase 3**	Submission and review of new drug application	**Phase 4**
Safety testing in animal	Emphasizes safety testing in healthy human volunteers	Emphasizes effectiveness of drug in trial *vs* standard of care, alternative drug or placebo in volunteers with disease	Continue studying safety and effectiveness	Review of drug's professional labeling	Post marketing safety analysis
Submission and review of investigational new drug application	Determine most frequent side effects		Evaluate various dosages of drug combinations utilizing larger groups of volunteers with disease	Inspection of facility where drug is to be manufactured	Review serious unexpected adverse events after drug has been released into the market
	Determine how drug is metabolized	Continued evaluation of safety and side effects		FDA issues response to manufacturer regarding approval	
		Based on results, determine scale of phase 3 trial			

DOI: 10.3748/wjg.v28.i35.5129 **Copyright** ©The Author(s) 2022.

Figure 1 Flow diagram of standard Food and Drug Administration drug approval process.

ballooning degeneration and 0-1 for inflammation) without worsening fibrosis; (2) Improvement in liver fibrosis greater than or equal to one stage without worsening NASH; or (3) NASH resolution and improvement in fibrosis by one stage or greater. Clinical benefit for these drugs was defined as superiority to placebo in delayed disease progression measured by a composite endpoint including progression to cirrhosis, hepatic decompensation, change in MELD score, liver transplantation, or all-cause mortality.

DRUGS IN DEVELOPMENT–PHASE 2

Key phase 2 trials for NASH therapeutics are summarized in Table 1. In brief, one major class being pursued is fibroblast growth factor 21 (FGF21) agonists such as pegbelfermin. FGF21 is endogenously produced by the liver and has a pleiotropic effect on metabolism that may benefit patients with NASH. Endogenous FGF21 concentrations are elevated as much as 10-fold in patients with obesity, NAFLD or NASH, leading to the hypothesis that these may represent an FGF21-resistant state which may benefit from exogenous stimulation to improve insulin sensitivity and lipid metabolism[8] . GLP-1 is an incretin hormone made by intestinal cells post prandially for which receptors are predominantly in the pancreas, adipose tissue and brain. It regulates plasma glucose by stimulating glucose release and inhibiting glucagon secretion. GLP-1 agonists have previously shown to improve hepatic steatosis, decrease liver inflammation, and ameliorate insulin resistance in murine models of fatty liver disease. Semaglutide and liraglutide have shown promising results with statistically significant NASH improvement or resolution compared to placebo[9,10]. Norursodeoxycholic acid is an orally administered side chain-shortened homologue of ursodeoxycholic acid that undergoes hepatic enrichment with hepatopro-tective, anti-inflammatory, and antifibrotic activity. It has shown significant reduction of serum alanine aminotransferase (ALT) within 12 wk of treatment when compared with placebo, encouraging further investigation[11]. Aldafermin is an analogue of fibroblast growth factor 19 (FGF19) which regulates bile acid metabolism and fat storage in the liver. FGF19 levels are lower in patients with NAFLD and insulin resistance. Activation of the FGF19 pathway has been shown to improve insulin sensitivity and liver steatosis. In a 24-wk placebo-controlled trial, the aldafermin group experienced a significant reduction in absolute liver fat content compared with placebo (P = 0.002) and fibrosis improvement of at least 1 stage (38% *vs* 18%, P = 0.10)[12]. The currently ongoing phase 2b ALPINE 4 study is designed to assess the efficacy, safety and tolerability of this agent (NCT04210245).

FXR agonists, which bind to the transcription factor FXR to help regulate bile acid metabolism are in multiple phases of clinical trial investigation. The FXR agonist tropifexor has demonstrated a robust and dose-dependent decrease in ALT, hepatic fat fractionation, and body weight with good safety and tolerability after 12 wk of treatment in a phase 2 trial[13]. The PPARα, β/δ and γ, play a central role in the regulation of glucose and lipid metabolism and of the inflammatory and fibrogenic pathways which contribute to NASH pathogenesis. Lanifibranor (IVA337), a pan-PPAR agonist, combines pharmaco-logical effects that could improve fatty acid oxidation, dyslipidemia, and insulin sensitivity, and has demonstrated anti-inflammatory, antifibrotic and hepatoprotective effects in preclinical models and phase 1/2 trials. TVB-2640 is an orally bioavailable, first-in-class fatty acid synthase (FASN) inhibitor. FASN is a key enzyme in the de novo lipogenesis pathway that is responsible for the synthesis of excess fat and activation of fibrogenic and inflammatory mechanisms in the liver of patients with NASH. TVB-2640 demonstrated significant improvement in several NASH endpoints in the FASCINATE-1 trial as

Table 1 Phase 2 trials in non-alcoholic steatohepatitis

Trial name/NCT number	Manufacturer	Drugs	Mechanism of action	Enrollment (targeted)	Study arms	Duration	Primary or relevant end point(s)	Results/SE
NCT03976401	Akero Therapeutics	AKR-001	FGF 21 receptor agonist	80	(1) AKR-001 50 mg QD; and (2) Placebo	112	Change in liver fat fraction measured by MRI-PDFF	Ongoing
NCT04541186	89bio	BIO89-100	FGF 21 receptor agonist	90	(1) BIO89-100 (QW or every 2 wk); and (2) Placebo	112	Change in various lab parameters TG, LDL, HDL, fasting glucose. Change in liver fat fraction measured by MRI-PDFF	Ongoing
NCT02097277	Bristol-Myers Squibb	Pegbelfermin (BMS-986036)	FGF 21 receptor agonist	120	(1) Pegbelfermin 1 mg QD; (2) Pegbelfermin 5 mg QD; (3) Pegbelfermin 20 mg QD; (4) Pegbelfermin 20 mg weekly; and (5) Placebo	84	Safety, tolerability, and change in HbA1c. Change in insulin sensitivity, lipids, adiponectin, and disease progression biomarkers	No significant effects of pegbelfermin versus placebo on HbA1c. Pegbelfermin 20 mg/d significantly improved high-density lipoprotein cholesterol and triglycerides. Most frequent adverse events were injection-site bruising and diarrhea
NCT01237119	Novo Nordisk	Liraglutide	GLP-1analogue	52	(1) Liraglutide 1.8 mg SC QD; and (2) Placebo	336	Resolution of NASH without worsening fibrosis	39% who received liraglutide and underwent end-of-treatment liver biopsy had resolution of definite non-alcoholic steatohepatitis compared with 9% in placebo ($P = 0.019$). Side effects diarrhea and loss of appetite
NCT02970942	Novo Nordisk	Semaglutide	GLP-1 analogue	320	(1) Semaglutide 0.1 mg SC QD; (2) Semaglutide 0.2 mg SC QD; (3) Semaglutide 0.4 mg SC QD; and (4) Placebo	504	Resolution of NASH without worsening fibrosis. Improvement in fibrosis, LFTs, A1c level	NASH resolution was achieved in 40% in the 0.1-mg group, 36% in the 0.2-mg group, 59% in the 0.4-mg group, and 17% in the placebo group ($P < 0.001$ for semaglutide 0.4 mg *vs* placebo). Side effects including nausea, constipation, and vomiting which was higher in the 0.4-mg group
2013-004605-38	Dr Falk Pharma GmbH	Norursodeoxycholic acid	homologue of ursodeoxy-cholic acid, undergoes hepatic enrichment with hepatoprotective, anti-inflammatory, and antifibrotic activity	198	(1) 500 mg norursodeoxy-cholic acid QD; (2) 1500 mg norursodeoxycholic acid QD; and (3) Placebo	112	Change in ALT levels	Dose-dependent reduction in ALT with norurs-odeoxycholic acid versus placebo, with a significant effect in the 1500 mg group ($P < 0.0001$). Side effects included headache, gastrointestinal disorders, and infections
COHORT 4/NCT02443116	NGM Biopharma-ceuticals	Aldafermin	Analog of fibroblast growth factor 19, inhibits bile acid synthesis and regulates metabolic homeostasis	78	(1) aldafermin 1 mg QD; and (2) Placebo	168	Improvement in liver fibrosis of greater or equal to one stage with no worsening of NASH	Aldafermin group with higher rate of liver fat content reduction compared to placebo (7.7% *vs* 2.7%, $P = 0.02$). Aldafermin produced significantly greater decrease in bile acids, liver enzymes. Fibrosis improvement without worsening NASH higher in aldafermin group (38% *vs* 18%, $P = 0.10$). NASH resolution without worsening fibrosis higher in aldafermin group (24% *vs* 9%, $P = 0.20$). Side effects include diarrhea, headache, abdominal distation and peripheral edema

ALPINE 4/NCT04210245	NGM Biopharma-ceuticals	Aldafermin	Analog of fibroblast growth factor 19, inhibits bile acid synthesis and regulates metabolic homeostasis	72	(1) Aldafermin 0.3 mg QD; (2) Aldafermin 1 mg QD; (3) Aldafermin 3 mg; and (4) Placebo	168	Improvement in liver fibrosis of greater or equal to one stage with no worsening of NASH	Ongoing
FLIGHT-FXR/NCT02855164	Novartis Pharma-ceutical	Tropifexor	FXR agonist	152	(1) TXR 140 g QD; (2) TXR 200gr QD; and (3) Placebo	84	Changes in liver fat fraction, liver enzymes, body weight	End point achieved in TXR 800 mg *vs* 1200 mg *vs* Placebo (51% *vs* 55% *vs* 34%, P = 0.001). Side effects include mild pruritus and increase in LDL
NATIVE/NCT03008070	Inventiva	Lanifibranor	PPAR agonist	247	(1) Lanifibranor 800 mg QD; (2) Lanifibranor 1200 mg QD; and (3) Placebo	168	Responder analysis based on the improvement of the SAF activity score	L800 mg *vs* 1200 mg *vs* Placebo (51% *vs* 55% *vs* 34%) P = 0.0015. SE weight gain, peripheral edema
FASCINATE-1/NCT03938246	Sagimet Biosciences Inc	TVB-2640	FASN inhibitor	99	(1) TVB2640 25 mg QD; (2) TVB2640 50 mg; and (3) Placebo	84	Change in hepatic fat fraction from baseline in subjects with NASH by proton-density fat fraction by magnetic resonance imaging	Dose-dependent relative changes in liver fat by MRI-PDFF were -28.2% with 50 mg (P < 0.005 *vs* placebo), -9.6% with 25 mg, and +4.5% with placebo. 30% relative reduction in liver fat at week 12 were 61% (P < 0.001 *vs* placebo)
NCT02856555	Gilead Sciences	Firsocostat	Acetyl-coenzyme A carboxylase Inhibitor	126	(1) Firsocostat 20 mg QD; (2) Firsocostat 5 mg QD; and (3) Placebo	84	Safety and tolerability. Secondary end point efficacy (NASH improvement without fibrosis)	Decrease of at least 30% from baseline in MRI-PDFF occurred in 48% of patients with 20 mg (P = 0.004), 23% given 5 mg (P = 0.43), and 15% given placebo. SE cause, abdominal pain, diarrhea
VOYAG/LBP20	Viking therapeutics	VK2809	Thyroid beta receptor agonist, selectively cleaved in hepatic tissue	45	(1) VK2809 5 mg QD; (2) VK2809 10 mg QOD; (3) VK280910 mg QD; and (4) Placebo	84	Safety, tolerability and efficacy in reducing liver fat content and LDL	< Liver fat content was 8.7% for 5 mg QD (P = 0.0014) *vs* 8.9% 10 mg QOD (P = 0.013) *vs* 10.6% for 10 mg QD (P = 0.0030), *vs* 1.1% for placebo. 70% in VK2809 therapy showed a ≥ 50%. Reduction in MRI-PDFF (P = 0.014)
NCT02912260	Madrigal Pharma-ceuticals	Resmetirom (MGL-3196)	Selective thyroid hormone receptor-β agonist	125	(1) Resmetirom 80 mg QD; and (2) Placebo	252	Change in liver fat fraction measured by MRI-PDFF	80 mg *vs* placebo reduction of hepatic fat at week 12 (-32.9% *vs* -10.4%; P < 0·0001) and week 36 (-37.3% *vs* -8.5%; P < 0·0001)
NCT02784444	Cirius Therapeutics	MSDC-0602K	Insulin sensitizer designed to preferentially target the mitochondrial pyruvate carrier with direct binding to the transcriptional factor PPARγ	392	(1) MSDC-0602K 62.5 mg QD; (2) MSDC-0602K 125 mg QD; (3) MSDC-0602K 250 mg QD; and (4) Placebo	364	Hepatic histological and activity score improvement in either ballooning or lobular inflammationNo increase in fibrosis stage at 12 mo	Primary end point placebo 29.7%, *vs* 62.5 mg 29.8%, *vs* 125 mg 32.9% *vs* 250 mg 39.5% (95%CI: 0.44–1.81) (95%CI: 0.60–2.48), (95%CI: 0.83–3.27)

FGF: Fibroblast growth factor; MRI-PDFF: Magnetic resonance imaging with proton density fat fraction; GLP-1: Glucagon-like peptide-1; FXR: Farnesoid X receptor; PPAR: Peroxisome proliferator-activated receptor; FASN: Fatty acid synthase.

summarized in Table 1[14]. Firsocostat (GS-0976) is an inhibitor of ACC (acetyl-coenzyme A carboxylase) which catalyzes de novo lipogenesis in the liver. In a randomized placebo-controlled trial, firsocostat 20 mg decreased hepatic steatosis and surrogate markers of fibrosis[15]. VK2809 is a small

molecule prodrug of a potent thyroid beta receptor agonist which has demonstrated favorable effects on lipid metabolism and biomarkers of hepatic steatosis and steatohepatitis in a phase 2 trial, supporting its potential role in patients with NASH[16]. MSDC-0602K is a novel insulin sensitizer designed to preferentially target the mitochondrial pyruvate carrier while minimizing direct binding to the transcriptional factor PPARγ. MSDC-0602K did not demonstrate statistically significant effects on primary and secondary histologic endpoints in a phase 2 trial, but favorable effects on liver cell injury and glucose metabolism support further investigation for in patients with type 2 diabetes[17].

DRUGS IN DEVELOPMENT–PHASE 3

Novel investigational agents which have completed are undergoing evaluation in phase 3 trials are summarized in Table 2. Obeticholic acid, an FXR agonist, has been shown to improve the histological features of NASH, with fibrosis improvement in 23% of patients treated with Obeticholic acid compared with 12% in placebo group[18]. Elafibranor, a PPAR agonist, improves liver enzymes, lipids, glucose levels, and markers of systemic inflammation and is being tested in a phase 3 study (NCT02704403)[19]. Aramchol inhibits steroyl-CoA desaturase 1, a key enzyme in hepatic lipogenesis that converts saturated fatty acids into monounsaturated fatty acid. In the phase 2b ARREST trial, aramchol demonstrated liver fat reduction, biochemical improvement, NASH resolution and fibrosis reduction in a dose response pattern[20]. It has since been included in an ongoing phase 3 trial to test its safety and efficacy (NCT04104321). Cenicriviroc is an oral, dual antagonist of C-C motif chemokine receptor (CCR) types 2 and 5. It has shown anti-inflammatory and anti-fibrotic properties, which are mediated by CCR types 2 and 5 (CCR2/CCR5) blockade. In a randomized double-blind phase 2b study of 289 subjects, cenicriviroc was associated with a statistically significant improvement in NASH fibrosis of one stage or greater *vs* placebo (20% *vs* 10%; P = 0.02)[21]. A phase 3 randomized, double-blind, placebo-controlled trial (AURORA) is currently ongoing with evaluation of 2000 adults with NASH who are treated with cenicriviroc or placebo for 52 wk[22]. Resmetirom is a liver-directed, orally active, selective thyroid hormone receptor-β agonist designed to improve NASH by increasing hepatic fat metabolism and reducing lipotoxicity. In a phase 2b study, resmetirom treated patients showed a relative reduction of hepatic fat compared with placebo with statistically significant NASH resolution *vs* placebo[23], and is currently under evaluation in a phase 3 registration trial (NCT03900429). GR-MD-02 (belapectin), is an inhibitor of galectin 3 that reduces liver fibrosis and portal hypertension. In a phase 2 trial, belapectin was safe but not associated with significant reduction in hepatic venous pressure gradient (HVPG) or fibrosis. However, in a subgroup analysis of patients without esophageal varices, 2 mg/kg belapectin reduced HVPG and development of varices, suggesting a possible benefit in patients with NASH cirrhosis without esophageal varices[24] . In the phase 3 NAVIGATE trial, the safety and efficacy of belapectin is under evaluation with primary clinical endpoints of development of varices and event-free survival (NCT04365868).

COMBINATION THERAPEUTICS

The rationale of combining two or more strategies for NASH therapy aims to augment rates of NASH resolution and NASH fibrosis improvement. By targeting the development of steatohepatitis, liver fibrosis as well as controlling metabolic syndrome, we may achieve response rates higher than 32% as seen currently *via* trials of drugs as monotherapy[6]. Table 3 is a collection of studies currently underway, and some completed, that evaluate multidrug regimens for the treatment of NASH. FXR agonists, which regulate bile acid metabolism, are one major class of drugs incorporated in many of these trials. Obeticholic acid, a promising drug in this class, has demonstrated the dose-dependent ability to improve liver fibrosis and steatohepatitis in NASH patients with stage F2/F3 fibrosis based on initial and secondary analysis of the REGENERATE trials[18,25]. Cilofexor, another FXR agonist, has been tested in combination with firsocostat, an ACC inhibitor and selonsertib, an ASK1 inhibitor, in the phase 2b ATLAS study that demonstrated improvements in liver enzymes, fibrosis, NAS score on histology and improvements in liver elastography in the cilofexor/firsocostat group compared to placebo[26]. Ongoing studies with tropifexor include combinations with cenicriviroc and LYS0006 with early results still pending and waiting to be reviewed.

By now it is well known that features of metabolic syndrome increase the risk of developing NAFLD. Type 2 diabetes, specifically, is a risk factor for NASH and its presence increases the risk of progression of NASH fibrosis[27,28]. Therefore, some of the ongoing trials in combination therapy for NASH include semaglutide, pioglitazone or licogliflozin; from drug classes that traditionally have been utilized for the management of T2DM. In one randomized, placebo controlled trial in patients with biopsy proven NASH, a GLP-1 analog, liraglutide, was associated with greater improvement in steatohepatitis and lower progression of fibrosis[9]. A proof-of-concept trial is currently underway including semaglutide along with cilofexor and firsocostat. Licogliflozin, which has shown benefit in lowering liver fat content, is being studied as part of a combination trial with tropifexor in the ELIVATE trial.

Table 2 Phase 3 trials in non-alcoholic steatohepatitis

Trial name/NCT number	Manufacturer	Drugs	Mechanism of action	Enrollment (targeted)	Study arms	Duration (weeks)	Primary or relevant end point(s)	Results
REGENERATE/NCT02548351	Intercept Pharmaceuticals	Obeticholic acid	Farnesoid X receptor agonist	2480	(1) Obeticholic acid 10 mg QD; (2) Obeticholic acid 25 mg QD; and (3) Placebo	72-378	Fibrosis improvement (≥ 1 stage) with no worsening of NASH, or NASH resolution with no worsening of fibrosis	Fibrosis improvement endpoint- (12%) placebo, (18%) obeticholic acid 10 mg, (23%) obeticholic acid group 25 mg. Safety most common adverse event was pruritus
RESOLVE-IT/NCT02704403	Genfit	Elafibranor	PPAR agonist	2157	(1) Elafibranor 120 mg QD; and (2) Placebo	72-216	Change in fibrosis. Change in histologic score of NASH	ongoing
ARMOR/NCT0410432	Galmed pharma-ceuticals	Aramchol	SCD-1 inhibitor	247	(1) Aramchol 600 mg QD; (2) Aramchol 400 mg qd; and (3) Placebo	364	(1) Evaluate the safety and efficacy as measured with % change in the liver triglycerides concen-tration; and (2) Safety	Ongoing
AURORA/NCT03028740	Tobira Therapeutics	Cenicriviroc	Dual antagonist of CCR types 2 and 5	2000	(1) Cenicriviroc 150 mg; and (2) Placebo	364	(1) Proportion of subjects with ≥ 1-stage improvement in liver fibrosis and no worsening of steatohepatitis at month 12 relative to screening; and (2) Safety	Ongoing
MAESTRO-NASH/ NCT03900429	Madrigal Pharmaceuticals	Resmetirom	Selective thyroid hormone receptor-β agonist	2000	(1) resmetirom 80 mg QD; (2) resmetirom 100 mg QD; and (3) Placebo	364	NASH resolution, with at least a 2-point reduction in NAS (NASH Activity Score-biopsy), and with no worsening of fibrosis. Secondary end p. (1) Liver fibrosis improvement of at least one stage, with no worsening of NASH; and (2) Lowering of LDL-cholesterol	Ongoing
NAVIGATE/NCT04365868	Galectin Therapeutics	GR-MD-02 (belapectin)	Inhibitor of galectin 3	1010	(1) Belapectin 2 mg/kg intravenously (IV) every other week; (2) Belapectin 4 mg/kg intravenously (IV) every other week; and (3) Placebo	504	Development of new esophageal varices at 78 weeks in the belapectin group Cumulative incidence rate of decompensations and event-free survival by time to first cirrhosis related clinical event	Ongoing

PPAR: Peroxisome proliferator-activated receptor; SCD-1: Steroyl-CoA desaturase 1; CCR: C-C motif chemokine receptor

Numerous trials have already established the benefit of pioglitazone in improving inflammation and fibrosis in patients with biopsy proven NASH and therefore it is included as recommended manage-ment for a select group of patients according to the most recent American Association for the Study of Liver Diseases guidelines on NAFLD[29].

Aside from the ability to decrease inflammation and fibrosis in NASH, allowing treatment with lower doses of various drugs in combination or improvement the side effect profile are two alternate motives for pursuing combination therapy. In Wister rat models for NASH, one group was able to demonstrate a synergistic therapeutic effect on inflammation and oxidative stress from combining elafibranor and obeticholic acid at lower doses than with each drug in monotherapy[30]. FXR agonists have been shown to increase low density lipoprotein (LDL) cholesterol concentrations. In the CONTROL study, the

Table 3 Multidrug regimens for the treatment of non-alcoholic steatohepatitis

Trial name/NCT number	Phase	Manufacturer	Drugs	Mechanism of action	Enrollment (targeted)	Study arms	Duration (weeks)	Primary or relevant end point(s)
NCT02781584 (Proof of Concept)	1	Gilead Sciences	Selonsertib, firsocostat, cilofexor, fenofibrate, icosapent ethyl	(1) Selonsertib-selective ASK1 inhibitor; (2) Firsocostat-ACC inhibitor; (3) Cilofexor-FXR agonist; (4) Fenofibrate-PPAR agonist; and (5) Icosapent ethyl-under investigation	220	(1) Selonsertib; (2) Firsocostat; (3) Cilofexor; (4) Selonsertib + cilofexor; (5) Selonsertib + firsocostat; (6) Firsocostat + cilofexor; (7) Firsocostat (cirrhotic patients); (8) Cilofexor (cirrhotic patients); (9) Selonsertib + firsocostat + cilofexor; (10) Firsocostat + fenofibrate 48 mg; (11) Firsocostat + fenofibrate 145 mg; and (12) Icosapent ethyl + firsocostat + cilofexor	12	(1) Adverse events; (2) Serious adverse events; and (3) Lab abnormalities
ATLAS/NCT03449446	2	Gilead Sciences	Selonsertib, firsocostat, cilofexor	(1) Selonsertib-selective ASK1 inhibitor; (2) Firsocostat-ACC inhibitor; and (3) Cilofexor-FXR agonist	395	(1) Selonsertib + firsocostat + placebo; (2) Selonsertib + cilofexor + placebo; (3) Firsocostat + cilofexor + placebo; (4) Selonsertib + placebo + placebo; (5) Firsocostat + placebo + placebo; (6) Cilofexor + placebo + placebo; and (7) 3 placebos	48	(1) Adverse events; (2) Lab abnormalities; and (3) Improvement of ≥ 1-stage in fibrosis without worsening of NASH
NCT03987074	2	Gilead Sciences, Novo Nordisk	Cilofexor, semaglutide, firsocostat	(1) Semaglutide-GLP-1 agonist; (2) Firsocostat-ACC inhibitor; and (3) Cilofexor-FXR agonist	109	(1) Semaglutide; (2) Firsocostat + semaglutide; (3) Semaglutide + cilofexor 30 mg; (4) Semaglutide + cilofexor 100 mg; and (5) Semaglutide + firsocostat + cilofexor	24	(1) Adverse events; (2) Serious adverse events; and (3) Lab abnormalities
ELIVATE/NCT04065841	2	Novartis	Tropifexor, licogliflozin	(1) Tropifexor-FXR agonist; and (2) Licogliflozin-SGLT1/2 inhibitor	380	(1) Tropifexor + licogliflozin; (2) Tropifexor + placebo; (3) Licogliflozin + placebo; and (4) 2 placebos	48	(1) Improvement of ≥ 1-stage in fibrosis without worsening of NASH; and (2) Resolution of NASH without worsening fibrosis
NCT03776175	2A	Pfizer	PF-05221304, PF-06865571	(1) PF-05221304-ACC inhibitor; and (2) PF-06865571 - DGAT 2 inhibitor	99	(1) ACC inhibitor + placebo; (2) DGAT2 inhibitor + placebo; (3) ACC inhibitor + DGAT2 inhibitor; and (4) 2 placebos	6	Improvement in fat fraction
TANDEM/NCT03517540	2	Novartis, Allergan	Tropifexor, cenicriviroc	(1) Tropifexor-FXR agonist; and (2) Cenicriviroc-CCR2/CCR5 inhibitor	193	(1) Tropifexor; (2) Cenicriviroc; (3) Tropifexor dose 1 + cenicriviroc; and (4) Tropifexor dose 2 + cenicriviroc	48	(1) improvement in fibrosis; and (2) Resolution of steato-hepatitis
CONTROL/NCT02633956	2	Intercept Pharmaceuticals	Obeticholic acid, atorvastatin	(1) Obeticholic acid-FXR agonist; and (2) Atorvastatin-HMG-CoA reductase inhibitor	84	(1) Obeticholic acid 5 mg/10 mg/25 mg + atorvastatin 10 mg/20 mg; and (2) Placebo + atorvastatin 10 mg/20 mg	16	(1) Change in LDL concen-tration; (2) Change in LDL particle size; and (3) Change in LDL particle concentration
NCT04235205	2	Albireo Pharma	Elobixibat, cholestyramine	(1) Elobixibat-IBAT inhibitor; and (2) Cholestyramine-bile acid binding resin	100	(1) Elobixibat + cholestyramine; (2) Elobixibat + placebo; (3) Placebo + cholestyramine; and (4) 2 placebos	16	(1) Change in liver fat fraction measured by MRI-PDFF; and (2) Change in fibrosis measured by MRE
PUVENAFLD/NCT04198805	2	DSM Nutritional Products	Vitamin E, omega-3 fatty acid	(1) Vitamin E-scavenging reactive oxidation species; and (2) Omega 3 FA-competing with omega 6 for cycloox-genase and lipoxygenase-mediated	200	(1) Vitamin E + placebo; (2) Omega-3 fatty acid + placebo; (3) Omega 3-fatty acid + vitamin E; and (4) 2 placebos	24	(1) Change in liver fat fraction measured by MRI-PDFF; (2) Change in liver enzymes; and (3) FIB-4 scores

				inflammatory eicosanoid production, forming anti-inflammatory compounds				
NEXSCOT/NCT04147195	2	Novartis	LYS006, tropifexor	(1) Tropifexor-FXR agonist; and (2) LYS006-leukotriene A4 hydrolase inhibitor	250	(1) LYS006; and (2) LYS006 + tropifexor	21	(1) Change in ELF score; and (2) Change in liver fat fraction measured by MRI-PDFF
NCT02466516	2	Gilead Sciences	Selonsertib, simtuzumab	(1) Selonsertib-selective ASK1 inhibitor; and (2) Simtuzumab-lysyl oxidase-like 2 inhibitor	72	(1) Selonsertib 6 mg; (2) Selonsertib 18 mg; (3) Selonsertib 6 mg + simtuzumab; (4) Selonsertib 18 mg + simtuzumab; and (5) Simtuzumab	24	(1) Adverse events; (2) Serious adverse events; (3) Lab abnormalities; and (4) Number of participants who prematurely discontinued study due to adverse events
NCT01703260	2	AstraZeneca	Roflumilast, pioglitazone	(1) Roflumilast-phosphodiesterase 4 inhibitor; and (2) Pioglitazone-PPAR agonist	16	(1) Roflumilast + pioglitazone; (2) Roflumilast + placebo; and (3) Pioglitazone + placebo	20	(1) Change in liver enzymes; and (2) Change in liver fat fraction measured by MRI-PDFF

ASK1: Apoptosis signal-regulating kinase-1; ACC: Acetyl-coenzyme A carboxylase; FXR: Farnesoid X receptor; PPAR: Peroxisome proliferator-activated receptor; GLP-1: Glucagon-like peptide-1; SGLT: Sodium/glucose transport protein; DGAT: Diacylglycerol acyltransferase; CCR: C-C motif chemokine receptor; IBAT: Ileal bile acid transporter.

authors were able to lower the LDL concentration below baseline with the addition of atorvastatin[31]. In a separate phase 2, proof-of-concept trial, fenofibrate was tested in combination with the ACC inhibitor, firsocostat, to help lower triglyceride levels[32].

CONCLUSION

In this concise review, we have discussed numerous possible therapeutic options for cessation or reversal of NASH and associated fibrosis. It is clear that NASH and particularly NASH fibrosis or cirrhosis is a leading topic garnering much interest in the study of liver diseases today, which would be appropriate considering the clinical impact. Although some of the above targets may seem promising, there are still a few concerns regarding study of this particular topic. Firstly, it is evident by reviewing the endpoints of each of the studies listed above that there is much heterogeneity. This is partly because the gold standard of liver biopsy to prove effectiveness in this endeavor is cumbersome, costly, and generally not favored by patients. The use of surrogates for liver fibrosis and resolution including markers of turnover, inflammation, or non-invasive assessments of liver scarring have not universally been agreed upon in the use of clinical trials. Secondly, for those studies that have utilized liver biopsies are part of their endpoint assessment, there can be considerable inter-observer variability in interpretation of liver biopsy specimens, assuming they are of adequate quality. Additionally, it is apparent that many of the study developers use magnetic resonance imaging with proton density fat fraction for assessment of liver fat content while there are additional tools such as the controlled attenuation parameter of transient elastography systems which might be more acceptable as a point of

care test. Lastly, endoscopic and surgical bariatrics represent an emerging area of therapeutic development for the management of obesity in context of NASH. In one prospective study of 180 patients, bariatric surgery was associated with NASH resolution in 84% of patients with improvement in fibrosis in 70% of patients at the 5 year mark after surgery[33]. Separately, in a 6 mo multi-center study of 85 patients with T2DM undergoing duodenal mucosal resurfacing, not only did their A1c improve, but so did their ALT levels and FIB-4 scores hinting at the possible insulin sensitizing, lipid lowering, anti-inflammatory and antioxidant effects of this procedure[34]. In conclusion, more effective treatments for NASH are urgently needed, and combination pharmacotherapy represents among the most promising approaches in develpoment.

FOOTNOTES

REFERENCES

1   **Paik JM**, Henry L, De Avila L, Younossi E, Racila A, Younossi ZM. Mortality Related to Nonalcoholic Fatty Liver Disease Is Increasing in the United States. *Hepatol Commun* 2019; **3**: 1459-1471 [PMID: 31701070 DOI: 10.1002/hep4.1419]

2   **Wong RJ**, Aguilar M, Cheung R, Perumpail RB, Harrison SA, Younossi ZM, Ahmed A. Nonalcoholic steatohepatitis is the second leading etiology of liver disease among adults awaiting liver transplantation in the United States. *Gastroenterology* 2015; **148**: 547-555 [PMID: 25461851 DOI: 10.1053/j.gastro.2014.11.039]

3   **Friedman SL**, Neuschwander-Tetri BA, Rinella M, Sanyal AJ. Mechanisms of NAFLD development and therapeutic strategies. *Nat Med* 2018; **24**: 908-922 [PMID: 29967350 DOI: 10.1038/s41591-018-0104-9]

4   **Kuchay MS**, Krishan S, Mishra SK, Farooqui KJ, Singh MK, Wasir JS, Bansal B, Kaur P, Jevalikar G, Gill HK, Choudhary NS, Mithal A. Effect of Empagliflozin on Liver Fat in Patients With Type 2 Diabetes and Nonalcoholic Fatty Liver Disease: A Randomized Controlled Trial (E-LIFT Trial). *Diabetes Care* 2018; **41**: 1801-1808 [PMID: 29895557 DOI: 10.2337/dc18-0165]

5   **Petit JM**, Cercueil JP, Loffroy R, Denimal D, Bouillet B, Fourmont C, Chevallier O, Duvillard L, Vergès B. Effect of Liraglutide Therapy on Liver Fat Content in Patients With Inadequately Controlled Type 2 Diabetes: The Lira-NAFLD Study. *J Clin Endocrinol Metab* 2017; **102**: 407-415 [PMID: 27732328 DOI: 10.1210/jc.2016-2775]

6   **Dufour JF**, Caussy C, Loomba R. Combination therapy for non-alcoholic steatohepatitis: rationale, opportunities and challenges. *Gut* 2020; **69**: 1877-1884 [PMID: 32381514 DOI: 10.1136/gutjnl-2019-319104]

7   **Services USD of H and H**. Noncirrhotic nonalcoholic steatohepatitis with liver fibrosis: developing drugs for treatment. *Guid Ind* 2018 [DOI: 10.1016/b978-0-323-99764-5.00013-5]

8   **Kaufman A**, Abuqayyas L, Denney WS, Tillman EJ, Rolph T. AKR-001, an Fc-FGF21 Analog, Showed Sustained Pharmacodynamic Effects on Insulin Sensitivity and Lipid Metabolism in Type 2 Diabetes Patients. *Cell Rep Med* 2020; **1**: 100057 [PMID: 33205064 DOI: 10.1016/j.xcrm.2020.100057]

9   **Armstrong MJ**, Gaunt P, Aithal GP, Barton D, Hull D, Parker R, Hazlehurst JM, Guo K; LEAN trial team, Abouda G, Aldersley MA, Stocken D, Gough SC, Tomlinson JW, Brown RM, Hübscher SG, Newsome PN. Liraglutide safety and efficacy in patients with non-alcoholic steatohepatitis (LEAN): a multicentre, double-blind, randomised, placebo-controlled phase 2 study. *Lancet* 2016; **387**: 679-690 [PMID: 26608256 DOI: 10.1016/S0140-6736(15)00803-X]

10 **Newsome PN**, Buchholtz K, Cusi K, Linder M, Okanoue T, Ratziu V, Sanyal AJ, Sejling AS, Harrison SA; NN9931-4296 Investigators. A Placebo-Controlled Trial of Subcutaneous Semaglutide in Nonalcoholic Steatohepatitis. *N Engl J Med* 2021; **384**: 1113-1124 [PMID: 33185364 DOI: 10.1056/NEJMoa2028395]

11   **Traussnigg S**, Schattenberg JM, Demir M, Wiegand J, Geier A, Teuber G, Hofmann WP, Kremer AE, Spreda F, Kluwe J, Petersen J, Boettler T, Rainer F, Halilbasic E, Greinwald R, Pröls M, Manns MP, Fickert P, Trauner M; Austrian/German NAFLD-norUDCA study group. Norursodeoxycholic acid versus placebo in the treatment of non-alcoholic fatty liver disease: a double-blind, randomised, placebo-controlled, phase 2 dose-finding trial. *Lancet Gastroenterol Hepatol* 2019; **4**: 781-793 [PMID: 31345778 DOI: 10.1016/S2468-1253(19)30184-0]

12   **Harrison SA**, Neff G, Guy CD, Bashir MR, Paredes AH, Frias JP, Younes Z, Trotter JF, Gunn NT, Moussa SE, Kohli A, Nelson K, Gottwald M, Chang WCG, Yan AZ, DePaoli AM, Ling L, Lieu HD. Efficacy and Safety of Aldafermin, an Engineered FGF19 Analog, in a Randomized, Double-Blind, Placebo-Controlled Trial of Patients With Nonalcoholic Steatohepatitis. *Gastroenterology* 2021; **160**: 219-231.e1 [PMID: 32781086 DOI: 10.1053/j.gastro.2020.08.004]

13   **Tropifexor SA**. A highly potent FXR agonist, produces robust and dose-dependent reductions in hepatic fat and serum alanine aminotransferase in patients with fibrotic NASH after 12 wk of therapy: FLIGH-FXR part C interim results. *Hepatology* 2019; 70 [DOI: 10.1016/j.dld.2019.12.129]

14   **Loomba R**, Rinella M, Harrison S, Wong VW-S, Ratziu V, Mohseni R, Lucas KJ, Perry RG, Rahmini R, Trotter JF. Novel first-in-class, fatty acid synthase inhibitor, TVB-2640 vs. placebo demonstrates clinically significant reduction in liver fat by MRI-PDFF in NASH: a phase 2 randomised controlled trial (FASCINATE-1). *J Hepatol* 2020; **73**: S53-S54 [DOI: 10.1016/s0168-8278(20)30653-x]

15   **Loomba R**, Kayali Z, Noureddin M, Ruane P, Lawitz EJ, Bennett M, Wang L, Harting E, Tarrant JM, McColgan BJ, Chung C, Ray AS, Subramanian GM, Myers RP, Middleton MS, Lai M, Charlton M, Harrison SA. GS-0976 Reduces Hepatic Steatosis and Fibrosis Markers in Patients With Nonalcoholic Fatty Liver Disease. *Gastroenterology* 2018; **155**: 1463-1473.e6 [PMID: 30059671 DOI: 10.1053/j.gastro.2018.07.027]

16   **Loomba R**, Neutel J, Mohseni R, Bernard D, Severance R, Dao M, Saini S, Margaritescu C, Homer K, Tran B, Mancini M, Masamune H, Lian B. LBP-20-VK2809, a Novel Liver-Directed Thyroid Receptor Beta Agonist, Significantly Reduces Liver Fat with Both Low and High Doses in Patients with Non-Alcoholic Fatty Liver Disease: A Phase 2 Randomized, Placebo-Controlled Trial. *J Hepatol* 2019; **70**: e150-1 [DOI: 10.1016/s0618-8278(19)30266-x]

17   **Harrison SA**, Alkhouri N, Davison BA, Sanyal A, Edwards C, Colca JR, Lee BH, Loomba R, Cusi K, Kolterman O, Cotter G, Dittrich HC. Insulin sensitizer MSDC-0602K in non-alcoholic steatohepatitis: A randomized, double-blind, placebo-controlled phase IIb study. *J Hepatol* 2020; **72**: 613-626 [PMID: 31697972 DOI: 10.1016/j.jhep.2019.10.023]

18   **Younossi ZM**, Ratziu V, Loomba R, Rinella M, Anstee QM, Goodman Z, Bedossa P, Geier A, Beckebaum S, Newsome PN, Sheridan D, Sheikh MY, Trotter J, Knapple W, Lawitz E, Abdelmalek MF, Kowdley KV, Montano-Loza AJ, Boursier J, Mathurin P, Bugianesi E, Mazzella G, Olveira A, Cortez-Pinto H, Graupera I, Orr D, Gluud LL, Dufour JF, Shapiro D, Campagna J, Zaru L, MacConell L, Shringarpure R, Harrison S, Sanyal AJ; REGENERATE Study Investigators. Obeticholic acid for the treatment of non-alcoholic steatohepatitis: interim analysis from a multicentre, randomised, placebo-controlled phase 3 trial. *Lancet* 2019; **394**: 2184-2196 [PMID: 31813633 DOI: 10.1016/S0140-6736(19)33041-7]

19   **Ratziu V**, Harrison SA, Francque S, Bedossa P, Lehert P, Serfaty L, Romero-Gomez M, Boursier J, Abdelmalek M, Caldwell S, Drenth J, Anstee QM, Hum D, Hanf R, Roudot A, Megnien S, Staels B, Sanyal A; GOLDEN-505 Investigator Study Group. Elafibranor, an Agonist of the Peroxisome Proliferator-Activated Receptor-α and -δ, Induces Resolution of Nonalcoholic Steatohepatitis Without Fibrosis Worsening. *Gastroenterology* 2016; **150**: 1147-1159.e5 [PMID: 26874076 DOI: 10.1053/j.gastro.2016.01.038]

20   **Ratziu V**, Ladron-De-Guevara L, Safadi R, Poordad F, Fuster F, Flores-Figueroa J, Harrison SA, Arrese M, Fargion S, Ben-Bashat D.   One-year results of the global phase 2b randomized placebo-controlled arrest trial of aramchol, a stearoyl CoA desaturase inhibitor, in patients with NASH. In: Hepatology. WILEY 111 RIVER ST, HOBOKEN 07030-5774, NJ United States, 2018: 1448A-1449A

21   **Friedman SL**, Ratziu V, Harrison SA, Abdelmalek MF, Aithal GP, Caballeria J, Francque S, Farrell G, Kowdley KV, Craxi A, Simon K, Fischer L, Melchor-Khan L, Vest J, Wiens BL, Vig P, Seyedkazemi S, Goodman Z, Wong VW, Loomba R, Tacke F, Sanyal A, Lefebvre E. A randomized, placebo-controlled trial of cenicriviroc for treatment of nonalcoholic steatohepatitis with fibrosis. *Hepatology* 2018; **67**: 1754-1767 [PMID: 28833331 DOI: 10.1002/hep.29477]

22   **Anstee QM**, Neuschwander-Tetri BA, Wong VW, Abdelmalek MF, Younossi ZM, Yuan J, Pecoraro ML, Seyedkazemi S, Fischer L, Bedossa P, Goodman Z, Alkhouri N, Tacke F, Sanyal A. Cenicriviroc for the treatment of liver fibrosis in adults with nonalcoholic steatohepatitis: AURORA Phase 3 study design. *Contemp Clin Trials* 2020; **89**: 105922 [PMID: 31881392 DOI: 10.1016/j.cct.2019.105922]

23   **Harrison SA**, Bashir MR, Guy CD, Zhou R, Moylan CA, Frias JP, Alkhouri N, Bansal MB, Baum S, Neuschwander-Tetri BA, Taub R, Moussa SE. Resmetirom (MGL-3196) for the treatment of non-alcoholic steatohepatitis: a multicentre, randomised, double-blind, placebo-controlled, phase 2 trial. *Lancet* 2019; **394**: 2012-2024 [PMID: 31727409 DOI: 10.1016/S0140-6736(19)32517-6]

24   **Chalasani N**, Abdelmalek MF, Garcia-Tsao G, Vuppalanchi R, Alkhouri N, Rinella M, Noureddin M, Pyko M, Shiffman M, Sanyal A, Allgood A, Shlevin H, Horton R, Zomer E, Irish W, Goodman Z, Harrison SA, Traber PG; Belapectin (GR-MD-02) Study Investigators. Effects of Belapectin, an Inhibitor of Galectin-3, in Patients With Nonalcoholic Steatohepatitis With Cirrhosis and Portal Hypertension. *Gastroenterology* 2020; **158**: 1334-1345.e5 [PMID: 31812510 DOI: 10.1053/j.gastro.2019.11.296]

25   **Sanyal AJ**, Ratziu V, Loomba R, Rinella M, Anstee QM, Goodman Z, Bedossa P, Khalili M, Boursier J, Stinton L. Obeticholic acid treatment in patients with non-alcoholic steatohepatitis: a secondary analysis in the regenerate study across fibrosis stages. In: AISF Annual Meeting 2020, 2020: 46–7

26   **Loomba R**, Noureddin M, Kowdley KV, Kohli A, Sheikh A, Neff G, Bhandari BR, Gunn N, Caldwell SH, Goodman Z, Wapinski I, Resnick M, Beck AH, Ding D, Jia C, Chuang JC, Huss RS, Chung C, Subramanian GM, Myers RP, Patel K, Borg BB, Ghalib R, Kabler H, Poulos J, Younes Z, Elkhashab M, Hassanein T, Iyer R, Ruane P, Shiffman ML, Strasser S, Wong VW, Alkhouri N; ATLAS Investigators. Combination Therapies Including Cilofexor and Firsocostat for Bridging Fibrosis and Cirrhosis Attributable to NASH. *Hepatology* 2021; **73**: 625-643 [PMID: 33169409 DOI: 10.1002/hep.31622]

27   **Neuschwander-Tetri BA**, Clark JM, Bass NM, Van Natta ML, Unalp-Arida A, Tonascia J, Zein CO, Brunt EM, Kleiner DE, McCullough AJ, Sanyal AJ, Diehl AM, Lavine JE, Chalasani N, Kowdley KV; NASH Clinical Research Network.

Clinical, laboratory and histological associations in adults with nonalcoholic fatty liver disease. *Hepatology* 2010; **52**: 913-924 [PMID: 20648476 DOI: 10.1002/hep.23784]

28   **Younossi ZM**, Gramlich T, Matteoni CA, Boparai N, McCullough AJ. Nonalcoholic fatty liver disease in patients with type 2 diabetes. *Clin Gastroenterol Hepatol* 2004; **2**: 262-265 [PMID: 15017611 DOI: 10.1016/s1542-3565(04)00014-x]

29   **Chalasani N**, Younossi Z, Lavine JE, Charlton M, Cusi K, Rinella M, Harrison SA, Brunt EM, Sanyal AJ. The diagnosis and management of nonalcoholic fatty liver disease: Practice guidance from the American Association for the Study of Liver Diseases. *Hepatology* 2018; **67**: 328-357 [PMID: 28714183 DOI: 10.1002/hep.29367]

30   **Noel B**, Ratziu V, Harrison S, Rigou G, degallaix nathalie, texier frederic, Brozek J, Daix V, Belanger C, roudot alice, megnien sophie, hum dean, staels bart, Walczak R, sanyal arun.   Combination drug therapy allows synergistic therapeutic dosereduction in NASH: A case study of ELAFIBRANOR (GFT505) and an FXR agonist combination in a model of severe NASH. 2017. [cited 10 January 2022]. Available from: https://linkinghub.elsevier.com/retrieve/pii/S0168827817304877

31   **Pockros PJ**, Fuchs M, Freilich B, Schiff E, Kohli A, Lawitz EJ, Hellstern PA, Owens-Grillo J, Van Biene C, Shringarpure R, MacConell L, Shapiro D, Cohen DE. CONTROL: A randomized phase 2 study of obeticholic acid and atorvastatin on lipoproteins in nonalcoholic steatohepatitis patients. *Liver Int* 2019; **39**: 2082-2093 [PMID: 31402538 DOI: 10.1111/liv.14209]

32   **Lawitz EJ**, Neff G, Ruane PJ, Younes Z, Zhang J, Jia C, Chuang J, Huss R, Chung C, Subramanian M.   Fenofibrate mitigates increases in serum triglycerides due to the ACC inhibitor firsocostat in patients with advanced fibrosis due to NASH: a phase 2 randomized trial. In: Hepatology. WILEY 111 RIVER ST, HOBOKEN 07030-5774, NJ United States, 2019: 1489A-1490A

33   **Lassailly G**, Caiazzo R, Ntandja-Wandji LC, Gnemmi V, Baud G, Verkindt H, Ningarhari M, Louvet A, Leteurtre E, Raverdy V, Dharancy S, Pattou F, Mathurin P. Bariatric Surgery Provides Long-term Resolution of Nonalcoholic Steatohepatitis and Regression of Fibrosis. *Gastroenterology* 2020; **159**: 1290-1301.e5 [PMID: 32553765 DOI: 10.1053/j.gastro.2020.06.006]

34   **van Baar ACG**, Beuers U, Wong K, Haidry R, Costamagna G, Hafedi A, Deviere J, Ghosh SS, Lopez-Talavera JC, Rodriguez L, Galvao Neto MP, Sanyal A, Bergman JJGHM. Endoscopic duodenal mucosal resurfacing improves glycaemic and hepatic indices in type 2 diabetes: 6-month multicentre results. *JHEP Rep* 2019; **1**: 429-437 [PMID: 32039394 DOI: 10.1016/j.jhepr.2019.10.006]

ORIGINAL ARTICLE

Basic Study

Long noncoding RNA negative regulator of antiviral response contributes to pancreatic ductal adenocarcinoma progression *via* targeting miR-299-3p

Hai-Quan Wang, Chun-Hua Qian, Zeng-Ya Guo, Pei-Ming Li, Zheng-Jun Qiu

Hai-Quan Wang, Zheng-Jun Qiu, Department of General Surgery, Shanghai General Hospital of Nanjing Medical University, Shanghai 200080, China

Hai-Quan Wang, Zeng-Ya Guo, Pei-Ming Li, Zheng-Jun Qiu, Department of General Surgery, Shanghai Jiao Tong University School of Medicine, Shanghai 200080, China

Chun-Hua Qian, Department of Endocrinology and Metabolism, Shanghai Tenth People's Hospital, Shanghai 200072, China

Corresponding author: Zheng-Jun Qiu, MD, Chief Doctor, Director, Surgeon, Department of General Surgery, Shanghai General Hospital of Nanjing Medical University, No. 100 Haining Road, Shanghai 200080, China. qiuzjdoctor@sina.com

Abstract

BACKGROUND
Pancreatic ductal cancer (PDAC) has high malignancy and poor prognosis. Long noncoding RNAs (lncRNAs) are associated with high levels of malignancy, including PDAC. However, the biological and clinical significance of negative regulator of antiviral response (NRAV) in PDAC is unclear.

AIM
To study the regulatory role of lncRNA NRAV in PDAC.

METHODS
GEPIA analyzed lncRNA NRAV and miRNA (miR-299-3p) expression levels in PDAC tissues and measured them in PDAC cells by quantitative measurements in real time. The specific role of NRAV and miR-299-3p in cell proliferation and transfer potential was evaluated by cell formation analysis, Cell Counting Kit-8 and Transwell analysis. The relationship between NRAV and miR-299-3p was studied by predictive bioinformatics, RNA immunoassay, and fluorescence enzyme analysis. *In vivo* experiments included transplantation of simulated tumor cells under naked mice.

RESULTS
The expression level of lncRNA NRAV was higher in both tumor tissues and cell lines of PDAC and was negatively associated with the clinical survival of PDAC

patients. Functionally, overexpression of NRAV promoted cell proliferation and metastasis of PDAC cells, while knockdown of NRAV reversed these effects. Finally, NRAV was performed as a molecular sponge of miR-299-3p. Moreover, overexpression of miR-299-3p could reverse the promoting effects of NRAV on cell proliferation and metastasis of PDAC cells.

CONCLUSION

NRAV facilitates progression of PDAC as a molecular sponge of miR-299-3p and may be a potential molecular marker for diagnosis and treatment of PDAC.

Core Tip: In the present research, the expression level of long noncoding RNA negative regulator of antiviral response (NRAV) in pancreatic ductal adenocarcinoma (PDAC) was detected, and the clinicopathological relationship between NRAV and PDAC was demonstrated. Moreover, cell and animal tests were conducted to assess the concrete roles of NRAV in the progression of PDAC. Finally, the existence of potential specific molecular mechanisms that can provide new ideas for finding new molecular markers for the diagnosis and treatment of PDAC is demonstrated.

INTRODUCTION

As an extremely malignant tumor, pancreatic ductal adenocarcinoma (PDAC) has shown a rapidly increasing incidence rate in recent years worldwide[1]. According to the latest cancer report in 2021, there are 495773 new cases reported globally every year and about 466003 people die of PDAC annually [2]. Due to insufficient means of early diagnosis and effective treatment, the 5-year survival rate of PDAC patients is only about 8% and will drop to about 3% in patients with advanced PDAC[1]. Therefore, it is urgent to establish a comprehensive pathological mechanism of PDAC and explore a more effective PDAC diagnosis and treatment center.

Long noncoding RNAs (lncRNAs) are new ncRNAs that are composed of > 200 nucleotides, accounting for the largest proportion of the entire human gene transcriptome[3,4]. lncRNAs mainly regulate gene expression in a variety of ways, including chromatin remodeling and transcriptional and post-transcriptional processing, and participate in regulating a variety of biological processes[5,6]. Recently, a large number of researches showed that lncRNAs are dysregulated in most tumors and function as key regulators in the process of tumor growth, metastasis, drug tolerance, and angiogenesis [7,8]. The lncRNA negative regulator of antiviral response (NRAV) is a newly identified lncRNA and is mainly related to immunity[9]. Xu *et al*[10] found that NRAV is highly expressed in the cell system of hepatocytes and regulates the course of hepatocellular carcinoma. However, the statements and specific role of NRAV in PDAC are still unclear.

lncRNAs play an important regulatory role in the occurrence and development of various cancers and may be considered a potential molecular marker. Many studies have shown that RNA plays its biological function of competing with endogenous RNAs[11,12]. Hsa-miR-299-3p plays an important role in the development of many cancers. Many studies describe the regulation of the relationship between miR-299-3p and lncRNAs[13,14]. Many experts conducted in-depth research on the regulation of the relationship between the two and stated that miR-299-3p increased the volume and cellular system and prevented proliferation and metastasis of pancreatic cancer cells with exposure to Notch1 [15]. The relationship between NRAV and miR-299-3p in PDAC has not yet been investigated.

In this study, we tested the expression of NRAV in PDAC and studied its function, and found that NRAV and PDAC have obvious overlaps. The results of functional experiments showed that the level of NRAV expression was directly associated with cell proliferation and metastasis and was closely related to the growth of tumors in naked mice. In addition, we found that NRAV, as a molecular sponge of miR-299-3p, contributes to PDAC progression. Therefore, the results of this study may provide new insights into the role of NRAV in PDAC. It can be a biomarker for the diagnosis and treatment of PDAC.

MATERIALS AND METHODS

Cell lines

PDAC cell lines (PANC-1, AsPC-1, Mia Paca-2 and BxPC-3) and human immortalized normal pancreatic duct epithelial (HPDE) cells were obtained from the American Type Culture Collection (Manassas, VA, United States). The cell lines were cultured at an appropriate concentration in a specific environment in a moistened cell incubator with a CO_2 concentration of 5% at 37 °C. Percentage of 10 fetal serum and 1% penicillin–streptomycin were added to the culture medium, including RPMI-1640 and Dulbecco's modified Eagle's medium.

RNA isolation and quantitative real-time polymerase chain reaction

Total cellular RNA was extracted from cultured cells using Trizol reagent (Invitrogen, Carlsbad, CA, United States). For lncRNA, FastKing gDNA Dispeeling RT Supermix (TIANGEN, China) was selected for reverse transclncRNAn. The specific cDNAs of miRNAs were obtained with a specific kit (miDETECT A Track RT Reagent Kit; RiboBio, China). The quantitative real-time polymerase chain reaction (qRT-PCR) system wasABI 7300 PCR (Foster City, CA, United States). *U6* and *ACTB* were respectively deemed as standardized internal controls of miRNA and lncRNA. The specific sequences of the primers were designed as follows. For NRAV, 5'-GGAGTTGATGCCTCCGAACA-3' (forward) and 5'-ATGACCGGAGCTGAAAGGTG-3' (reverse); for β-actin, 5'-TCCCTGGAGAAGAGCTACGA-3' (forward) and 5'-AGCACTGTGTTGGCGTACAG-3' (reverse); for miR-299-3p, 5'-ACACTCCAGCTGG-GTATGTGGGATGGTAAAC-3' (forward) and 5'-GTGCAGGGTCCGAGGT-3' (reverse); and for U6, 5'-CTCGCTTCGGCAGCACA-3' (forward) and 5'-AACGCTTCACGAATTTGCGT-3' (reverse). The relative expression level of each gene was calculated with the $2^{-\Delta\Delta Ct}$ method.

Cell transfection

Lipofectamine 2000 kit (Invitrogen) was used to conduct cell transfection. Short hairpin RNAs (shRNAs) targeting NRAV were designed by Genepharma (Shanghai, China). The specific sequences targeting NRAV were designed as follows: For sh-NRAV #1, 5'-CACCTCATCCACAAGTAGGAC-3'; for sh-NRAV #2, 5'-TTGGAGCCAAGGACTGTACTG-3'; and negative control: 5'-TTCTCCGAACGT-GTCACGT-3'. NRAV overexpression plasmid and shRNAs against NRAV were inserted into the pcDNA3.1 vector and pGpU6/GFP/Neo vector, respectively. The miR-299-3p mimic was purchased from RiboBio. qRT-PCR was performed to examine the transfection efficiency.

Cell Counting Kit-8 assay

A 96-well plate was selected, and 2000 tumor cells were cultured in each well. The cells were transfected with different vectors and allowed to stand for 48 h. Cell Counting Kit-8 (CCK-8) solution (10 µL; Mashiki, Japan) was added to each well, and incubated for 2 h. A microplate reader (Winooski, VT, United States) was used to check cell viability.

Colony formation assay

The specific PDAC cells transfected with different plasmids were inoculated into six-well plates and incubated at 37°C for 10 d. Tumor cells were fixed for 20 min in methanol after being washed with phosphate-buffered saline in triplicate. Cell colonies were stained and counted.

Transwell assay

In migration and invasion assays, PDAC cells were added to resuspension after setting a concentration of 10^5 mL in a serum-free environment. Two hundred microliters of cell suspension was added to the upper layer of each Transwell chamber and 600 µL of complete media containing 10% fetal serum was added to the lower layer. To set up the invasion analysis phase, the Matrigel layer (BD Biosciences, United States) was first applied to the chamber membrane, and the cell suspension was placed on top of the transition chamber. A 24-h incubation was followed and the invasive cells were finally fixed and monitored and compared in five random fields.

Tumor xenograft experiments

All animal studies were approved by the Ethics Committee for Animal Studies at Shanghai 10th People's Hospital. Specific PANC-1 cells ($2 × 10^6$, 200/L) were transplanted subcutaneously to the right side of naked male mice aged 4 wk. The condition of the mice was monitored daily and the size of the tumor was measured every 5 d. Tumor volume was calculated according to tumor length and length formula volume = length through × wide^2/2. Twenty days after inoculation, mice were killed and the entire tumor removed and weighed.

Immunohistochemical analysis

Mouse tumors were removed for immunohistochemical staining to visualize Ki-67 expression. Paraffin-embedded sections were prepared and wax removed in 100% xylene, followed by rehydration with

various gradients of ethanol and distilled water. The fabric is dyed with a protractor for 1 h at room temperature and removed during washing with distilled water. Tissue sections were incubated for 20 min with secondary antibodies bound to horseradish peroxidase. To facilitate visualization, 3,3'-diaminobenzidine tetrahydrochloride Ki-67 was selected for positive staining.

Nuclear/cytoplasmic fractionation assay

The PARIS Kit (Life Technologies, United States) was used to isolate RNA from the nucleus and cytoplasm. qRT-PCR assays were conducted as described above.

RNA immunoprecipitation assay

RNA immunoprecipitation (RIP) assays were performed by EZ-Magna RNA Immunosuppression Kit (Millipore, United States). The cells were collected and resuspended in an immunodeposition buffer and kept on ice for 30 min. The cell suspension was incubated with a separate RIP buffer containing magnetic beads. Proteinase K was added to the bead state after buffering for further digestion of proteins. All RNA was extracted with Trizol and measured with qRT-PCR.

Dual-luciferase activity assay

According to a special combination of software for network prediction starbes 3.0 and NRAV miR-299-3p (http://starbase.sysu.edu.cn/ b). Other matters according to the V2 specification (enzyme, China), it is a rapid mutation reagent for NRAV, and supplementary DNA and mutant miR-299-3p are added to psicheck2 (US Promega) (NRAV wild and music) satellite. Paycheck-2 and miR-229-3p plasmid samples or miR-229-3p negative control were transferred to PDAC cells. After 48 h, the fluorescent enzyme activity of each well was examined by the Promega reporting system. The relative activity of luciferase is used for normalization.

Statistical analysis

Statistical analysis was performed using GraphPad Prisma 8.2 (LA Jolla, CA, United States) and SPSS 22.0 (IBM, Armonk, NY, United States). Student t test was used to compare the differences between the two groups and calculate the P value. $P < 0.05$ was statistically significant.

RESULTS

NRAV was significantly upregulated in PDAC and predicted poor prognosis

We used GEPIA to determine NRAV expression levels as an online bioinformatics tool for gene expression analysis based on the cancer genome database (TCGA)[16]. NRAV expression of PDAC in tissues was significantly higher than that in nonmedical tissues (Figure 1A and B). The survival curve showed that the total life cycle ($P = 0.034$; Figure 1D) and disease-free life cycle ($P = 0.046$; Figure 1E) of PDAC patients were decreasing. The data of the TCGA database showed that the level of emotional expression was negatively correlated with the level of clinical pathology (Figure 1C). The level of NRAV expression in HPDE cells and four PDAC systems was tested. NRAV in the PDAC cell system was significantly higher than that in HPDE cells (Figure 1F). Based on these data, we believe that NRAV may be a potential carcinogen related to lncRNA.

Knockdown of NRAV inhibited proliferation, migration and invasion of PDAC cells

We studied the biological role of NRAV in the PDAC cell system. We used heterogeneous RNA transplantation to reduce NRAV expression in PANC-1 and AsPC-1 cells. qRT-PCR showed a significant decrease in expression after NRAV (Figure 2A). After showing the results of CCK-8 tests and colony formation, there was a significant reduction after removal of signs of proliferation and abscision of PANC-1 and AsPC-1 cells (Figure 2B and C). We performed Transwell analysis to test whether NRAV affected metastasis and damage to police cells. Similarly, after the removal of PANC-1 and AsPC-1 cells, migration and invasion rates slowed significantly (Figure 2D and E). Knockdown of NRAV inhibited proliferation, migration and invasion of PDAC cells.

Overexpression of NRAV promoted PDAC cell proliferation, migration and invasion

High expression of NRAV in BXPC-3 and Mia PaCa-2 cells used to display exogenous particles confirmed the effectiveness of the expression (Figure 3A). The CCK-8 test and the product reduction test showed that NRAV overexpression significantly supported proliferation and formation of PDAC cells (Figure 3B and C). Transwell analysis found that NRAV overexpression significantly increased displacement and invasion of Mia PaCa-2 and BXPC-3 cells (Figure 3D and E). Overall, the results showed that NRAV promotes proliferation, metastasis and invasion of PDAC cells.
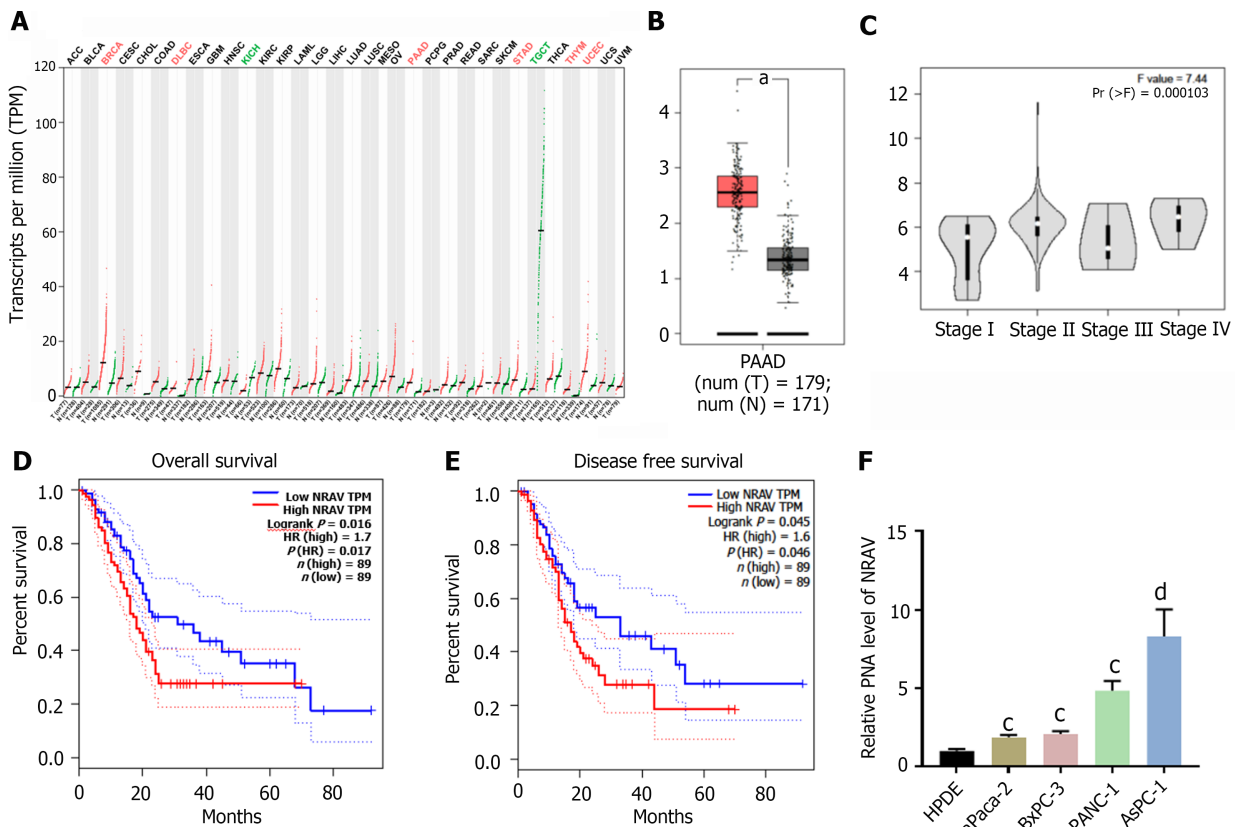
DOI: 10.3748/wjg.v28.i35.5141 **Copyright** ©The Author(s) 2022.

Figure 1 Relative expression of negative regulator of antiviral response in pancreatic cancer tissues and cells and its clinical significance. A: The negative regulator of antiviral response (NRAV) expression profile across all tumor samples and paired normal tissues; B: The NRAV expression of pancreatic adenocarcinoma in tissues was significantly higher than that in normal pancreas tissues; C: Expression of NRAV in patients divided by cancer stages using expression data from The Cancer Genome Atlas (TCGA) database; D: Overall survival analyzed by GEPIA based on the TCGA database; E: Disease-free survival analyzed by GEPIA based on the TCGA database; F: Quantitative real-time polymerase chain reaction analysis measured NRAV expression level in four pancreatic cancer and normal cell lines. $^cP < 0.001$; $^dP < 0.0001$. PAAD: Pancreatic adenocarcinoma; TPM: Transcripts per million; NRAV: Negative regulator of antiviral response; HR: Hazard ratio.

NRAV ablation inhibited tumor growth in vivo

To further investigate whether NRAV supports tumor growth *in vivo*, PANC-1 cells were injected into naked mice treated with sh-NRAV and internal control cells. The tumor volume of the NRAV genotype was significantly lower than the negative control volume (Figure 4A and B). Similarly, the mass of the tumor in the NRAV group (Figure 4C) was significantly reduced compared to the control group. Ki-67 was analyzed for lignin content and immunochemical staining. Reduction of NRAV led to a significant reduction of Ki-67 and inhibition of tumor growth (Figure 4D and E). Overall, these findings suggest that NRAV does not inhibit tumor growth *in vivo*.

NRAV acted as a molecular sponge for miR-299-3p in PDAC

To study how NRAV plays a catalytic role in PDAC, we used the nuclear/cell separation method to determine the location of NRAV in PDAC. Spleen qi was mainly located in cells (Figure 5A), and it can exert its biological function as a competitive endogenous RNA[17,18]. We used starbase V3.0 (http://starbase.sysu.edu.cn/) Interactive Bio information Analysis Software to identify potential miRNAs that may interact with genes. miR-299-3p was selected as the tempered target due to potential point complementarity (Figure 5B). Rip analysis confirms this point[19]. As shown in Overexpression in PDAC cells resulted in significant enrichment of miR-299-3p on ago2 (Figure 5C). The miR-299-3p simulator significantly reduced the fluorescence activity of the wild-type NRAV group, while this change did not occur in the modified NRAV group (Figure 5D). qRT-PCR showed that expression of miR-299-3p in PDAC cells was significantly enhanced after removing the traits (Figure 5E). Spearman's analysis showed that expression of NRAV and miR-299-3p in PDAC tissue was opposite (Figure 5F). Therefore, these results suggest that temper may play the role of molecular sponge miR-299-3p.

miR-299-3p reversed the effect of NRAV on PDAC cells

To validate whether NRAV affected proliferation and metastasis of PDAC cells through sponging miR-299-3p, specific miR-299-3p mimic or mimic NC vector was cotransfected into PDAC cells after overex-
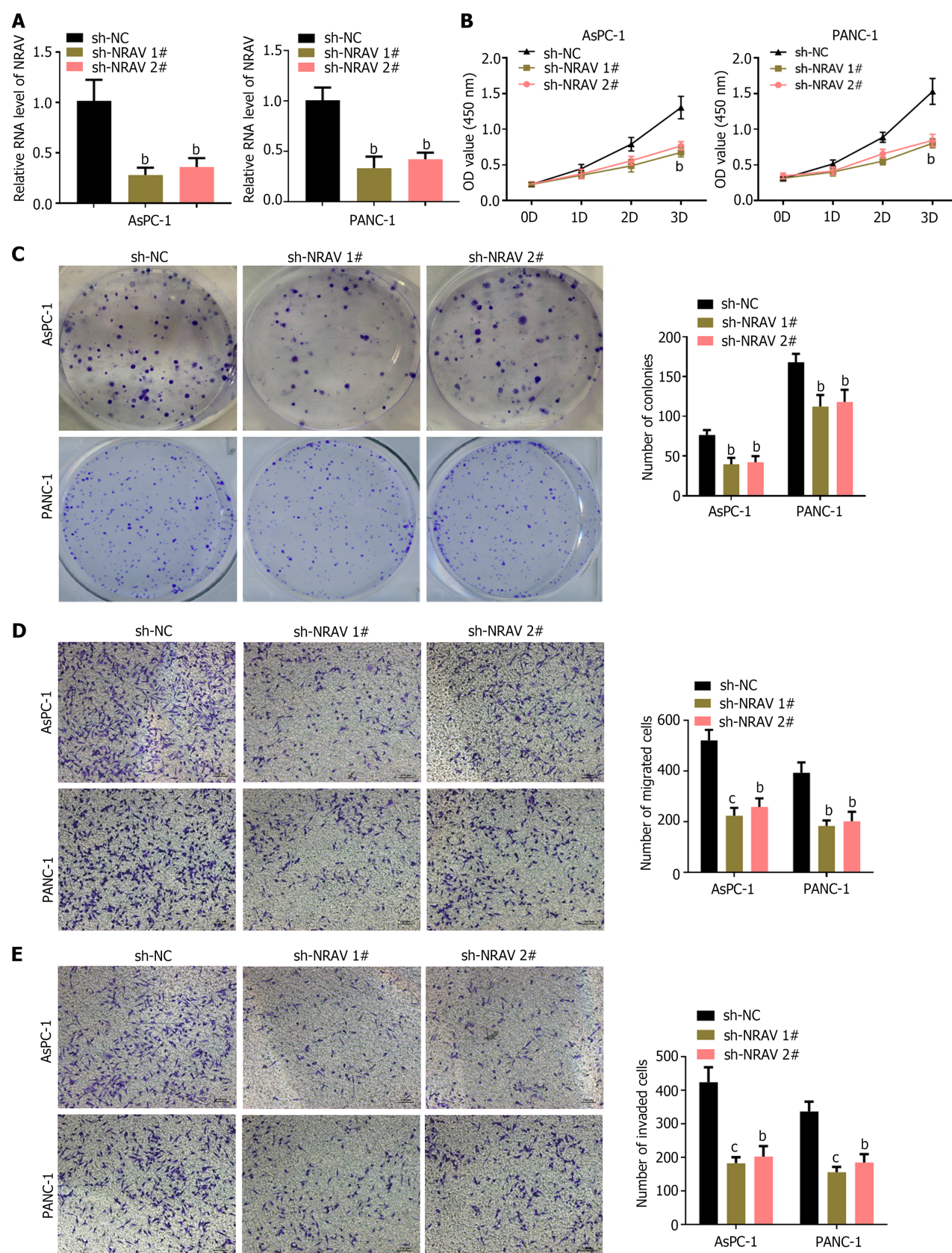
DOI: 10.3748/wjg.v28.i35.5141 **Copyright** ©The Author(s) 2022.

Figure 2 Knockdown of negative regulator of antiviral response inhibited proliferation, migration and invasion of pancreatic cancer cells.
A: Quantitative real-time polymerase chain reaction analysis assessed expression of NRAV in PANC-1 and AsPC-1 cells transfected with shNC, shRNA #1 and shRNA #2 targeting negative regulator of antiviral response; B: Cell Counting Kit-8 analysis showed that compared with the NC group, NRAV gene knockout significantly reduced the proliferation of PANC-1 and AsPC-1 cells; C: The colony formation test showed that NRAV ablation inhibited the colony numbers of PANC-1 and AsPC-1 cells; D: Transwell assays were performed to measure migration of PANC-1 and AsPC-1 cells; E: Transwell assays were performed to measure invasion of PANC-1 and AsPC-1 cells. $^{b}P < 0.01$; $^{c}P < 0.001$. NRAV: Negative regulator of antiviral response; sh: Short hairpin; NC: Negative control.
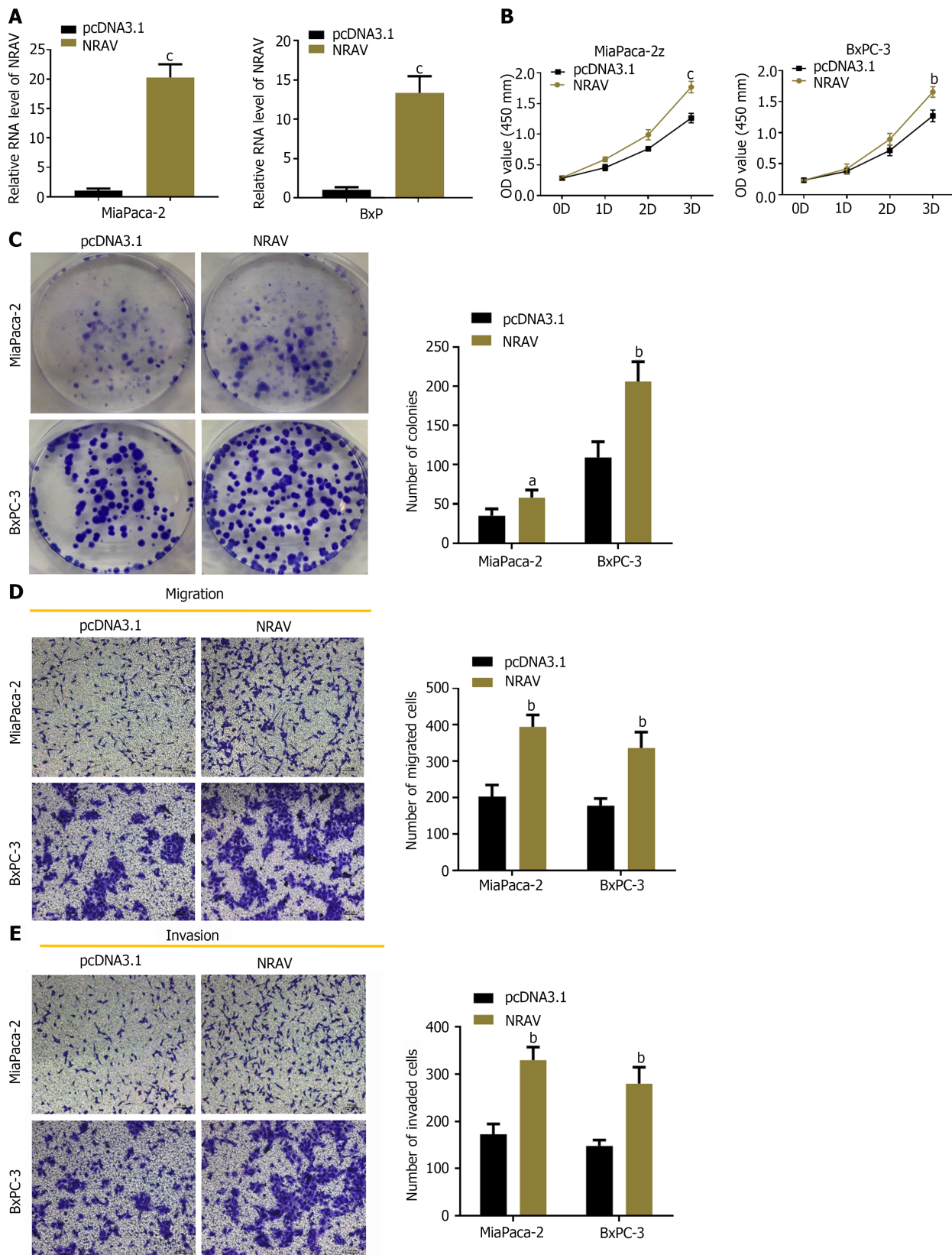
Figure 3 Overexpression of negative regulator of antiviral response promoted pancreatic cancer cell proliferation, migration and invasion. A: Quantitative real-time polymerase chain reaction measured negative regulator of antiviral response (NRAV) expression in Mia Paca-2 and BxPC-3 cells transfected with pcDNA3.1 empty vector or pcDNA3.1-NRAV; B: Cell Counting Kit-8 was performed to detect proliferation of Mia Paca-2 and BxPC-3 cells; C: Colony formation test showed that NRAV overexpression increased the number of clones of Mia-Paca-2 and BXPC-3 cells; D: Transwell assays were performed to measure migration of Mia Paca-2 and BxPC-3 cells; E: Transwell assays were performed to measure invasion of Mia Paca-2 and BxPC-3 cells. [a]$P < 0.05$; [b]$P < 0.01$; [c]$P < 0.001$. NRAV: Negative regulator of antiviral response.

DOI: 10.3748/wjg.v28.i35.5141 **Copyright** ©The Author(s) 2022.
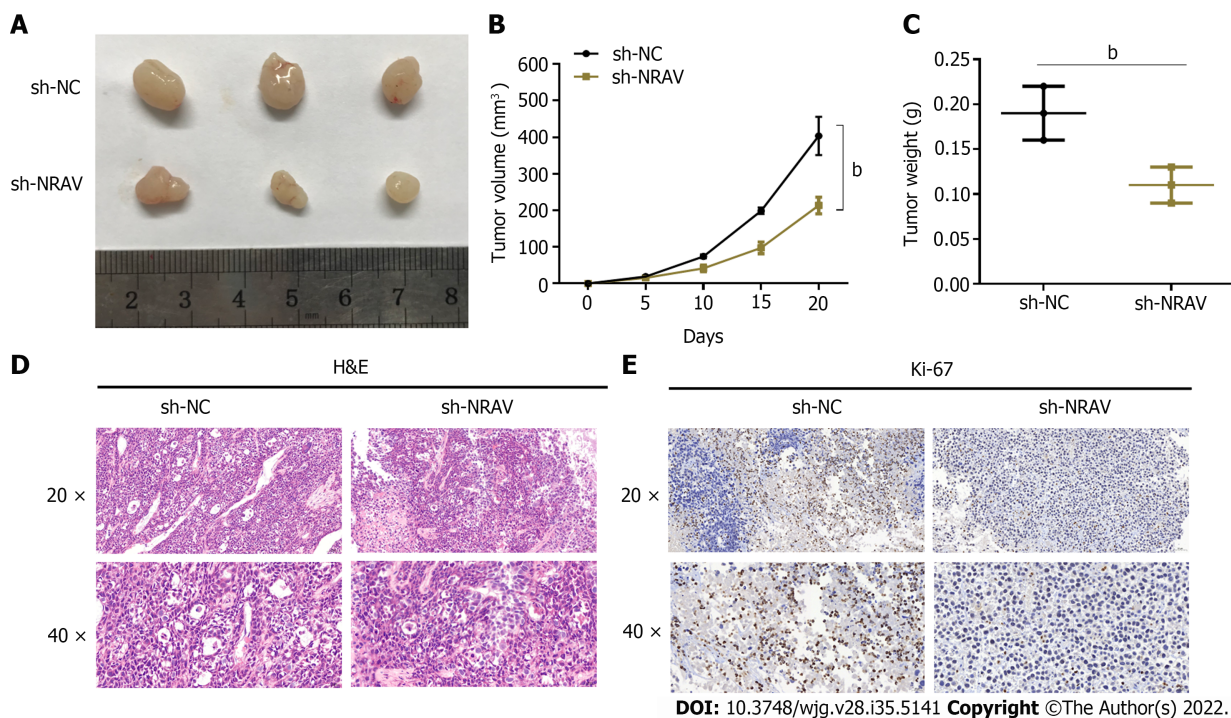
Figure 4 Negative regulator of antiviral response ablation inhibited tumor growth in a mouse xenograft models. A: Representative images of xenograft tumors after transfection with short hairpin NC or sh-negative regulator of antiviral response (NRAV); B: Tumor volume was measured; C: Tumor weight was measured; D: Representative images of hematoxylin and eosin staining for xenograft tumor tissue samples; E: Expression pattern of Ki-67 in the harvested tumor tissues was detected by immunohistochemical staining. [b]$P < 0.01$. sh: Short hairpin; NRAV: Negative regulator of antiviral response; NC: Negative control.

pression of NRAV. Subsequently, we evaluated the cell proliferation, migration and invasion of PDAC cells. miR-299-3p mimic reversed the dramatic promotion by overexpression of NRAV on proliferation (Figure 6A and B). Similarly, miR-299-3p mimic inhibited the promoting effects of NRAV overexpression on migration and invasion of PDAC cells (Figure 6C and D). These results indicated that miR-299-3p mediated the promoting effects of NRAV on PDAC cell proliferation, migration and invasion.

DISCUSSION

An increasing number of studies have shown that lncRNAs play an important role in the development of various malignant tumors. Recent studies have shown that large amounts of lncRNAs are abnormally expressed in PDAC and participate in the tumor process[20,21]. Guo *et al*[22] found that under hypoxia, lncRNAs extract of PDAC *UCA1* cells increased to promote angiogenesis. We used the TCGA database to identify NRAV in PDAC. We confirmed that the code of good conduct is a key element related to the program of action, and that significant progress has been made in the program of action. In addition, in PDAC patients, high levels of NRAV expression inhibit overall and disease-free survival. It is worth noting that NRAV may participate in PDAC progression.

The specific role of NRAV in oncology is not clear due to increased immunization. Recent studies have shown that NRAV expression is significantly increased in liver cancer and myeloma and can play a key role in the development of these two tumors[10,23]. To verify the biological function of NRAV in PDAC, function loss and acquisition studies were carried out. The results of *in vitro* experiments showed that temper has a major contribution to the migration, invasion and reproduction of PDAC cells. In addition, ablation temperament significantly reduced the tumor of the nude mouse model overall, these results show that the NRAV plays an important role in promoting cancer and can be used as a new biometric index for diagnosis and prediction of diseases caused by PDAC.

To further study the potential mechanism of NRAV, nuclear/cell division experiments were carried out in PDAC, and NRAV was mainly in the cytoplasm. Further analysis of the rip report analysis showed that NRAV may play the role of miR-299-3p molecular sponge (Figure 7). In addition, the stimulation effect of NRAV on malignant tumors in PDAC cells was also proved in the rescue experiment. The role of NRAV in promoting progression of PDAC mainly depends on miR-299-3p.

At the beginning of the study, it was emphasized that the significant increase in lncRNA was negatively correlated with overall and disease-free survival in PDAC patients. In addition, it also plays a carcinogenic role by promoting the proliferation and metastasis of cells in the sponge world. Our research shows that NRAV/miR-299-3p play a key role in PDAC and can be used as potential
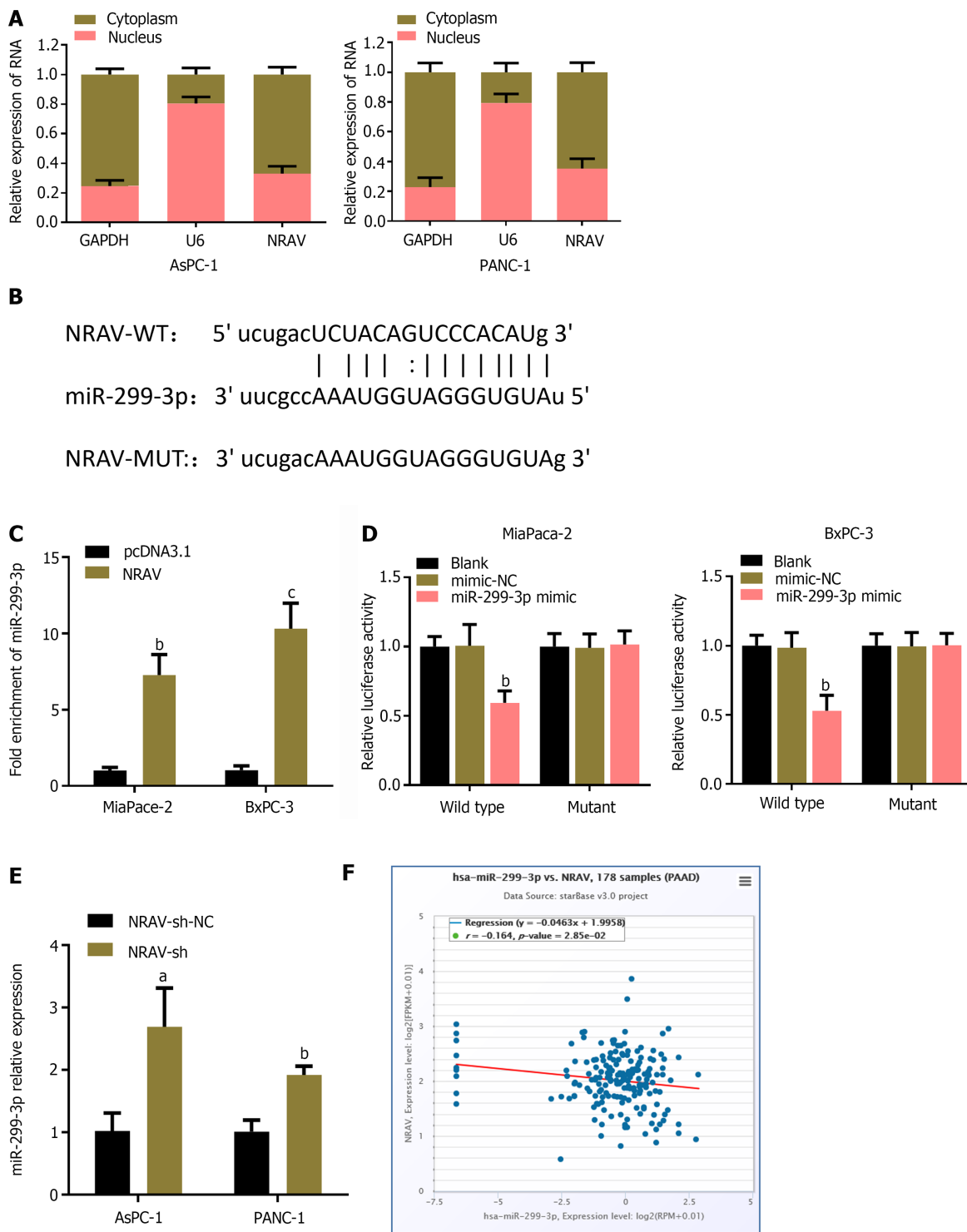
Figure 5 Negative regulator of antiviral response acted as a molecular sponge for miR-299-3p. A: Subcellular fractionation assay was used to determine the subcellular localization of NRAV; B: A complementary binding site of *NRAV* in miR-299-3p was predicted *via* starBase v3.0 online database; C: RNA immunoprecipitation assays were performed to validate whether *NRAV* could interact with miR-299-3p in MiaPaca-2 and BxPC-3 cells; D: Luciferase reporter assays were carried out to verify the direct binding of *NRAV* and miR-299-3p in MiaPaca-2 and BxPC-3 cells; E: Relative expression of miR-299-3p in AsPC-1 and PANC-1 cells following knockdown of *NRAV*; F: Spearman's correlation analysis between *NRAV* and miR-299-3p expression in PAAD by the starBase v3.0 project. [a]$P < 0.05$; [b]$P < 0.01$; [c]$P < 0.001$. NRAV: Negative regulator of antiviral response; MUT: Mutant; NC: Negative control; WT: Wild-type.

biomarkers for PDAC diagnosis and treatment.

However, because no samples from patients with pancreatic cancer were collected, there was a lack of correlation analysis between temperament expression and PDAC clinicopathological features. In addition, it is also of great significance to study the significance of NRAV and miR-299-3p in PDAC organization.
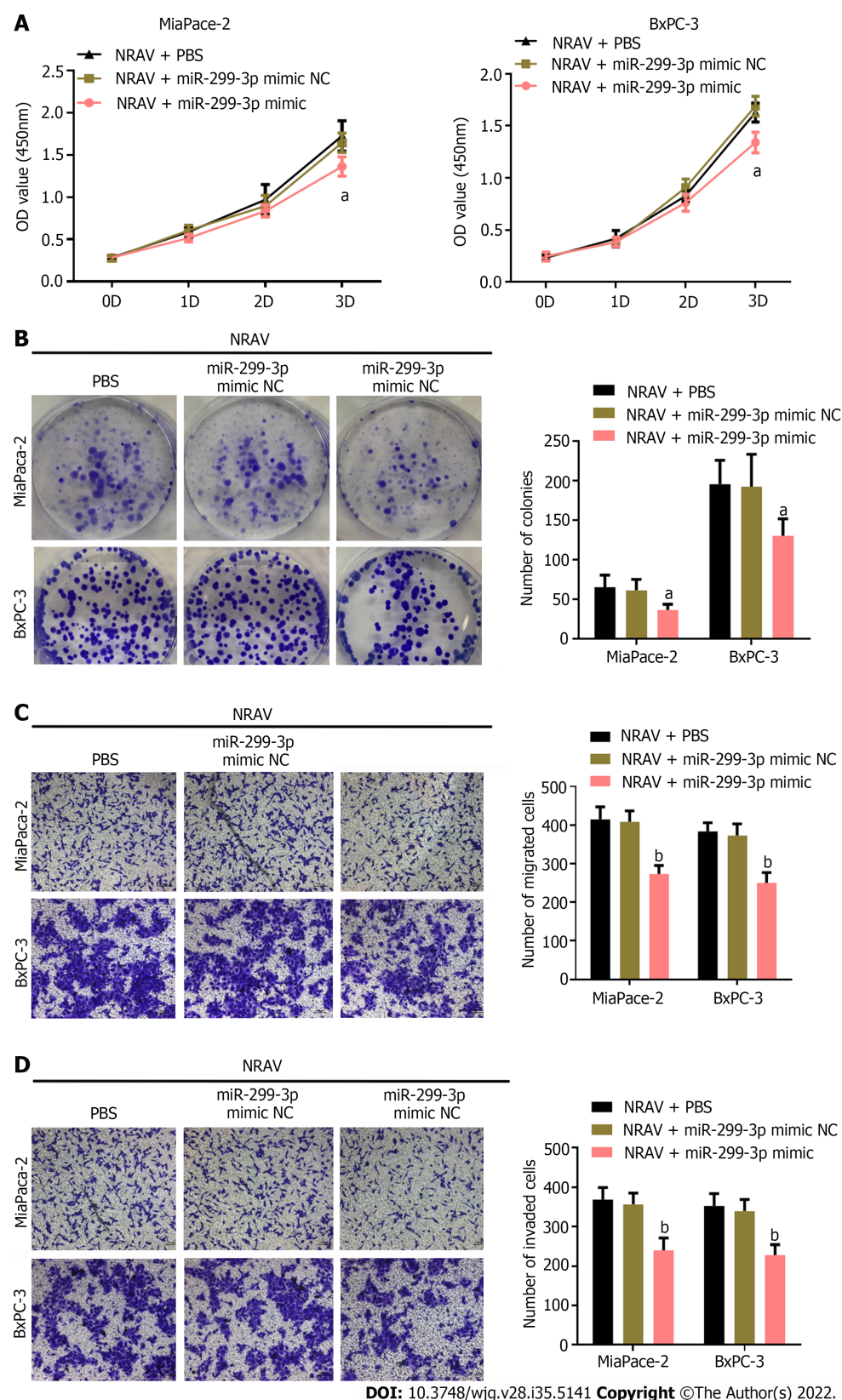
DOI: 10.3748/wjg.v28.i35.5141 **Copyright** ©The Author(s) 2022.

Figure 6 miR-299-3p reversed the effect of negative regulator of antiviral response on pancreatic cancer cells. A: Viability of MiaPaca-2 and BxPC-3 cells was determined following transfection with pcDNA3.1-*NRAV* and miR-299-3p mimic by Cell Counting Kit-8 assay; B: Proliferation of MiaPaca-2 and BxPC-3 cells was detected by colony formation assay; C: Transwell assays of cell migration was performed in MiaPaca-2 and BxPC-3 cells transfected with pcDNA3.1-*NRAV* and miR-299-3p mimic; D: Transwell assays of cell invasion were performed in MiaPaca-2 and BxPC-3 cells transfected with pcDNA3.1-*NRAV* and miR-299-3p mimic. [a]$P < 0.05$; [b]$P < 0.01$. NRAV: Negative regulator of antiviral response; NC: Negative control; PBS: Phosphate-buffered saline.
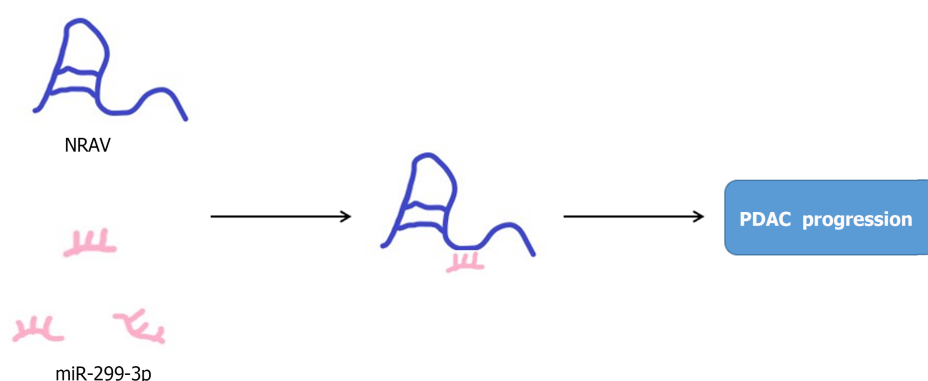
Figure 7 Negative regulator of antiviral response plays the role of miR-299-3p molecular sponge to promote the progress of pancreatic ductal cancer.

CONCLUSION

NRAV can act as a molecular sponge of miR-299-3p and significantly promote the proliferation and metastasis of PDAC cells.

ARTICLE HIGHLIGHTS

Research background

Pancreatic ductal adenocarcinoma (PDAC) has high malignancy and poor prognosis. Long noncoding RNAs (lnRNAs) are recognized as crucial factors and associated with progression of PDAC. However, the specific biological role and practical clinical significance of lnRNAs and negative regulator of antiviral response (NRAV) in PDAC remain unclear.

Research motivation

Early and timely diagnosis and treatment of PDAC are still scarce. Therefore, it is a matter of urgency to comprehensively understand the pathogenesis of PDAC and explore more effective targets for its diagnosis and treatment.

Research objectives

To study the role of NRAV in the growth and metastasis of PDAC.

Research methods

Real-time polymerase chain reaction detected expression of NRAV and miR-299-3p in PDAC cells. The temperament correction and miR-299-3p in the process of cell proliferation, metastasis and invasion were verified by Cell Counting Kit-8, precipitation test, and Transwell assay. RNA and fluorescent enzyme immunoprecipitation test to test the interaction between NRAV and miR-299-3p. Verify the interaction between NRAV and miR-299-3p.

Research results

According to our data, NRAV in PDAC was significantly increased, which is related to the negative survival rate of PDAC patients. NRAV overexpression was conducive to the proliferation and metastasis of PDAC cells, and NRAV knockout reversed these effects. Finally, in terms of mechanism, NRAV acts as a miR-299-3p molecular sponge. Overexpression of miR-299-3p significantly changed the role of NRAV in the proliferation, metastasis and invasion of PDAC cells.

Research conclusions

NRAV promotes proliferation and metastasis of PDAC by playing the molecule sponge function of miR-299-3p.

Research perspectives

NRAV facilitated the progression of PDAC, which provides a potential biological marker for diagnosis and therapeutic target for PDAC.

FOOTNOTES

REFERENCES

1. **Siegel RL**, Miller KD, Fuchs HE, Jemal A. Cancer Statistics, 2021. *CA Cancer J Clin* 2021; **71**: 7-33 [PMID: 33433946 DOI: 10.3322/caac.21654]

2. **Sung H**, Ferlay J, Siegel RL, Laversanne M, Soerjomataram I, Jemal A, Bray F. Global Cancer Statistics 2020: GLOBOCAN Estimates of Incidence and Mortality Worldwide for 36 Cancers in 185 Countries. *CA Cancer J Clin* 2021; **71**: 209-249 [PMID: 33538338 DOI: 10.3322/caac.21660]

3. **Esteller M**. Non-coding RNAs in human disease. *Nat Rev Genet* 2011; **12**: 861-874 [PMID: 22094949 DOI: 10.1038/nrg3074]

4. **Nagano T**, Fraser P. No-nonsense functions for long noncoding RNAs. *Cell* 2011; **145**: 178-181 [PMID: 21496640 DOI: 10.1016/j.cell.2011.03.014]

5. **Guttman M**, Rinn JL. Modular regulatory principles of large non-coding RNAs. *Nature* 2012; **482**: 339-346 [PMID: 22337053 DOI: 10.1038/nature10887]

6. **Yao RW**, Wang Y, Chen LL. Cellular functions of long noncoding RNAs. *Nat Cell Biol* 2019; **21**: 542-551 [PMID: 31048766 DOI: 10.1038/s41556-019-0311-8]

7. **Bhan A**, Soleimani M, Mandal SS. Long Noncoding RNA and Cancer: A New Paradigm. *Cancer Res* 2017; **77**: 3965-3981 [PMID: 28701486 DOI: 10.1158/0008-5472.CAN-16-2634]

8. **Arun G**, Diermeier SD, Spector DL. Therapeutic Targeting of Long Non-Coding RNAs in Cancer. *Trends Mol Med* 2018; **24**: 257-277 [PMID: 29449148 DOI: 10.1016/j.molmed.2018.01.001]

9. **Ouyang J**, Zhu X, Chen Y, Wei H, Chen Q, Chi X, Qi B, Zhang L, Zhao Y, Gao GF, Wang G, Chen JL. NRAV, a long noncoding RNA, modulates antiviral responses through suppression of interferon-stimulated gene transcription. *Cell Host Microbe* 2014; **16**: 616-626 [PMID: 25525793 DOI: 10.1016/j.chom.2014.10.001]

10. **Xu Q**, Wang Y, Huang W. Identification of immune-related lncRNA signature for predicting immune checkpoint blockade and prognosis in hepatocellular carcinoma. *Int Immunopharmacol* 2021; **92**: 107333 [PMID: 33486322 DOI: 10.1016/j.intimp.2020.107333]

11. **Chan JJ**, Tay Y. Noncoding RNA:RNA Regulatory Networks in Cancer. *Int J Mol Sci* 2018; **19** [PMID: 29702599 DOI: 10.3390/ijms19051310]

12. **Chen W**, Zhang K, Yang Y, Guo Z, Wang X, Teng B, Zhao Q, Huang C, Qiu Z. MEF2A-mediated lncRNA HCP5 Inhibits Gastric Cancer Progression *via* MiR-106b-5p/p21 Axis. *Int J Biol Sci* 2021; **17**: 623-634 [PMID: 33613117 DOI: 10.7150/ijbs.55020]

13. **Duan H**, Li X, Chen Y, Wang Y, Li Z. LncRNA RHPN1-AS1 promoted cell proliferation, invasion and migration in cervical cancer *via* the modulation of miR-299-3p/FGF2 axis. *Life Sci* 2019; **239**: 116856 [PMID: 31525429 DOI: 10.1016/j.lfs.2019.116856]

14   **Bai N**, Ma Y, Zhao J, Li B. Knockdown of lncRNA HCP5 Suppresses the Progression of Colorectal Cancer by miR-299-3p/PFN1/AKT Axis. *Cancer Manag Res* 2020; **12**: 4747-4758 [PMID: 32606965 DOI: 10.2147/CMAR.S255866]

15   **Xu K**, Zhang L. Inhibition of TUG1/miRNA-299-3p Axis Represses Pancreatic Cancer Malignant Progression *via* Suppression of the Notch1 Pathway. *Dig Dis Sci* 2020; **65**: 1748-1760 [PMID: 31655908 DOI: 10.1007/s10620-019-05911-0]

16   **Tang Z**, Li C, Kang B, Gao G, Zhang Z. GEPIA: a web server for cancer and normal gene expression profiling and interactive analyses. *Nucleic Acids Res* 2017; **45**: W98-W102 [PMID: 28407145 DOI: 10.1093/nar/gkx247]

17   **Salmena L**, Poliseno L, Tay Y, Kats L, Pandolfi PP. A ceRNA hypothesis: the Rosetta Stone of a hidden RNA language? *Cell* 2011; **146**: 353-358 [PMID: 21802130 DOI: 10.1016/j.cell.2011.07.014]

18   **Batista PJ**, Chang HY. Long noncoding RNAs: cellular address codes in development and disease. *Cell* 2013; **152**: 1298-1307 [PMID: 23498938 DOI: 10.1016/j.cell.2013.02.012]

19   **Gregory RI**, Chendrimada TP, Cooch N, Shiekhattar R. Human RISC couples microRNA biogenesis and posttranscriptional gene silencing. *Cell* 2005; **123**: 631-640 [PMID: 16271387 DOI: 10.1016/j.cell.2005.10.022]

20   **Wang Y**, Zhou L, Lu J, Jiang B, Liu C, Guo J, Xiao GG. Research progress on long non-coding RNAs and their roles as potential biomarkers for diagnosis and prognosis in pancreatic cancer. *Cancer Cell Int* 2020; **20**: 457 [PMID: 32973402 DOI: 10.1186/s12935-020-01550-y]

21   **Tasaki Y**, Suzuki M, Katsushima K, Shinjo K, Iijima K, Murofushi Y, Naiki-Ito A, Hayashi K, Qiu C, Takahashi A, Tanaka Y, Kawaguchi T, Sugawara M, Kataoka T, Naito M, Miyata K, Kataoka K, Noda T, Gao W, Kataoka H, Takahashi S, Kimura K, Kondo Y. Cancer-Specific Targeting of Taurine-Upregulated Gene 1 Enhances the Effects of Chemotherapy in Pancreatic Cancer. *Cancer Res* 2021; **81**: 1654-1666 [PMID: 33648930 DOI: 10.1158/0008-5472.CAN-20-3021]

22   **Guo Z**, Wang X, Yang Y, Chen W, Zhang K, Teng B, Huang C, Zhao Q, Qiu Z. Hypoxic Tumor-Derived Exosomal Long Noncoding RNA UCA1 Promotes Angiogenesis *via* miR-96-5p/AMOTL2 in Pancreatic Cancer. *Mol Ther Nucleic Acids* 2020; **22**: 179-195 [PMID: 32942233 DOI: 10.1016/j.omtn.2020.08.021]

23   **Maimaiti A**, Jiang L, Wang X, Shi X, Pei Y, Hao Y, Paerhati H, Zibibula Y, Abudujielili A, Kasimu M. Identification and validation of an individualized prognostic signature of lower-grade glioma based on nine immune related long non-coding RNA. *Clin Neurol Neurosurg* 2021; **201**: 106464 [PMID: 33454543 DOI: 10.1016/j.clineuro.2020.106464]

ORIGINAL ARTICLE

Basic Study

Alcohol promotes epithelial mesenchymal transformation-mediated premetastatic niche formation of colorectal cancer by activating interaction between laminin-γ2 and integrin-β1

Fei-Fei Nong, Yu-Qi Liang, Shang-Ping Xing, Yin-Fang Xiao, Hui-Hui Chen, Bin Wen

Fei-Fei Nong, Yin-Fang Xiao, Hui-Hui Chen, Bin Wen, Pi-Wei Institute, Science and Technology Innovation Center, Guangzhou University of Chinese Medicine, Guangzhou 510000, Guangdong Province, China

Yu-Qi Liang, The Second Clinical College of Guangzhou University of Chinese Medicine, Guangzhou University of Chinese Medicine, Guangzhou 510000, Guangdong Province, China

Shang-Ping Xing, Guangxi Key Laboratory of Bioactive Molecules Research and Evaluation, School of Pharmacy, Guangxi Medical University, Nanning 530022, Guangxi Zhuang Autonomous Region, China

Corresponding author: Bin Wen, PhD, Academic Research, Full Professor, Pi-Wei Institute, Science and Technology Innovation Center, Guangzhou University of Chinese Medicine, No. 232 Waihuandong Road, Guangzhou 510000, Guangdong Province, China. wenbin@gzucm.edu.cn

Abstract

BACKGROUND
Colorectal cancer (CRC) is a common malignant tumor. Alcohol consumption is positively correlated with CRC malignant metastasis; however, the mechanism is unclear. The interaction between laminin-γ2 (LAMC2) and integrin-β1 (ITGB1) plays a role in premetastatic niche signaling, which may induce epithelial mesenchymal transformation (EMT) and lead to metastasis.

AIM
To investigate the effects of alcohol on CRC metastasis from the molecular mechanism of the premetastatic niche.

METHODS
The interaction between LAMC2 and ITGB1 was measured by Duolink assay, and the expression levels of LAMC2, ITGB1 and focal adhesion kinase (FAK), snail, fibronectin, N-cadherin and special AT-rich sequence binding protein 1 (SATB1) were measured by quantitative real-time polymerase chain reaction, immunohistochemistry and western blotting. Interleukin-1β (IL-1β), tumor necrosis factor-α (TNF-α) and IL-6 levels were measured *via* enzyme-linked immunosorbent assay, histopathological assessment *via* hematoxylin eosin staining, and determination of

aberrant crypt foci *via* methylene blue.

RESULTS
The lymph node metastasis rate was higher in the alcohol group than non-alcohol group. There was a significant increase in interaction signals between LAMC2 and ITGB1, and an increase in phosphorylate-FAK/FAK, snail, fibronectin, N-cadherin and SATB1, whereas E-cadherin was reduced in the alcohol group compared to the non-alcohol group in both animal and clinical samples. Serum IL-1β, TNF-α and IL-6 were higher in alcohol group than in non-alcohol group. Alcohol may promote CRC metastasis by influencing the molecular mechanism of the premeta-static niche.

CONCLUSION
Our study suggests that alcohol promotes EMT-mediated premetastatic niche formation of CRC by activating the early interaction between LAMC2 and ITGB1 and lead to CRC metastasis.

Key Words: Alcohol; Colorectal cancer; Premetastatic niche; Epithelial mesenchymal transformation; Metastasis

Core Tip: Our study indicated that alcohol promotes epithelial mesenchymal transformation-mediated premetastatic niche formation of colorectal cancer (CRC) by activating the early interaction between laminin-γ2 and integrin-β1 and lead to CRC metastasis.

INTRODUCTION

Colorectal cancer (CRC) is the third most commonly diagnosed malignancy worldwide[1]. A majority of colorectal cancers are associated with the environmental factors such as lifestyle changes including diet, obesity, smoking and alcohol consumption[2,3]. It is reported that long-term alcohol consumption is associated with an increased risk of CRC metastasis[3]. In the presence of concomitant metastasis, the maximum survival rates after surgical intervention do not exceed 20%[4,5]. Therefore, the relationship between alcohol consumption and CRC metastasis should be investigated. However, the mechanism that the alcohol promotes CRC metastasis has not been clearly explained[6,7].

Accumulating evidence suggests that metastasis develops from disseminated cancer cells that can remain dormant, and the dissemination may occur during the early stage of tumor evolution[7,8]. The microenvironment around the early disseminated cancer cells, also known as the premetastatic niche[9,10], may play an important role during the proliferation and migration of disseminated cancer cells in the early stage of tumors[11-13]. The extracellular matrix (ECM) is an important part of the premeta-static niche[14-17].

As an important component of the ECM, laminins are important for adhesion, differentiation, migration, and resistance to apoptosis of various cells, including cancer cells[18-21]. Reports have indicated that laminins are involved in the formation of the premetastatic niche[22,23]. Laminin-γ2 (LAMC2), a subunit of laminin-332, has been reported to be an important component in the survival dependent environment of epithelial cells in CRC and plays a key role in the regulation of tumor cell motility in premetastatic niche formation[24-27]. The interaction between LAMC2 and integrin-β1 (ITGB1) may stimulate the formation of premetastatic focal contacts by activating the premetastatic niche signaling, which promotes the migration of cancer cells[28]. Focal adhesion kinase (FAK) is a premetastatic focal contact involved in LAMC2 and β1 integrin signal transduction[29]. Signaling cascades triggered by integrin-laminin interactions in cells phosphorylate FAK, which induced epithelial mesenchymal transformation (EMT). EMT is a key initiating step during the metastasis and invasion of cancer[30,31] and involved in the formation of the premetastatic niche[32,33].

Alcohol consumption may influence the ECM remodeling and thus induce EMT, which may be closely related to the premetastatic niche[34]. Therefore, we explore its effect on CRC metastasis from the view of the premetastatic niche.

MATERIALS AND METHODS

Antibodies and reagents

The following antibodies were used: LAMC2 monoclonal antibody (YT5379, Immunoway, United States), ITGB1 monoclonal antibody (sc-9970, Santa Cruz, United States), glyceraldehyde-3-phosphate dehydrogenase (GAPDH) monoclonal antibody (ab125247, ABCAM, United Kingdom), phosphorylate-FAK (p-FAK)-Y397 (AP0302, ABclonal, Wuhan, China), FAK monoclonal antibody (A11131, ABclonal, Wuhan, China), snail monoclonal antibody (ab53519, ABCAM, United Kingdom), E-cadherin polyclonal antibody (ab1416, ABCAM, United Kingdom), N-cadherin polyclonal antibody (22018-1-AP, Proteintech, United States), fibronectin polyclonal antibody (A16678, ABclonal, Wuhan, China) and special AT-rich sequence binding protein 1 (SATB1) polyclonal antibody (A5800, ABclonal, Wuhan, China). Secondary antibodies were ab288151 and ab150113 (ABCAM, United Kingdom). Polyvinylidene difluoride membranes with a pore size of 0.45 mm (Millipore, United States) were used. RNAEX reagent (Accurate Biotechnology, Beijing, China), Evo M-MLV RT Premix (Accurate Biotechnology, Beijing, China), SYBR Green Premix Pro Taq HS qPCR Kit (Accurate Biotechnology, China). Interleukin-6 (IL-6), IL-1β and tumor necrosis factor-α (TNF-α) enzyme-linked immunosorbent assay (ELISA) kits (Enzyme-linked Biotechnology Co., LTD, Shanghai, China) were used. Duolink proximity ligation assay (PLA) kits (DUO92012, Merck, United States), Duolink PLA Rabbit PLUS (DUO92002, Merck, United States), and PLA Mouse MINUS (DUO92004, Merck, United States) proximity probes were purchased from Sigma-Aldrich. All above the mentioned antibodies can be used in both in rats and in humans.

Patients and clinical data

A total of 63 patients (26-86 years old) at The First Affiliated Hospital of Guangzhou University of Chinese Medicine (Guangzhou, China) from July 2019 to February 2020 was enrolled in this study. The baseline characteristics were collected, and data on alcohol consumption were collected at baseline using a direct interview method[35]. Participants were asked to answer whether they drank alcoholic beverages ("Yes", "Yes, but not now", or "No" were the answer options to the question, "Have you ever drunk alcohol?"), and for "ever drinkers", consumption frequency and average quantity of one serving over the past year by beverage type was recorded. CRC patients who never drank alcohol were added into the non-alcohol group, and CRC patients who drank alcohol over 3 times a week for more than 5 years were added into the alcohol group. And patients with smoking, family history, blood lipids, obesity, and chronic diseases were excluded. The present study was approved by the Ethics Committee of First Affiliated Hospital of Guangzhou University of Chinese Medicine [No. Y (2019) 172] and carried out in accordance with the "Helsinki Declaration". All CRC patients have sighed informed consent. Patients who received neoadjuvant chemotherapy or radiotherapy or had a history of malignancy were excluded. Clinicopathological data including pathological report, sex, age, macroscopic classification, tumor location, tumor size, tumor differentiation, lymphatic infiltration and invasion depth were collected *via* medical record. The American Joint Council on Cancer tumor, node and metastasis (TNM) staging system is used for the clinical staging of tumors[36].

Animals, induction of CRC and treatments

A total of 32 male Wistar rats, 7 wk old and weighing 200 ± 20 g, were obtained from the Experimental Animal Center of Southern Medical University [Certificate of quality: SCXK (Yue) 2016-0041]. All rats were housed in cages (25 cm × 30 cm × 30 cm, four rats per cage) under specified-pathogens free conditions at 25℃, 40%-60% relative humidity, and a 12-h light/dark cycle in the experimental animal center of Guangzhou University of Chinese Medicine. All rats had ad libitum access to standard rodent chow and filtered water and were acclimatized for 1 wk prior to the initiation of the experiment. The use of laboratory animals was checked by the "Institutional Animal Ethical Committee" and all procedures were approved by the Ethics Committee of Guangzhou University of Chinese Medicine, and performed according to the "Principles of Laboratory Animal Care" as well as specific national laws where applicable. All experimental protocols and handling of the animals followed the guide for the care and use of laboratory animals[37].

A total of 32 rats were randomly divided into two groups: the non-alcohol group and the alcohol group, with 16 rats in each group. Non-alcohol group: The rats were fed water (10 mL/kg b.wt.) every day and from the 6th week on, the rats were administered a subcutaneous injection of 1,2-dimethylhydrazine hydrochloride (DMH) at a dose of 30, 35, 25 or 20 mg/kg b.wt. once a week for 12 wk in order to induce CRC. Alcohol group (DMH + ethanol): The rats were fed 30% ethanol (10 mL/kg b.wt.) every day, and from the 6th week on, they were administered a subcutaneous injection of DMH at a dose of 30, 35, 25 or 20 mg/kg b.wt. once a week for 12 wk in order to induce CRC. The details of the specific modeling method of each group were shown in Figure 1. The blood samples were collected through the posterior orbital venous plexus. And the rats were sacrificed by cervical dislocation, then the colons were removed and used in further experiments.

Hematoxylin and eosin staining and histological evaluation

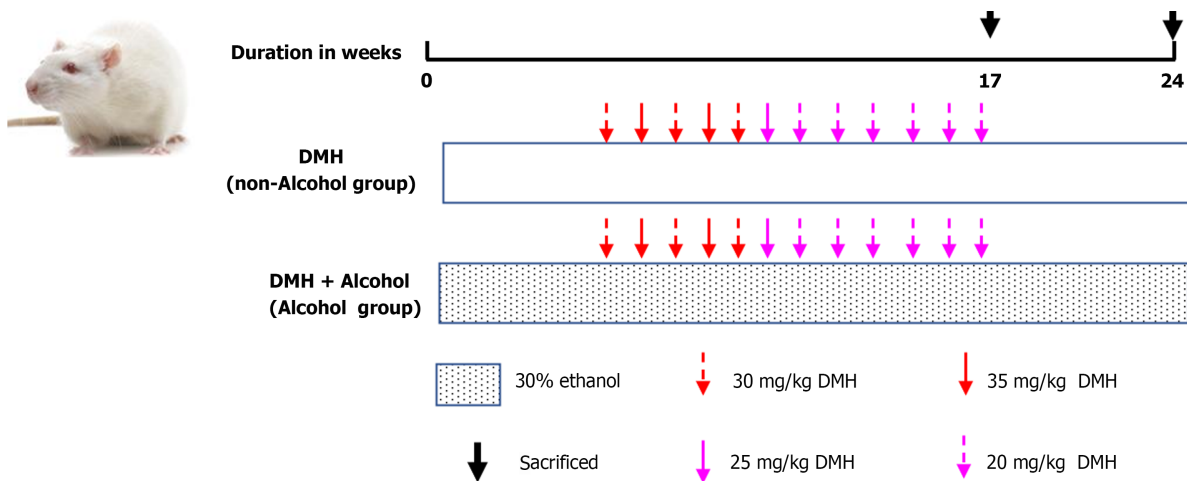All specimens were fixed in 4% paraformaldehyde solution for 24 h and embedded in paraffin and

Figure 1 Schematic diagram of animal experimental modeling. DMH: 1,2-Dimethylhydrazine hydrochloride.

processed by standard histological processing techniques. Tissue sections (4-μm thick) were obtained from each sample. The hematoxylin and eosin results were observed under a light microscope at 40× magnifications (Olympus, BX51) to observe the colonic histology differences by the method of Martin B [38].

Determination of aberrant crypt foci

Aberrant crypt foci (ACF) were determined according to the method described by Bird *et al*[39]. Then, the formalin-fixed colon was stained with 0.2% methylene blue for 3 min and observed under light microscope. The diagnosis of colonic pathology and ACF was performed by two pathologists. The number of ACF was counted as described by Sivaranjani *et al*[40].

Cytokines detection by ELISA

Serum samples of rats were collected, and the inflammatory factors (TNF-α, IL-6 and IL-1β) were determined using ELISA kits according to the manufacturers' instructions. The optical density of the colorimetric reaction was measured at 450 nm with a flat microplate reader.

Western blotting

For western blotting, 50 μg of extracted protein was fractionated on a 10% SDS-PAGE gel and then transferred to a polyvinylidene fluoride membrane with a 0.45-mm pore size (Millipore, MA, United States). The membrane was blocked in 5% milk for 3 h at room temperature and probed with antibodies against acetylated LAMC2 (1:1000), integrinβ1 (1:1000), p-FAK (1:1000), FAK (1:1000), snail (1:1000), E-cadherin (1:1000), fibronectin (1:1000) and N-cadherin (1:1000) at 4°C overnight. Horseradish peroxide-conjugated goat anti-rabbit and rabbit anti-mouse was used as the secondary antibodies. FAK and GAPDH (1:8000) were used as loading controls. Band intensity was visualized by ChemiDoc TMXRS+ (Bio-Rad, United States).

Immunohistochemical staining

The immunohistochemical (IHC) was performed by the method described in previous studies[41,42], all colonic tissue were fixed with 4% paraformaldehyde and paraffin embedded, then thin 4μm sections were obtained and deparaffinized in xylene and rehydrated through decreasing grades of alcohol. The sections were placed in a 95°C antigen retrieval solution for 15 min. After cooling the retrieval solutions for 20 min at room temperature, the slides were treated with hydrogen peroxide (H_2O_2) for 10 min to block endogenous peroxidase activity. Then, slides were incubated with primary antibodies against ITGB1 (dilution 1:100), LAMC2 (dilution 1:500), p-FAK (dilution 1:500), snail (dilution 1:500), E-cadherin (dilution 1:100), N-cadherin (dilution 1:800), fibronectin (dilution 1:200), and SATB1 (dilution 1:200) overnight at 4°C. The next day, biotin-conjugated secondary antibody and streptavidin-biotin peroxidase were applied each for 20 min. 3,3'-Diaminobenzidine tetrahydrochloride was used as the substrate, and nuclear contrast was performed using hematoxylin counterstaining. The negative controls for IHC are performed with PBS instead of primary antibody. The results were observed under a light microscope at 40× magnifications (Olympus, BX51). For quantitative analyses, the IHC images were analyzed by Image-Pro Plus 6.0 to calculate the average optical density (AOD), and the following equation: AOD = integrated optical density/area.

Table 1 Primer sequences for quantitative real-time polymerase chain reaction

Gene name	Forward (5'>3')	Reverse (5'>3')
For human		
LAMC2	TTCTACAACGATCCGCACGAC	GAGTTAAAAGCAGCCCTGGT
ITGB1	CCTACTTCTGCACGATGTGATG	CCTTTGCTACGGTTGGTTACATT
FAK	GTCTGCCTTCGCTTCACG	GAATTTGTAACTGGAAGATGCAAG
Snail	CTAGCGAGTGGTTCTTCTGC	GTAGTTAGGCTTCCGATTGGG
E-cadherin	GACCGGTGCAATCTTCAAA	TTGACGCCGAGAGCTACAC
N-cadherin	AGCTTCTCACGGCATACACC	GTGCATGAAGGACAGCCTCT
Fibronectin	GCCTGGTACAGAATA TGTAGTG	ATCCCAGCTGATC AGTAGGCTGGTG
SATB1	GTGGAAGCCTTGGGAATCC	CTGACAGCTCTTCTTCTAGTT
GAPDH	GGAGCGAGATCCCTCCAAAAT	GGCTGTTGTCATACTTCTCATGG
For rats		
LAMC2	GTGAAGCTTCCCTGCAAAAC	CATTTGGCCCCACGTAGT
ITGB1	TCGAAGGACCACTAGACCTGA	TTCCATGGGAACAAAAGGTAA
FAK	TTGGGTTGCAAACTATCTCTAGAAC	TGGTACAAAACTGGCACAGAA
Snail	TTCACATCCGAGTGGGTCTG	ACCCACACTGGTGAGAAGCC
E-cadherin	AAAGCAGGAAGAAAACACCACTC	AAAGGGCACGCTATCAACATTAG
N-cadherin	TCAGTGGCGGAGATCCTAC	GTGCTGAATTCCCTTGGCTA
Fibronectin	TGTCACCCACCACCTTGA	CTGATTGTTCTTCAGTGCGA
SATB1	AGATGCAGGGAGTGCCTTTA	TGCTCCTCCTTGCAATCATA
GAPDH	TGCCCTCATGTTCCTGATAAAT	CATTACATCACAGCTTTCCAGG

ITGB1: Integrin-β1; LAMC2: Laminin-γ2; SATB1: Special AT-rich sequence binding protein 1; FAK: Focal adhesion kinase; GAPDH: Glyceraldehyde-3-phosphate dehydrogenase.

Table 2 Number of rats with mucosal pathological tissue changes in different time periods

Wk	Group	n	Normal	Atypical hyperplasia	Adenoma	Adenocarcinoma Mucosal carcinoma	Adenocarcinoma Infiltrating carcinoma	With lymphatic metastasis Metastasis	With lymphatic metastasis Tumor metastasis rate
17	Non-alcohol	8	3	5	0	0	0	0	0.00%
	Alcohol	8	0	6	2	0	0	0	0.00%
24	Non-alcohol	8	0	0	0	6	2	0	0.00%
	Alcohol	8	0	0	0	2	6	3	37.5%

Duolink PLA

The Duolink PLA in situ was used in this study to detect the interaction between LAMC2 and ITGB1 in tissue samples, and it was performed as previously described by Bai *et al*[43]. Briefly, after washing, permeabilizing, and blocking as histological analysis, colon sections were incubated with primary antibodies against LAMC2 (1:200) and ITGB1 (1:400) overnight at 4℃. Then the slides were incubated with Duolink PLA Rabbit MINUS and PLA Mouse PLUS proximity probes for 1 h at 37℃. Ligation and amplification were conducted using the Duolink in situ detection reagent kit according to the protocol. Images were captured under the light microscope (Olympus, BX51).

RNA extraction and quantitative real-time polymerase chain reaction

The total RNA was extracted from tissues using RNAEX reagent (Accurate Biotechnology, China). It
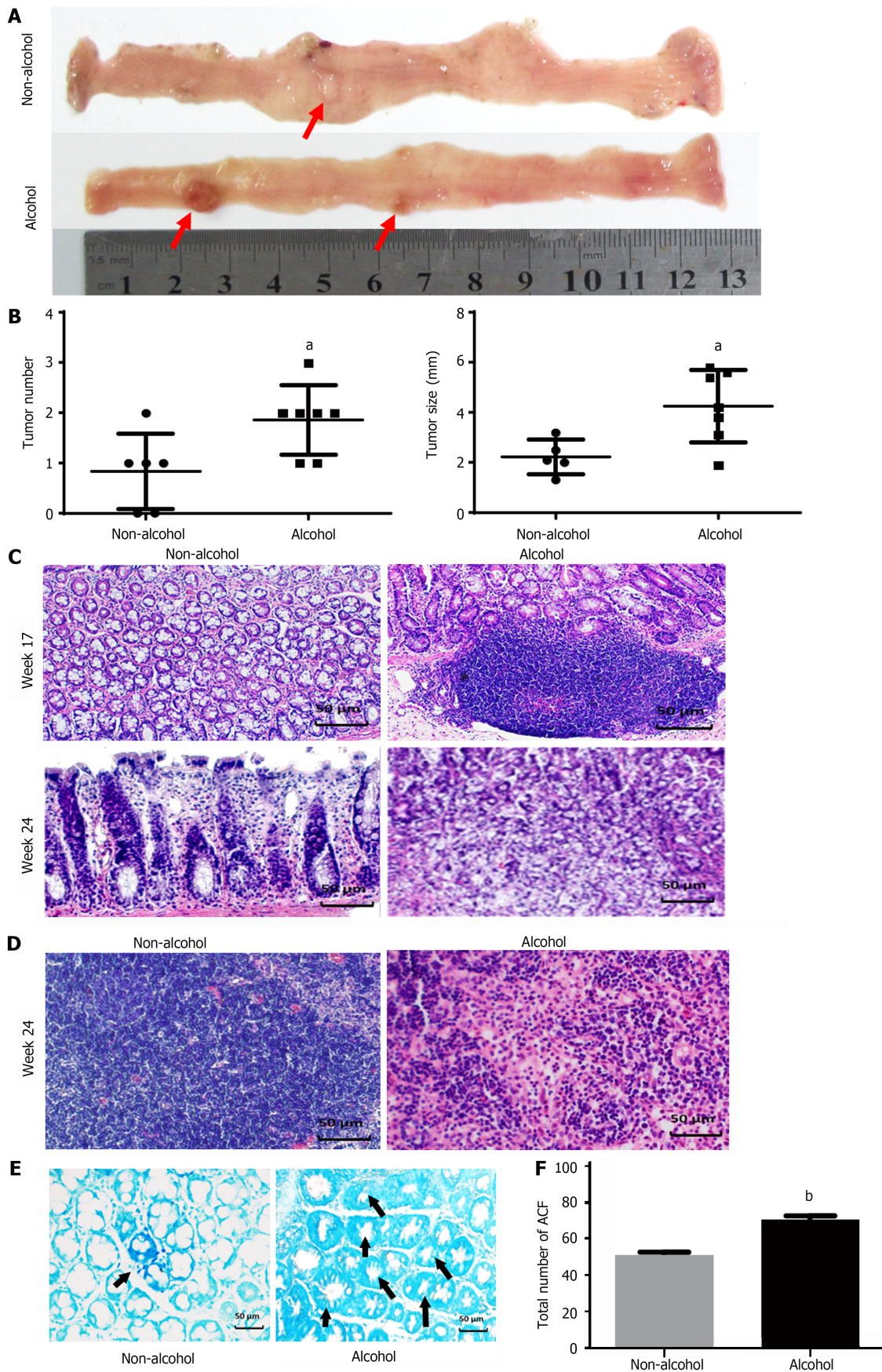
Figure 2 Alcohol consumption promotes colorectal cancer progression. A: Morphological view of colonic tumors; B: Average tumor number and tumor size in each group; C: Colon pathology of different groups (× 400); D: Pathology of colonic lymph node in different groups at the 24th week (× 400); E: Methylene blue staining for aberrant crypt foci (ACF) in the sectioned rat colon (× 400); F: Bar graph of ACF with different crypt multiplicity. The bars represent the mean ± SD (*n* = 8). Compared with the non-alcohol group: b*P* < 0.01, a*P* < 0.05. ACF: Aberrant crypt foci.

Table 3 Baseline characteristics of colorectal cancer patients

Baseline characteristics	Alcohol group (*n* = 29)	Non-alcohol group (*n* = 34)	*P* value
Gender			
Male, *n* (%)	18 (62.1)	16 (47.1)	0.233
Female, *n* (%)	11 (37.9)	18 (52.9)	
Age (yr old)			
< 55, *n* (%)	10 (34.5)	14 (41.2)	0.586
≥ 55, *n* (%)	19 (65.5)	20 (58.8)	
Differentiation			
Medium, *n* (%)	24 (82.8)	30 (88.2)	0.536
Poor, *n* (%)	5 (17.2)	4 (11.8)	
Clinical stage			
Stage I-II, *n* (%)	12 (41.4)	24 (70.6)	0.020[a]
Stage III-IV, *n* (%)	17 (58.6)	10 (29.4)	
T stage			
T1-T2, *n* (%)	6 (20.7)	12 (35.3)	0.201
T3-T4, *n* (%)	23 (79.3)	22 (64.7)	
Tumor metastasis conditions			
Distant metastasis	12 (41.4)	23 (70.6)	0.046[a]
Lymphatic metastasis	9 (31)	8 (20.6)	
Non-metastasis	8 (27.6)	3 (8.8)	

[a]$P < 0.05$.

was reverse transcribed into cDNA by using Evo M-MLV RT premix (Accurate Biotechnology, China) and quantitative real-time polymerase chain reaction (RT-PCR) system (TaKaRa, Japan). Then a SYBR Green Premix Pro Taq HS qPCR Kit (Accurate Biotechnology, China) was used for PCR. The PCR liquid volume was 20 μL. Quantitative PCR was performed using an RT-PCR system (BioRad, Singapore). At 95℃, 40 cycles were amplified after 90 s of initial denaturation, 10 s desaturation at 95℃, and 34 s of extension at 60℃. GAPDH was used as the reference gene for calculation. And the primer sequences are shown in Table 1.

Statistical analysis

The data were described using the mean (standard deviation), median (range), or frequency (percentage). An independent-samples *t* test or the Mann-Whitney U test was applied for the comparison between two groups (non-alcohol group and alcohol group). The associations between the clinical parameters and immunohistochemical results were analyzed using the χ^2 test. Statistical analyses were conducted using SPSS version 25.0 for Windows (SPSS, Inc.). Statistical analysis was performed: [b]$P < 0.01$; [a]$P < 0.05$; [ns]$P > 0.05$.

RESULTS

Alcohol consumption promoted malignant progression in CRC rats

The total number of ACFs detected in the alcohol group was 70.33 ± 5.16 and 51.6 ± 4.5 in the non-alcohol group (Figure 2E and F), which implied that alcohol consumption may significantly increase considerably raise the risk of precancerous lesions of colorectal cancer ($P < 0.05$). Furthermore, CRC rats in alcohol group had more tumors and larger tumor size was observed in the alcohol group than those in the non-alcohol group (Figure 2A and B). Histopathological analysis revealed that at 17th week, 62.5% of rats in the non-alcohol group showed atypical hyperplasia, and the other 37.5% showed normal colonic tissues. Atypical hyperplasia was seen in 75% of the rats in the alcohol group; however, 25% of the rats in the alcohol group had many heteroepithelial cells in the colonic epithelium and one or more large nucleoli in the pleomorphic cystic nucleus, indicating a carcinoma adenoma. At the 24th week, 25%
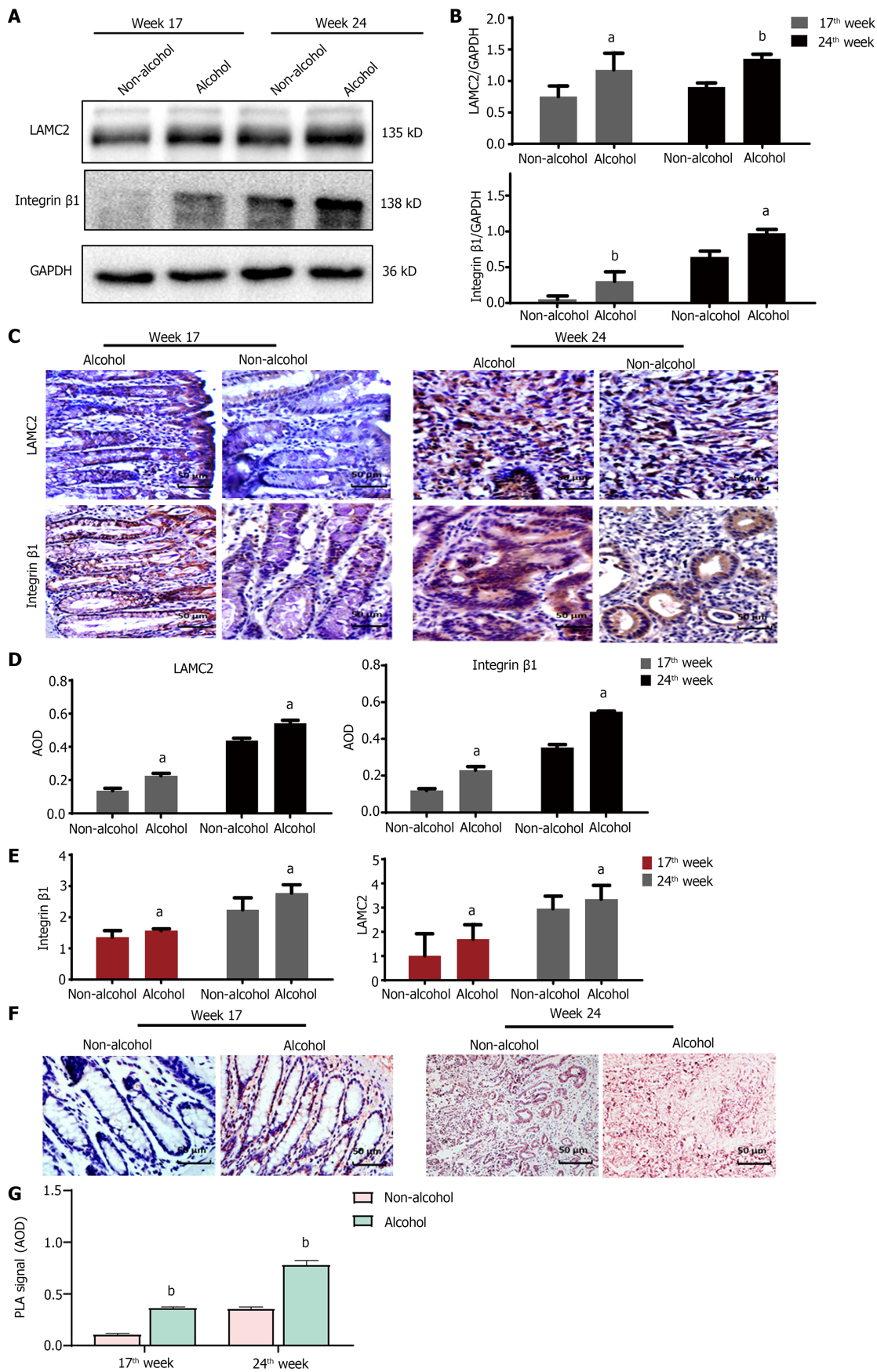
Figure 3 Alcohol consumption regulates the expression and interaction of integrin-β1 and laminin-γ2 in animal samples. The bars represent the mean ± SD (n = 8). A and B: Quantification of the protein levels of integrin-β1 (ITGB1) and laminin-γ2 (LAMC2) detected by western blotting in animal samples; C and D: Quantification of the protein levels of ITGB1 and LAMC2 by immunohistochemical (IHC) in animal samples; E: Quantification of the mRNA levels of ITGB1 and LAMC2 by quantitative real-time polymerase chain reaction in clinical samples; F: Statistical analysis of IHC was performed by counting the average optical density

(AOD). In Duolink proximity ligation assay (PLA), the brown dot particles observed under the microscope represent the interactions between LAMC2 and ITGB1; G: The statistical analysis of PLA positive signals was performed by counting the AOD under a light microscope. Compared with the non-alcohol group: [b]$P < 0.01$, [a]$P < 0.05$. ITGB1: Integrin-β1; LAMC2: Laminin-γ2; GAPDH: Glyceraldehyde-3-phosphate dehydrogenase; PLA: Proximity ligation assay; IHC: Immunohistochemical staining; AOD: Average optical density.

of rats in the alcohol group showed intramucosal carcinoma (mucosal carcinoma), which was characterized by less mucus secretion of colonic epithelial cells, compact and irregular arrangement of glandular ducts, and clear invasion of cancer cells into lamina propria in colons. The other 75% of rats in the alcohol group had invasive mucosal infiltrating carcinoma (infiltrating carcinoma), which manifested as abnormal tubular or mucinous structures invading through the muscularis mucosa or deep intestinal wall. In total, 75% and 25% of rats in the non-alcohol group showed mucosal carcinoma and infiltrating carcinoma, respectively. We found no lymphatic metastasis in the non-alcohol group, while cancer cell infiltration was found in the lymph nodes of the alcohol group and the lymph node metastasis rate was 37.5% (Figure 2C and D; Table 2). The abovementioned results indicated that alcohol consumption promoted CRC metastasis.

Alcohol consumption increased the expression of LAMC2, ITGB1 and FAK in CRC rats

The protein levels of LAMC2 and ITGB1 measured by western blotting (Figure 3A and B) and IHC (Figure 3C and D). The result showed that at both of 17th week and 24th week, the protein levels of LAMC2 and ITGB1 in the alcohol group were higher than those in the non-alcohol group ($P < 0.05$). Furthermore, the mRNA levels of LAMC2 and ITGB1 in alcohol group were higher than those in non-alcohol group at both of 17th week and 24th week ($P < 0.05$; Figure 3E). In addition, the protein level of FAK in the alcohol group was higher than that in the non-alcohol group at the 17th and 24th weeks (Figures 4 and 5, $P < 0.05$). However, there was no significant difference in the mRNA level of FAK between the alcohol and non-alcohol group at both of the 17th and 24th week ($P > 0.05$; Figure 6A).

Alcohol consumption enhanced the early interaction between LAMC2 and ITGB1 in CRC rats

Duolink PLA were used to detect the interaction between ITGB1 and LAMC2, and the red spots represent the interactions between LAMC2 and ITGB1. The results revealed that (Figure 3F and G) at 17th week, more early interacting signals between LAMC2 and ITGB1 were found in the alcohol group than that in non-alcohol group. At week 24, the results were consistent with that of week 17. The present study suggested that alcohol consumption may enhance the early interaction between LAMC2 and ITGB1 in CRC rats.

Alcohol consumption increased the expression of the CRC metastasis marker SATB1 in CRC rats

High expression level of SATB1 significantly influenced the malignant phenotypic characteristics of CRC. As shown in Figures 4 and 5, the results of IHC and western blotting indicated that at 17th week, the protein level of SATB1 in the alcohol group was higher than that in non-alcohol group, and the results of qRT-PCR (Figure 6A) showed that the mRNA level of SATB1 was higher than that in non-alcohol group.

Alcohol consumption regulates the protein and mRNA levels of EMT-associated markers in CRC rats

EMT is one of the key events that occur during the formation of premetastatic niche[44]. The results of western blotting (Figure 4A) and IHC (Figure 5) suggested that at the 17th week, long-term alcohol consumption resulted in an increase in the proteins involved in triggering the EMT process including p-FAK, N-cadherin, fibronectin and snail; however, there was a decrease in E-cadherin in the alcohol group. At week 24, the results were similar to those of week 17. In addition, the mRNA levels of FAK, E-cadherin, N-cadherin, fibronectin and snail were measured by qRT-PCR, and the results were consistent with those of protein levels (Figure 6A). The abovementioned results indicated that alcohol consumption may abnormally change the expression levels of EMT biomarkers in CRC rats in early stage.

Alcohol consumption increased the expression of proinflammatory factors associated with premetastatic niche in CRC rats

The results of ELISA (Figure 6B) showed that IL-1β, IL-6 and TNF-α levels in the alcohol group were higher than those in the non-alcohol group at week 17. The results at week 24 were consistent with those at week 17, indicating that the concentrations of IL-1β, IL-6, and TNF-α were higher in the alcohol group than in the non-alcohol group during precancerous lesions, which may be one of the reasons for lymph node metastasis in CRC patients in the alcohol group.

The obtained results showed that in early stages of CRC, the contents of IL-6, IL-1β and TNF-α in the alcohol group were higher than those in the non-alcohol group. This might be one of the explanations for the higher metastatic rate in the alcohol group.
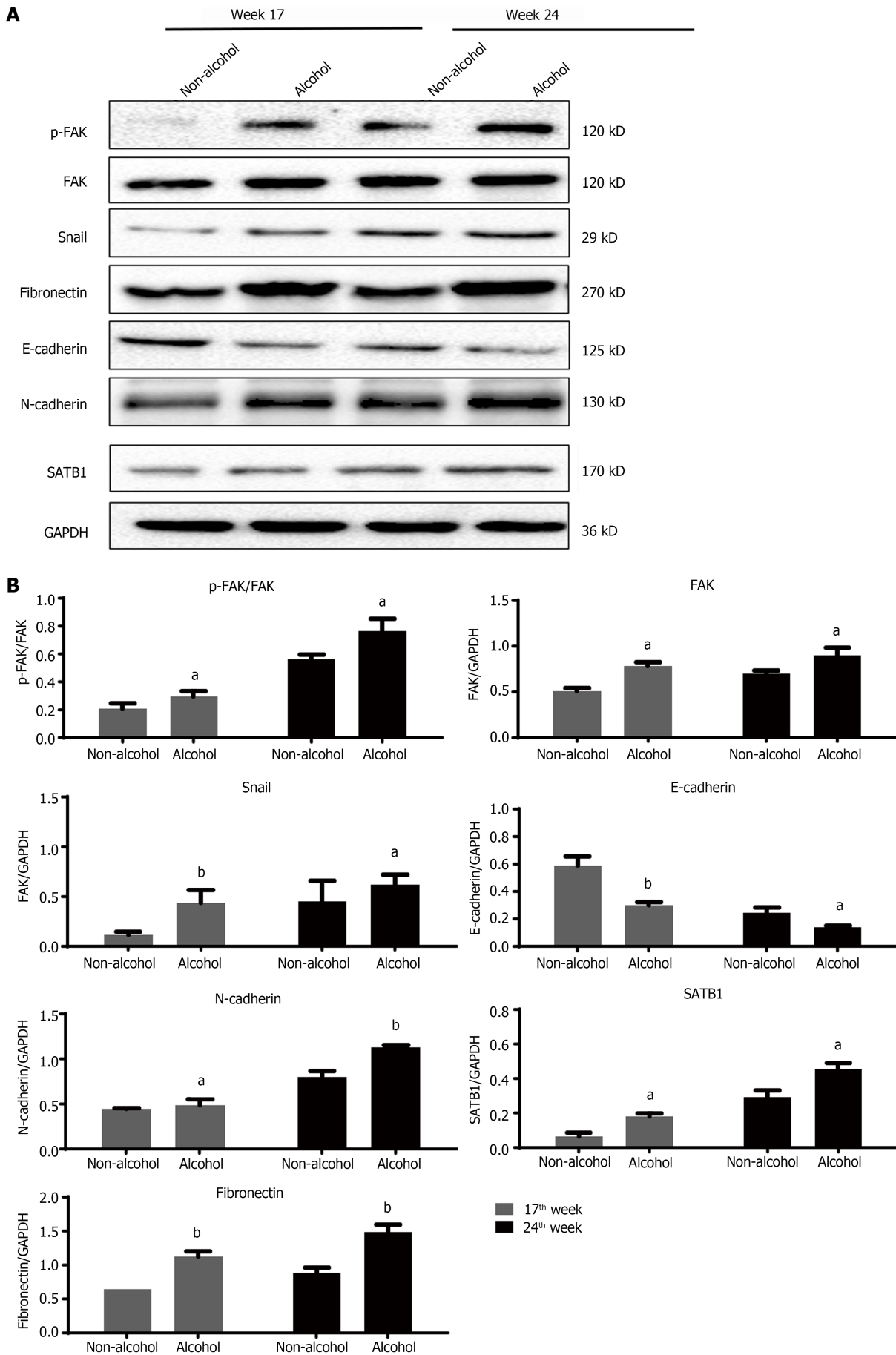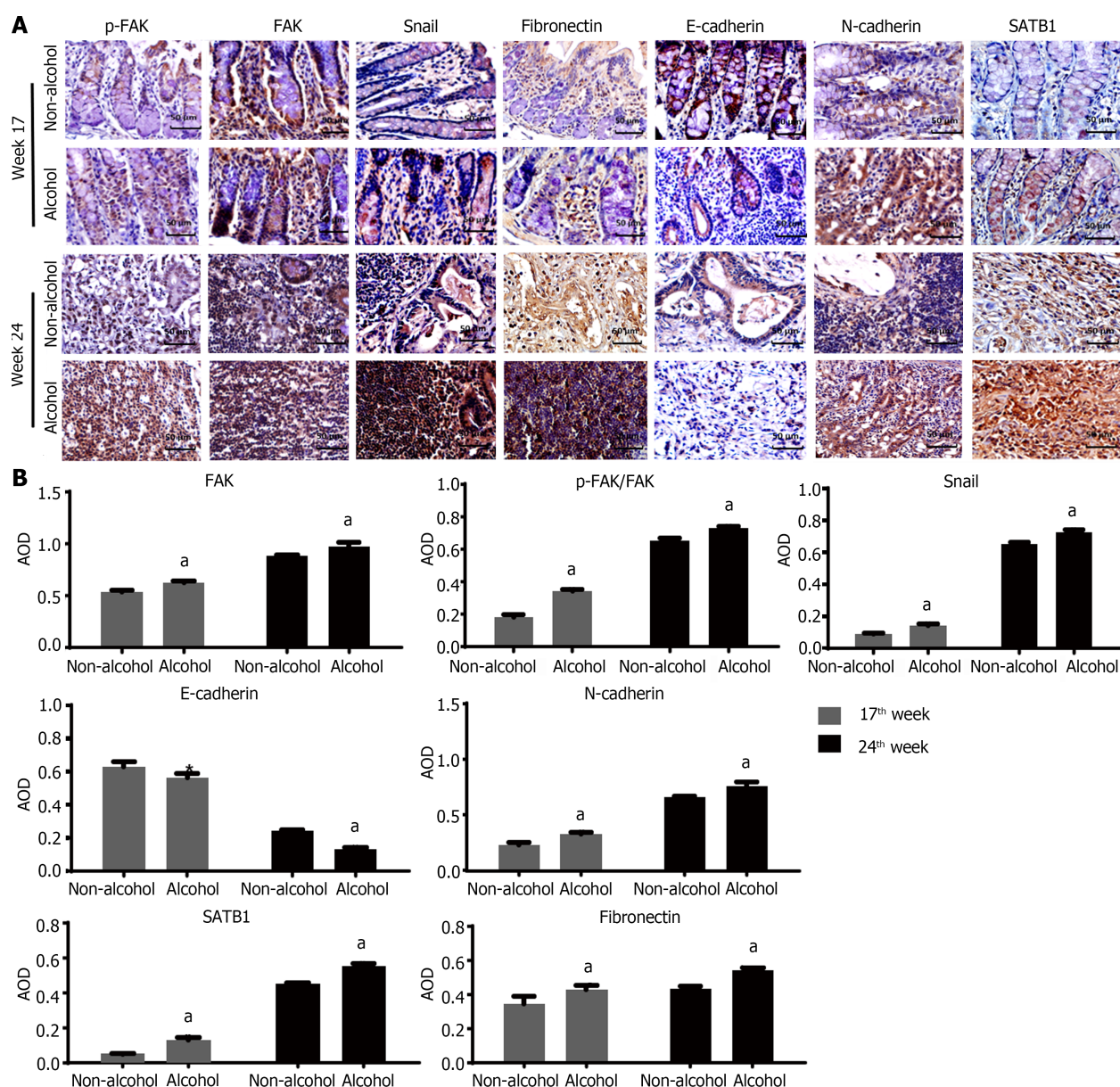
Figure 4 Quantification of the protein levels of epithelial mesenchymal transformation-related markers in colorectal cancer rats by using

western blotting. The bars represent the mean ± SD (*n* = 3). A: The western blotting images of phosphorylate-focal adhesion kinase (p-FAK), FAK, snail, fibronectin, E-cadherin, N-cadherin and special AT-rich sequence binding protein 1 (SATB1) in animal samples; B: Quantification of the protein levels of FAK, p-FAK/FAK, snail, fibronectin, E-cadherin, N-cadherin and SATB1 in animal samples. Compared with the non-alcohol group: [b]*P* < 0.01, [a]*P* < 0.05. SATB1: Special AT-rich sequence binding protein 1; FAK: Focal adhesion kinase; p-FAK: Phosphorylate focal adhesion kinase; GAPDH: Glyceraldehyde-3-phosphate dehydrogenase.

Figure 5 Immunohistochemical staining detected the protein level of epithelial mesenchymal transformation-related markers in colorectal cancer rats. The bars represent the mean ± SD (*n* = 3). A: The images of immunohistochemical (IHC) in animal samples; B: Quantification of the protein levels of focal adhesion kinase (FAK), phosphorylate-FAK (p-FAK)/FAK, snail, Fibronectin, E-cadherin, N-cadherin and special AT-rich sequence binding protein 1 detected by IHC counting the average optical density. Compared with the non-alcohol group: [b]*P* < 0.01, [a]*P* < 0.05. SATB1: Special AT-rich sequence binding protein 1; FAK: Focal adhesion kinase; p-FAK: Phosphorylate focal adhesion kinase; qRT-PCR: Quantitative real-time polymerase chain reaction; IHC: Immunohistochemical staining; AOD: Average optical density.

Baseline characteristics of CRC patients

A total of 63 patients with a preliminary diagnosis of colorectal cancer participated in the trial. According to the baseline characteristics and data on alcohol consumption of 63 CRC patients, 29 CRC patients who had been drinking alcohol over 3 times each week for more than 5 years were classified in alcohol group, while the remaining 34 CRC patients who have never drunk alcohol before were classified in non-alcohol group. As shown in Table 3, there are significant differences in clinical stage and tumor metastasis (*P* < 0.05) between alcohol group and non-alcohol group. There were no significant differences in sex, age, degree of differentiation or T stage (*P* > 0.05). The experimental
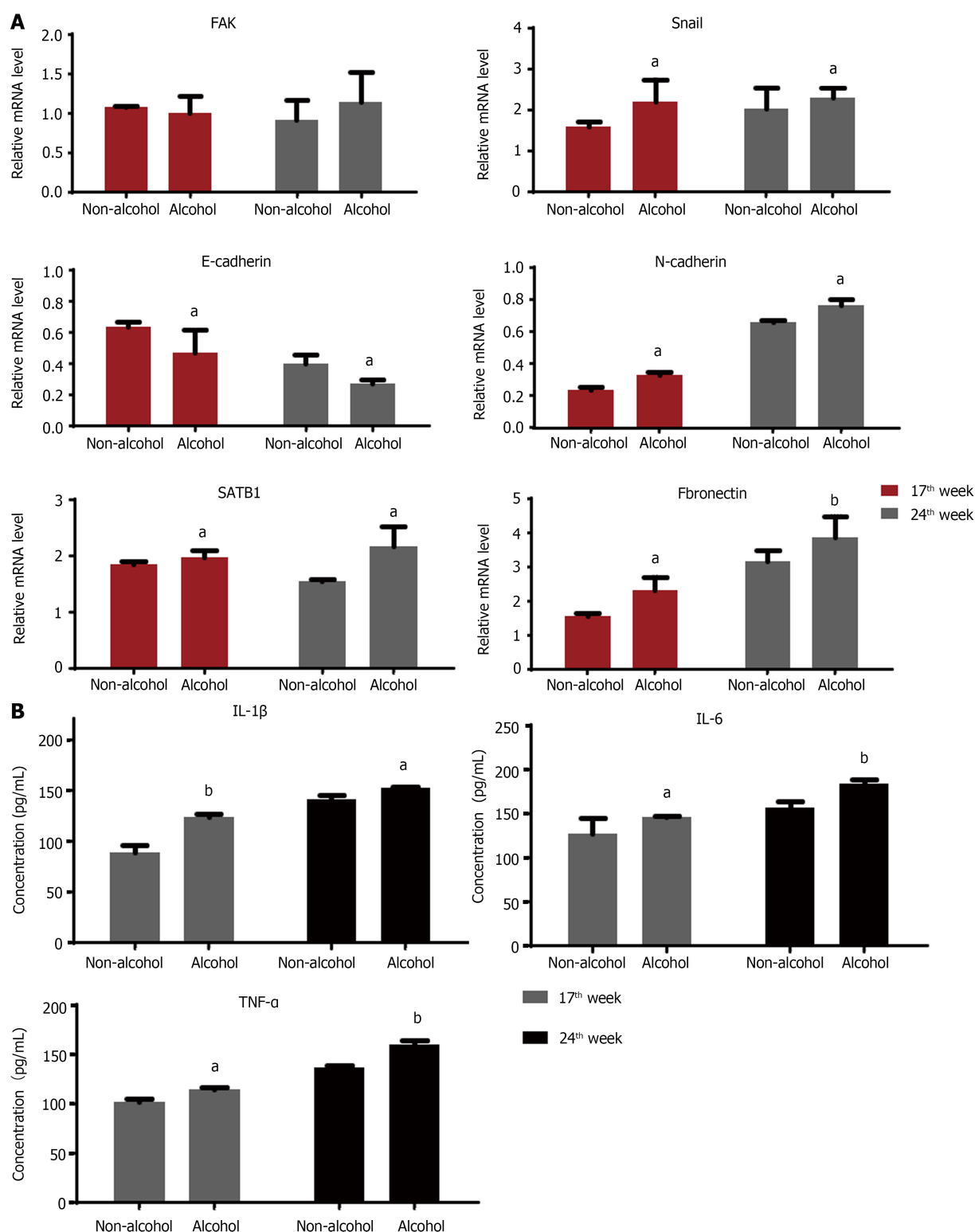
Figure 6 Alcohol consumption regulated the mRNA expression of epithelial mesenchymal transformation-related markers and proinflammatory factors in colorectal cancer rats. The bars represent the mean ± SD (*n* = 8). A: Quantification of the mRNA levels of snail, focal adhesion kinase, fibronectin, N-cadherin, E-cadherin and special AT-rich sequence binding protein 1 in each group analyzed by quantitative real-time polymerase chain reaction; B: Tumor necrosis factor-α, interleukin-6 (IL-6) and IL-1β levels in each group. Compared with the non-alcohol group: [b]*P* < 0.01, [a]*P* < 0.05. SATB1: Special AT-rich sequence binding protein 1; FAK: Focal adhesion kinase; IL-1β: Interleukin-1β; IL-6: Interleukin-6; TNF-α: Tumor necrosis factor-α.

results were consistent with the results of animal experiments. The degree of tumor deterioration in CRC patients in the alcohol group was significantly higher than that in non-alcohol group.

Alcohol consumption increased the expression and interaction of LAMC2 and ITGB1 in CRC patients

The expression of LAMC2 and ITGB1 in clinical samples determined by IHC (shown in Figure 7C and D). In cancer tissues, the mRNA and protein levels of LAMC2 and ITGB1 in alcohol group were significantly higher than those in non-alcohol group (Figure 7B). In addition, according to the survival analysis of 392 CRC patient samples from the GSE39582 dataset, we explored the prognostic significance of LAMC2 and ITGB1. As shown in Figure 7A, the overexpression of LAMC2 and ITGB1 was closely related to poor CRC prognosis. The abovementioned results were consistent with the results of animal experiments. Alcohol consumption may increase the expression levels and the interaction of LAMC2 and ITGB1 in CRC patients.

The interactions of LAMC2-ITGB1 are pivotal in CRC progression. Animal experiments revealed that more interactions between LAMC2 and ITGB1 were found in the alcohol group than in the non-alcohol group in the early stage of CRC. And it has been validated in clinical samples. According to the results of duolink PLA (Figure 7E and F), more interacting signals between LAMC2 and ITGB1 were found in alcohol group than those in non-alcohol group.

Alcohol consumption influenced the protein and mRNA expression of EMT-associated markers in CRC patients

In the animal experiment, we found that alcohol may abnormally change the expression levels of EMT-associated biomarkers in CRC rats in the early stage. To verify the clinical implications of this finding, the levels of EMT biomarkers were detected in clinical samples. The results of IHC (Figure 8A and B) showed that there were significant differences in EMT-associated biomarkers ($P < 0.01$) in cancer tissues between the alcohol and non-alcohol group. In cancer tissues, the protein levels of p-FAK, N-cadherin, fibronectin and snail were significantly higher in alcohol group was significantly higher than that in non-alcohol group; however, the expression of E-cadherin in alcohol group was significantly lower in alcohol group than that in non-alcohol group. The qRT-PCR results (Figure 8C) also showed that the mRNA levels of N-cadherin, fibronectin and snail in the cancer tissues of alcohol group was higher than that in non-alcohol group. The abovementioned findings were consistent with the results of animal experiments. The abnormal expression of EMT biomarkers in CRC patients was different from that in alcohol group, and the abnormal expression of LAMC2 and ITGB1 was more severe in alcohol group.

Alcohol consumption increased the expression of the CRC metastasis marker SATB1 in CRC patients

In animal experiments, alcohol consumption was found to increase the expression of SATB1 in CRC rats. IHC and qRT-PCR were used to evaluate the protein and mRNA levels of SATB1 in clinical samples (Figure 8A-C). The obtained results showed that protein and mRNA levels of SATB1 in cancer tissues were significantly higher in alcohol group than that in non-Alcohol group. Our results indicate that the expression of SATB1 is higher in alcohol group than those in non-Alcohol group, which is consistent with the higher metastasis rate of CRC patients who drink alcohol as described by TNM staging. The above results suggest that alcohol consumption may up-regulate the expression of SATB1, thereby induce the early EMT event and leads to malignant metastasis of the tumor[45].

DISCUSSION

Metastasis is the prominent cause of death in CRC[7]. Chronic alcohol intake has been extensively reported to enhance CRC metastasis; nevertheless, the specific mechanism remains unknown. In the present study, the results of TNM stage, pathological grade and other clinicopathological parameters suggested that the tumor deterioration rate of patients in alcohol group was higher than that in non-alcohol group, and the results were consistent with previous reports[6,7]. The present study demonstrated that the metastasis rate in alcohol group was higher than that in non-alcohol group. Similar to the clinical results, in animal experiments, the number of ACFs in the alcohol group was significantly higher than that in the non-alcohol group, and the pathological evaluation results were similar to the ACF screening results, suggesting that the alcohol group had a higher risk of precolonic lesions in CRC rats. And the number and size of tumors in the alcohol group were higher than those in the non-alcohol group. Lymph node metastasis was found in 37.5% of patients in the alcohol group, while no metastasis was found in the non-alcohol group. The present study indicated a higher risk of precancerous lesions and malignant metastasis of CRC were found in alcohol group compared with the non-alcohol group. Thus, we hypothesized that alcohol may promote the metastasis of CRC, however, the molecular mechanism is still unclear.

A key step in the formation of metastasis is the extravasation of circulating tumor cells to distant organs and their adaptation to the new environment[46,47]. Thus, the interaction between disseminated cancer cells and the microenvironment of the premetastatic niche is necessary for metastasis[10]. Primary tumor cells regulate the metastasis by secreting a variety of molecules that promote the mobilization and recruitment of various cells to the premetastatic niche and alter ECM protein expression and ECM properties in secondary organs[25,48]. The ECM constitutes a scaffold that
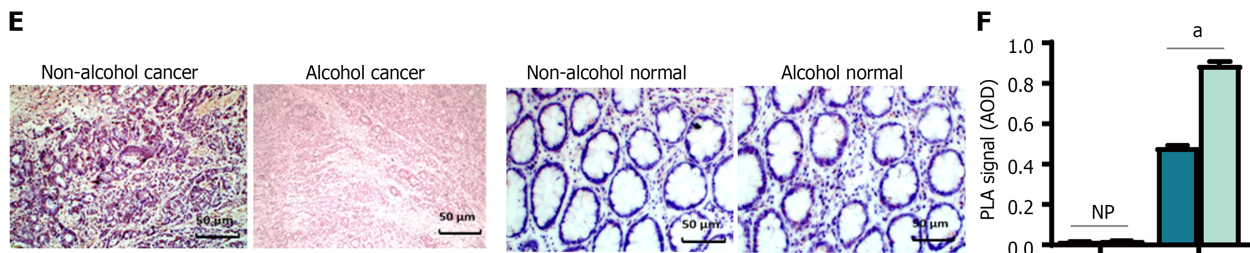
A

B

C

D

E

F
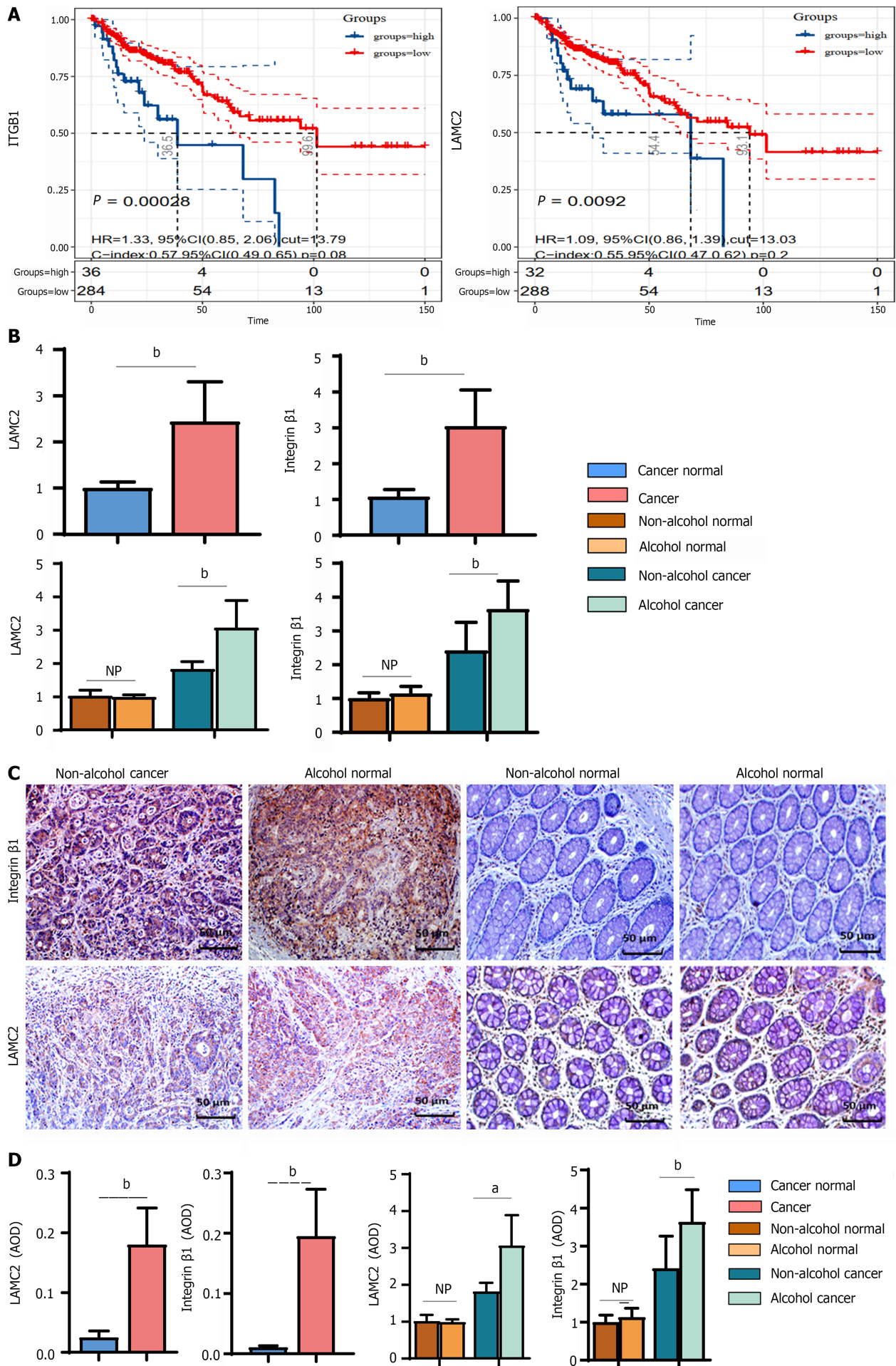
Figure 7 Alcohol consumption increased the expression and interaction of laminin-γ2 and integrin-β1 in colorectal cancer rats. The bars represent the mean ± SD (*n* = 8). A: Survival analysis of integrin-β1 (ITGB1) and laminin-γ2 (LAMC2) in colorectal cancer; B: The mRNA levels of ITGB1 and LAMC2 determined by quantitative real-time polymerase chain reaction in clinical samples; C: Representative immunohistochemical (IHC) images of ITGB1 and LAMC2 in clinical samples (× 400); D: The quantifications of the protein levels of ITGB1 and LAMC2 determined by IHC in clinical samples; E and F: Duolink proximity ligation assay (PLA) verified the interactions between ITGB1 and LAMC2 in clinical samples. The statistical analysis of PLA positive signals was performed by counting the average optical density under a light microscope. Compared with the non-alcohol group: [b]$P < 0.01$, [a]$P < 0.05$. LAMC2: Laminin-γ2; ITGB1: Integrin-β1; qRT-PCR: Quantitative real-time polymerase chain reaction; PLA: Proximity ligation assay; IHC: Immunohistochemical staining; AOD: Average optical density. Cancer normal group: cancer adjacent tissue group. NP: No statistical difference.

supports the attachment and thus reactivation of survival signaling in cancer cells[16]. And the remodeling of ECM is essential during formation of premetastatic niche, which may support cancer cell attachment, metabolism and migration of recruited cells[17,18]. Laminin, as an important component of the ECM and the main structural component of basement membrane, is involved in the formation of pre-metastasis niche[49]. Among them, LAMC2 is an important component of the survival-dependent environment of colorectal cancer epithelial cells and plays a key role in the regulation of tumor cell motility by premetastatic niche formation[50]. LAMC2 plays a role in premetastatic niche signaling by stimulating the formation of premetastatic local contacts and promoting the migration of cancer cells through its interaction with ITGB1[51]. It has been reported that the interaction of ITGB1 and LAMC2 may promote the tumor budding of CRC cells, which leads to malignant metastasis of CRC, and the focal adhesion formed by the interaction of LAMC2 and ITGB1 plays an important role in the prognosis of CRC. This adhesion is not only the basis of cancer cell survival but is also closely related to the migration and metastasis of cancer cells[52]. FAK is involved in LAMC2 and ITGB1 signal transduction, and the overexpression of FAK was found to play a key regulatory role in ITGB1-mediated signal transduction. As the phosphorylated FAK is activated, it transmits signals to the transcription factor snail, thereby inducing EMT[32,33]. The interaction of LAMC2 and ITGB1 and the overexpression of FAK were seen as markers of premetastatic niche formation, which may lead to malignant metastasis of CRC[52]. According to the results of our study, more interacting signals between LAMC2 and ITGB1, and higher level of FAK were found in the alcohol group than those in the non-alcohol group at early stage. In addition, the higher ratio of p-FAK/FAK in the alcohol group in the early stage indicates a higher degree of FAK activation, which may induce early EMT events and promote CRC metastasis.

CRC metastasis depends on EMT, during EMT, epithelial cells lose the connectivity and top-to-base polarity, resulting in a mesenchymal phenotype capability of migration and invasion[32]. There is evidence that some cancer cells may acquire the ability to spread and metastasize before they are fully malignant, which suggests that EMT may be an early event involving in the metastasis[53]. In addition, SATB1 has been found to be associated with early EMT events and can be used as a marker of CRC metastasis[54]. SATB1 was found to be a driver of the malignant phenotype in CRC, and its expression was shown to be positively associated with invasion depth, poor degree of differentiation and advanced TNM stage of CRC. And SATB1 organizes chromatin into spatial rings that provide the necessary "docking sites" for further binding of transcription factors and chromatin modifying enzymes[45]. SATB1 was found to regulate entire genes, even those located on distant chromosomes[55]. The results of the animal experiment suggested that the expression of SATB1 was significantly higher in the alcohol group than that in the non-alcohol group during precancerous lesions, which may predict the early EMT events.

In addition, there is an increasing evidence that proinflammatory cytokines play an important role in the formation of premetastatic niches. Previous studies have shown that the high expression of IL-6 and IL-1β may activate ITGB1[56,57] to stimulate the adhesion of bone marrow cells to endothelial cells, thereby promote the formation of premetastatic niche, and inducing EMT to promote metastasis[58]. Pal *et al*[55] found that TNF-α induces EMT in human HCT116 cells and promotes colorectal cancer invasion and metastasis. According to our study, the levels of the proinflammatory cytokines IL-1β, TNF-α and IL-6 in CRC rats in the alcohol group were significantly increased at the early stage of precancerous lesions, which may serve as paracrine signals to enhance the proliferation and invasion of early disseminated cancer cells. It may help cancer cells change their phenotypes through EMT to enhance metastasis.
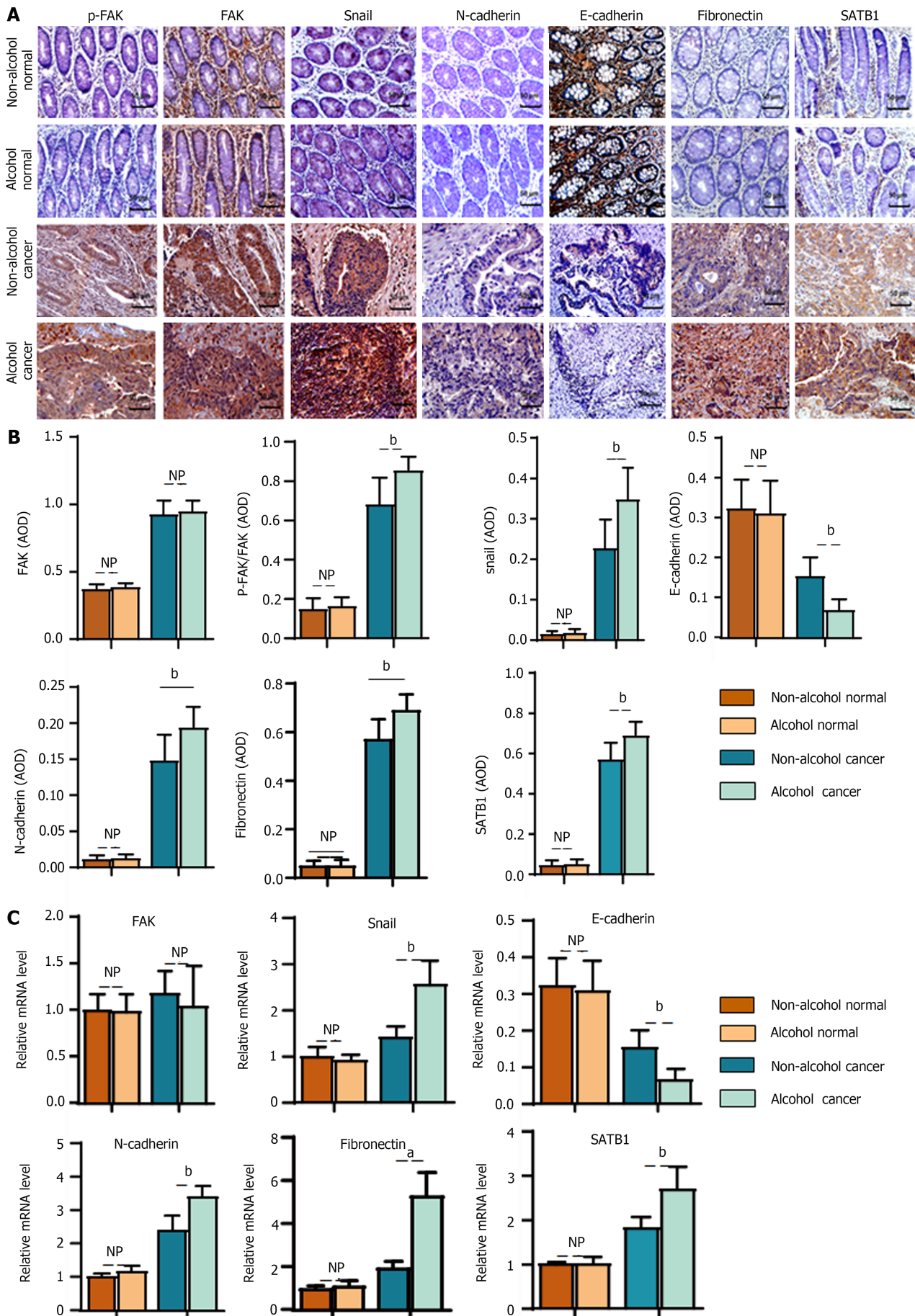
Figure 8 Alcohol consumption influenced the protein and mRNA levels of epithelial mesenchymal transformation -associated markers in

colorectal cancer patients. The bars represent the mean ± SD (*n* = 8). A: Representative immunohistochemical images of phosphorylate-focal adhesion kinase (p-FAK), FAK, snail, fibronectin, E-cadherin, N-cadherin and special AT-rich sequence binding protein 1 (SATB1) in different groups in clinical samples (× 400); B: Quantification of the protein levels of FAK, p-FAK/FAK, snail, fibronectin, E-cadherin, N-cadherin and SATB1 by counting the average optical density in clinical samples; C: Quantification of the mRNA levels of FAK, snail, fibronectin, E-cadherin, N-cadherin and SATB1 by quantitative real-time polymerase chain reaction in clinical samples. Compared with the non-alcohol group: [b]*P* < 0.01, [a]*P* < 0.05. SATB1: Special AT-rich sequence binding protein 1; FAK: Focal adhesion kinase; p-FAK: Phosphorylate focal adhesion kinase; AOD: Average optical density. NP: No statistical difference.
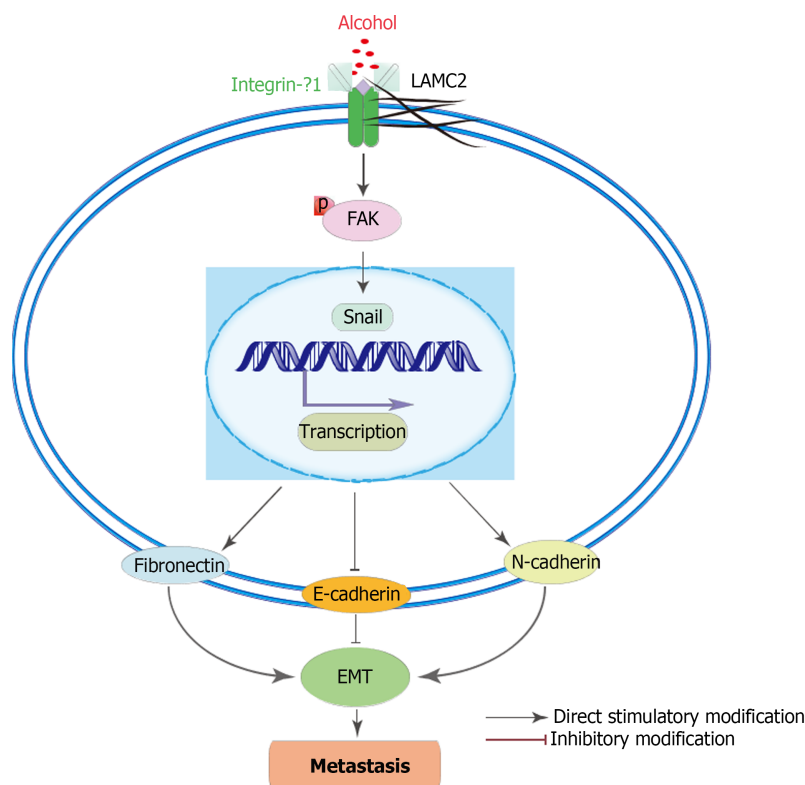
Figure 9 Schematic diagram of the possible signaling pathway regulated by alcohol. EMT: Epithelial mesenchymal transformation; LAMC2: Laminin-γ2; ITGB1: Integrin-β1; FAK: Focal adhesion kinase; p-FAK: Phosphorylate focal adhesion kinase.

The EMT event is also a key event involving in the formation of the premetastatic niche[32,33], which is almost featuring the loss of E-cadherin expression and overexpression of snail, N-cadherin and fibronectin[56,59]. The results of animal experiments suggested that long-term alcohol consumption (shown in Figure 9), as a risk factor of CRC, may further activate p-FAK by enhancing the interaction between LAMC2 and ITGB1 and forming a premetastatic niche, thus upregulating the expression of snail in precancerous lesions. Thus, the expression levels of N-cadherin and fibronectin were increased and the expression level of E-cadherin was downregulated, leading to the mesenchymal phenotype of cancer cells and colorectal cancer metastasis. This may be one of the reasons for the higher metastasis rate of CRC rats in the alcohol group. We found the similar results in clinical samples. The main limitation of the clinical study is the relatively small sample size. Larger-scale functional studies are required to improve our understanding of the effects of alcohol on the premetastatic niche in CRC. However, the obtained results provide some interesting suggestions for future studies with an increased sample size. Based on the abovementioned results, the present study demonstrated that alcohol may promote the formation of premetastatic niche *via* enhancing the EMT event mediated by the LAMC2-ITGB1 interaction, leading to the high incidence of CRC metastasis in the alcohol group.

CONCLUSION

In summary, the present study attempted to examine the nonspecific effect of alcohol on the premetastatic niche of colorectal cancer. Our study suggests that alcohol has an effect on the colorectal carcinogenesis paradigm and may accelerate the malignant metastasis of CRC. The molecular mechanism may involve the effect of alcohol on the early EMT-mediated premetastatic niche of colorectal cancer induced by LAMC2 and ITGB1 interactions.

ACKNOWLEDGMENT

ARTICLE HIGHLIGHTS

Research background
Colorectal cancer (CRC) is a common malignant tumor.

Research motivation
Alcohol consumption is positively correlated with CRC malignant metastasis; however, the mechanism is unclear.

Research objectives
To investigate the effects of alcohol on CRC metastasis

Research methods
The interaction between laminin-γ2 (LAMC2) and integrin-β1 (ITGB1) was measured by Duolink assay, and the expression levels of LAMC2, ITGB1 and focal adhesion kinase, snail, fibronectin, N-cadherin and special AT-rich sequence binding protein 1 were measured by quantitative real-time polymerase chain reaction, immunohistochemistry and western blotting. Interleukin-1β (IL-1β), tumor necrosis factor-α and IL-6 levels were measured *via* enzyme-linked immunosorbent assay, histopathological assessment *via* hematoxylin eosin staining, and determination of aberrant crypt foci *via* methylene blue.

Research results
Alcohol may promote CRC metastasis by influencing the molecular mechanism of the premetastatic niche.

Research conclusions
Our study suggests that alcohol promotes epithelial mesenchymal transformation-mediated premetastatic niche formation of CRC by activating the early interaction between LAMC2 and ITGB1 and lead to CRC metastasis.

Research perspectives
To explore the effect of alcohol on colorectal cancer metastasis.

FOOTNOTES

ORCID number: Fei-Fei Nong 0000-0002-2306-0108; Yu-Qi Liang 0000-0002-7481-116X; Shang-Ping Xing 0000-0001-7252-7176; Yin-Fang Xiao 0000-0001-5196-641X; Hui-Hui Chen 0000-0002-0129-6718; Bin Wen 0000-0001-9096-3115.

REFERENCES

1   **Ladabaum U**, Dominitz JA, Kahi C, Schoen RE. Strategies for Colorectal Cancer Screening. *Gastroenterology* 2020; **158**: 418-432 [PMID: 31394083 DOI: 10.1053/j.gastro.2019.06.043]

2   **Akimoto N**, Ugai T, Zhong R, Hamada T, Fujiyoshi K, Giannakis M, Wu K, Cao Y, Ng K, Ogino S. Rising incidence of early-onset colorectal cancer - a call to action. *Nat Rev Clin Oncol* 2021; **18**: 230-243 [PMID: 33219329 DOI: 10.1038/s41571-020-00445-1]

3   **Murphy N**, Moreno V, Hughes DJ, Vodicka L, Vodicka P, Aglago EK, Gunter MJ, Jenab M. Lifestyle and dietary environmental factors in colorectal cancer susceptibility. *Mol Aspects Med* 2019; **69**: 2-9 [PMID: 31233770 DOI: 10.1016/j.mam.2019.06.005]

4   **Zheng K**, Yu J, Chen Z, Zhou R, Lin C, Zhang Y, Huang Z, Yu L, Zhao L, Wang Q. Ethanol promotes alcohol-related colorectal cancer metastasis *via* the TGF-β/RUNX3/Snail axis by inducing TGF-β1 upregulation and RUNX3 cytoplasmic mislocalization. *EBioMedicine* 2019; **50**: 224-237 [PMID: 31757777 DOI: 10.1016/j.ebiom.2019.11.011]

5   **Mohr AM**, Gould JJ, Kubik JL, Talmon GA, Casey CA, Thomas P, Tuma DJ, McVicker BL. Enhanced colorectal cancer metastases in the alcohol-injured liver. *Clin Exp Metastasis* 2017; **34**: 171-184 [PMID: 28168393 DOI: 10.1007/s10585-017-9838-x]

6   **Diao XY**, Peng T, Kong FG, Huang JG, Han S, Shang YS, Liu H. Alcohol consumption promotes colorectal cancer by altering intestinal permeability. *Eur Rev Med Pharmacol Sci* 2020; **24**: 9370-9377 [PMID: 33015778 DOI: 10.26355/eurrev_202009_23020]

7   **Hosseini H**, Obradović MMS, Hoffmann M, Harper KL, Sosa MS, Werner-Klein M, Nanduri LK, Werno C, Ehrl C, Maneck M, Patwary N, Haunschild G, Gužvić M, Reimelt C, Grauvogl M, Eichner N, Weber F, Hartkopf AD, Taran FA, Brucker SY, Fehm T, Rack B, Buchholz S, Spang R, Meister G, Aguirre-Ghiso JA, Klein CA. Early dissemination seeds metastasis in breast cancer. *Nature* 2016; **540**: 552-558 [PMID: 27974799 DOI: 10.1038/nature20785]

8   **Tsai HW**, Yuan CC, Wang PH. Umbilicus as the only site of metastasis in recurrent ovarian cancer. *J Chin Med Assoc* 2006; **69**: 233-235 [PMID: 16835987 DOI: 10.1016/S1726-4901(09)70225-4]

9   **Attaran S**, Bissell MJ. The role of tumor microenvironment and exosomes in dormancy and relapse. *Semin Cancer Biol* 2022; **78**: 35-44 [PMID: 34757184 DOI: 10.1016/j.semcancer.2021.09.008]

10   **Radin DP**, Tsirka SE. Interactions between Tumor Cells, Neurons, and Microglia in the Glioma Microenvironment. *Int J Mol Sci* 2020; **21** [PMID: 33187183 DOI: 10.3390/ijms21228476]

11   **Osipov A**, Saung MT, Zheng L, Murphy AG. Small molecule immunomodulation: the tumor microenvironment and overcoming immune escape. *J Immunother Cancer* 2019; **7**: 224 [PMID: 31439034 DOI: 10.1186/s40425-019-0667-0]

12   **Zhang Z**, Qiao J, Zhang D, Zhu W, Zhu J, Leng X, Li S. Noncoding RNAs Act as Tumor-Derived Molecular Components in Inducing Premetastatic Niche Formation. *Biomed Res Int* 2019; **2019**: 9258075 [PMID: 31309120 DOI: 10.1155/2019/9258075]

13   **Han P**, Cao P, Hu S, Kong K, Deng Y, Zhao B, Li F. Esophageal Microenvironment: From Precursor Microenvironment to Premetastatic Niche. *Cancer Manag Res* 2020; **12**: 5857-5879 [PMID: 32765088 DOI: 10.2147/CMAR.S258215]

14   **Jing B**, Wang T, Sun B, Xu J, Xu D, Liao Y, Song H, Guo W, Li K, Hu M, Zhang S, Ling J, Kuang Y, Zhang T, Zhou BP, Yao F, Deng J. IL6/STAT3 Signaling Orchestrates Premetastatic Niche Formation and Immunosuppressive Traits in Lung. *Cancer Res* 2020; **80**: 784-797 [PMID: 31848193 DOI: 10.1158/0008-5472.CAN-19-2013]

15   **Doglioni G**, Parik S, Fendt SM. Interactions in the (Pre)metastatic Niche Support Metastasis Formation. *Front Oncol* 2019; **9**: 219 [PMID: 31069166 DOI: 10.3389/fonc.2019.00219]

16   **Choi J**, Gyamfi J, Jang H, Koo JS. The role of tumor-associated macrophage in breast cancer biology. *Histol Histopathol* 2018; **33**: 133-145 [PMID: 28681373 DOI: 10.14670/HH-11-916]

17   **Dong Q**, Liu X, Cheng K, Sheng J, Kong J, Liu T. Pre-metastatic Niche Formation in Different Organs Induced by Tumor Extracellular Vesicles. *Front Cell Dev Biol* 2021; **9**: 733627 [PMID: 34616739 DOI: 10.3389/fcell.2021.733627]

18   **Kim H**, Chung H, Kim J, Choi DH, Shin Y, Kang YG, Kim BM, Seo SU, Chung S, Seok SH. Macrophages-Triggered Sequential Remodeling of Endothelium-Interstitial Matrix to Form Pre-Metastatic Niche in Microfluidic Tumor Microenvironment. *Adv Sci (Weinh)* 2019; **6**: 1900195 [PMID: 31179226 DOI: 10.1002/advs.201900195]

19   **Najafi M**, Farhood B, Mortezaee K. Extracellular matrix (ECM) stiffness and degradation as cancer drivers. *J Cell Biochem* 2019; **120**: 2782-2790 [PMID: 30321449 DOI: 10.1002/jcb.27681]

20   **Trapani V**, Bonaldo P, Corallo D. Role of the ECM in notochord formation, function and disease. *J Cell Sci* 2017; **130**: 3203-3211 [PMID: 28883093 DOI: 10.1242/jcs.175950]

21   **Mal'tseva DV**, Makarova YA, Raigorodskaya MP, Rodin SA. Effects of Laminins 332 and 411 on the Epithelial-

Mesenchymal Status of Colorectal Cancer Cells. *Bull Exp Biol Med* 2019; **166**: 377-382 [PMID: 30627897 DOI: 10.1007/s10517-019-04354-x]

22 **Urooj T**, Wasim B, Mushtaq S, Shah SNN, Shah M. Cancer Cell-derived Secretory Factors in Breast Cancer-associated Lung Metastasis: Their Mechanism and Future Prospects. *Curr Cancer Drug Targets* 2020; **20**: 168-186 [PMID: 31858911 DOI: 10.2174/1568009620666191220151856]

23 **Maltseva DV**, Rodin SA. [Laminins in Metastatic Cancer]. *Mol Biol (Mosk)* 2018; B: 411-434 [PMID: 29989574 DOI: 10.7868/S0026898418030059]

24 **Chang YC**, Wang JD, Chang HY, Zhou P, Hahn RA, Gordon MK, Laskin JD, Gerecke DR. Expression of Laminin γ2 Proteolytic Fragments in Murine Skin Following Exposure to Sulfur Mustard. *Anat Rec (Hoboken)* 2020; **303**: 1642-1652 [PMID: 32421930 DOI: 10.1002/ar.24405]

25 **Meireles Da Costa N**, Mendes FA, Pontes B, Nasciutti LE, Ribeiro Pinto LF, Palumbo Júnior A. Potential Therapeutic Significance of Laminin in Head and Neck Squamous Carcinomas. *Cancers (Basel)* 2021; **13** [PMID: 33920762 DOI: 10.3390/cancers13081890]

26 **Tohmatsu Y**, Imura J, Sakai T, Takagi K, Minamisaka T, Tanaka S, Noguchi A, Nakajima T, Nagata T, Makino T, Shimizu T, Fujii T. Expression of laminin-5 gamma 2 chain predicts invasion of extramammary Paget's disease cell. *APMIS* 2021; **129**: 3-8 [PMID: 32996218 DOI: 10.1111/apm.13086]

27 **Huang C**, Chen J. Laminin332 mediates proliferation, apoptosis, invasion, migration and epithelialtomesenchymal transition in pancreatic ductal adenocarcinoma. *Mol Med Rep* 2021; **23** [PMID: 33179081 DOI: 10.3892/mmr.2020.11649]

28 **Wang SH**, Liou GG, Liu SH, Chang JS, Hsiao JR, Yen YC, Chen YL, Wu WL, Chang JY, Chen YW. Laminin γ2-enriched extracellular vesicles of oral squamous cell carcinoma cells enhance in vitro lymphangiogenesis *via* integrin α3-dependent uptake by lymphatic endothelial cells. *Int J Cancer* 2019; **144**: 2795-2810 [PMID: 30485433 DOI: 10.1002/ijc.32027]

29 **Liu CC**, Lin JH, Hsu TW, Hsu JW, Chang JW, Su K, Hsu HS, Hung SC. Collagen XVII/laminin-5 activates epithelial-to-mesenchymal transition and is associated with poor prognosis in lung cancer. *Oncotarget* 2018; **9**: 1656-1672 [PMID: 29416721 DOI: 10.18632/oncotarget.11208]

30 **Brenner H**, Chen C. The colorectal cancer epidemic: challenges and opportunities for primary, secondary and tertiary prevention. *Br J Cancer* 2018; **119**: 785-792 [PMID: 30287914 DOI: 10.1038/s41416-018-0264-x]

31 **Erin N**, Grahovac J, Brozovic A, Efferth T. Tumor microenvironment and epithelial mesenchymal transition as targets to overcome tumor multidrug resistance. *Drug Resist Updat* 2020; **53**: 100715 [PMID: 32679188 DOI: 10.1016/j.drup.2020.100715]

32 **Wang Y**, Shi J, Chai K, Ying X, Zhou BP. The Role of Snail in EMT and Tumorigenesis. *Curr Cancer Drug Targets* 2013; **13**: 963-972 [PMID: 24168186 DOI: 10.2174/15680096113136660102]

33 **Wu X**, Cai J, Zuo Z, Li J. Collagen facilitates the colorectal cancer stemness and metastasis through an integrin/PI3K/AKT/Snail signaling pathway. *Biomed Pharmacother* 2019; **114**: 108708 [PMID: 30913493 DOI: 10.1016/j.biopha.2019.108708]

34 **Wang Y**, Xu M, Ke ZJ, Luo J. Cellular and molecular mechanisms underlying alcohol-induced aggressiveness of breast cancer. *Pharmacol Res* 2017; **115**: 299-308 [PMID: 27939360 DOI: 10.1016/j.phrs.2016.12.005]

35 **Cho S**, Shin A, Park SK, Shin HR, Chang SH, Yoo KY. Alcohol Drinking, Cigarette Smoking and Risk of Colorectal Cancer in the Korean Multi-center Cancer Cohort. *J Cancer Prev* 2015; **20**: 147-152 [PMID: 26151048 DOI: 10.15430/JCP.2015.20.2.147]

36 **Ferretti S**, Patriarca S, Carbone A, Zanetti R. [TNM classification of malignant tumours, VII edition 2009. Changes and practical effects on cancer epidemiology]. *Epidemiol Prev* 2010; **34**: 125-128 [PMID: 20852350]

37 **National Research Council (US) Committee for the Update of the Guide for the Care and Use of Laboratory Animals**. Guide for the Care and Use of Laboratory Animals. 8th edition. Washington (DC): National Academies Press (US); 2011 [PMID: 21595115]

38 **Martin B**, Schäfer E, Jakubowicz E, Mayr P, Ihringer R, Anthuber M, Schenkirsch G, Schaller T, Märkl B. Interobserver variability in the H&E-based assessment of tumor budding in pT3/4 colon cancer: does it affect the prognostic relevance? *Virchows Arch* 2018; **473**: 189-197 [PMID: 29626253 DOI: 10.1007/s00428-018-2341-1]

39 **Bird RP**, Lafave LM. Varying effect of dietary lipids and azoxymethane on early stages of colon carcinogenesis: enumeration of aberrant crypt foci and proliferative indices. *Cancer Detect Prev* 1995; **19**: 308-315 [PMID: 7553672]

40 **Sivaranjani A**, Sivagami G, Nalini N. Chemopreventive effect of carvacrol on 1,2-dimethylhydrazine induced experimental colon carcinogenesis. *J Cancer Res Ther* 2016; **12**: 755-762 [PMID: 27461646 DOI: 10.4103/0973-1482.154925]

41 **Mansour DF**, Abdallah HMI, Ibrahim BMM, Hegazy RR, Esmail RSE, Abdel-Salam LO. The Carcinogenic Agent Diethylnitrosamine Induces Early Oxidative Stress, Inflammation and Proliferation in Rat Liver, Stomach and Colon: Protective Effect of Ginger Extract. *Asian Pac J Cancer Prev* 2019; **20**: 2551-2561 [PMID: 31450931 DOI: 10.31557/APJCP.2019.20.8.2551]

42 **Huang G**, Bao J, Shao X, Zhou W, Wu B, Ni Z, Wang L. Inhibiting pannexin-1 alleviates sepsis-induced acute kidney injury *via* decreasing NLRP3 inflammasome activation and cell apoptosis. *Life Sci* 2020; **254**: 117791 [PMID: 32416166 DOI: 10.1016/j.lfs.2020.117791]

43 **Bai N**, Zhang Q, Zhang W, Liu B, Yang F, Brann D, Wang R. G-protein-coupled estrogen receptor activation upregulates interleukin-1 receptor antagonist in the hippocampus after global cerebral ischemia: implications for neuronal self-defense. *J Neuroinflammation* 2020; **17**: 45 [PMID: 32007102 DOI: 10.1186/s12974-020-1715-x]

44 **Suarez-Carmona M**, Lesage J, Cataldo D, Gilles C. EMT and inflammation: inseparable actors of cancer progression. *Mol Oncol* 2017; **11**: 805-823 [PMID: 28599100 DOI: 10.1002/1878-0261.12095]

45 **Coupland LA**, Parish CR. Platelets, selectins, and the control of tumor metastasis. *Semin Oncol* 2014; **41**: 422-434 [PMID: 25023359 DOI: 10.1053/j.seminoncol.2014.04.003]

46 **Høye AM**, Erler JT. Structural ECM components in the premetastatic and metastatic niche. *Am J Physiol Cell Physiol* 2016; **310**: C955-C967 [PMID: 27053524 DOI: 10.1152/ajpcell.00326.2015]

47 **Zhuyan J**, Chen M, Zhu T, Bao X, Zhen T, Xing K, Wang Q, Zhu S. Critical steps to tumor metastasis: alterations of

tumor microenvironment and extracellular matrix in the formation of pre-metastatic and metastatic niche. *Cell Biosci* 2020; **10**: 89 [PMID: 32742634 DOI: 10.1186/s13578-020-00453-9]

48   **Guo Y**, Ji X, Liu J, Fan D, Zhou Q, Chen C, Wang W, Wang G, Wang H, Yuan W, Ji Z, Sun Z. Effects of exosomes on pre-metastatic niche formation in tumors. *Mol Cancer* 2019; **18**: 39 [PMID: 30857545 DOI: 10.1186/s12943-019-0995-1]

49   **Wang Y**, Shi M, Yang N, Zhou X, Xu L. GPR115 Contributes to Lung Adenocarcinoma Metastasis Associated With LAMC2 and Predicts a Poor Prognosis. *Front Oncol* 2020; **10**: 577530 [PMID: 33330053 DOI: 10.3389/fonc.2020.577530]

50   **Xu L**, Hou Y, Tu G, Chen Y, Du YE, Zhang H, Wen S, Tang X, Yin J, Lang L, Sun K, Yang G, Liu M. Nuclear Drosha enhances cell invasion *via* an EGFR-ERK1/2-MMP7 signaling pathway induced by dysregulated miRNA-622/197 and their targets LAMC2 and CD82 in gastric cancer. *Cell Death Dis* 2017; **8**: e2642 [PMID: 28252644 DOI: 10.1038/cddis.2017.5]

51   **Moon YW**, Rao G, Kim JJ, Shim HS, Park KS, An SS, Kim B, Steeg PS, Sarfaraz S, Changwoo Lee L, Voeller D, Choi EY, Luo J, Palmieri D, Chung HC, Kim JH, Wang Y, Giaccone G. LAMC2 enhances the metastatic potential of lung adenocarcinoma. *Cell Death Differ* 2015; **22**: 1341-1352 [PMID: 25591736 DOI: 10.1038/cdd.2014.228]

52   **Cavaco ACM**, Eble JA. A 3D Spheroid Model as a More Physiological System for Cancer-Associated Fibroblasts Differentiation and Invasion In Vitro Studies. *J Vis Exp* 2019 [PMID: 31449247 DOI: 10.3791/60122]

53   **Wang G**, Yang Q, Li M, Zhang Y, Cai Y, Liang X, Fu Y, Xiao Z, Zhou M, Xie Z, Huang H, Huang Y, Chen Y, He Q, Peng F, Chen Z. Quantitative proteomic profiling of tumor-associated vascular endothelial cells in colorectal cancer. *Biol Open* 2019; **8** [PMID: 31036754 DOI: 10.1242/bio.042838]

54   **Pavan Kumar P**, Purbey PK, Sinha CK, Notani D, Limaye A, Jayani RS, Galande S. Phosphorylation of SATB1, a global gene regulator, acts as a molecular switch regulating its transcriptional activity in vivo. *Mol Cell* 2006; **22**: 231-243 [PMID: 16630892 DOI: 10.1016/j.molcel.2006.03.010]

55   **Pal M**, Bhattacharya S, Kalyan G, Hazra S. Cadherin profiling for therapeutic interventions in Epithelial Mesenchymal Transition (EMT) and tumorigenesis. *Exp Cell Res* 2018; **368**: 137-146 [PMID: 29674112 DOI: 10.1016/j.yexcr.2018.04.014]

56   **Schmid MC**, Avraamides CJ, Foubert P, Shaked Y, Kang SW, Kerbel RS, Varner JA. Combined blockade of integrin-α4β1 plus cytokines SDF-1α or IL-1β potently inhibits tumor inflammation and growth. *Cancer Res* 2011; **71**: 6965-6975 [PMID: 21948958 DOI: 10.1158/0008-5472.CAN-11-0588]

57   **Jones SA**, Jenkins BJ. Recent insights into targeting the IL-6 cytokine family in inflammatory diseases and cancer. *Nat Rev Immunol* 2018; **18**: 773-789 [PMID: 30254251 DOI: 10.1038/s41577-018-0066-7]

58   **Deng Y**, Chakraborty P, Jolly MK, Levine H. A Theoretical Approach to Coupling the Epithelial-Mesenchymal Transition (EMT) to Extracellular Matrix (ECM) Stiffness *via* LOXL2. *Cancers (Basel)* 2021; **13** [PMID: 33807227 DOI: 10.3390/cancers13071609]

59   **Noronha C**, Ribeiro AS, Taipa R, Castro DS, Reis J, Faria C, Paredes J. Cadherin Expression and EMT: A Focus on Gliomas. *Biomedicines* 2021; **9** [PMID: 34680444 DOI: 10.3390/biomedicines9101328]

ORIGINAL ARTICLE

Retrospective Cohort Study

Natural history and outcomes of patients with liver cirrhosis complicated by hepatic hydrothorax

Sarah Romero, Andy KH Lim, Gurpreet Singh, Chamani Kodikara, Rachel Shingaki-Wells, Lynna Chen, Samuel Hui, Marcus Robertson

Sarah Romero, Chamani Kodikara, Rachel Shingaki-Wells, Samuel Hui, Marcus Robertson, Department of Gastroenterology, Monash Health, Clayton 3168, Victoria, Australia

Andy KH Lim, Marcus Robertson, Department of General Medicine, School of Clinical Sciences, Monash University, Clayton 3168, Victoria, Australia

Gurpreet Singh, Lynna Chen, Gastroenterology and Liver Transplant Unit, Austin Health, Heidelberg 3084, Victoria, Australia

Corresponding author: Sarah Romero, FRACP, MBBS, Doctor, Department of Gastroenterology, Monash Health, 246 Clayton Road, Clayton 3168, Victoria, Australia. s.romero.md@gmail.com

Abstract

BACKGROUND
Hepatic hydrothorax (HH) is an uncommon and difficult-to-manage complication of cirrhosis with limited treatment options.

AIM
To define the clinical outcomes of patients presenting with HH managed with current standards-of-care and to identify factors associated with mortality.

METHODS
Cirrhotic patients with HH presenting to 3 tertiary centres from 2010 to 2018 were retrospectively identified. HH was defined as pleural effusion in the absence of cardiopulmonary disease. The primary outcomes were overall and transplant-free survival at 12-mo after the index admission. Cox proportional hazards analysis was used to determine factors associated with the primary outcomes.

RESULTS
Overall, 84 patients were included (mean age, 58 years) with a mean model for end-stage liver disease score of 29. Management with diuretics alone achieved long-term resolution of HH in only 12% patients. At least one thoracocentesis was performed in 73.8% patients, transjugular intrahepatic portosystemic shunt insertion in 11.9% patients and 33% patients received liver transplantation within 12-mo of index admission. Overall patient survival and transplant-free survival at 12 mo were 68% and 41% respectively. At multivariable analysis, current smoking

[hazard ratio (HR) = 8.65, 95% confidence interval (CI): 3.43-21.9, $P < 0.001$) and acute kidney injury (AKI) (HR = 2.91, 95%CI: 1.21-6.97, $P = 0.017$) were associated with a significantly increased risk of mortality.

CONCLUSION
Cirrhotic patients with HH are a challenging population with a poor 12-mo survival despite current treatments. Current smoking and episodes of AKI are potential modifiable factors affecting survival. HH is often refractory of diuretic therapy and transplant assessment should be considered in all cases.

Key Words: Cirrhosis; Portal hypertension; Hepatic hydrothorax; Ascites; Liver transplantation

Core Tip: The development of hepatic hydrothorax (HH) in cirrhotic patients continues to be associated with a very poor prognosis despite current standards-of-care. In one of the largest series to investigate the natural history of patients with hepatic hydrothoraces, a 45-d overall survival rate of 80% and 12-mo transplant-free survival of 41% was observed after index hospitalisation with HH. At multivariate analysis, current smoking and development of acute kidney injury were both independently associated with mortality, and represent important modifiable risk factors.

INTRODUCTION

Hepatic hydrothorax (HH) is an uncommon but serious complication occurring in patients with decompensated cirrhosis. HH is defined as the accumulation of more than 500 mL of transudative pleural fluid in a patient with cirrhosis and portal hypertension, where primary cardiopulmonary or malignant aetiologies have been excluded[1]. HH has been reported to occur in 5% to 11% of patients with cirrhosis, with more than 90% of cases occurring in Child-Pugh B or C disease[1,2]. HH is thought to arise from direct passage of fluid from the peritoneal cavity to the pleural cavity through diaphragmatic fenestrations[1]. Nuclear medicine studies, using labelled albumin have confirmed unidirectional passage of fluid from the abdominal to the pleural cavity[3], thus supporting a diaphragmatic defect process.

Clinically significant HH develops when accumulation of ascites in the pleural cavity exceeds the absorptive capacity of the pleura and patients typically present with shortness of breath, cough, hypoxia or chest discomfort[1,3]. Most cases occur in patients with appreciable ascites, however ascites may not be a prominent finding in up to 42%[1]. HH is most often unilateral and right-sided (59%-80%), however, there are increasing reports of left-sided (12%-17%) or bilateral (8%-24%) involvement[1,4]. Similar to the development of spontaneous bacterial peritonitis (SBP) in patients with ascites, patients with HH may develop spontaneous infections within the pleural fluid, which are termed spontaneous bacterial empyema (SBEM)[3].

The clinical management of HH remains complex and challenging. Treatment priorities in cirrhotic patients presenting with a pleural effusion include confirming a diagnosis of HH and excluding alternative pathology, relieving symptoms, preventing pulmonary complications and managing the underlying ascites. Diagnostic or therapeutic thoracocentesis is typically performed to confirm the presence of transudative fluid and to exclude SBEM or alternative pathology[5]. Recently developed American Association for the Study of Liver Disease (AASLD) guidelines state that first-line management should include sodium restriction and diuresis[6]. It is recognised, however, that 20%-30% of patients with cirrhosis and HH will develop persistent or recurrent pleural effusion despite these measures[6]. Refractory HH represents a particularly challenging management issue and patients are often considered for repeat therapeutic thoracocentesis and transjugular intrahepatic portosystemic shunt (TIPS) placement. Liver transplantation (LT) is the definitive treatment for HH, and post-transplant outcomes are comparable to outcomes for alternative indications[6].

Currently, there remains a paucity of literature examining the natural history and prognostic significance of HH. No randomised controlled trials have been performed in this population and clinical guidelines were only published for the first time in 2020[6]. Previous small studies have indicated the development of HH is associated with significant morbidity and extremely poor survival in the absence of LT[2,7,8]. The aims of this study were to: (1) Evaluate the probability of survival in a cohort of patients with liver cirrhosis presenting with HH and to examine factors associated with mortality; and (2) Provide a descriptive analysis of the treatments and complications associated with HH treatment during hospitalisation.

MATERIALS AND METHODS

Study design and setting
We conducted a multi-centre retrospective cohort study of patients with cirrhosis and HH presenting to three Australian metropolitan tertiary hospitals, one of which was a liver transplant centre, over a 9-year period from 2010 to 2018. Across all study sites, patients with decompensated cirrhosis were admitted under a specialist gastroenterology or liver transplant unit. Individual patient management was at the discretion of the attending gastroenterologist.

Ethics approval
The Human Research Ethics Committee at Monash Health and Austin Health approved the study as a quality assurance activity and the committee provided a waiver for informed consent (RES-19-0000-343Q).

Study participants
International Classification of Diseases (10th revision) codes for cirrhosis and chronic liver disease (K74, K74.6), HH (J 94.8) and pleural effusion (J90, J91) were used to retrospectively identify eligible patients with cirrhosis and HH[9]. The study eligibility criteria were: (1) Adult patients ≥ 18 years; (2) A confirmed diagnosis of cirrhosis, either biopsy-proven or based on clinical complications of cirrhosis; (3) Confirmed diagnosis of pleural effusion, based on imaging (plain X-ray or computed tomography); (4) Evidence of portal hypertension, as established by the presence of oesophageal varices, ascites and/or thrombocytopenia; and (5) Exclusion of cardiopulmonary or malignant pathology as a cause for the pleural fluid collection. Eligible patients were excluded if they had previously undergone LT. Included patients were followed for 12-mo from the date of the index admission.

Outcomes
The primary outcomes were 12-mo overall and transplant-free patient survival following index hospital admission with HH. Patients were followed-up from the date of first hospital admission with HH to an endpoint of death, LT or end of the study period. We report the 12-mo overall survival using the endpoint of death, censored for LT; and the 12-mo transplant-free survival using a composite endpoint of death and LT. The secondary outcomes included the incidence of specific treatments of HH and associated complications and to determine patient-specific prognostic factors associated with mortality.

HH definition and treatment protocols
HH was defined as the presence of a pleural effusion occurring in a patient with liver cirrhosis where no alternative aetiology was identified. Each patient was reviewed by a specialist hepatologist to ensure that the aetiology of pleural effusion was secondary to HH. Patients were excluded if the pleural effusion was felt to be due to primary infection, cardiopulmonary or malignant pathology.

Paracentesis was performed following radiological marking and thoracocentesis was performed by an interventional radiologist or the unit treating doctor with ultrasound guidance. In all cases, baseline observations were recorded, and the procedure was performed using sterile technique. Intravenous albumin (100 mL of 20% concentrated human albumin) was administered after every 2 liters of ascites or pleural fluid drained as per institutional protocol. Clinical observations were performed every 30 min for the duration of the procedure. Pleural and ascitic fluid was sent for analysis at the discretion of the physician performing the procedure according to indication and specimen viability. Where available, serum-pleural ascites gradient (SPAG) or serum-ascites albumin gradient values were obtained. SPAG greater than 11 g/L is consistent with a transudate[2], and was used to confirm portal hypertensive pathophysiology. SBEM was defined as pleural fluid with polymorphonuclear count of > 500 cells/mm³ or > 250 cells/mm³ with a positive culture, where parapneumonic effusion had been excluded[3]. Thoracocentesis without significant fluid drainage (diagnostic aspiration) was not considered in this analysis. TIPS insertion was available at all study centres and was performed by interventional radiology.

Treatment modalities pertaining to HH were categorized as: (1) Medical therapy with diuretics, and/or thoracocentesis; (2) TIPS; and (3) LT. All patients were risk stratified using the model for end-

stage liver disease (MELD) score which was calculated at the time of presentation for each admission. An in-hospital complication was defined as the occurrence of one or more of the following: Infection, procedural complication (hematoma, pneumothorax, death), acute kidney injury (AKI, defined as at least 1.5-1.9 times baseline or ≥ 26.5 mmol/L increase from baseline[10]), and new-onset acute hepatic encephalopathy which was not present on admission.

Data sources

For each patient, baseline demographic data, aetiology of liver disease, comorbidities, medication use, radiology results and laboratory results were extracted from electronic medical records. For patients with recurrent hospital admissions due to HH during the study period, data was collected for each presentation. Death was determined through hospital medical records and confirmed with a patient's Local Medical Officer if required.

Statistical analysis

mean ± SD was used to describe normally distributed continuous data, and median and interquartile range (IQR) for data that was significantly skewed. χ^2 analysis was used to examine the association between categorical variables. For the primary outcome, we used the Cox proportional hazards regression survival model to analyze the time of onset of HH to death. The time at risk begins at the first admission for HH (the index admission, t_0) and patients were censored at the time of LT or study conclusion (365 d after t_0). For transplant-free survival analysis, we omitted censoring LT and treated the transplant date as an outcome event. For each readmission, further clinical data was collected for analysis. The model incorporates enduring baseline variables (age, sex, comorbidities, smoking, alcohol intake, aetiology of cirrhosis) as well as a number of time-varying covariates (MELD score, AKI, encephalopathy, treatment-related complications, functional status, and TIPS).

From the univariable analyses, we included variables with a $P < 0.20$ into the multivariable model. Through backward elimination steps, we retained covariates with a $P < 0.05$ and checked the general model fit using partial Cox-Snell residuals. We used fractional polynomials to assist parameterization of continuous variables. The proportional hazards assumption was tested by examining the Schoenfeld residuals. The DFBETA estimates were used to detect influential observations. To validate our findings, we conducted bootstrapping of the Cox regression analysis with 1000 replications to generate bootstrapped confidence intervals (CIs). All analyses were conducted with STATA 16.1 (StataCorp, TX, United States), and a $P < 0.05$ was considered statistically significant.

RESULTS

Patient characteristics

A total of 246 patients with cirrhosis presenting to hospital with a pleural effusion were identified during the study period, of which 162 were excluded as the pleural effusion did not meet the criteria for HH. The final analysis included 84 patients who had a total of 167 hospital admissions over the study period. The baseline characteristics of the patients are summarized in Table 1. The mean age was 58.3 years, with only 11% patients over the age of 70, and there was a slight predominance of males. All patients had established liver cirrhosis and clinical evidence of portal hypertension. The median MELD score at time of hospital admission was 29 (IQR: 25-33). A diagnosis of hepatocellular carcinoma was present in 27.4% patients.

Across all hospital admissions, 59% of patients were treated with lactulose (13% variation within patients between admissions), 27% of patients were treated with rifaximin (average 12% variation within patients between admissions), and 56% of patients were receiving prophylaxis for SBP (average 12% variation within patients between admissions). Prior to hospital presentation with HH, 93% patients were prescribed diuretic therapy, with median furosemide and spironolactone doses of 40 mg and 100 mg per day respectively and 70% of these patients were receiving dual diuretic treatment.

HH clinical features and management

The clinical features and management of HH are summarized in Table 2. The majority of the hydrothoraces were unilateral on the right side. Of the 167 episodes of HH, 20 (12.0%) were managed solely with increased diuretics. Concurrent treatment with diuretics and ascitic fluid drainage was commonly performed, with abdominal paracentesis performed during 47 (28.1%) presentations, where the median volume of fluid drained was 5 litres. The proportion of patients requiring thoracocentesis, abdominal paracentesis and the complications rates were similar for readmissions compared to the index admission. However, the dose of diuretics used was higher on readmissions than during the index admission.

Thoracocentesis and complications: In total, 115 thoracocentesis procedures were performed in 62 (73.8%) patients with a median of 3 litres drained per procedure. Thoracocentesis was performed in 53 of 84 (63%) patients during the index admission. A further 62 thoracocentesis procedures were

Table 1 Baseline characteristics of patients with cirrhosis during the index hospital admission for hepatic hydrothorax (*n* = 84)

Characteristic	Statistic
Age, mean ± SD, yr	58.3 ± 11.5
Male, *n* (%)	46 (54.8)
Diabetes mellitus, *n* (%)	23 (27.4)
Ischaemic heart disease, *n* (%)	7 (8.3)
Heart failure, *n* (%)	4 (4.8)
Chronic obstructive lung disease, *n* (%)	5 (6.0)
Hepatocellular carcinoma, *n* (%)	23 (27.4)
Other cancer, *n* (%)	3 (3.6)
Chronic kidney disease, *n* (%)	11 (13.1)
Current smoker, *n* (%)	12 (14.3)
Current alcohol drinker, *n* (%)	9 (10.7)
Aetiology of liver disease[1], *n* (%)	
Hepatitis C virus	25 (29.8)
Non-alcoholic fatty liver	17 (20.2)
Alcoholic liver disease	13 (15.5)
Hepatitis B virus	9 (10.7)
Primary biliary cirrhosis/sclerosing cholangitis	7 (8.3)
Cryptogenic	7 (8.3)
Autoimmune hepatitis	6 (7.1)
Budd-Chiari syndrome	3 (3.6)
Metabolic/others[2]	7 (8.3)
MELD score, mean ± SD	26.8 ± 7.1
Platelet count, median (IQR), per nL	103 (65-132)
Platelet count < 50/nL, *n* (%)	9 (10.7)
Anticoagulation, *n* (%)	6 (7.1)
Previous ascitic taps, *n* (%)	69 (82.1)
Beta-blockers, *n* (%)	11 (13.1)
Lactulose, *n* (%)	34 (40.5)
Rifaximin, *n* (%)	14 (16.7)
SBP prophylaxis, *n* (%)	32 (38.1)

[1]Categories are not mutually exclusive as > 1 aetiology may be attributed to each patient.

[2]Hemochromatosis, α1-antitrypsin deficiency, sarcoidosis.

MELD: Model for end-stage liver disease; SBP: Spontaneous bacterial peritonitis; IQR: Interquartile range.

performed in 33 of 43 patients who required one or more readmissions. On average, the probability of receiving another thoracocentesis was 77% during each readmission episode. Sufficient laboratory data to perform pleural/ascitic fluid analysis was available in 31% of procedures. Of these, SBEM was detected in 10 (8.7%) thoracocentesis procedures.

Blood products, including pooled platelets, fresh frozen plasma, cryoprecipitate, were administered in 29% of patients prior to or following thoracocentesis. Sixteen patients received an indwelling intercostal catheter for ongoing drainage rather than simple thoracocentesis in the setting of acute instability (*n* = 4) or refractory disease (*n* = 12). A pneumothorax complicated 17 (15%) thoracocentesis procedures, of which 7 were managed conservatively, 9 required an intercostal catheter insertion, and 1 patient died. Bleeding complications from thoracocentesis were uncommon and we could not determine if blood product infusions (platelets, fresh frozen plasma, cryoprecipitate, or prothrombin complex

Table 2 Clinical features of hepatic hydrothorax, management, and complications

Characteristic	Index admission (*n* = 84)	Readmissions (*n* = 83)
NYHA severity of dyspnoea, *n* (%)		
Class I	13 (15.5)	4 (4.3)
Class II	23 (27.4)	37 (39.4)
Class III	28 (33.3)	22 (23.4)
Class IV	20 (23.8)	31 (33.0)
Distribution of hydrothorax, *n* (%)		
Unilateral, left	13 (15.5)	10 (12.1)
Unilateral, right	68 (81.0)	72 (86.8)
Bilateral	3 (3.6)	1 (1.2)
Admission hepatic encephalopathy, *n* (%)	12 (14.3)	14 (16.9)
De novo hepatic encephalopathy, *n* (%)	11 (13.1)	10 (12.0)
Thoracocentesis performed, *n* (%)	53 (63.1)	62 (74.7)
Pneumothorax, *n* (% of procedures)	6 (11.3)	11 (17.7)
Haematoma, *n* (% of procedures)	2 (3.8)	1 (1.6)
Pre-procedure platelet infusion, *n* (%)	11 (13.3)	6 (7.2)
Pre-procedure blood products[1], *n* (%)	18 (21.7)	12 (14.5)
Pleural fluid drained, mean ± SD, litres	2.8 ± 1.7	3.0 ± 1.5
Indwelling intercostal catheter, *n* (%)	10 (11.9)	8 (9.6)
Infection, *n* (%)	17 (20.2)	14 (16.9)
Acute kidney injury, *n* (%)	30 (35.7)	28 (33.7)
Concurrent ascites drainage, *n* (%)	23 (27.1)	24 (28.9)
Volume drained, mean ± SD, litres	6.0 ± 3.1	5.5 ± 2.1
TIPS performed, *n* (%)	2 (2.4)	8 (9.6)
Furosemide, *n* (%)		
None	27 (32.1)	9 (10.8)
20 to < 100 mg daily	52 (61.9)	60 (72.3)
100 to 240 mg daily	5 (5.6)	14 (16.9)
Spironolactone, *n* (%)		
None	27 (32.1)	18 (21.7)
25 to < 100 mg daily	15 (17.9)	22 (26.5)
100 to 300 mg daily	42 (50.0)	43 (51.8)

[1]One or more of fresh frozen plasma, cryoprecipitate, or prothrombin complex concentrate.

NYHA: New York Heart Association; TIPS: Transjugular intrahepatic portosystemic shunt.

concentrate) reduced procedural complications or affected patient survival.

Other complications: One or more non-pleural complications were recorded in 80 (48%) of HH admissions. The most frequent complications were AKI in 58 (35%) patients, followed by infection in 31 (19%) and new-onset hepatic encephalopathy in 21 (13%). The incidence of these complications was similar for the index admission and readmissions.

TIPS insertion: Ten (12%) patients received a TIPS insertion, with 2 patients receiving TIPS insertion during the index admission, and 8 patients on a readmission. Significantly more females than males received a TIPS (21% *vs* 4%, *P* = 0.038), but age and MELD score did not differ between patients who received TIPS and those who did not. No patient who received a TIPS proceeded to LT within 12 mo of

the index admission.

LT: Forty-seven patients (56%) were referred for liver transplant assessment and 28 patients (33%) were successfully transplanted in the 12-mo following their index admission. The median time to transplantation from the index admission was 105 d (IQR: 55-200 d). The effect of LT on survival could not be estimated as there were no deaths amongst the transplanted patients within the study period.

Hospital length of stay and readmissions

The median hospital length of stay was 8 d (IQR: 4-17) for the index admission and 6 d (IQR: 4-14) for subsequent hospital readmissions. Within 12-mo of the index admission, 22 (26%) patients had 1 readmission, 9 (11%) had 2 readmissions, and 12 (14%) had ≥ 3 readmissions. In the 43 patients who required readmission, the median time interval between the index admission and the first readmission was 32 d (IQR: 12-74 d). The primary reasons for hospital readmissions were recurrent hydrothorax in 24 (38%) patients and decompensated cirrhosis in 26 (41%). There was strong evidence for an association between the New York Health Association (NYHA) functional class of dyspnoea and total number of readmissions (χ^2 = 46.2, P < 0.001) but the strength of the association was weak (Kendall's tau-b = 0.11). Intensive care unit (ICU) admission was required in 13 (15%) patients during the index admission, and 10 (12%) of 83 readmission episodes.

Mortality

There were 23 deaths (27.4% of the cohort) within 12-mo of the index admission. The total time-at-risk was 17850 patient-days with a mortality rate of 1.3 deaths per 1000 patient-days. The Kaplan-Meier survivor functions for overall and transplant-free patient survival are shown in Figure 1. Most deaths occurred early after the index admission, with 30-d overall survival of 87% (95%CI: 78%-93%), 45-d survival of 80% (95%CI: 70%-87%), and 12-mo survival of 68% (95%CI: 56%-78%). For transplant-free survival, the 30-d survival was 85% (95%CI: 75%-91%), 45-d survival of 76% (95%CI: 66%-84%), and 12-mo survival of 41% (95%CI: 30%-51%). Most deaths were due to complications of end-stage liver disease and multiorgan failure (75%) or hepatocellular carcinoma (10%), but a small number were due to cardiovascular events (15%). We noted that the mortality rate for current smokers was 5.58 per 1000 patient-days, compared to non-smokers of 0.86 per 1000 patient-days, giving a mortality rate ratio for current smokers of 6.5 (95%CI: 2.5-16.1, P < 0.001).

Univariable and multivariable Cox regression analysis

The results of univariable analyses are summarised in Table 3. Factors consistently associated with an increased hazard of death were current smoking, episodes of AKI, higher MELD score, and hepatic encephalopathy. In addition, when analysing transplant-free survival, diabetes and TIPS insertion were associated with a lower hazard for death or LT while incident pneumothoraces were associated with greater hazard.

The results of the multivariable analyses are summarised in Table 4. When examining the overall patient survival model, we decided not to include hepatic encephalopathy in the multivariable model as there were only 4 cases of severe encephalopathy on admission which were associated with an increased risk of death. In the transplant-free survival model, age, diabetes, TIPS and incident pneumothoraces were not statistically significant after adjusting for MELD, smoking, AKI, and hepatic encephalopathy. There were no significant statistical interactions between variables in the final models, and the models were a reasonable fit for the data when assessed by partial Cox-Snell residuals.

Due to the cohort size, we conducted bootstrapped analysis to validate our findings (Table 4). The significance of current smoking and AKI remained robust. In the overall survival model, a current smoker had 8.7 times the hazard of death of a non-smoker or ex-smoker; and one or more episodes of AKI was associated with a 2.9-fold increase in the hazard of death, after allowing for age and MELD score. In the transplant-free survival model, a current smoker had 3.1 times the hazard of death of a non-smoker or ex-smoker; and AKI was associated with a 2.2-fold increase in the hazard of death; after allowing for MELD and hepatic encephalopathy. These findings are represented in Figure 2.

Other analysis

To compare with the traditional Cox model, we also performed a competing risks regression analysis (Fine-Gray subdistribution proportional hazards) using the same covariates, with the assumption that all patients were on the active liver transplant waiting list. In this analysis, the effect of smoking and AKI on survival remained significant, and our conclusions remained unchanged. The subhazard ratio (SHR) of smoking on mortality was 6.26 (95%CI: 2.75-14.3), P < 0.001. The SHR of AKI on mortality was 2.60 (95%CI: 1.25-5.36), P = 0.01. The clear effect of smoking can be illustrated by examining the cumulative incidence function for active smokers compared to non-smokers (see Supplementary Figure 1).

Table 3 Univariable Cox regression on patient survival to 12 mo

Enduring variables	Overall[1], 12-mo survival HR (95%CI)	Transplant-free, 12-mo survival HR (95%CI)
Age, per 5-yr	1.13 (0.94-1.35)	0.95 (0.85-1.07)
Male sex	2.05 (0.84-4.99)	1.68 (0.94-3.00)
Diabetes	0.56 (0.25-1.50)	0.39 (0.19-0.81)
Ischaemic heart disease	2.00 (0.68-5.92)	0.80 (0.29-2.23)
Heart failure	0.86 (0.12-6.38)	0.35 (0.05-2.55)
Chronic obstructive lung disease	NE	1.02 (0.32-3.30)
Chronic kidney disease	1.13 (0.38-3.32)	0.82 (0.37-1.83)
Hepatocellular carcinoma	2.11 (0.92-4.81)	1.55 (0.87-2.76)
Hepatitis B	3.36 (1.32-8.53)	1.68 (0.75-3.74)
Hepatitis C	0.81 (0.32-2.05)	1.28 (0.71-2.28)
Alcoholic liver disease	0.76 (0.22-2.55)	0.94 (0.44-2.01)
Non-alcoholic fatty liver	0.51 (0.15-1.73)	0.43 (0.18-1.02)
Current smoking	5.01 (2.15-11.7)	2.27 (1.13-4.56)
Current alcohol intake	0.68 (0.42-1.13)	0.93 (0.68-1.26)
Time varying variables		
MELD score, per 5-points	1.28 (0.93-1.77)	1.82 (1.41-2.34)
NYHA functional class	1.14 (0.74-1.75)	1.09 (0.81-1.46)
TIPS procedure	0.37 (0.05-2.83)	0.13 (0.02-0.96)
Acute kidney injury	2.57 (1.13-5.88)	2.36 (1.35-4.11)
Thoracocentesis	0.51 (0.23-1.16)	1.28 (0.70-2.34)
Pneumothorax	2.37 (0.80-7.00)	2.78 (1.39-5.56)
Intercostal catheter inserted	1.56 (0.53-4.62)	1.85 (0.90-3.82)
Admission hepatic encephalopathy		
None	1.00 (reference)	1.00 (reference)
Mild	0.75 (0.17-3.25)	1.21 (0.54-2.70)
Severe	11.4 (3.28-39.6)	7.93 (2.36-26.6)
Encephalopathy during admission[2]	2.30 (0.84-6.32)	3.20 (1.65-6.24)
Any encephalopathy	2.30 (0.97-5.45)	2.21 (1.22-4.03)

[1]Censored at time of liver transplantation.

[2]New-onset during admission not present on admission, all episodes were mild.

HR: Hazard ratio; CI: Confidence interval; MELD: Model for end-stage liver disease; NYHA: New York Heart Association; TIPS: Transjugular intrahepatic portosystemic shunt; NE: Not estimable.

DISCUSSION

HH remains an uncommon but extremely challenging complication in patients with liver cirrhosis. This study represents one of the largest series to analyse the natural history and outcomes of patients with HH and to our knowledge, is the first study to examine factors associated with survival in this population. We demonstrated that development of HH was associated with poor prognosis despite current therapeutic modalities, with a 45-d overall survival of 80% and 12-mo transplant-free survival of 41%. HH is a refractory disease, and the use of diuretics in isolation was rarely effective in this cohort, with 52% of patients experiencing recurrence of HH and rehospitalisation. At multivariable analysis, smoking status and the presence of AKI confer significant additional mortality risk.

Table 4 Multivariable Cox regression on patient survival to 12 mo

Model and variables	AHR (95%CI)	P value	Bootstrap CI	P value
Overall survival[1]				
Age, per 5-yr increase	1.30 (1.01-1.67)	0.043	0.91-1.85	0.15
MELD score, per 5 points	1.53 (1.06-1.67)	0.025	0.89-2.66	0.13
Current smoking	8.65 (3.43-21.9)	< 0.001	2.54-29.5	0.001
Acute kidney injury	2.91 (1.21-6.97)	0.017	1.04-8.12	0.042
Transplant-free survival				
Hepatic encephalopathy	2.00 (1.08-3.67)	0.030	0.93-4.28	0.078
MELD score, per 5 points	1.78 (1.38-2.29)	< 0.001	1.31-2.44	< 0.001
Current smoking	3.11 (1.49-6.52)	0.003	1.16-8.30	0.024
Acute kidney injury	2.18 (1.20-3.96)	0.011	1.10-4.31	0.026

[1]Censored for liver transplantation.

MELD: Model for end-stage liver disease; AHR: Adjusted hazard ratio; CI: Confidence interval.

DOI: 10.3748/wjg.v28.i35.5175 **Copyright** ©The Author(s) 2022.
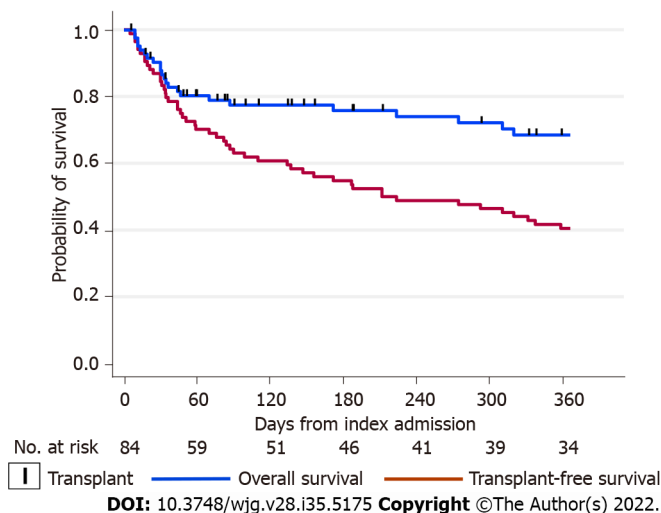
Figure 1 Kaplan-Meier survival curves. Kaplan-Meier survival curves showing transplant-free survival at 12 mo, with liver transplantation and death treated as composite endpoints, and overall patient survival at 12 mo, with patients censored at the time of liver transplantation (ticks on survival curve).

Hospitalisation with symptomatic HH is an uncommon presentation, with 84 patients recruited over a 9-year period to 3 metropolitan tertiary hospitals. The majority of patients presented with a right-sided pleural effusion and concurrent ascites, which is consistent with previous series[1,2,4]. The median MELD score of 29 in our cohort highlights that HH typically occurs in patients with advanced cirrhosis who often have other decompensating events such as hepatic encephalopathy. The median MELD score in our study was higher than that reported in other smaller studies[2,4,11], which may reflect use of data from a LT centre.

Patient management in this study aligns with recent AASLD guidelines, which recommend diuresis as the first-line therapy[6]. Most patients in our study were receiving diuretic therapy at the time of hospital presentation, with 70% receiving 2 diuretic agents, however the median doses of furosemide and spironolactone was well below the recommended maximum doses of 160 mg and 400 mg daily respectively[1]. Nonetheless, only 12% patients achieved long-term resolution of HH with diuretic therapy alone. An important limiting factor in relation to diuretic therapy is the propensity for AKI in patients with advanced cirrhosis. AKI was recorded in nearly one-third of presentations, and this was associated with a significantly higher risk of mortality. This suggests that diuretic therapy should be titrated cautiously in patients with HH with close monitoring of renal function.

There remains no consensus on universal diagnostic thoracocentesis in hospitalised patients with HH. In practice, whilst HH may be suspected on the basis of imaging and clinical presentation, thoraco-centesis is useful to confirm transudative fluid and exclude other causes of a pleural effusion. We demonstrated that thoracocentesis in the HH population was associated with a significant higher risk of

DOI: 10.3748/wjg.v28.i35.5175 **Copyright** ©The Author(s) 2022.
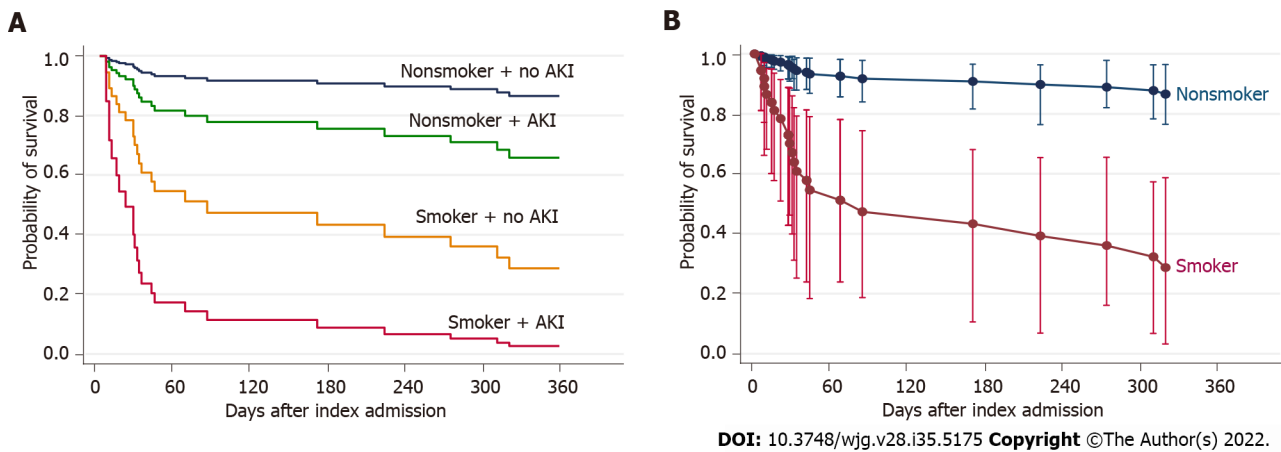
Figure 2 Multivariate survival analysis. A: Multivariable Cox regression of overall patient survival (censored for transplantation), showing survival estimates for patients with hepatic hydrothorax by smoking and acute kidney injury status, with age and model for end-stage liver disease (MELD) scores held at the mean values; B: Bootstrapped pointwise confidence intervals for survival functions by active smoking status, in the absence of acute kidney injury and with age and MELD held at the means, demonstrating a robust association between active smoking and mortality in patients with hepatic hydrothorax. AKI: Acute kidney injury.

pneumothorax of 15% compared to the standard pneumothorax risk of 6% in non-cirrhotic populations, despite being performed under ultrasound guidance[12]. Shojaee *et al*[13] reported that repeat thoracocentesis in cirrhotic patients was associated with a higher rate of major complications compared to thoracocentesis for other aetiologies (8% *vs* 0%). In addition, Xiol *et al*[5], observed a pneumothorax rate of 25% in cirrhotic patients undergoing serial therapeutic thoracocentesis. Our analysis suggested that pneumothorax complications were associated with lower transplant-free survival [hazard ratio (HR) = 2.78; 95%CI: 1.39-5.56], however this was not significant in multivariable analysis. Other series have also suggested that HH requiring thoracocentesis independently confers significant morbidity and increased mortality[7,14]. Given the greater complications associated with thoracocentesis in cirrhotic patients, it was concerning that 74.7% of patients who were readmitted underwent repeat thoracocentesis. Further study is needed to elucidate the cause of the high complication rate and strategies to mitigate this risk. For example, it remains unclear if abdominal paracentesis effectively prevents HH recurrence[1].

In relation to other treatment modalities, indwelling intercostal catheter drains are thought to carry substantial risk and are not recommended by current guidelines, with some studies observing complication rates of 80%-90%[11,15]. In our cohort, an indwelling intercostal catheter was placed in 19% of patients, most commonly due to respiratory compromise and rapid re-accumulation of pleural fluid. In contrast, consideration of TIPS insertion is recommended by AASLD guidelines, based on evidence of a 70%-80% response rate in patients with refractory HH[3,6,16-18]. The outcomes following TIPS insertion may be comparable to those for management of refractory ascites and although a survival benefit in HH has not been established[19], the study by Badillo and Rockey[2] suggests a trend toward improved survival in patients proceeding to TIPS. Only 10 (17.9%) of the 56 patients in our cohort who were deemed not suitable for LT received TIPS insertion. No overall survival benefit from TIPS insertion was demonstrated, but transplant-free survival was higher (HR = 0.13; 95%CI: 0.02-0.96), as no patient who had TIPS insertion underwent LT.

Multiple studies have demonstrated that development of HH is associated with a poor prognosis[2, 20,21], but mortality is difficult to compare due to heterogeneity between studies[2,4,11,15,21,22]. Our 12-mo transplant-free survival of 41%, however, is comparable to the 12-mo mortality of 57% reported by Badillo and Rockey[2]. In multivariable analysis, increasing age and MELD score, hepatic encephalopathy, development of AKI and active smoking were important factors independently associated with mortality. Given that the majority of deaths in our cohort were observed within 45-d of hospital admission and were most frequently due to complications of end-stage liver disease, we would advocate that in all patients presenting with HH, the appropriateness of transplantation should be considered with early referral for suitable candidates. Indeed, no deaths were recorded in patients who received LT, highlighting the successful outcomes of transplantation in patients with HH.

The strong association between smoking and poor outcomes has not previously been reported in patients with HH. Our study echoes a growing body of literature demonstrating an association between cigarette smoking and poorer outcomes in patients with liver disease[23,24]. Current smokers with cirrhosis have up to a 3.6 times higher mortality risk and cigarette smoking has been linked with progression of fibrosis in non-alcoholic fatty liver disease[24], hepatitis C and primary biliary cholangitis and is associated with an increased incidence of hepatocellular carcinoma[23]. Cigarette smoking represents an important modifiable risk factor that should be actively addressed in all patients with cirrhosis but appears critical in the HH population.

Study strengths and limitations

This is one of the largest, multicentre studies to investigate the prognostic significance of HH requiring hospitalisation in cirrhotic patients. Study inclusion criteria were broad and pragmatic, and represent generalisable real-world data. The Victorian Liver Transplant Centre was established in 1988 and currently performs over 100 transplants annually. The cohort had comprehensive assessments by gastroenterology specialists to confirm HH, which also assured treatment consistent with current standard-of-care practice guidelines. We used multivariable analysis to allow for confounders of mortality, and were able to identify smoking as a novel factor associated with significantly lower 12-mo survival in patients with HH. This study was able to elucidate the less well-described challenges in HH patients, such as need for ICU admission, hospital readmissions, and blood product requirement.

This study is limited by its retrospective design, with the inherent risks of missing information or extraction of inaccurate records. Complete pleural fluid analysis was only available in 31% of patients, which limited our ability to detect complications such as SBEM. SBEM has been associated in other studies with high short-term mortality (20% to 38%)[1]. SBEM was detected in 8.7% of thoracocentesis procedures in our study, which is almost certainly an underrepresentation of the true rate and lower than a study by Xiol *et al*[5], which found SBEM was present in 13% of patients with HH on pre-sentation. Reasons for the low rate of complete pleural fluid analysis included the large number of hospital settings in which thoracocentesis was performed (including the emergency department, ICU, gastroenterology ward, radiology department or other acute hospital wards) with associated hetero-geneity in process, incorrect requests for fluid analysis, incorrect tube collection to facilitate fluid analysis, clotting of fluid which precluded analysis, emergency procedures due to patient distress or instability and thoracocentesis performed prior to a diagnosis of HH being made. This reflects the real-world nature of the study and pleural fluid analysis rates were similar across all study sites. As such, we were not able to determine if specific pleural fluid findings were associated with refractory symptoms, rehospitalisation, or poor survival. In addition, factors associated with treatment failure or rehospital-isation such as compliance with diuretics were difficult to discern. The observational nature of the study also limits any causality inferences and eliminates the ability to ensure standardisation, which is partic-ularly relevant to thoracocentesis technique. We could not exclude the possibility that some patients may have been admitted to a non-study hospital, although in practice this would be uncommon, and thus readmissions and complications may be underestimated.

In order to assess if TIPS may have provided clinical benefit apart from survival, we examined the readmissions, thoracocentesis, or ascitic drainage procedures in patients who received TIPS. Four patients had a single readmission post-TIPS, of which 3 occurred < 30 d and one at 6 mo post-TIPS. Thoracocentesis was performed in 3 of 4 of these readmitted patients, and ascitic drainage in 1 of 4 of these readmitted patients. Due to these low frequencies and different timing of TIPS, we cannot provide a meaningful statistical comparison with patients who did not have TIPS.

CONCLUSION

The development of HH is associated with poor transplant-free survival despite current standards-of-care and should prompt consideration of the appropriateness of LT in all patients. HH is often refractory to both conservative and invasive management and patients frequently require repeat hospit-alisations. Active smoking and AKI may be important modifiable risk factors to reduce mortality in cirrhotic patients with HH.

ARTICLE HIGHLIGHTS

Research background

Hepatic hydrothorax (HH) is an important complication of cirrhosis, however management is often challenging and the natural history is poorly understood.

Research motivation

HH is a significant complication of cirrhosis, with a paucity of literature studying natural history and factors affecting survival.

Research objectives

This study sought to: (1) Evaluate factors associated with survival in a cohort of patients hospitalised with HH; and (2) Provide descriptive analysis of treatments, complications and outcomes following HH hospitalisation.

Research methods

Cirrhotic patients with HH presenting to three tertiary centres from 2010 to 2018 were retrospectively identified. Patients were followed-up from the date of first hospital admission with HH to an endpoint of death, liver transplantation (LT) or end of the study period. The primary outcomes were overall and transplant free survival at 12 mo after the index admission. The secondary outcomes included the incidence of specific treatments of HH and associated complications and to determine patient-specific prognostic factors associated with mortality.

Research results

Only 12% of patients achieved long-term resolution of HH with diuretic therapy alone. 74% of patients required thoracocentesis, with 15% of procedures being complicated by pneumothorax. 12-mo transplant free survival was 41%. 45-d overall survival was 80%.

Research conclusions

The development of HH is associated with poor transplant-free survival despite current standards-of-care and should prompt consideration of the appropriateness of LT in all patients. HH is often refractory to both conservative and invasive management and patients frequently require repeat hospitalisations. Active smoking and acute kidney injury may be important modifiable risk factors to reduce mortality in cirrhotic patients with HH.

Research perspectives

This study represents one of the largest series examining survival in persons hospitalised with HH, and importantly has identified modifiable risk factors that may alter the natural history in this challenging patient population.

FOOTNOTES

ORCID number: Sarah Romero 0000-0003-2707-6390; Andy KH Lim 0000-0001-7816-4724; Gurpreet Singh 0000-0001-6760-566X; Chamani Kodikara 0000-0002-2381-2875; Rachel Shingaki-Wells 0000-0002-8714-591X; Lynna Chen 0000-0002-7093-2036; Samuel Hui 0000-0002-2839-6209; Marcus Robertson 0000-0002-8848-1771.

REFERENCES

1   **Chaaban T**, Kanj N, Bou Akl I. Hepatic Hydrothorax: An Updated Review on a Challenging Disease. *Lung* 2019; **197**: 399-405 [PMID: 31129701 DOI: 10.1007/s00408-019-00231-6]

2   **Badillo R**, Rockey DC. Hepatic hydrothorax: clinical features, management, and outcomes in 77 patients and review of the literature. *Medicine (Baltimore)* 2014; **93**: 135-142 [PMID: 24797168 DOI: 10.1097/MD.0000000000000025]

3   **Cardenas A**, Kelleher T, Chopra S. Review article: hepatic hydrothorax. *Aliment Pharmacol Ther* 2004; **20**: 271-279 [PMID: 15274663 DOI: 10.1111/j.1365-2036.2004.02081.x]

4   **Gurung P**, Goldblatt M, Huggins JT, Doelken P, Nietert PJ, Sahn SA. Pleural fluid analysis and radiographic, sonographic, and echocardiographic characteristics of hepatic hydrothorax. *Chest* 2011; **140**: 448-453 [PMID: 21273292 DOI: 10.1378/chest.10-2134]

5   **Xiol X**, Castellote J, Cortes-Beut R, Delgado M, Guardiola J, Sesé E. Usefulness and complications of thoracentesis in cirrhotic patients. *Am J Med* 2001; **111**: 67-69 [PMID: 11448663 DOI: 10.1016/s0002-9343(01)00744-6]

6   **Banini BA**, Alwatari Y, Stovall M, Ogden N, Gershman E, Shah RD, Strife BJ, Shojaee S, Sterling RK. Multidisciplinary Management of Hepatic Hydrothorax in 2020: An Evidence-Based Review and Guidance. *Hepatology* 2020; **72**: 1851-1863 [PMID: 32585037 DOI: 10.1002/hep.31434]

7   **Hung TH**, Tseng CW, Tsai CC, Tseng KC, Hsieh YH. The long-term outcomes of cirrhotic patients with pleural effusion. *Saudi J Gastroenterol* 2018; **24**: 46-51 [PMID: 29451184 DOI: 10.4103/sjg.SJG_336_17]

8   **Yoon JH**, Kim HJ, Jun CH, Cho SB, Jung Y, Choi SK. Various Treatment Modalities in Hepatic Hydrothorax: What Is Safe and Effective? *Yonsei Med J* 2019; **60**: 944-951 [PMID: 31538429 DOI: 10.3349/ymj.2019.60.10.944]

9   **World Health Organization**. ICD-10: international statistical classification of diseases and related health problems: tenth revision, 2nd ed. [cited 12 December 2021]. Available from: https://apps.who.int/iris/handle/10665/42980

10 **Kellum JA**, Lameire N, Aspelin P, Barsoum RS, Burdmann EA, Goldstein SL, Herzog CA, Joannidis M, Kribben A, Levey AS, MacLeod AM, Mehta RL, Murray PT, Naicker S, Opal SM, Schaefer F, Schetz M, Uchino S. Kidney disease: Improving global outcomes (KDIGO) acute kidney injury work group. KDIGO clinical practice guideline for acute kidney injury. *Kidney Int Suppl* 2012; **2**: 1-138 [DOI: 10.1038/kisup.2012.1]

11 **Orman ES**, Lok AS. Outcomes of patients with chest tube insertion for hepatic hydrothorax. *Hepatol Int* 2009; **3**: 582-586 [PMID: 19669710 DOI: 10.1007/s12072-009-9136-z]

12 **Gordon CE**, Feller-Kopman D, Balk EM, Smetana GW. Pneumothorax following thoracentesis: a systematic review and meta-analysis. *Arch Intern Med* 2010; **170**: 332-339 [PMID: 20177035 DOI: 10.1001/archinternmed.2009.548]

13 **Shojaee S**, Khalid M, Kallingal G, Kang L, Rahman N. Repeat Thoracentesis in Hepatic Hydrothorax and Non-Hepatic Hydrothorax Effusions: A Case-Control Study. *Respiration* 2018; **96**: 330-337 [PMID: 29991046 DOI: 10.1159/000490001]

14 **Kallingal G**, Khalid M, Kang L, Shojaee S.   Complications Associated With Serial Thoracenteses in Cirrhotic Patients With Hepatic Hydrothorax. Proceedings of the Chest Conference; 2016 Oct 22-26; Los Angeles, USA. Netherlands: Elsevier, 2016: 997A

15 **Liu LU**, Haddadin HA, Bodian CA, Sigal SH, Korman JD, Bodenheimer HC Jr, Schiano TD. Outcome analysis of cirrhotic patients undergoing chest tube placement. *Chest* 2004; **126**: 142-148 [PMID: 15249455 DOI: 10.1378/chest.126.1.142]

16 **Siegerstetter V**, Deibert P, Ochs A, Olschewski M, Blum HE, Rössle M. Treatment of refractory hepatic hydrothorax with transjugular intrahepatic portosystemic shunt: long-term results in 40 patients. *Eur J Gastroenterol Hepatol* 2001; **13**: 529-534 [PMID: 11396532 DOI: 10.1097/00042737-200105000-00011]

17 **Strauss RM**, Martin LG, Kaufman SL, Boyer TD. Transjugular intrahepatic portal systemic shunt for the management of symptomatic cirrhotic hydrothorax. *Am J Gastroenterol* 1994; **89**: 1520-1522 [PMID: 8079930]

18 **Gordon FD**, Anastopoulos HT, Crenshaw W, Gilchrist B, McEniff N, Falchuk KR, LoCicero J 3rd, Lewis WD, Jenkins RL, Trey C. The successful treatment of symptomatic, refractory hepatic hydrothorax with transjugular intrahepatic portosystemic shunt. *Hepatology* 1997; **25**: 1366-1369 [PMID: 9185754 DOI: 10.1002/hep.510250611]

19 **Young S**, Bermudez J, Zhang L, Rostambeigi N, Golzarian J. Transjugular intrahepatic portosystemic shunt (TIPS) placement: A comparison of outcomes between patients with hepatic hydrothorax and patients with refractory ascites. *Diagn Interv Imaging* 2019; **100**: 303-308 [PMID: 30522911 DOI: 10.1016/j.diii.2018.10.006]

20 **Liu WL**, Kuo PH, Ku SC, Huang PM, Yang PC. Impact of therapeutic interventions on survival of patients with hepatic hydrothorax. *J Formos Med Assoc* 2010; **109**: 582-588 [PMID: 20708509 DOI: 10.1016/S0929-6646(10)60095-2]

21 **Mouelhi L**, Daboussi O, Cheffi N, El Jery K, Said Y, Khedher S, Salem M, Dabbèche R, Houissa F, Najjar T. Hepatic hydrothorax: About a hospital serie of 63 cases. *Tunis Med* 2016; **94**: 867 [PMID: 28994887]

22 **Luh SP**, Chen CY. Video-assisted thoracoscopic surgery (VATS) for the treatment of hepatic hydrothorax: Report of twelve cases. *J Zhejiang Univ Sci B* 2009; **10** [DOI: 10.1631/jzus.B0820374]

23 **Rutledge SM**, Asgharpour A. Smoking and Liver Disease. *Gastroenterol Hepatol (N Y)* 2020; **16**: 617-625 [PMID: 34035697]

24 **Carter BD**, Abnet CC, Feskanich D, Freedman ND, Hartge P, Lewis CE, Ockene JK, Prentice RL, Speizer FE, Thun MJ, Jacobs EJ. Smoking and mortality--beyond established causes. *N Engl J Med* 2015; **372**: 631-640 [PMID: 25671255 DOI: 10.1056/NEJMsa1407211]

ORIGINAL ARTICLE

Observational Study

Gut microbiota of hepatitis B virus-infected patients in the immune-tolerant and immune-active phases and their implications in metabolite changes

Ya-Nan Li, Na-Ling Kang, Jia-Ji Jiang, Yue-Yong Zhu, Yu-Rui Liu, Da-Wu Zeng, Fei Wang

Ya-Nan Li, Na-Ling Kang, Jia-Ji Jiang, Yue-Yong Zhu, Yu-Rui Liu, Da-Wu Zeng, Department of Hepatology, Hepatology Research Institute, The First Affiliated Hospital, Fujian Medical University, Fuzhou 350001, Fujian Province, China

Fei Wang, Department of Pharmacy, Fujian Geriatric Hospital, Fuzhou 350001, Fujian Province, China

Corresponding author: Da-Wu Zeng, MD, Associate Chief Physician, Associate Professor, Department of Hepatology, Hepatology Research Institute, The First Affiliated Hospital, Fujian Medical University, No. 20 Chazhong Road, Fuzhou 350001, Fujian Province, China. zengdw1980@fjmu.edu.cn

Abstract

BACKGROUND
The microbes and metabolomics of microbiota dysbiosis in the gut in the different phases of hepatitis B virus (HBV) infection are not fully understood.

AIM
To investigate the specific gut microbiota and metabolites of the immune-tolerant (IT) and immune-active (IA) phases of chronic hepatitis B (CHB).

METHODS
Clinical fecal samples from healthy individuals and patients in the IT and IA phases of HBV infection were collected. Next, non-target metabolomics, bioinformatics, and 16S rDNA sequencing analyses were performed.

RESULTS
A total of 293 different metabolites in 14 phyla, 22 classes, 29 orders, 51 families, and 190 genera were identified. The four phyla of *Firmicutes*, *Bacteroidetes*, *Actinobacteria*, and *Proteobacteria* were the most abundant, accounting for 99.72%, 99.79%, and 99.55% in the healthy controls, IT-phase patients, and IA-phase patients, respectively. We further identified 16 genera with different richness in the IT phase and IA phase of HBV infection. Of the 134 named metabolites, 57 were upregulated and 77 were downregulated. A total of 101 different metabolic functions were predicted in this study, with 6 metabolic pathways having the highest enrichments, namely carbohydrate metabolism (14.85%), amino acid

metabolism (12.87%), lipid metabolism (11.88%), metabolism of cofactors and vitamins (11.88%), xenobiotic biodegradation (9.9%), and metabolism of terpenoids and polyketides (7.92%).

CONCLUSION
These findings provide observational evidence of compositional alterations of the gut microbiome and some related metabolites in patients with IT-phase or IA-phase HBV infection. Further studies should investigate whether microbiota modulation can facilitate the progression of CHB and the cause-effect relationship between the gut microbiota and CHB.

Key Words: Microbes; Metabolomics; Gut microbiota; Immune-tolerant phase; Hepatitis B virus

Core Tip: This article provided observational evidence of compositional alterations of gut microbiome and some related metabolite in patients with immune-tolerant phase hepatitis B virus (HBV) infection and immune-active phase HBV infection.

INTRODUCTION

As a disease of public health significance, hepatitis B often leads to liver cirrhosis or hepatocellular carcinoma (HCC). Currently, there are few effective treatments and strategies for eliminating hepatitis B virus (HBV) infection. The immune-tolerant (IT) phase is the first stage of HBV infection, and recent studies suggest that HBV-infected patients in this phase suffer from a high risk of HCC and death[1-3]. However, anti-HBV treatment is not generally recommended at this stage. The IT status of patients largely determines the patients' outcomes. Thus, the identification of factors that affect the consequences of HBV infection is crucial for eliminating this disease.

Recent studies indicate that the gut microbiota is involved in chronic hepatitis B (CHB) as well as other liver diseases[4-6]. Some commensal bacteria regulate the host metabolic pathways by improving food-derived energy or modulating the host-derived compounds that alter metabolism[7-9]. In addition, there are various gut microbiota in patients with CHB, hepatitis B-related liver cirrhosis, or HCC[10-12]. To date, information about the gut microbiota in patients at the initial phase of HBV infection remains largely unknown. We believe that studies on the gut microbiota of HBV-infected patients in the IT phase would help to elucidate the underlying mechanism of HBV IT as it will provide valuable information about the immune environment for HBV and its long-term existence.

Most studies on the microbiome have been cross-sectional with samples collected at a single time point, and only some studies have been performed with samples from different stages of HBV infection [12-15]; moreover, few comparisons of HBV-infected patients and healthy individuals have been carried out in these studies. CHB patients may develop recurrent active hepatitis, while the IT phase may change into the immune-active (IA) phase at a later stage in patients[16], which can lead to a substantial change in the composition of the gut microbiota. Therefore, understanding how the gut microbiota change from the IT phase to the IA phase will be important for the development of potential microbiome-targeting therapeutic drugs to combat HBV infection. Furthermore, this dynamic variation in gut microbiota in HBV-infected patients may help us to identify unique bacterial taxa that would contribute to postponing disease progression.

The present study focused on the dynamic profiles of the gut microbiota in IT-phase patients and IA-phase HBV-infected patients without liver fibrosis by 16S rDNA sequencing and analysis. We aimed to identify changes of bacteria involved in the transition from the IT phase to the IA phase in HBV-infected patients and to illustrate the regulation of both microbiota and metabolites. The results will provide a new perspective for the noninvasive diagnosis and treatment of IT-phase HBV-infected patients.

MATERIALS AND METHODS

Recruitment of participants

HBV-infected patients in the IT phase or the IA phase were recruited from The First Affiliated Hospital of Fujian Medical University from January 2018 to December 2020. All HBV-infected patients were at least 18-years-old, hepatitis B surface antigen positive for ≥ 6 mo, and hepatitis B virus e-antigen positive; moreover, the IT patients had a normal alanine aminotransferase level (< 40 IU/L), HBV DNA > 1 million IU/mL, and no fibrosis found by FibroScan analysis[17]. The IA patients had an HBV DNA serum concentration of > 20000 IU/mL as well as elevated alanine aminotransferase and/or aspartate aminotransferase levels[17]. However, patients who suffered from other non-HBV diseases/infections were excluded from the study. Samples from healthy volunteers were blindly collected, and participants who had received antiviral therapy, immunotherapy, probiotics, or antibiotics within 8 wk before enrollment were excluded. Verbal informed consent was provided by all participants. The experimental protocol and participant enrollment procedure were approved by the Ethics Review Committee of the university and were conducted according to the Declaration of Helsinki guidelines.

Clinical measurements

Liver stiffness measurements were conducted using a FibroScan instrument. Measurements with more than ten successful acquisitions were obtained (with a rate > 60% and an interquartile range < 30%). In addition, the alanine aminotransferase, aspartate aminotransferase, glutamyl transpeptidase, total bilirubin, albumin, globulin, and alpha-fetoprotein levels were measured. HBV serological testing was performed with the Architect platform (Abbott Laboratories, Chicago, IL, United States). HBV DNA was tested by a quantitative PCR assay (PG Company, Shenzhen, China).

Sampling, DNA extraction, and PCR

Fecal samples were obtained from all participants, filtered with a 2-mm sieve to remove interferents, and then stored at -80 °C for the following experiments. Total bacterial DNA extraction was performed with a PowerSoil DNA Isolation Kit (MoBio Laboratories, Carlsbad, CA, United States), and the purity and quality of the genomic DNA were checked by electrophoresis on 0.8% agarose gels. The V3-4 hypervariable region of bacterial 16S rDNA was amplified by previously reported conserved primers: 338F (5'-ACTCCTACGGGAGGCAGCAG-3') and 806R (5'-GGACTACHVGGGTWTCTAAT-3')[18]. For each sample, the 10-digit barcode sequence was added to the 5'-end of the forward and reverse primers (provided by Allwegene Company, Beijing, China). The PCR was carried out on a Mastercycler Gradient (Eppendorf, Germany) using a reaction volume of 25 µL, containing 12.5 µL of KAPA 2G Robust Hot Start Ready Mix, 1 µL of forward primer (5 µmol/L), 1 µL of reverse primer (5 µmol/L), 5 µL of DNA (total template quantity of 30 ng), and 5.5 µL of H_2O. The cycling parameters were 95 °C for 5 min, followed by 28 cycles of 95 °C for 45 s, 55 °C for 50 s, and 72 °C for 45 s, with a final extension at 72 °C for 10 min.

Three PCR products per sample were pooled to mitigate reaction-level PCR biases. The PCR products were purified using a QIAquick Gel Extraction Kit (QIAGEN, Germany), quantified using real-time PCR, and sequenced at Allwegene Company, Beijing, China. Deep sequencing was done with the Miseq platform at the Allwegene Company (Beijing, China). The raw data were first screened, and sequences were removed from consideration if they were shorter than 200 bp, had a low quality score (≤ 20), contained ambiguous bases, or did not exactly match the primer sequences and barcode tags. Qualified reads were separated using the sample-specific barcode sequences and trimmed with Illumina Analysis Pipeline Version 2.6. Thereafter, the dataset after cleaning was analyzed using the Quantitative Insights into Microbial Ecology (QIIME) platform.

All sequences were clustered into operational taxonomic units (OTUs) at a similarity level of 97%[19] to generate rarefaction curves. The Ribosomal Database Project classifier tool was used to analyze different taxonomic groups[20]. The Venn diagram was built by the R package program. Shared taxa presented in all groups were defined as the core microbiota. Clustering analysis and principal component analysis were performed by using the R package, as described previously[21]. The evolution distances were analyzed with the unweighted pair group method and an arithmetic mean clustering tree[22]. Heatmaps of the top 20 OTUs were generated using Mothur, as described in a previous study [23].

Metabolic pathway and non-target metabolomics

Phylogenetic Investigation of Communities by Reconstruction of Unobserved States (PICRUSt) analysis based on the 16S rDNA was performed. The OTU table derived from QIIME was compared using the Kyoto Encyclopedia of Genes and Genomes and MetaboAnalyst (http://www.metaboanalyst.ca/) databases, and the metabolic function of the gut microbiota was predicted based on the findings. The abundances of functional genes were visualized as heatmaps by the R package.

For metabolite extraction, a 10-µL aliquot of each sample was mixed with 990 µL of the extraction solvent (acetonitrile/methanol/water, 2:2:1), and the mixture was vortexed for 30 s, incubated at -20 °C for 1 h, and then centrifuged at 12000 rpm and 4 °C for 15 min. Finally, the supernatant was diluted 10

times for ultra-high-performance liquid chromatography-tandem mass spectrometry (UHPLC-MS/MS) analysis[24]. UHPLC separation was performed on an Agilent 1290 Infinity II series UHPLC system (Agilent Technologies). Mobile phase A included both 10 mmol/L ammonium formate and 10 mmol/L ammonia, while mobile phase B was acetonitrile. The temperatures for the column and the autosampler were set at 35 °C and 4 °C, respectively[25].

Statistical analysis

One-way analysis of variance was performed to compare continuous variables between two groups. The Wilcoxon signed rank test, Kruskal–Wallis test, χ^2 test, or Student's t test was used to compare categorical variables between groups. All statistical analyses were calculated either in the R package (version 3.6.1) or SPSS (version 26.0). P values less than 0.05 were considered as significant differences.

RESULTS

Overview of gut microbial community shift in patients

To differentiate the characteristics of the gut microbiota in IT-phase HBV-infected patients, IA-phase HBV-infected patients, and healthy individuals, 16S rDNA gene sequencing was performed on the stool samples from 14 IT-phase HBV-infected patients, 10 IA-phase HBV-infected patients, and 13 healthy donors (Table 1). A total of 1521813, 411189, and 1109236 sequences were acquired for the IT, IA, and healthy groups, respectively, after excluding low-quality reads. A total of 19556 clean tags were obtained, of which 824 OTUs were matched. After applying strict trimming criteria to exclude low-quality clean tags, the numbers of OTUs for healthy individuals, IT-phase patients, and IA-phase patients were 633, 662, and 489, respectively, as shown in Table 2. A total of 95, 132, and 27 OTUs existed independently in the healthy controls, IT-phase patients, and IA-phase patients, respectively (Figure 1). There were no significant differences in the Chao1, Shannon, and Simpson indices among the IT, IA, and healthy groups (all P values > 0.05, Table 2). The bacterial communities in the healthy individuals were relatively more heterogeneous than those found in the IT- or IA-phase patients. The IT and IA patients could be separated from the healthy individuals by non-metric multidimensional scaling and principal component analysis (Figure 2A and B). Partial least squares discriminant analysis showed structural differences in the gut bacterial community structure among the groups, indicating that the classification model was effective (Figure 2C).

Predominant bacteria at different levels

To show the abundance of bacteria of all fecal samples, 14 phyla, 22 classes, 29 orders, 51 families, and 190 genera were identified, and the dominant gut microbiota are shown in Supplementary Table 1 and Figure 3. The four phyla of *Firmicutes*, *Bacteroidetes*, *Actinobacteria*, and *Proteobacteria* were the most abundant, accounting for 99.72%, 99.79%, and 99.55% in the healthy controls, IT-phase patients, and IA-phase patients, respectively. In detail, the highest relative abundance of *Actinobacteria*, which reached 7.32%, was found in the healthy group. Meanwhile, compared with the healthy control and the IA-phase patients, the IT patients had the highest abundance of *Bacteroidetes* (33.27%). The IT-phase patients had less *Firmicutes* (61.00%) and *Actinobacteria* (2.71%) than the IA-phase patients. *Clostridiales*, *Bacteroidales*, *Selenomonadales*, *Bifidobacteriales*, *Coriobacteriales*, *Erysipelotrichales*, *Lactobacillales*, and *Enterobacteriales* were the most abundant bacteria at the order level in all three groups.

For the genus level, an abundance of *Bacteroides* (16.19%), *Prevotella 9* (9.04%), and *Megamonas* (7.66%) was found in the IT-phase patients. However, *Blautia* (19.20%) and *Faecalibacterium* (12.68%) were enriched in the IA-phase patients. Interestingly, the healthy groups had more *Eubacterium rectale* (6.69%), *Eubacterium hallii* (4.03%), *Bifidobacterium* (3.87%), and *Dorea* (3.23%). In addition, *Faecalibacterium* and *Blautia* accounted for a high proportion in the IA-phase patients; these bacteria are involved in butyrate short-chain fatty acid metabolism and inhibit inflammation.

Linear discriminant analysis effect size analysis to identify specific microbial taxa related to IT and IA patients

Linear discriminant analysis (LDA) effect size modeling was applied to identify specific bacterial taxa associated with different stages of CHB (Figure 2D and E). There were markedly significant differences in the community compositions in CHB patients compared with the healthy individuals. There were 12 and 6 significantly different taxa in the IT- and IA-phase patients, respectively. The five most enriched genera in the IT-phase patients were *Senegalimassilia* (LDA score = 4.38, $P < 0.05$), *Prevotella 2* (LDA score = 4.24, $P < 0.01$), *Alloprevotella* (LDA score = 4.09, $P < 0.05$), *Sutterella* (LDA score = 3.67, $P < 0.001$), and *Haemophilus* (LDA score = 3.58, $P < 0.05$). The four most enriched genera in the IA-phase patients included *Blautia* (LDA score = 4.78, $P < 0.01$), *Faecalibacterium* (LDA score = 4.51, $P < 0.05$), *Clostridium innocuum* group (LDA score = 4.23, $P < 0.01$), and *Faecalitalea* (LDA score = 3.76, $P < 0.05$) (Supplementary Table 2). These significantly different gut microbial taxa can be used as potential noninvasive biomarkers for the diagnosis of different immune phases of infection in CHB.

Table 1 Basic information and clinical characteristics of healthy individuals, immune-tolerant phase hepatitis B virus infection patients, and immune-active phase hepatitis B virus infection patients

Characteristic	H, *n* = 13	IT, *n* = 14	IA, *n* = 10	*P* value
Sex, M/F	9/4	9/5	7/3	0.949
Age in yr	26.4 ± 0.8	26.9 ± 5.8	36.2 ± 11.3	0.004
HBsAg as log10 IU/mL	NA	4.62 ± 0.18	3.83 ± 0.81	< 0.001
HBeAg as log10 S/Co	NA	3.18 ± 0.08	1.21 ± 1.70	< 0.001
HBV DNA as log10 IU/mL	NA	7.81 ± 0.80	6.28 ± 1.70	< 0.001
AFP in ng/mL	2.06 ± 0.82	2.49 ± 1.05	22.61 ± 40.82	0.045
TBIL in μmol/L	5.9 ± 3.1	12.7 ± 5.3	19.5 ± 9.2	< 0.001
ALB in g/L	48.8 ± 3.5	45.8 ± 2.9	43.0 ± 4.9	0.002
GLO in g/L	24.4 ± 4.0	26.6 ± 4.4	29.3 ± 4.3	0.017
ALT in U/L	22.0 (18.0, 29.0)	29.5 (23.7, 33.0)	277.5 (101.5, 410.8)	< 0.001
AST in U/L	16.0 (12.0, 22.0)	23.0 (19.5, 27.8)	111.0 (67.0, 143.5)	0.006
GGT in U/L	25.7 ± 11.5	18.5 ± 9.4	72.7 ± 64.9	0.001
TBA in μmol/L	2.3 (1.9, 3.4)	5.6 (4.2, 8.4)	13.9 (5.5, 31.1)	0.012
LSM in kPa	4.99 ± 0.99	5.11 ± 1.01	6.38 ± 0.72	0.026

H: Healthy; IT: Immune-tolerant; IA: Immune-active; HBsAg: Hepatitis B surface antigen; HBeAg: Hepatitis B virus e-antigen; HBV: Hepatitis B virus; AFP: Alpha-fetoprotein; TBIL: Total bilirubin; ALB: Albumin; GLO: Globulin; ALT: Alanine aminotransferase; AST: Aspartate aminotransferase; GGT: Gamma glutamyl transpeptidase; TBA: Total bile acid; LSM: Liver stiffness measurement; M: Male; F: Female; NA: Not available.

Table 2 Species richness indices in the fecal samples

Group	Healthy controls, *n* = 14	IT phase HBV infection, *n* = 13	IA phase HBV infection, *n* = 10	*P* value
OTUs	633	662	489	
α-diversity indexes, median				
Chao1	264.310	233.825	227.000	0.924
Shannon	5.020	4.720	4.705	1.739
Simpson	0.940	0.885	0.915	1.666

IT: Immune-tolerant; IA: Immune-active; HBV: Hepatitis B virus; OTUs: Operational taxonomic units.

Furthermore, the Wilcoxon and Kruskal-Wallis rank sum tests showed the abundance at different taxonomic levels with *P* < 0.05 and FDR q < 0.1 (Supplementary Table 3). The top 20 gut microbiota at the genus level consisted of *Bacteroides, Prevotella 9, Megamonas, Blautia, Faecalibacterium, Roseburia, Fusicatenibacter, Anaerostipes, Prevotella 2, Ruminococcus 2, Phascolarctobacterium, Alloprevotella, Bifidobacterium, Subdoligranulum, Dialister, Eubacterium rectale, Eubacterium eligens, Dorea, Eubacterium hallii*, and *Streptococcus*. Moreover, the shared species between the significantly different gut microbiota and the top 20 gut microbiota were *Blautia, Faecalibacterium, Fusicatenibacter, Prevotella 2, Alloprevotella*, and *Eubacterium hallii* group, which might be highly associated with the outcomes of CHB in different phases. The differences found in this study revealed the dysbiosis involved in the development of CHB and the aberrant ecological networks of microbial communities during infection.

Longitudinal analysis of patients in the IT phase of HBV infection

Longitudinal follow-up analysis showed that 3 patients progressed from the IT phase to the IA phase and required medical treatments. The change in the microbiota of these 3 patients during treatment was studied. The abundance of *Firmicutes* and *Actinobacteria* increased, while the abundance of *Bacteroidetes* and *Proteobacteria* decreased at the phylum level (Figure 4A). Moreover, *Bacteroides, Alistipes*, and *Bilophila* were mostly abundant in the IT phase, while *Actinomyces, Adlercreutzia*, and *Streptococcus* were more abundant in the IA phase (Figure 4B and C). A decreased ratio of *Bacteroidetes* to *Firmicutes* was observed, which might be involved in inflammatory disorders in the IA phase.
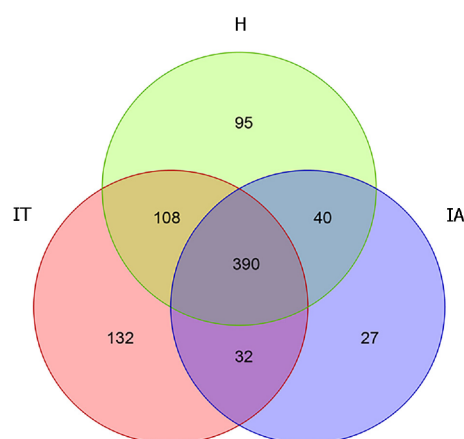
Figure 1 Operational taxonomic units in healthy controls, immune-tolerant phase patients, and immune-active phase patients. IT: Immune-tolerant; IA: Immune-active; H: Healthy.

Microbial functional dysbiosis in IT and IA patients and co-occurrence network analysis

To identify the bacterial functional alteration in IT and IA patients, we analyzed the functional potential of gut microbiota with PICRUSt analysis. A total of 101 different metabolic functions were predicted in this study, with 6 metabolic pathways having the highest enrichments, namely carbohydrate metabolism (14.85%), amino acid metabolism (12.87%), lipid metabolism (11.88%), metabolism of cofactors and vitamins (11.88%), xenobiotic biodegradation (9.90%), and metabolism of terpenoids and polyketides (7.92%). In addition, the functional roles of the bacteria were highly related to infectious diseases, including bacterial infection (50.00%) and parasitic infection (33.33%) as well as cardiovascular disease (10.00%) and neurodegenerative disease (10.00%) (Supplementary Table 4). The parasitic infectious disease-related gene subgroups ($P = 0.03$) in the IA-phase patients were highly enriched (Figure 5). The cell motility-related genes were highly enriched in the IA-phase patients (Figure 5A), while the transport and catabolism-related genes ($P = 0.03$) were significantly enriched in the IT-phase patients. However, signal transduction-related genes were significantly enriched in the healthy controls ($P < 0.01$) (Figure 5B). The replication repair-related genes and digestive system-related genes in the IT-phase patients were more abundant than in the other groups, but the difference between the three groups was not statistically significant (Figure 5C and E). Moreover, the digestive system disease-related gene subset ($P = 0.02$) was highly enriched in the IT-phase patients (Figure 5D). Genes that are related to the amino acid metabolism glycosyl biosynthesis cofactors and vitamin metabolism were more enriched in the IT-phase patients than in the healthy controls ($P < 0.01$) (Figure 5F). These observed results suggested that changes in the bacterial composition can significantly alter gene function, which may contribute to the development of CHB.

As shown in the co-occurrence network analysis using Cytoscape software (Supplementary Figure 1), five genera (Dorea, Bifidobacterium, Bacteroides, Blautia, and Romboutsia) were highly positively correlated. Dorea and Bifidobacterium exhibited the highest degree of linkage, while Dorea and Bacteroides had the least degree of linkage.

Non-target metabolomics analysis

A total of 293 substantially different metabolites were identified, among which 134 metabolites had an MS2.name provided by the mass spectrometry qualitative matching analysis. A total of 57 metabolites were upregulated, while 77 were downregulated. The different metabolites are shown in Supplementary Table 5.

DISCUSSION

To date, there are limited studies showing the role of dysbiosis of the gut microbiota in HBV-infected patients during the different immune phases of infection. This study revealed the profiles of the gut microbiota during HBV infection from the IT phase to the IA phase. The results suggested that the diversity, composition, and functionality of the microbiota changed from the IT phase to the IA phase and were related to the progression of CHB.

In our study, analysis of α-diversity using the Chao1, Shannon, and Simpson diversity indices showed no significant differences among the three groups. Nevertheless, one study has reported that the α-diversity is increased in cirrhosis patients compared to healthy controls and positively correlated to the Child-Pugh score[26]. In our study, a decreased ratio of *Bacteroidetes* to *Firmicutes* was observed as
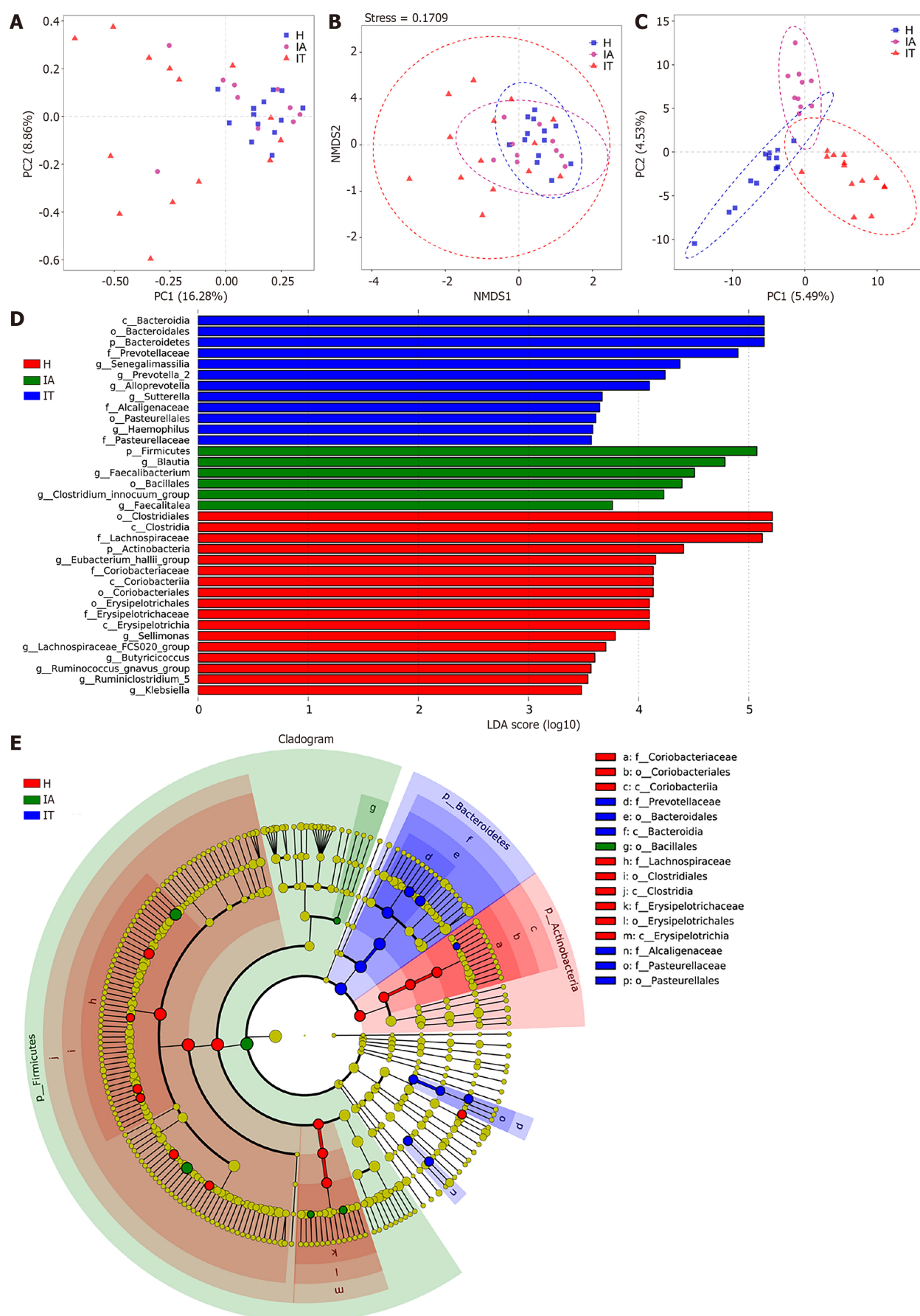
Figure 2 Beta-diversity analysis and comparison of variation in microbiota in the three groups using the linear discriminant analysis effect size online tool. A: Principal component analysis on the relative abundance. Each point represents a sample, plotted by the second principal component on

the Y-axis and the first principal component on the X-axis and colored by group; B: Comparison of the sample distribution of different subgroups using weighted non-metric multidimensional scaling analysis. Each sample is represented by a dot; C: Partial least squares discrimination analysis. Each point represents a sample; D: Histogram of the linear discriminant analysis (LDA) scores for differentially abundant genera between groups (a logarithmic LDA score > 3 indicated a higher relative abundance in the corresponding group compared to the other group); E: The taxonomic cladogram obtained from the LDA effect size analysis of 16S sequences and taxonomic representation of statistically significant differences between groups. The diameter of each circle is proportional to the taxon abundance. LDA: Linear discriminant analysis; IT: Immune-tolerant; IA: Immune-active; H: Healthy.
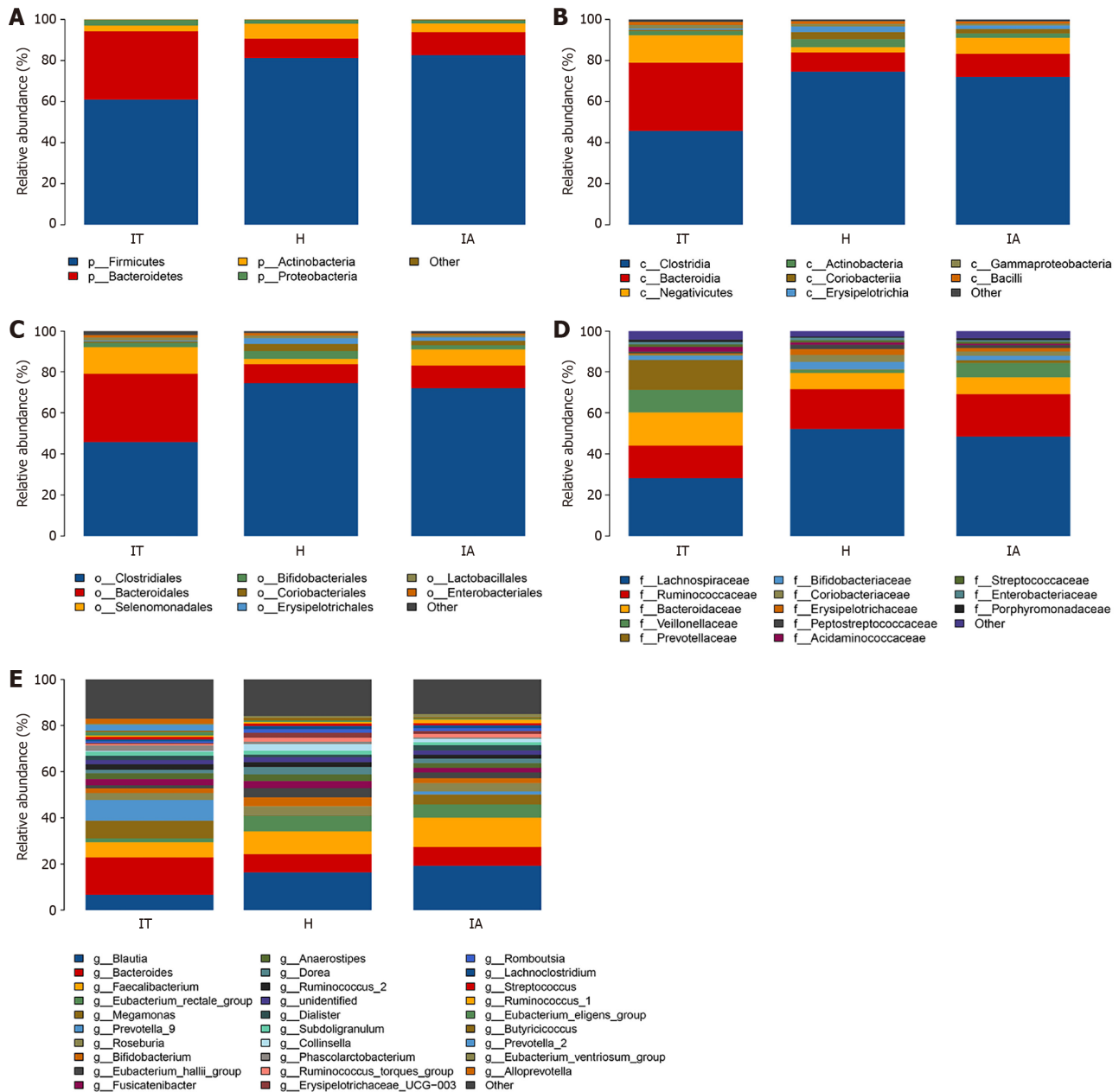
DOI: 10.3748/wjg.v28.i35.5188 **Copyright** ©The Author(s) 2022.

Figure 3 Distribution of the predominant bacteria at different taxonomic levels (phylum, class, order, family, and genus). A-E: Stacked bars of the phylum, class, order, family, and genus level in healthy controls, immune-tolerant phase hepatitis B virus infection, and immune-active phase hepatitis B virus infection. IT: Immune-tolerant; IA: Immune-active; H: Healthy.

patients progressed from the IT phase to the IA phase, while another study has demonstrated that the ratio of *Bacteroidetes* to *Firmicutes* increased in patients with HBV-related cirrhosis compared to that of healthy individuals[27]. These results in different studies indicate that the results may vary greatly depending on the grouping. In addition, our results suggest that the composition of the gut microbiota had changed in the early stages of HBV infection. Furthermore, metabolic changes at different stages of HBV infection were also observed by PICRUSt analysis. Consistent with another study[27], these results suggest that changes in the composition of the gut microbiota can significantly alter gene function,
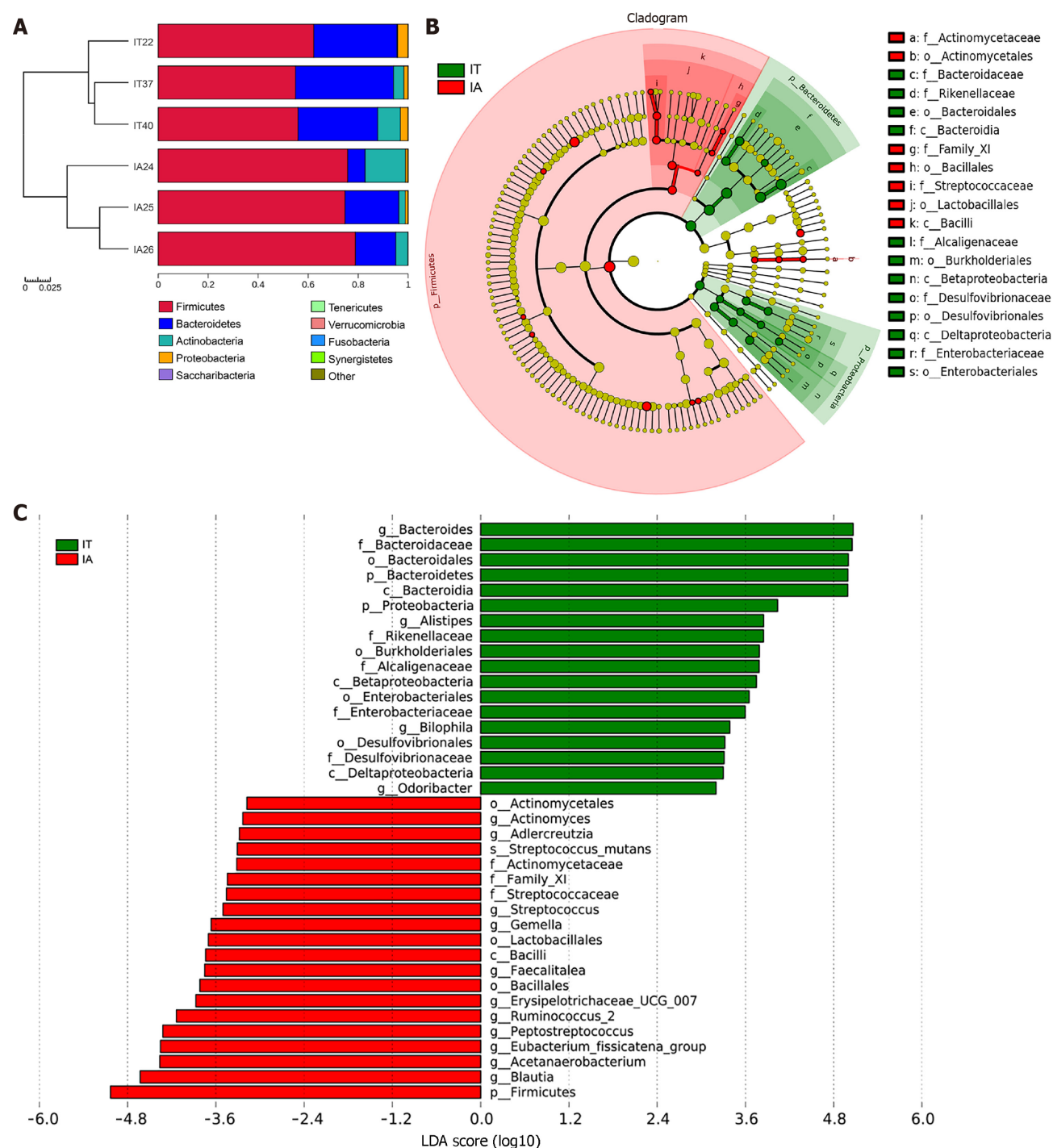
Figure 4 Comparison of variations in the microbiota of 3 patients before and after disease progression using the linear discriminant analysis effect size online tool. A: Distribution of the predominant bacteria at the phylum level in the 3 patients in the immune-tolerant and immune-active phases; B: The taxonomic cladogram obtained from linear discriminant analysis effect size analysis of 16S sequences and taxonomic representation of statistically significant differences between the two groups. The diameter of each circle is proportional to the taxon abundance; C: Histogram of the linear discriminant analysis scores for differentially abundant genera between the two groups (a logarithmic linear discriminant analysis score > 3 indicated a higher relative abundance in the corresponding group compared to the other group). LDA: Linear discriminant analysis; IT: Immune-tolerant; IA: Immune-active.

which may have a potential role in HBV-infected patients.

When compared to the healthy controls, there was a correlation between some gut microbiota in patients at the IT and IA phases. Notably, the IT group presented a high relative abundance of *Senegali-massilia*, *Prevotella 2*, *Alloprevotella*, *Sutterella*, and *Haemophilus*; while the IA group showed a high relative abundance of *Blautia*, *Faecalibacterium*, *Clostridium innocuum* group, and *Faecalitalea*. Some *Prevotella* strains have been reported as potentially clinically important pathobionts in human diseases by increasing the levels of interleukin (IL)-23, IL-1, IL-8, IL-6, and C-C motif chemokine ligand 20[28]. In addition, *Alloprevotella* is enriched in fecal samples from patients with chronic kidney disease[29].

A Cellular processes
B Environmental information processing
C Genetic information processing
D Human diseases
E Organismal system
F Metabolism

DOI: 10.3748/wjg.v28.i35.5188 **Copyright** ©The Author(s) 2022.
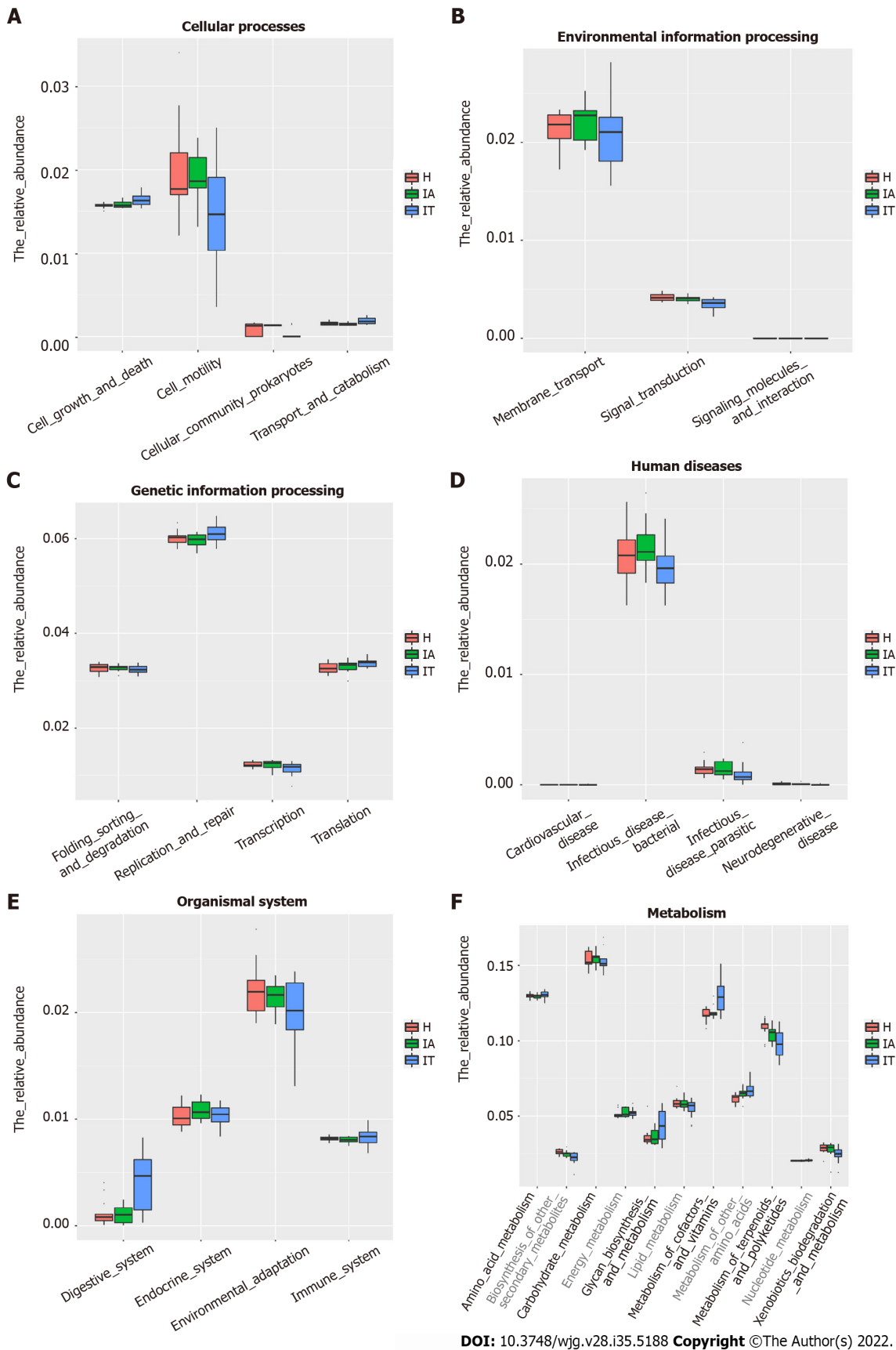
Figure 5 Alteration of the predicted microbial functional composition from the 16S rDNA sequencing data, analyzed using Phylogenetic Investigation of Communities by Reconstruction of Unobserved States. A and B: Representing the differences at the cellular processes among healthy and patients in the immune-tolerant and immune-active phases; C and D: Representing the differences at the genetic information processing and human diseases among healthy and patients in the immune-tolerant and immune-active phases; E and F: Representing the differences at the organismal systems and metabolism among healthy and patients in the immune-tolerant and immune-active phases. IT: Immune-tolerant; IA: Immune-active; H: Healthy.

Moreover, the gut microbiota in prediabetic individuals was found to be aberrant, with decreased *Clostridium* and increased *Sutterella* levels[30]. Furthermore, *Sutterella* has the capacity to degrade IgA, causing failure of therapeutics treating ulcerative colitis[31]. These findings reveal that *Prevotella 2*, *Alloprevotella*, and *Sutterella* are involved in chronic human diseases. Our results also indicate that *Prevotella 2*, *Alloprevotella*, and *Sutterella* are specifically related to HBV infection in the IT phase, suggesting their role of mediating viral escape from the host immune response.

Blautia, *Faecalibacterium*, *Clostridium innocuum* group, and *Faecalitalea* were identified as signature gut microbiota related to HBV infection in the IA phase. Notably, an elevated abundance of *Blautia* has been shown to alleviate the severity of lethal acute graft-versus-host disease[32]. In addition, Benítez-Páez *et al*[33] proposed that *Blautia luti* and *Blautia wexlerae* might help to reduce the inflammation that is linked to obesity-related complications. Moreover, *Blautia* is positively associated with the pathophysiology of type 2 diabetes[34]. Furthermore, *Faecalibacterium prausnitzii*, belonging to *Faecalibacterium*, is a major constituent of the gut microbiota in healthy individuals. This bacterium, which has anti-inflammatory activity, is decreased in patients with inflammatory bowel diseases such as Crohn's disease. Interestingly, *Blautia* and *Faecalibacterium* have been shown to be beneficial in a healthy gut[35]; these bacteria enhance the production of butyrate succinate and lactate, thus providing energy and reducing inflammation[36].

Additionally, a recent finding indicated that in patients with early HBV-related HCC, genera belonging to butyrate-producing bacterial families, including *Ruminococcus*, *Oscillibacter*, *Faecalibacterium*, *Clostridium IV*, and *Coprococcus* decreased, while the lipopolysaccharide-producing bacteria *Klebsiella* and *Haemophilus* increased compared to the levels in cirrhosis patients[37]. Herein, the proportions of *Blautia*, *Faecalibacterium*, and *Clostridium innocuum* group were higher in the IA-phase patients than in the controls, indicating that enrichment of these three signature microbial taxa might be a sign of severe inflammation or exacerbation of disease. Notably, these beneficial gut microbiota might help to clear viral infection in the IA phase, while some gut microbiota in the IT phase might help the virus to escape from host immune responses. Taken together, these findings highlight an important role for the composition of the gut microbiota in the progression of HBV infection, which has significant clinical implications.

Based on the composition and structure of the gut microbiota, the metabolic function of the microflora was further analyzed through PICRUSt. In this study, the genes involved in glycan biosynthesis and metabolism as well as cofactor and vitamin metabolism were more enriched in the IT-phase patients than in the healthy controls. One explanation for this finding is that *Senegalimassilia*, *Prevotella 2*, *Alloprevotella*, *Sutterella*, and *Haemophilus* are enriched in the IT phase and consume glycan as their energy source; the genes found in these bacteria are related to cofactor and vitamin metabolism. In contrast, terpenoid and polyketide metabolism-related genes were more abundant in the IA phase, suggesting that *Senegalimassilia*, *Prevotella 2*, *Alloprevotella*, *Sutterella*, and *Haemophilus* participate in the metabolism of terpenoids and polyketides. These results may indicate that the gut microbiota and metabolites contribute to the abnormal metabolism status in CHB.

Previous research has shown that the gut microbiota composition is closely related to the occurrence of various chronic liver diseases[38-40]. Our current study demonstrated that potential links exist between certain bacteria and different pathological mechanisms during CHB progression from the IT phase to the IA phase.

Studies using mouse models have uncovered that the gut microbiota have a vital role in overcoming the IT phase of viral infection at different ages[41] and that gut microbiota lead to Kupffer cell-mediated T cell suppression, which is associated with HBV persistence[42]. In addition, fecal microbiota transplantation therapy has been shown to improve the clearance rate of HBV antigens in CHB patients after long-term therapy[43]. Our study demonstrated that the gut microbiota composition changed at different phases of HBV infection. Changes in the gut microbiota composition could be a biological factor for the progression of CHB. We believe that the gut microbiome of CHB patients may provide a useful prognostic marker for disease progression, outcome prediction, and treatment and that further microbiome-based study may provide new insights into the pathogenesis of CHB, the etiology of its progression, and novel therapeutic strategies such as the use of probiotics or fecal microbiota transplantation.

Although this study uncovered some insightful findings, some limitations remain. First, all patients enrolled in this study were from different families. Having different genetic backgrounds and dietary habits might affect the gut microbiota composition. In addition, the healthy donors should have had a similar age to the patients; however, the controls were not age-matched to the patients in this study. Second, only 3 patients were followed up from the IT phase to the IA phase. A larger longitudinal sample size will strengthen the results. Third, a real-world cross-sectional study would be beneficial to understand the impact of the microbiota on the progression of liver disease. Fourth, the methods we used have some limitations. Although transcriptomics also contributes to gene expression, the findings could be further confirmed if we used metagenomic sequencing rather than 16S rDNA gene sequencing. Metagenomic sequencing not only sequences the 16S rDNA genes, but it also sequences the whole genome of each bacterium. Thus, only by doing metagenomic sequencing, one can get the complete picture. Fifth, the functional studies of the gut microbiota are based on statistical predictions; therefore, further studies using germ-free animal models and related functional studies are required to investigate

the specific roles of the gut microbiota in CHB. Furthermore, the IT phase is an important phase that needs more attention.

CONCLUSION

These findings provide observational evidence of compositional alterations of the gut microbiome and some related metabolites in patients with IT-phase or IA-phase HBV infection. Further studies should investigate whether microbiota modulation can facilitate the progression of CHB and the cause-effect relationship between the gut microbiota and CHB.

ARTICLE HIGHLIGHTS

Research background

Chronic hepatitis B virus (HBV) infection (CHB) represents a public health problem that may progress to cirrhosis and hepatocellular carcinoma (HCC). HBV-infected individuals in immune tolerance (IT) are generally not recommended for anti-HBV treatment, owing to the absence of curative treatment and the evidence of a low risk of progressive liver injury in the IT patients. However, recent studies indicated hepatocarcinogenesis may occur in IT-phase patients; the body's IT status is a key factor affecting the outcome of the disease. Therefore, finding out the factors that affect the prognosis of HBV infection is of paramount significance for the rapid elimination of virus and the reduction of CHB.

Research motivation

The bacterial diversity level and composition varied between CHB, hepatitis B-related liver cirrhosis, and HCC. Gut microbiota of healthy controls is more consistent, whereas those of CHB, hepatitis B-related liver cirrhosis and HCC varied substantially. As the first phase of HBV progression, IT phase provides a favorable immune environment for HBV invasion and long-term existence, then transitions to immune clearance in the third decade. Therefore, in-depth study of the disease status and changes in the body during the IT phase is conducive to the development of new antiviral treatment methods to break the IT of the body and improve the antiviral efficacy and thus improve the long-term prognosis.

Research objectives

This study aimed to find some potential bacteria, linking different pathological mechanisms of IT phase HBV infection and some related metabolites to the IT phase of CHB infection.

Research methods

Clinical fecal samples from healthy individuals and patients in the IT and IA phases of HBV infection were collected. Next, non-target metabolomics, bioinformatics, and 16S rDNA sequencing analyses were performed.

Research results

A total of 293 different metabolites in 14 phyla, 22 classes, 29 orders, 51 families, and 190 genera were identified. The four phyla of *Firmicutes*, *Bacteroidetes*, *Actinobacteria*, and *Proteobacteria* were the most abundant, accounting for 99.72%, 99.79%, and 99.55% in the healthy controls, IT-phase patients, and IA-phase patients, respectively. We further identified 16 genera with different richness in the IT phase and IA phase of HBV infection. Of the 134 named metabolites, 57 were upregulated and 77 were downregulated. A total of 101 different metabolic functions were predicted in this study, with 6 metabolic pathways having the highest enrichments, namely carbohydrate metabolism (14.85%), amino acid metabolism (12.87%), lipid metabolism (11.88%), metabolism of cofactors and vitamins (11.88%), xenobiotic biodegradation (9.9%), and metabolism of terpenoids and polyketides (7.92%).

Research conclusions

The composition of the gut microbiota changed in the early stages of HBV infection, and changes in the composition of the gut microbiota can significantly alter gene function, which may have a potential role in HBV-infected patients.

Research perspectives

It is relatively difficult to fully understand the causal relationship between gut microbiota and HBV-induced chronic liver disease at different stages in this real-world cross-sectional study. Nevertheless, it should be noted that germ-free animals are good models to study the effect of gut microbiota on human diseases. In a future study, it is imperative to use germ-free animal models and additional biofunctional assays to reveal the cause-effect relationship between gut microbiota and chronic HBV infection.

FOOTNOTES

REFERENCES

1   **Mason WS**, Gill US, Litwin S, Zhou Y, Peri S, Pop O, Hong ML, Naik S, Quaglia A, Bertoletti A, Kennedy PT. HBV DNA Integration and Clonal Hepatocyte Expansion in Chronic Hepatitis B Patients Considered Immune Tolerant. *Gastroenterology* 2016; **151**: 986-998.e4 [PMID: 27453547 DOI: 10.1053/j.gastro.2016.07.012]

2   **Kennedy PTF**, Litwin S, Dolman GE, Bertoletti A, Mason WS. Immune Tolerant Chronic Hepatitis B: The Unrecognized Risks. *Viruses* 2017; **9** [PMID: 28468285 DOI: 10.3390/v9050096]

3   **Kim GA**, Lim YS, Han S, Choi J, Shim JH, Kim KM, Lee HC, Lee YS. High risk of hepatocellular carcinoma and death in patients with immune-tolerant-phase chronic hepatitis B. *Gut* 2018; **67**: 945-952 [PMID: 29055908 DOI: 10.1136/gutjnl-2017-314904]

4   **Xu D**, Huang Y, Wang J. Gut microbiota modulate the immune effect against hepatitis B virus infection. *Eur J Clin Microbiol Infect Dis* 2015; **34**: 2139-2147 [PMID: 26272175 DOI: 10.1007/s10096-015-2464-0]

5   **Wang B**, Li L. Who determines the outcomes of HBV exposure? *Trends Microbiol* 2015; **23**: 328-329 [PMID: 25864882 DOI: 10.1016/j.tim.2015.04.001]

6   **Maslennikov R**, Ivashkin V, Efremova I, Poluektova E, Kudryavtseva A, Krasnov G. Gut dysbiosis and small intestinal bacterial overgrowth as independent forms of gut microbiota disorders in cirrhosis. *World J Gastroenterol* 2022; **28**: 1067-1077 [PMID: 35431497 DOI: 10.3748/wjg.v28.i10.1067]

7   **Tremaroli V**, Bäckhed F. Functional interactions between the gut microbiota and host metabolism. *Nature* 2012; **489**: 242-249 [PMID: 22972297 DOI: 10.1038/nature11552]

8   **Nicholson JK**, Holmes E, Kinross J, Burcelin R, Gibson G, Jia W, Pettersson S. Host-gut microbiota metabolic interactions. *Science* 2012; **336**: 1262-1267 [PMID: 22674330 DOI: 10.1126/science.1223813]

9   **Hernández-Ceballos W**, Cordova-Gallardo J, Mendez-Sanchez N. Gut Microbiota in Metabolic-associated Fatty Liver Disease and in Other Chronic Metabolic Diseases. *J Clin Transl Hepatol* 2021; **9**: 227-238 [PMID: 34007805 DOI: 10.14218/JCTH.2020.00131]

10   **Liu Q**, Li F, Zhuang Y, Xu J, Wang J, Mao X, Zhang Y, Liu X. Alteration in gut microbiota associated with hepatitis B and non-hepatitis virus related hepatocellular carcinoma. *Gut Pathog* 2019; **11**: 1 [PMID: 30675188 DOI: 10.1186/s13099-018-0281-6]

11   **Wang J**, Wang Y, Zhang X, Liu J, Zhang Q, Zhao Y, Peng J, Feng Q, Dai J, Sun S, Zhao L, Zhang Y, Hu Y, Zhang M. Gut Microbial Dysbiosis Is Associated with Altered Hepatic Functions and Serum Metabolites in Chronic Hepatitis B Patients. *Front Microbiol* 2017; **8**: 2222 [PMID: 29180991 DOI: 10.3389/fmicb.2017.02222]

12   **Zeng Y**, Chen S, Fu Y, Wu W, Chen T, Chen J, Yang B, Ou Q. Gut microbiota dysbiosis in patients with hepatitis B virus-

induced chronic liver disease covering chronic hepatitis, liver cirrhosis and hepatocellular carcinoma. *J Viral Hepat* 2020; **27**: 143-155 [PMID: 31600845 DOI: 10.1111/jvh.13216]

13   **Li R**, Yi X, Yang J, Zhu Z, Wang Y, Liu X, Huang X, Wan Y, Fu X, Shu W, Zhang W, Wang Z. Gut Microbiome Signatures in the Progression of Hepatitis B Virus-Induced Liver Disease. *Front Microbiol* 2022; **13**: 916061 [PMID: 35733959 DOI: 10.3389/fmicb.2022.916061]

14   **Chen Z**, Xie Y, Zhou F, Zhang B, Wu J, Yang L, Xu S, Stedtfeld R, Chen Q, Liu J, Zhang X, Xu H, Ren J. Featured Gut Microbiomes Associated With the Progression of Chronic Hepatitis B Disease. *Front Microbiol* 2020; **11**: 383 [PMID: 32265857 DOI: 10.3389/fmicb.2020.00383]

15   **Yang XA**, Lv F, Wang R, Chang Y, Zhao Y, Cui X, Li H, Yang S, Li S, Zhao X, Mo Z, Yang F. Potential role of intestinal microflora in disease progression among patients with different stages of Hepatitis B. *Gut Pathog* 2020; **12**: 50 [PMID: 33117435 DOI: 10.1186/s13099-020-00391-4]

16   **Sarin SK**, Kumar M, Lau GK, Abbas Z, Chan HL, Chen CJ, Chen DS, Chen HL, Chen PJ, Chien RN, Dokmeci AK, Gane E, Hou JL, Jafri W, Jia J, Kim JH, Lai CL, Lee HC, Lim SG, Liu CJ, Locarnini S, Al Mahtab M, Mohamed R, Omata M, Park J, Piratvisuth T, Sharma BC, Sollano J, Wang FS, Wei L, Yuen MF, Zheng SS, Kao JH. Asian-Pacific clinical practice guidelines on the management of hepatitis B: a 2015 update. *Hepatol Int* 2016; **10**: 1-98 [PMID: 26563120 DOI: 10.1007/s12072-015-9675-4]

17   **European Association for the Study of the Liver**. EASL 2017 Clinical Practice Guidelines on the management of hepatitis B virus infection. *J Hepatol* 2017; **67**: 370-398 [PMID: 28427875 DOI: 10.1016/j.jhep.2017.03.021]

18   **Munyaka PM**, Eissa N, Bernstein CN, Khafipour E, Ghia JE. Antepartum Antibiotic Treatment Increases Offspring Susceptibility to Experimental Colitis: A Role of the Gut Microbiota. *PLoS One* 2015; **10**: e0142536 [PMID: 26605545 DOI: 10.1371/journal.pone.0142536]

19   **Edgar RC**. UPARSE: highly accurate OTU sequences from microbial amplicon reads. *Nat Methods* 2013; **10**: 996-998 [PMID: 23955772 DOI: 10.1038/nmeth.2604]

20   **Cole JR**, Wang Q, Cardenas E, Fish J, Chai B, Farris RJ, Kulam-Syed-Mohideen AS, McGarrell DM, Marsh T, Garrity GM, Tiedje JM. The Ribosomal Database Project: improved alignments and new tools for rRNA analysis. *Nucleic Acids Res* 2009; **37**: D141-D145 [PMID: 19004872 DOI: 10.1093/nar/gkn879]

21   **Wang Y**, Sheng HF, He Y, Wu JY, Jiang YX, Tam NF, Zhou HW. Comparison of the levels of bacterial diversity in freshwater, intertidal wetland, and marine sediments by using millions of illumina tags. *Appl Environ Microbiol* 2012; **78**: 8264-8271 [PMID: 23001654 DOI: 10.1128/AEM.01821-12]

22   **Jiang XT**, Peng X, Deng GH, Sheng HF, Wang Y, Zhou HW, Tam NF. Illumina sequencing of 16S rRNA tag revealed spatial variations of bacterial communities in a mangrove wetland. *Microb Ecol* 2013; **66**: 96-104 [PMID: 23649297 DOI: 10.1007/s00248-013-0238-8]

23   **Jami E**, Israel A, Kotser A, Mizrahi I. Exploring the bovine rumen bacterial community from birth to adulthood. *ISME J* 2013; **7**: 1069-1079 [PMID: 23426008 DOI: 10.1038/ismej.2013.2]

24   **Zhou B**, Xiao JF, Tuli L, Ressom HW. LC-MS-based metabolomics. *Mol Biosyst* 2012; **8**: 470-481 [PMID: 22041788 DOI: 10.1039/c1mb05350g]

25   **Dunn WB**, Broadhurst D, Begley P, Zelena E, Francis-McIntyre S, Anderson N, Brown M, Knowles JD, Halsall A, Haselden JN, Nicholls AW, Wilson ID, Kell DB, Goodacre R; Human Serum Metabolome (HUSERMET) Consortium. Procedures for large-scale metabolic profiling of serum and plasma using gas chromatography and liquid chromatography coupled to mass spectrometry. *Nat Protoc* 2011; **6**: 1060-1083 [PMID: 21720319 DOI: 10.1038/nprot.2011.335]

26   **Sanduzzi Zamparelli M**, Rocco A, Compare D, Nardone G. The gut microbiota: A new potential driving force in liver cirrhosis and hepatocellular carcinoma. *United European Gastroenterol J* 2017; **5**: 944-953 [PMID: 29163959 DOI: 10.1177/2050640617705576]

27   **Shu W**, Shanjian C, Jinpiao L, Qishui O. Gut microbiota dysbiosis in patients with hepatitis B virus-related cirrhosis. *Ann Hepatol* 2022; **27**: 100676 [PMID: 35093600 DOI: 10.1016/j.aohep.2022.100676]

28   **Larsen JM**. The immune response to Prevotella bacteria in chronic inflammatory disease. *Immunology* 2017; **151**: 363-374 [PMID: 28542929 DOI: 10.1111/imm.12760]

29   **Li F**, Wang M, Wang J, Li R, Zhang Y. Alterations to the Gut Microbiota and Their Correlation With Inflammatory Factors in Chronic Kidney Disease. *Front Cell Infect Microbiol* 2019; **9**: 206 [PMID: 31245306 DOI: 10.3389/fcimb.2019.00206]

30   **Allin KH**, Tremaroli V, Caesar R, Jensen BAH, Damgaard MTF, Bahl MI, Licht TR, Hansen TH, Nielsen T, Dantoft TM, Linneberg A, Jørgensen T, Vestergaard H, Kristiansen K, Franks PW; IMI-DIRECT consortium, Hansen T, Bäckhed F, Pedersen O. Aberrant intestinal microbiota in individuals with prediabetes. *Diabetologia* 2018; **61**: 810-820 [PMID: 29379988 DOI: 10.1007/s00125-018-4550-1]

31   **Kaakoush NO**. Sutterella Species, IgA-degrading Bacteria in Ulcerative Colitis. *Trends Microbiol* 2020; **28**: 519-522 [PMID: 32544438 DOI: 10.1016/j.tim.2020.02.018]

32   **Jenq RR**, Taur Y, Devlin SM, Ponce DM, Goldberg JD, Ahr KF, Littmann ER, Ling L, Gobourne AC, Miller LC, Docampo MD, Peled JU, Arpaia N, Cross JR, Peets TK, Lumish MA, Shono Y, Dudakov JA, Poeck H, Hanash AM, Barker JN, Perales MA, Giralt SA, Pamer EG, van den Brink MR. Intestinal Blautia Is Associated with Reduced Death from Graft-versus-Host Disease. *Biol Blood Marrow Transplant* 2015; **21**: 1373-1383 [PMID: 25977230 DOI: 10.1016/j.bbmt.2015.04.016]

33   **Benítez-Páez A**, Gómez Del Pugar EM, López-Almela I, Moya-Pérez Á, Codoñer-Franch P, Sanz Y. Depletion of *Blautia* Species in the Microbiota of Obese Children Relates to Intestinal Inflammation and Metabolic Phenotype Worsening. *mSystems* 2020; **5** [PMID: 32209719 DOI: 10.1128/mSystems.00857-19]

34   **Gurung M**, Li Z, You H, Rodrigues R, Jump DB, Morgun A, Shulzhenko N. Role of gut microbiota in type 2 diabetes pathophysiology. *EBioMedicine* 2020; **51**: 102590 [PMID: 31901868 DOI: 10.1016/j.ebiom.2019.11.051]

35   **Lopez-Siles M**, Duncan SH, Garcia-Gil LJ, Martinez-Medina M. Faecalibacterium prausnitzii: from microbiology to diagnostics and prognostics. *ISME J* 2017; **11**: 841-852 [PMID: 28045459 DOI: 10.1038/ismej.2016.176]

36   **Abaidullah M**, Peng S, Kamran M, Song X, Yin Z. Current Findings on Gut Microbiota Mediated Immune Modulation against Viral Diseases in Chicken. *Viruses* 2019; **11** [PMID: 31349568 DOI: 10.3390/v11080681]

37   **Ren Z**, Li A, Jiang J, Zhou L, Yu Z, Lu H, Xie H, Chen X, Shao L, Zhang R, Xu S, Zhang H, Cui G, Sun R, Wen H, Lerut JP, Kan Q, Li L, Zheng S. Gut microbiome analysis as a tool towards targeted non-invasive biomarkers for early hepatocellular carcinoma. *Gut* 2019; **68**: 1014-1023 [PMID: 30045880 DOI: 10.1136/gutjnl-2017-315084]

38   **Aron-Wisnewsky J**, Vigliotti C, Witjes J, Le P, Holleboom AG, Verheij J, Nieuwdorp M, Clément K. Gut microbiota and human NAFLD: disentangling microbial signatures from metabolic disorders. *Nat Rev Gastroenterol Hepatol* 2020; **17**: 279-297 [PMID: 32152478 DOI: 10.1038/s41575-020-0269-9]

39   **Qin N**, Yang F, Li A, Prifti E, Chen Y, Shao L, Guo J, Le Chatelier E, Yao J, Wu L, Zhou J, Ni S, Liu L, Pons N, Batto JM, Kennedy SP, Leonard P, Yuan C, Ding W, Hu X, Zheng B, Qian G, Xu W, Ehrlich SD, Zheng S, Li L. Alterations of the human gut microbiome in liver cirrhosis. *Nature* 2014; **513**: 59-64 [PMID: 25079328 DOI: 10.1038/nature13568]

40   **Albhaisi SAM**, Bajaj JS, Sanyal AJ. Role of gut microbiota in liver disease. *Am J Physiol Gastrointest Liver Physiol* 2020; **318**: G84-G98 [PMID: 31657225 DOI: 10.1152/ajpgi.00118.2019]

41   **Chou HH**, Chien WH, Wu LL, Cheng CH, Chung CH, Horng JH, Ni YH, Tseng HT, Wu D, Lu X, Wang HY, Chen PJ, Chen DS. Age-related immune clearance of hepatitis B virus infection requires the establishment of gut microbiota. *Proc Natl Acad Sci U S A* 2015; **112**: 2175-2180 [PMID: 25646429 DOI: 10.1073/pnas.1424775112]

42   **Zhou W**, Luo J, Xie X, Yang S, Zhu D, Huang H, Yang D, Liu J. Gut Microbiota Dysbiosis Strengthens Kupffer Cell-mediated Hepatitis B Virus Persistence through Inducing Endotoxemia in Mice. *J Clin Transl Hepatol* 2022; **10**: 17-25 [PMID: 35233369 DOI: 10.14218/JCTH.2020.00161]

43   **Ren YD**, Ye ZS, Yang LZ, Jin LX, Wei WJ, Deng YY, Chen XX, Xiao CX, Yu XF, Xu HZ, Xu LZ, Tang YN, Zhou F, Wang XL, Chen MY, Chen LG, Hong MZ, Ren JL, Pan JS. Fecal microbiota transplantation induces hepatitis B virus e-antigen (HBeAg) clearance in patients with positive HBeAg after long-term antiviral therapy. *Hepatology* 2017; **65**: 1765-1768 [PMID: 28027582 DOI: 10.1002/hep.29008]

ORIGINAL ARTICLE

Observational Study

Dynamic blood presepsin levels are associated with severity and outcome of acute pancreatitis: A prospective cohort study

Hong-Li Xiao, Guo-Xing Wang, Yan Wang, Zhi-Min Tan, Jie Zhou, Han Yu, Miao-Rong Xie, Chun-Sheng Li

Hong-Li Xiao, Guo-Xing Wang, Yan Wang, Zhi-Min Tan, Jie Zhou, Miao-Rong Xie, Chun-Sheng Li, Department of Emergency Medicine, Beijing Friendship Hospital, Capital Medical University, Beijing 100050, China

Han Yu, Department of Emergency Medicine, Beijing Chao-Yang Hospital, Capital Medical University, Beijing 100020, China

Corresponding author: Chun-Sheng Li, MD, Professor, Department of Emergency Medicine, Beijing Friendship Hospital, Capital Medical University, No. 95 Yongan Road, Xicheng District, Beijing 100050, China. lcscyyy@163.com

Abstract

BACKGROUND

Acute pancreatitis (AP) is an inflammatory disorder of the pancreas with an unpredictable course of illness. A major challenge of AP is the early identification of patients at high-risk for organ failure and death. However, scoring systems are complicated and time consuming, and the predictive values for the clinical course are vague.

AIM

To determine whether the dynamic changes in presepsin levels can be used to evaluate the severity of disease and outcome of AP.

METHODS

In this multicentric cohort study, 133 patients with AP were included. Clinical severity was dynamically evaluated using the 2012 revised Atlanta Classification. Blood presepsin levels were measured at days 1, 3, 5 and 7 after admission by chemiluminescent enzyme immunoassay.

RESULTS

The median concentration of presepsin increased and the clearance rate of presepsin decreased with disease severity and organ failure in AP patients. The presepsin levels on days 3, 5 and 7 were independent predictors of moderately severe and severe AP with time-specific area under the curve (AUC) values of 0.827, 0.848 and 0.867, respectively. The presepsin levels positively correlated with bedside index of severity in AP, Ranson, acute physiology and chronic health evaluation II, computed tomography severity index and Marshall scores. Presepsin levels on days 3, 5 and 7 were independent predictors of 28-d mortality of

AP patients with AUC values of 0.781, 0.846 and 0.843, respectively.

CONCLUSION
Blood presepsin levels within 7 d of admission were associated with and may be useful to dynamically predict the severity of disease course and 28-d mortality in AP patients.

Key Words: Presepsin; Acute pancreatitis; Severity; Mortality; Disease severity

Core Tip: Acute pancreatitis has diverse clinical manifestations with an unpredictable clinical course. A major challenge of acute pancreatitis is the early identification of patients at high-risk for organ failure and death. Scoring systems are complicated and time consuming with limited predictive value for the clinical course. In this study, we investigated the association between the dynamic levels of blood presepsin, a new infection biomarker, and the changes of severity in the early course of acute pancreatitis. We found the predictive value of presepsin for 28-d mortality was similar to the bedside index of severity in acute pancreatitis, Ranson and acute physiology and chronic health evaluation II scores.

INTRODUCTION

Acute pancreatitis (AP) is an inflammatory disorder of the pancreas that can lead to systemic inflammatory response syndrome, organ failure and sepsis. AP is one of the most common causes of abdominal emergencies and is associated with mortality rates up to 35%[1,2]. Gallstones and alcohol consumption are the most frequent causes of AP. Irrespective of the etiology, AP has diverse clinical manifestations with an unpredictable clinical course. Various clinical scoring systems such as the bedside index of severity in acute pancreatitis (BISAP) score, Ranson criteria, computed tomography severity index (CTSI) and acute physiology and chronic health evaluation (APACHE) II scores have been developed to predict the illness severity at admission[3]. However, accurate prediction of the clinical course remains difficult[4]. A major challenge of AP is the early identification of patients at high risk for organ failure and death. Moreover, some of these scoring systems are complicated and time consuming with limited predictive value for the clinical course. Therefore, it is necessary to develop simple and convenient biomarkers to dynamically predict the severity of AP in its early course.

Presepsin is a subtype of soluble CD14 formed by a 13 kDa fragment and is an emerging biomarker of infection[5]. CD14 is a glycoprotein receptor for lipopolysaccharide. After lipopolysaccharide binds to CD14, presepsin is released into the blood and cleared by the kidney[6]. Presepsin has been confirmed to predict illness severity[7], number of organs experiencing dysfunction[8] and septic 90-d death rates [9,10]. This study aimed to assess the predictive value of blood presepsin levels for the severity of disease course and outcomes in patients with AP.

MATERIALS AND METHODS

Study population

This prospective, multicentric, and observational cohort study was conducted at the Emergency Departments of Beijing Friendship Hospital and Beijing Chaoyang Hospital affiliated with Capital Medical University. This study was approved by the Beijing Friendship Hospital Ethics Committee (Approval No. 2017-P2-103-02). Written informed consent was obtained from patients or their relatives. Patients diagnosed with AP as per the 2012 revised Atlanta Classification[11] were screened within 24 h of admission and followed up for 28 d. Patients were classified into one of three groups (mild, moderately severe and severe AP) based on the hospital course. Patients with mild AP had neither local complications nor organ failure. Patients with moderately severe AP had transient (< 48 h) organ failure or local complications or both, whereas patients with severe AP had persistent (> 48 h) organ failure. Organ failure was defined as a Marshall score > 2[11]. Patients were subsequently divided into one of

two groups [mild and non-mild (moderately severe and severe) AP] based on their presentation during the first, third, 5th and 7th day of admission. Pregnant women and patients younger than 18 years of age were excluded. All patients received standardized treatment according to the 2012 revised Atlanta Classification[11].

Data collection
The collected data included age, sex, comorbidities, etiologies, scoring, pancreatic imaging and interventions. Abdominal ultrasonography at admission and abdominal computed tomography scans 72 h after symptom onset were performed. The BISAP score, Ranson score, CTSI, APACHE II score, Marshall score and severity of AP were determined at 1, 3, 5 and 7 d post-admission. BISAP and APACHE II scores were evaluated within 24 h. The Ranson score was calculated within 48 h. Levels of the conventional inflammatory biomarkers procalcitonin and C-reactive protein were obtained from the clinical laboratory data. AP patients were classified into survival and non-survival groups based on their 28-d survival.

Determination of blood presepsin concentration
Venous blood samples were collected in tubes containing heparin at days 1, 3, 5 and 7 after admission and stored at 4 °C for analysis within 24 h. Presepsin concentration in the blood was measured using a chemiluminescent enzyme immunoassay[12] with a compact automated immunoanalyzer (PATHFAST; Mitsubishi Chemical Medience Corporation, Tokyo, Japan). The lower and upper detection limits of presepsin concentrations were 20 pg/mL and 200000 pg/mL, respectively.

Statistical analysis
All analyses were performed using SPSS version 25.0 (SPSS, Chicago, IL, United States). With a two-sided α = 0.05, a β = 0.2 and 70% of patients with mild pancreatitis[13], it was determined that 106 patients were required for enrollment, 74 with mild pancreatitis and 32 with non-mild pancreatitis. This study enrolled 137 patients to account for 20% of patients lost to follow-up. The clearance ratio of presepsin was calculated using the following formula: the presepsin level on day 1 minus the presepsin level on days 3, 5 or 7, divided by the presepsin level on day 1 and multiplied by 100%. Data with normal distribution were expressed as mean ± SD and were analyzed by Student's *t* test or variance analysis. Data with non-normal distribution were expressed as the median with quartiles and were analyzed by the Mann-Whitney *U* or Kruskal-Wallis tests. The χ^2 test or Fisher's exact test was used for comparison of frequencies. A receiver operating characteristic (ROC) curve was constructed to assess the predictive value of presepsin for moderate/severe AP and 28-d mortality. Prognostic parameters including sensitivity, specificity, positive predictive value and negative predictive value were calculated based on ROC curve analysis. The areas under the ROC curves (AUCs) were compared by MedCalc version 11.4 (MedCalc Software, Ostend, Belgium). The correlation was analyzed by Spearman rank correlation. Binary logistic regression analyses were used to determine the independent predictors for disease severity and 28-d mortality of AP patients. Cox proportional hazards regression model was used to estimate the independent contribution of presepsin for the prediction of 28-d mortality. All statistical tests were two-tailed, and a *P* value < 0.05 was considered statistically significant.

RESULTS

Patient characteristics
A total of 137 patients were screened in the emergency departments of the two hospitals from January 2018 to September 2019. Of these, 4 patients were excluded from analysis: 1 patient was diagnosed with pancreatic cancer, and 3 patients were lost to follow-up. Thus, 133 patients were enrolled and classified throughout the course of the disease as mild AP (*n* = 95 patients), moderately severe AP (*n* = 21 patients) and severe AP (*n* = 17 patients) according to the Atlanta 2012 classification. Patient characteristics are described in Table 1. The median age of patients was 65 years. There were 86 males and 47 females. The etiologies of AP included gallstones (63.2%), hypertriglyceridemia (9.0%), post-endoscopic retrograde cholangiopancreatography (11.3%), idiopathic (13.5%) and alcohol (3.0%). The BISAP, Ranson, CTSI and APACHE II scores increased with the severity of disease (all *P* < 0.01). The incidence of organ failure, mortality and the cost of hospitalization increased with the severity of disease (all *P* < 0.001).

The role of serial blood presepsin concentration in predicting severity of AP
Compared to patients with mild or moderately severe AP, the presepsin concentration at days 3 and 5 were significantly higher in patients with severe AP (Figure 1A). Compared with the mild group, the presepsin concentration in the moderately severe group at days 5 and 7 and in the severe group at day 7 were significantly higher (Figure 1A). The median clearance rate of presepsin on days 3 and 5 in moderately severe and severe patients were reduced compared to patients in the mild group (Figure 1B).

Table 1 Overall characteristics of the study population

Characteristic	Overall, *n* = 133	Mild, *n* = 95	Moderately severe, *n* = 21	Severe, *n* = 17	*P* value
Demographics					
Male, %	86 (64.7)	56 (58.9)	16 (76.2)	14 (82.4)	0.086
Age, yr	65 (54.0-76.0)	65 (54.0-76.0)	68 (40.5-72.5)	59 (43.0-82.0)	0.860
Comorbidities					
CHF, %	19 (17.4)	16 (18.8)	3 (18.8)	0 (0)	0.402
COPD, %	3 (2.8)	2 (2.4)	0 (0)	1 (12.5)	0.188
Diabetes, %	25 (22.9)	20 (23.5)	3 (18.8)	2 (25.0)	0.907
Immunosuppression, %	8 (7.3)	7 (8.2)	0 (0)	1 (12.5)	0.432
Etiology					0.003
Gallstones, %	84 (63.2)	65 (68.4)	12 (57.1)	7 (41.2)	
Hypertryglyceridemia, %	12 (9.0)	9 (9.5)	0 (0)	3 (17.6)	
Alcohol, %	4 (3.0)	2 (2.1)	2 (9.5)	0 (0)	
Post-ERCP, %	15 (11.3)	13 (13.7)	1 (4.8)	1 (5.9)	
Idiopathic, %	18 (13.5)	6 (6.3)	6 (28.6)	6 (35.3)	
Scoring					
BISAP score at admission	2.0 (1.0-2.0)	1.0 (1.0-2.0)	2.0 (2.0-3.0)	3.0 (2.0-3.0)	< 0.001
Ranson score at 48 h	2.0 (1.0-4.0)	2.0 (1.0-3.0)	3.0 (2.0-5.5)	4.0 (3.5-6.5)	< 0.001
CTSI score	4.0 (2.0-4.0)	2.0 (2.0-4.0)	4.0 (2.0-6.0)	4.0 (4.0-5.0)	0.002
APACHE II score at admission	8.0 (5.0-12.5)	7.0 (3.0-10.0)	9.0 (6.0-15.0)	18.0 (9.0-19.0)	< 0.001
Imaging					
Pancreatic necrosis, %	14 (10.5)	5 (5.3)	6 (28.6)	3 (17.6)	0.013
Mechanical ventilation, %	3 (2.3)	0 (0)	0 (0)	3 (17.6)	< 0.001
CRRT, %	1 (0.8)	0 (0)	0 (0)	1 (5.9)	0.027
Length of hospital stay in d	11.74 ± 5.21	11.08 ± 3.73	13.24 ± 8.40	13.59 ± 6.72	0.067
Outcomes					
Single organ failure, %	30 (22.6)	0 (0)	20 (95.2)	10 (58.8)	< 0.001
Multiple organ failure, %	8 (6.0)	0 (0)	1 (4.8)	7 (41.2)	< 0.001
28-d deaths, %	7 (5.3)	0 (0)	0 (0)	7 (41.2)	< 0.001
Cost in $	5276.14 (3265.34-7739.10)	4482.18 (3127.06-6493.38)	7242.67 (3356.87-8785.31)	11222.04 (7457.31-23045.12)	< 0.001

Data are presented as mean ± SD, *n* (%), or median (25th-75th percentile). CHF: Chronic heart failure; COPD: Chronic obstructive pulmonary disease; BISAP: Bedside index of severity in acute pancreatitis; CTSI: Computed tomography severity index; APACHE: Acute physiology and chronic health evaluation; CRRT: Continuous renal replacement therapy; ERCP: Endoscopic retrograde cholangiopancreatography.

Moreover, presepsin concentration remained significantly higher in the non-mild group compared to the mild group at days 3, 5 and 7 (Figure 1C). The concentrations of presepsin through the 7 d increased progressively with the number of organs failing as defined by the Marshall score (Figure 1D).

Independent predictors of severity of AP
Compared to the mild group, the proportion of patients with biliary etiology in the non-mild group was significantly less (69.4% *vs* 45.7%; *P* = 0.013) and those with idiopathic AP was significantly higher (6.1% *vs* 34.3%; *P* < 0.001). The median presepsin concentration on day 1 in patients with biliary AP was higher compared to those with other etiologies [1154.00 (728.75-2108.50) *vs* 749.00 (474.00-1174.00); *P* = 0.001]. The presepsin concentration on day 1 and etiology were independent predictive factors for non-mild AP on day 1 (Table 2). The presepsin concentrations on days 3, 5 and 7, but not etiology, were

Table 2 Independent factors for time-specific prediction of non-mild (moderately severe and severe) acute pancreatitis

Variable	β	Standard error	Wald statistic	Degrees of freedom	*P* value	Odds ratio	95%CI	
							Lower limit	Upper limit
Non-mild AP day 1								
Etiology	0.456	0.133	11.707	1	0.001	1.578	1.215	2.050
Presepsin day 1	0.000	0.000	5.872	1	0.015	1.001	1.000	1.001
Non-mild AP day 3								
Etiology	0.259	0.178	2.115	1	0.146	1.296	0.914	1.836
Presepsin day 3	0.001	0.000	8.567	1	0.003	1.001	1.000	1.001
Non-mild AP day 5								
Etiology	0.315	0.199	2.502	1	0.114	1.371	0.927	2.026
Presepsin day 5	0.002	0.000	13.141	1	< 0.001	1.002	1.001	1.003
Non-mild AP day 7								
Etiology	0.292	0.215	1.836	1	0.175	1.339	0.878	2.041
Presepsin day 7	0.002	0.000	13.203	1	< 0.001	1.002	1.001	1.003

AP: Acute pancreatitis.

independent predictive factors for non-mild AP on days 3, 5 and 7, respectively (Table 2). Presepsin concentration showed time-specific AUCs of 0.827, 0.848 and 0.867 on days 3, 5 and 7, respectively, in predicting moderately severe and severe AP (Table 3).

Correlation of presepsin concentration with scoring systems and other biomarkers

The Spearman correlation analysis revealed that the presepsin levels through day 7 in AP patients positively correlated with BISAP and Ranson scores (all *P* < 0.05, Figure 2). Positive correlations were also observed between the presepsin concentration on days 5 and 7 with the APACHE II scores. Presepsin levels at days 3, 5 and 7 also positively correlated with CTSI and Marshall scores (all *P* < 0.05, Figure 2). There was a positive correlation between presepsin and procalcitonin levels on days 1 and 3 and between presepsin and C-reactive protein levels on days 3 and 7 (Table 4).

Dynamic changes in presepsin concentrations and clearance rates in survivors and non-survivors

Presepsin levels decreased persistently through the first 7 d after admission in survivors but tended to decrease on day 3 and then increase on day 5 in non-survivors. The presepsin concentration in non-survivors on days 3, 5 and 7 were significantly higher when compared with survivors (Figure 3A). Moreover, the median clearance rate of presepsin on day 3 in the survivors was higher than that in the non-survivors (Figure 3B; *P* < 0.01).

Presepsin concentration for predicting 28-d mortality in patients with AP

The clinical characteristics between survival and non-survival groups are presented in Table 5. The binary logistic regression analysis showed that the presepsin levels on days 3, 5 and 7 and the BISAP, Ranson and APACHE II scores were independent predictors of 28-d mortality in patients with AP (Table 6). The AUC of presepsin for predicting 28-d mortality in AP patients was 0.781 on day 3, 0.846 on day 5 and 0.843 on day 7, which were slightly lower compared to APACHE II (0.955; all *P* > 0.05) and Ranson (0.900; all *P* > 0.05) scores but similar to BISAP (0.811; all *P* > 0.05) scores (Figure 4). The optimal prognostic cutoff values for predicting 28-d mortality on days 3, 5 and 7 were 681.5 pg/mL, 613 pg/mL and 770 pg/mL of presepsin, respectively.

Using the cutoff values determined by ROC curves, the Cox proportional hazards regression model was adjusted for age, sex and etiology to analyze the 28-d survival curves of patients (Figure 5). The hazard ratio (HR) of presepsin at day 3 was 9.475 (95%CI: 1.133-79.226; *P* = 0.038), the HR of presepsin at day 5 was 11.191 (95%CI: 1.297-96.518; *P* = 0.028), and the HR of presepsin at day 7 was 16.495 (95%CI: 2.759-98.615; *P* = 0.002).

Table 3 Time-specific area under the receiver operating characteristic curve of presepsin for prediction of moderately severe and severe acute pancreatitis

Time point	Cutoff (pg/mL)	Sensitivity	Specificity	PPV	NPV	AUROC (95%CI)	*P* value
Day 3	657.5	92.9%	71.4%	76.5%	90.9%	0.827 (0.730-0.923)	< 0.001
Day 5	593.5	84.6%	80.4%	81.2%	83.9%	0.848 (0.751-0.945)	< 0.001
Day 7	601.5	72.7%	89.8%	87.7%	76.7%	0.867 (0.756-0.977)	< 0.001

AUROC: Area under the receiver operating characteristic curve; NPV: Negative predictive value; PPV: Positive predictive value.

Table 4 Correlation between presepsin and procalcitonin or C-reactive protein levels

Variables	Procalcitonin	C-reactive protein
Presepsin day 1	$r = 0.464$	$r = 0.179$
	$P < 0.001$	$P = 0.080$
Presepsin day 3	$r = 0.318$	$r = 0.254$
	$P = 0.002$	$P = 0.016$
Presepsin day 5	$r = 0.208$	$r = 0.183$
	$P = 0.084$	$P = 0.091$
Presepsin day 7	$r = 0.239$	$r = 0.312$
	$P = 0.053$	$P = 0.007$

DISCUSSION

The current findings demonstrated that blood presepsin levels correlated with the severity of AP, and the clearance rate of presepsin was lower in patients with moderately severe or severe AP compared to patients with mild AP. Furthermore, the presepsin levels on days 1, 3, 5 and 7 during the hospital stay independently predicted the severity of AP. High levels of presepsin through the first 7 d after admission were associated with organ failure. It was also found that presepsin positively correlated with the BISAP, Ranson, CTSI, APACHE II, and Marshall scores as well as conventional biomarkers such as procalcitonin and C-reactive protein. Dynamic changes in the concentration of presepsin can be used for ongoing risk stratification of disease course and prediction of 28-d mortality in AP patients. Both presepsin and the clearance rate of presepsin on day 3 may be used as early biomarkers to predict the severity and prognosis of AP.

Recently, the blood presepsin concentration has been shown to be an early biomarker of various infections[14,15] as well as a valuable biomarker for diagnosing the occurrence[16], severity[17] or prognosis[7] of sepsis. Presepsin levels were shown to have good diagnostic and prognostic value for bacterial community-acquired pneumonia (CAP) and intensive care unit (ICU) mortality[18]. Similarly, our previous study showed that presepsin could predict acute respiratory distress syndrome, severe CAP, and 28-d mortality[19]. Recently, Yao *et al*[20] found that presepsin has a better predictive ability than existing biomarkers for bacterial infection following major hepato-biliary-pancreatic surgery. The study of Hiraki *et al*[21] showed that a higher concentration of presepsin in the drainage fluid was an independent predictive marker for clinically relevant postoperative pancreatic fistula after pancreaticoduodenectomy.

For noninfectious diseases, presepsin correlates with the disease activity of autoimmune diseases, such as systemic lupus erythematosus[22]. Higher presepsin levels are associated with renal and liver dysfunction[10]. Presepsin is a 13 kDa peptide that may be cleared by the kidney[6]. Presepsin levels have been shown to increase as the glomerular filtration rate (GFR) decreases and are markedly high in patients with chronic renal failure or receiving hemodialysis[23]. Presepsin concentrations correlate with serum creatinine and GFR levels in patients with chronic kidney disease[24]. Recently, presepsin was found to be a predictor of acute kidney injury and initiation of renal replacement therapy in sepsis patients[25]. Masson *et al*[10] found that presepsin levels are significantly higher in septic patients with shock than those without shock. A gender- and age-matched study on patients with severe AP and healthy volunteers showed that presepsin was an independent predictor of local complications, organ failure and in-hospital mortality[26].

In this study, we observed the dynamic changes of plasma presepsin levels and clearance rate of presepsin with time in patients with mild, moderate and severe AP and found that the presepsin

Table 5 Comparison of clinical characteristics between survival and non-survival groups

Characteristic	28-d survival outcome		P value
	Survival (*n* = 126)	Non-survival (*n* = 7)	
Demographics			
Male, %	79 (62.7)	7 (100.0)	0.051
Age, yr	65 (54-75)	75 (54-82)	0.417
Comorbidities			
CHF, %	19 (18.1)	0 (0)	1.000
COPD, %	2 (1.9)	1 (25.0)	0.107
Diabetes, %	24 (22.9)	1 (25.0)	1.000
Immunosuppression, %	7 (6.7)	1 (25.0)	0.266
Etiology			0.634
Gallstones, %	80 (63.5)	4 (57.1)	
Hypertryglyceridemia, %	11 (8.7)	1 (14.3)	
Alcohol, %	4 (3.2)	0 (0.0)	
Post-ERCP, %	15 (11.9)	0 (0.0)	
Idiopathic, %	16 (12.7)	2 (28.6)	
Scoring			
BISAP score at admission	1.0 (1.0-2.0)	3.0 (2.0-4.0)	0.003
Ranson score at 48 h	2.0 (1.0-3.0)	5.0 (4.0-8.0)	< 0.001
CTSI score	2.0 (2.0-4.0)	4.0 (4.0-4.0)	0.181
APACHE II score at admission	8.0 (4.8-11.0)	19.0 (15.0-31.0)	< 0.001
Imaging			
Pancreatic necrosis, %	13 (10.3)	1 (14.3)	0.550
Mechanical ventilation, %	0 (0.0)	3 (42.9)	< 0.001
CRRT, %	0 (0.0)	1 (14.3)	0.053
Length of hospital stay in d	11 (9-14)	13 (5-21)	0.568
Outcomes			
Single organ failure, %	27 (22.1)	3 (100.0)	0.013
Multiple organ failure, %	4 (4.0)	4 (100.0)	< 0.001
Cost in $	4718.99 (3065.47-7104.78)	22243.29 (10432.63-36309.99)	0.001

Data are presented as *n* (%), or median (25th-75th percentile). CHF: Chronic heart failure; COPD: Chronic obstructive pulmonary disease; ERCP: Endoscopic retrograde cholangiopancreatography; BISAP: Bedside index of severity in acute pancreatitis; CTSI: Computed tomography severity index; APACHE: Acute physiology and chronic health evaluation; CRRT: Continuous renal replacement therapy.

concentrations on days 3, 5 and 7 (but not day 1) increased with the severity of AP. A high presepsin value and low clearance rate of presepsin at day 3 were found to be more valuable in early identification of mild or moderate *vs* severe compared to mild *vs* moderate disease. Inconsistently, the concentrations of presepsin on day 1 through 7 increased significantly with the number of organs experiencing failure.

In most high-income countries, gallstones (45%) and alcohol abuse (20%) are the most frequent causes of AP[27]. In the current study, gallstones (63.2%), but not alcohol (3.0%), was the most common etiology of AP, which is consistent with the conclusion of an 8-year Chinese study by Zhu *et al*[28]. Upon multivariate analysis, after adjusting for the confounding factor of etiology, it was found that presepsin levels were independent predictors for the severity of AP on days 1, 3, 5 and 7. In this study, the proportion of patients with biliary etiology were significantly less, and those with idiopathic AP were significantly higher in the moderately severe or severe AP group compared to the mild AP group. It was shown that the presepsin values on day 1, but not on days 3, 5 or 7, were higher in patients with biliary AP than in other etiologies, which is in line with the procalcitonin values of the study of Modrau

Table 6 Independent factors for the prediction of 28-d mortality in patients with acute pancreatitis

Variable	β	Standard error	Wald statistic	Degrees of freedom	*P* value	Odds ratio	95%CI	
							Lower limit	Upper limit
Presepsin day 3	0.001	0.000	5.013	1	0.025	1.001	1.000	1.001
Presepsin day 5	0.002	0.000	11.406	1	0.001	1.002	1.001	1.003
Presepsin day 7	0.002	0.001	11.672	1	0.001	1.002	1.001	1.003
BISAP score at admission	1.217	0.390	9.700	1	0.002	3.376	1.571	7.255
Ranson score at 48 h	0.868	0.249	12.202	1	< 0.001	2.383	1.464	3.880
APACHE II score at admission	0.477	0.166	8.251	1	0.004	1.611	1.164	2.230

BISAP: Bedside index of severity in acute pancreatitis; APACHE: Acute physiology and chronic health evaluation.

DOI: 10.3748/wjg.v28.i35.5203 **Copyright** ©The Author(s) 2022.
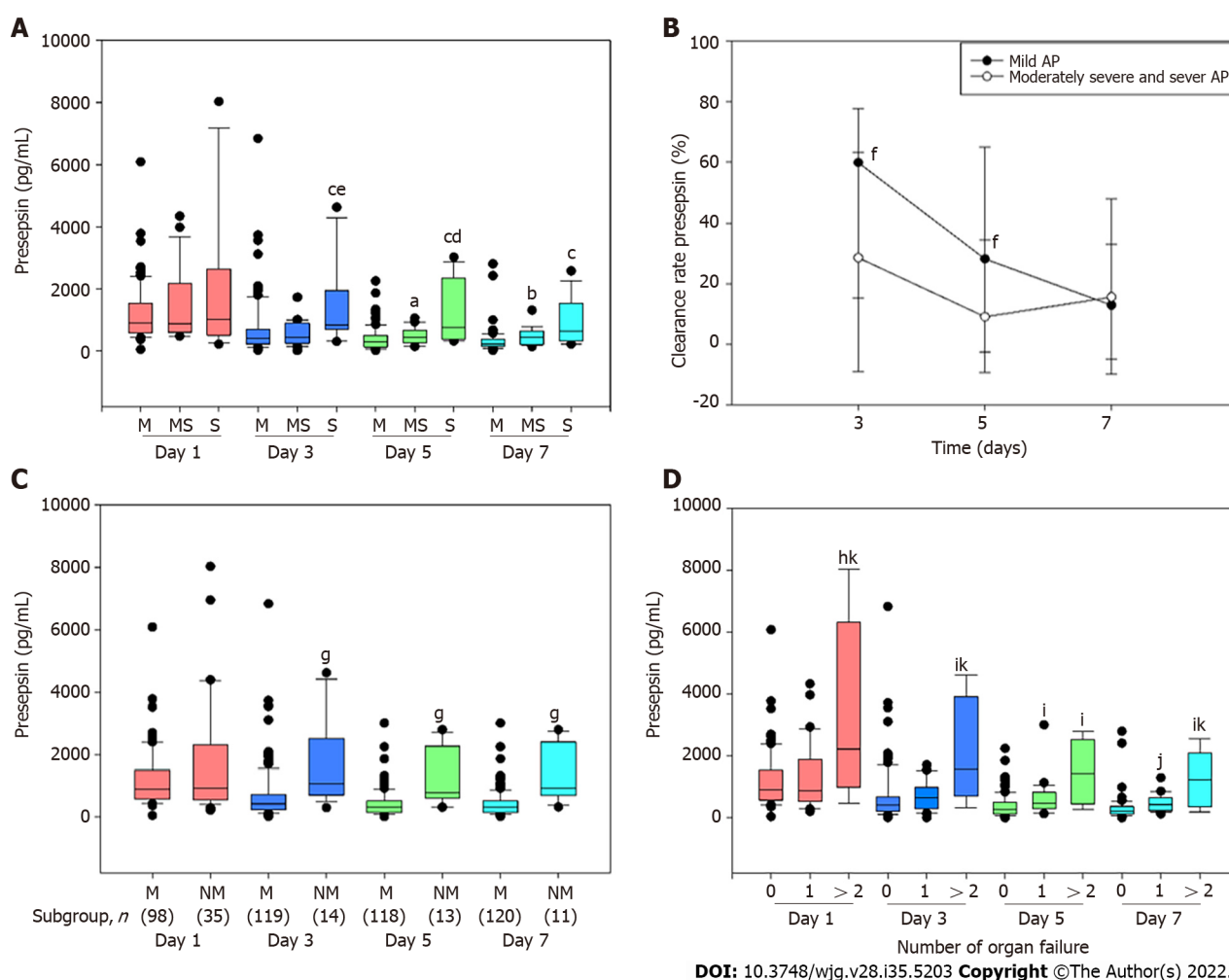
Figure 1 Association between dynamic blood presepsin levels and severity of acute pancreatitis. A: Presepsin levels on days 1, 3, 5 and 7 after admission in mild (M), moderately severe (MS) and severe (S) acute pancreatitis (AP). [a]$P < 0.05$ *vs* M AP; [b]$P < 0.01$ *vs* M AP; [c]$P < 0.001$ *vs* M AP; [d]$P < 0.05$ *vs* MS AP; [e]$P < 0.01$ *vs* MS AP; B: Clearance rate of presepsin in patients with M and non-mild (NM) (MS and S) AP; [f]$P < 0.05$ *vs* MS and S AP; C: Time-specific concentrations of presepsin in patients with M and NM AP; [g]$P < 0.001$ *vs* M AP; D: Correlation between presepsin and organ failure in patients with AP. [h]$P < 0.05$ *vs* no organ failure; [i]$P < 0.01$ *vs* no organ failure; [j]$P < 0.001$ *vs* no organ failure; [k]$P < 0.05$ *vs* 1 organ failure. Lines denote median values, boxes represent 25th to 75th percentiles, and whiskers indicate the range.

et al[29]. It is likely that the increase in circulating presepsin found in the present study was associated with organ dysfunction and biliary tract infection, though infectious complications are rare during the early course of severe AP[30].

DOI: 10.3748/wjg.v28.i35.5203 **Copyright** ©The Author(s) 2022.
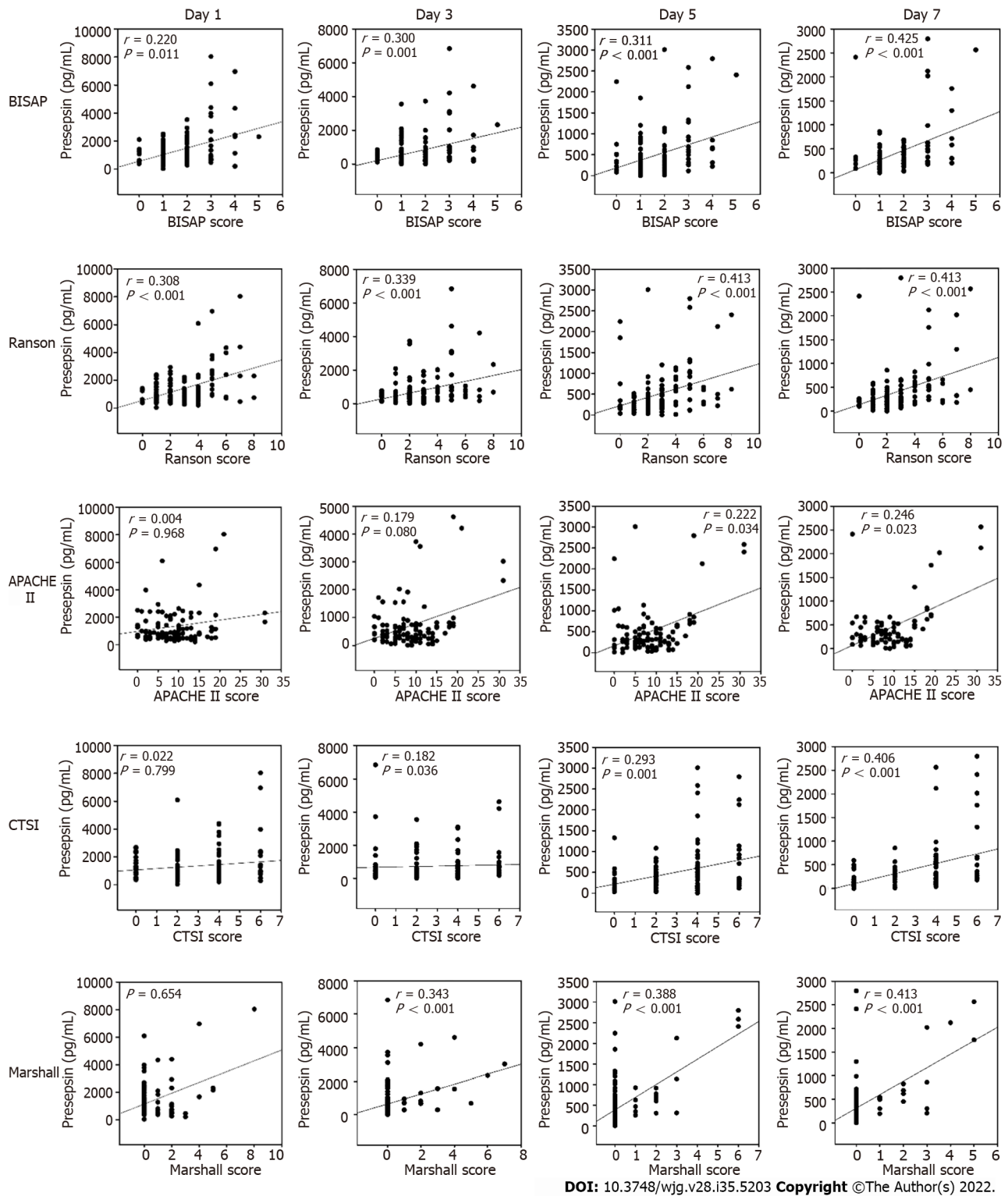
Figure 2 Correlation between presepsin and bedside index of severity in acute pancreatitis, Ranson, acute physiology and chronic health evaluation-II, computed tomography severity index and Marshall scores. BISAP: Bedside index of severity in acute pancreatitis; APACHE: Acute physiology and chronic health evaluation; CTSI: Computed tomography severity index.

Procalcitonin is a sensitive biomarker for the detection of pancreatic infection, and C-reactive protein levels ≥ 150 mg/L at day 3 is a prognostic indicator for severe AP[13]. The current study illustrated that presepsin levels were positively correlated with procalcitonin levels on days 1 and 3 and with C-reactive protein levels on days 3 and 7. There was a positive correlation between the presepsin levels and Marshall scores (including respiratory function, cardiovascular system, renal dysfunction) on days 3, 5 and 7. Meanwhile, the current study found a significant positive correlation between the presepsin levels and other AP scores, such as BISAP, Ranson and APACHE II. In this study, increased presepsin levels were found to be an accurate predictor of disease severity. For the prediction of moderately
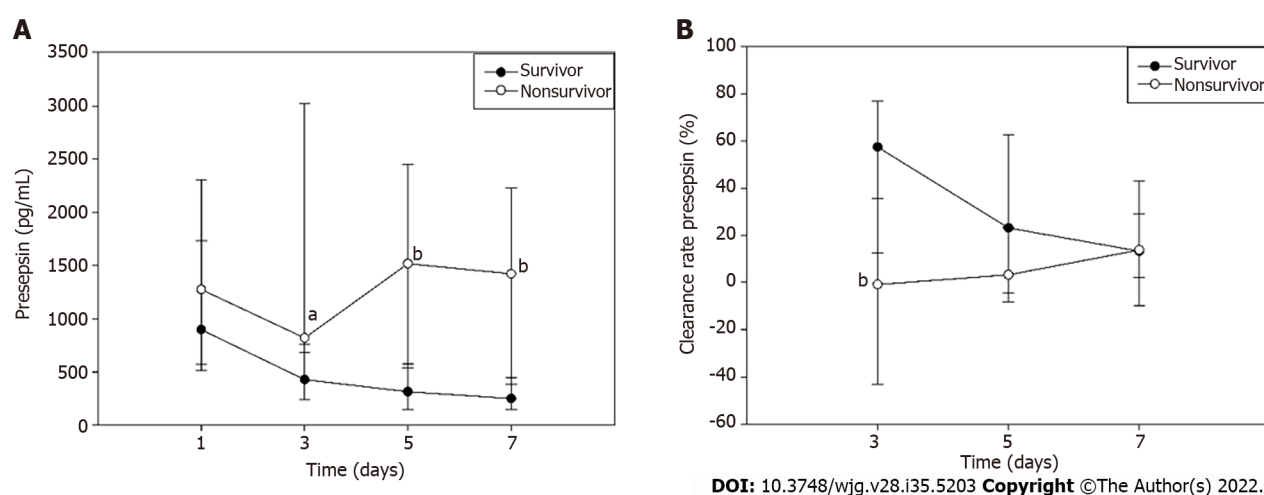
Figure 3 Dynamic changes in presepsin concentration and clearance rate in survivors and non-survivors. A: Presepsin concentration; B: Clearance rate. [a]$P < 0.05$ *vs* survivors; [b]$P < 0.01$ *vs* survivors.

DOI: 10.3748/wjg.v28.i35.5203 **Copyright** ©The Author(s) 2022.
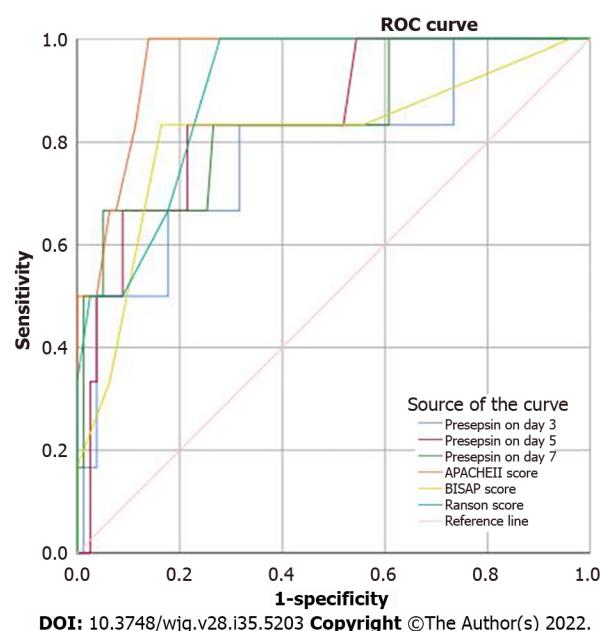
Figure 4 Receiver operating characteristic curves of presepsin, acute physiology and chronic health evaluation-II, index of severity in acute pancreatitis and Ranson scores for 28-d mortality of patients with acute pancreatitis. ROC: Receiver operating characteristic; APACHE: Acute physiology and chronic health evaluation; BISAP: Bedside index of severity in acute pancreatitis.

severe or severe AP, the AUCs of presepsin on days 3, 5 and 7 were 0.827, 0.848 and 0.867, respectively, with high sensitivity and specificity.

The dynamic changes in presepsin were different in survivors and non-survivors of this study. In survivors, presepsin levels showed a decreasing trend over time but in non-survivors presepsin levels first decreased and then increased. Similar trends in presepsin levels have been reported in patients with severe sepsis[31]. In addition, clearance rates of presepsin in non-survivors were lower than that of survivors in the early stage of AP (day 3). Potential explanations involve a reduced clearance of presepsin due to reduced kidney function[22-24] and circulatory dysfunction[10]. The most common organ systems to fail in non-survivors were circulatory [71.4% (5/7 patients)], respiratory [85.7% (6/7 patients)] and renal [42.8% (3/7 patients)] systems. Studies have showed that higher presepsin levels were associated with ICU death and mortality in sepsis[7], CAP[18], cardiac arrest patients after return of spontaneous circulation[32] and severe AP[25]. Interestingly, the presepsin levels on days 3, 5,and 7 were found to independently predict 28-d mortality in AP.

This study has certain limitations. First, the patient population was heterogeneous. Second, the study did not compare presepsin with other biomarkers. Third, the relevance of presepsin during the latter course of AP was not studied. Fourth, the association between presepsin levels and hepatorenal

DOI: 10.3748/wjg.v28.i35.5203 **Copyright** ©The Author(s) 2022.
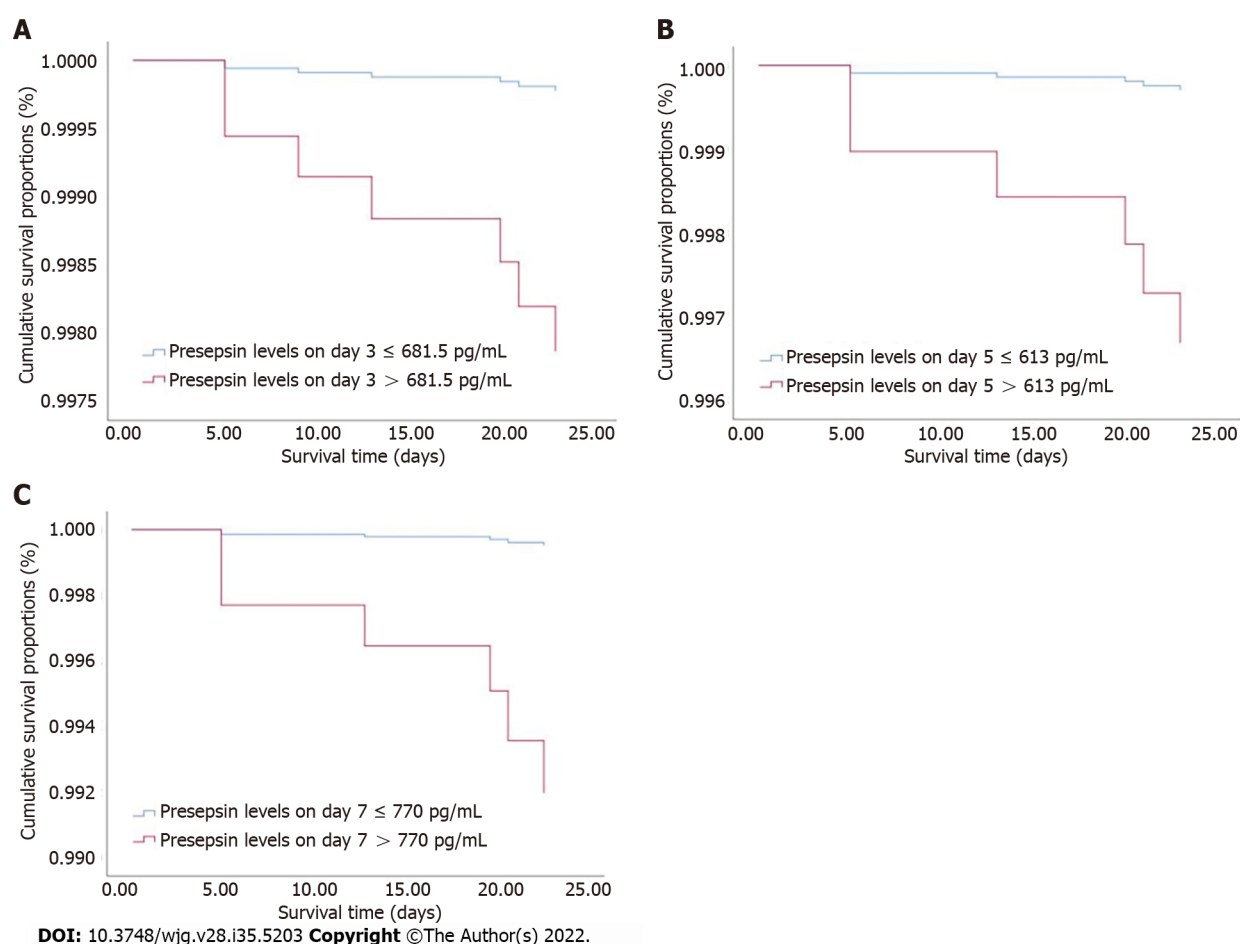
Figure 5 Cox regression survival curves. A: Acute pancreatitis (AP) patients with presepsin levels higher than 681.5 pg/mL on day 3 had a lower probability of survival at 28 d compared to patients with lower levels; B and C: Similarly, AP patients with presepsin levels on day 5 (B) and day 7 (C) higher than 613 pg/mL and 770 pg/mL, respectively, had a lower probability of survival at 28 d than patients with lower levels. AP: acute pancreatitis.

function was not evaluated. Future multicentric studies with larger cohorts that consider these factors should be conducted to validate the findings of this study.

CONCLUSION

This cohort study found that blood presepsin levels in the first 7 d after admission could accurately predict the severity of disease course and 28-d mortality in patients with AP and may be a promising prognostic marker.

ARTICLE HIGHLIGHTS

Research background

Acute pancreatitis (AP) is one of the most common causes of abdominal emergencies and is associated with sepsis, organ failure and high mortality rates (up to 35%). AP has diverse clinical manifestations with an unpredictable clinical course. It is necessary to predict the severity of AP rapidly and accurately.

Research motivation

A major challenge in AP is the early identification of patients at high-risk for organ failure and death. However, scoring systems are complicated and time consuming with limited predictive value for the clinical course. Biomarkers are promising for the dynamic prediction of disease severity.

Research objectives

To determine whether the dynamic levels of an emerging biomarker, presepsin, can be used to evaluate the severity of disease course and outcome of AP.

Research methods
In this prospective and multicentric cohort study, 133 patients with AP were included from January 2018 to September 2019. Clinical severity (mild, moderately severe and severe AP) was dynamically evaluated using the 2012 revised Atlanta Classification. Blood presepsin levels were measured at days 1, 3, 5 and 7 after admission by chemiluminescent enzyme immunoassay. The patients were followed up for 28 d.

Research results
The median concentration of presepsin increased, and the clearance rate of presepsin decreased with disease severity and organ failure in AP patients. The presepsin levels on days 3, 5 and 7 were independent predictors of moderately severe and severe AP with time-specific area under the curve (AUC) values of 0.827, 0.848 and 0.867, respectively. The presepsin levels positively correlated with bedside index of severity in acute pancreatitis, Ranson, acute physiology and chronic health evaluation-II, computed tomography severity index and Marshall scores and conventional biomarkers such as procalcitonin and C-reactive protein. Presepsin levels on days 3, 5 and 7 were independent predictors of 28-d mortality of AP patients with AUC values of 0.781, 0.846 and 0.843, respectively.

Research conclusions
The blood presepsin levels within 7 d of admission were associated with and may be useful to dynamically predict the severity of disease course and 28-d mortality in AP patients. Both presepsin and clearance rate of presepsin on day 3 may be used as early biomarkers to predict the severity and prognosis of AP.

Research perspectives
Prospective cohort studies report the predictive value of presepsin in the severity of AP. Future research should focus on the guiding significance of presepsin in the treatment of AP, such as antibiotic use.

Country/Territory of origin: China

ORCID number: Hong-Li Xiao 0000-0002-7353-114X; Guo-Xing Wang 0000-0003-1379-5749; Yan Wang 0000-0002-7950-8696; Zhi-Min Tan 0000-0002-8731-4293; Jie Zhou 0000-0003-1298-6789; Han Yu 0000-0002-0529-7152; Miao-Rong Xie 0000-0003-2479-9470; Chun-Sheng Li 0000-0002-3161-4457.

REFERENCES

1   **van Santvoort HC**, Bakker OJ, Bollen TL, Besselink MG, Ahmed Ali U, Schrijver AM, Boermeester MA, van Goor H, Dejong CH, van Eijck CH, van Ramshorst B, Schaapherder AF, van der Harst E, Hofker S, Nieuwenhuijs VB, Brink MA, Kruyt PM, Manusama ER, van der Schelling GP, Karsten T, Hesselink EJ, van Laarhoven CJ, Rosman C, Bosscha K, de Wit RJ, Houdijk AP, Cuesta MA, Wahab PJ, Gooszen HG; Dutch Pancreatitis Study Group. A conservative and minimally invasive approach to necrotizing pancreatitis improves outcome. *Gastroenterology* 2011; **141**: 1254-1263 [PMID: 21741922 DOI: 10.1053/j.gastro.2011.06.073]

2   **van Dijk SM**, Hallensleben NDL, van Santvoort HC, Fockens P, van Goor H, Bruno MJ, Besselink MG; Dutch Pancreatitis Study Group. Acute pancreatitis: recent advances through randomised trials. *Gut* 2017; **66**: 2024-2032 [PMID: 28838972 DOI: 10.1136/gutjnl-2016-313595]

3   **Harshit Kumar A**, Singh Griwan M. A comparison of APACHE II, BISAP, Ranson's score and modified CTSI in predicting the severity of acute pancreatitis based on the 2012 revised Atlanta Classification. *Gastroenterol Rep (Oxf)* 2018; **6**: 127-131 [PMID: 29780601 DOI: 10.1093/gastro/gox029]

4   **Zerem E**. Treatment of severe acute pancreatitis and its complications. *World J Gastroenterol* 2014; **20**: 13879-13892 [PMID: 25320523 DOI: 10.3748/wjg.v20.i38.13879]

5   **Shirakawa K**, Naitou K, Hirose J, Takahashi T, Furusako S. Presepsin (sCD14-ST): development and evaluation of one-step ELISA with a new standard that is similar to the form of presepsin in septic patients. *Clin Chem Lab Med* 2011; **49**: 937-939 [PMID: 21345045 DOI: 10.1515/CCLM.2011.145]

6   **Ackland GL**, Prowle JR. Presepsin: solving a soluble (CD14) problem in sepsis? *Intensive Care Med* 2015; **41**: 351-353 [PMID: 25608923 DOI: 10.1007/s00134-014-3642-8]

7   **Liu B**, Chen YX, Yin Q, Zhao YZ, Li CS. Diagnostic value and prognostic evaluation of Presepsin for sepsis in an emergency department. *Crit Care* 2013; **17**: R244 [PMID: 24138799 DOI: 10.1186/cc13070]

8   **Nakamura Y**, Ishikura H, Nishida T, Kawano Y, Yuge R, Ichiki R, Murai A. Usefulness of presepsin in the diagnosis of sepsis in patients with or without acute kidney injury. *BMC Anesthesiol* 2014; **14**: 88 [PMID: 25309126 DOI: 10.1186/1471-2253-14-88]

9   **Kerr KF**, Wang Z, Janes H, McClelland RL, Psaty BM, Pepe MS. Net reclassification indices for evaluating risk prediction instruments: a critical review. *Epidemiology* 2014; **25**: 114-121 [PMID: 24240655 DOI: 10.1097/EDE.0000000000000018]

10   **Masson S**, Caironi P, Fanizza C, Thomae R, Bernasconi R, Noto A, Oggioni R, Pasetti GS, Romero M, Tognoni G, Latini R, Gattinoni L. Circulating presepsin (soluble CD14 subtype) as a marker of host response in patients with severe sepsis or septic shock: data from the multicenter, randomized ALBIOS trial. *Intensive Care Med* 2015; **41**: 12-20 [PMID: 25319385 DOI: 10.1007/s00134-014-3514-2]

11   **Banks PA**, Bollen TL, Dervenis C, Gooszen HG, Johnson CD, Sarr MG, Tsiotos GG, Vege SS; Acute Pancreatitis Classification Working Group. Classification of acute pancreatitis--2012: revision of the Atlanta classification and definitions by international consensus. *Gut* 2013; **62**: 102-111 [PMID: 23100216 DOI: 10.1136/gutjnl-2012-302779]

12   **Okamura Y**, Yokoi H. Development of a point-of-care assay system for measurement of presepsin (sCD14-ST). *Clin Chim Acta* 2011; **412**: 2157-2161 [PMID: 21839732 DOI: 10.1016/j.cca.2011.07.024]

13   **Leppäniemi A**, Tolonen M, Tarasconi A, Segovia-Lohse H, Gamberini E, Kirkpatrick AW, Ball CG, Parry N, Sartelli M, Wolbrink D, van Goor H, Baiocchi G, Ansaloni L, Biffl W, Coccolini F, Di Saverio S, Kluger Y, Moore E, Catena F. 2019 WSES guidelines for the management of severe acute pancreatitis. *World J Emerg Surg* 2019; **14**: 27 [PMID: 31210778 DOI: 10.1186/s13017-019-0247-0]

14   **Marazzi MG**, Randelli F, Brioschi M, Drago L, Romanò CL, Banfi G, Massaccesi L, Crapanzano C, Morelli F, Corsi Romanelli MM, Galliera E. Presepsin: A potential biomarker of PJI? *Int J Immunopathol Pharmacol* 2018; **31**: 394632017749356 [PMID: 29251000 DOI: 10.1177/0394632017749356]

15   **Chenevier-Gobeaux C**, Borderie D, Weiss N, Mallet-Coste T, Claessens YE. Presepsin (sCD14-ST), an innate immune response marker in sepsis. *Clin Chim Acta* 2015; **450**: 97-103 [PMID: 26164388 DOI: 10.1016/j.cca.2015.06.026]

16   **Kweon OJ**, Choi JH, Park SK, Park AJ. Usefulness of presepsin (sCD14 subtype) measurements as a new marker for the diagnosis and prediction of disease severity of sepsis in the Korean population. *J Crit Care* 2014; **29**: 965-970 [PMID: 25042676 DOI: 10.1016/j.jcrc.2014.06.014]

17   **Behnes M**, Bertsch T, Lepiorz D, Lang S, Trinkmann F, Brueckmann M, Borggrefe M, Hoffmann U. Diagnostic and prognostic utility of soluble CD 14 subtype (presepsin) for severe sepsis and septic shock during the first week of intensive care treatment. *Crit Care* 2014; **18**: 507 [PMID: 25190134 DOI: 10.1186/s13054-014-0507-z]

18   **Klouche K**, Cristol JP, Devin J, Gilles V, Kuster N, Larcher R, Amigues L, Corne P, Jonquet O, Dupuy AM. Diagnostic and prognostic value of soluble CD14 subtype (Presepsin) for sepsis and community-acquired pneumonia in ICU patients. *Ann Intensive Care* 2016; **6**: 59 [PMID: 27389015 DOI: 10.1186/s13613-016-0160-6]

19   **Liu B**, Yin Q, Chen YX, Zhao YZ, Li CS. Role of Presepsin (sCD14-ST) and the CURB65 scoring system in predicting

severity and outcome of community-acquired pneumonia in an emergency department. *Respir Med* 2014; **108**: 1204-1213 [PMID: 24931899 DOI: 10.1016/j.rmed.2014.05.005]

20   **Yao S**, Kaido T, Uozumi R, Hirata M, Iwamura S, Miyachi Y, Macshut M, Sharshar M, Yagi S, Uemoto S. Diagnostic potential of presepsin in bacterial infection following hepato-biliary-pancreatic surgery: A prospective observational study. *J Hepatobiliary Pancreat Sci* 2020; **27**: 756-766 [PMID: 32654388 DOI: 10.1002/jhbp.802]

21   **Hiraki M**, Miyoshi A, Sadashima E, Shinkai Y, Yasunami M, Manabe T, Kitahara K, Noshiro H. The novel early predictive marker presepsin for postoperative pancreatic fistula: A pilot study. *Exp Ther Med* 2020; **20**: 2298-2304 [PMID: 32765708 DOI: 10.3892/etm.2020.8919]

22   **Tanimura S**, Fujieda Y, Kono M, Shibata Y, Hisada R, Sugawara E, Nakamura H, Ohmura K, Shimamura S, Mitani A, Shida H, Watanabe T, Kato M, Oku K, Bohgaki T, Amengual O, Yasuda S, Shimizu C, Atsumi T. Clinical significance of plasma presepsin levels in patients with systemic lupus erythematosus. *Mod Rheumatol* 2018; **28**: 865-871 [PMID: 29239264 DOI: 10.1080/14397595.2017.1408755]

23   **Nagata T**, Yasuda Y, Ando M, Abe T, Katsuno T, Kato S, Tsuboi N, Matsuo S, Maruyama S. Clinical impact of kidney function on presepsin levels. *PLoS One* 2015; **10**: e0129159 [PMID: 26030716 DOI: 10.1371/journal.pone.0129159]

24   **Miyoshi M**, Inoue Y, Nishioka M, Ikegame A, Nakao T, Kishi S, Doi T, Nagai K. Clinical evaluation of presepsin considering renal function. *PLoS One* 2019; **14**: e0215791 [PMID: 31490935 DOI: 10.1371/journal.pone.0215791]

25   **Shimoyama Y**, Umegaki O, Kadono N, Minami T. Presepsin and prognostic nutritional index are predictors of septic acute kidney injury, renal replacement therapy initiation in sepsis patients, and prognosis in septic acute kidney injury patients: a pilot study. *BMC Nephrol* 2021; **22**: 219 [PMID: 34118899 DOI: 10.1186/s12882-021-02422-x]

26   **Lin J**, Li Z, Zheng Y, Zhang Y, Shao C, Liu G, Li J. Elevated Presepsin Levels are Associated with Severity and Prognosis of Severe Acute Pancreatitis. *Clin Lab* 2016; **62**: 1699-1708 [PMID: 28164588 DOI: 10.7754/Clin.Lab.2016.160134]

27   **Roberts SE**, Morrison-Rees S, John A, Williams JG, Brown TH, Samuel DG. The incidence and aetiology of acute pancreatitis across Europe. *Pancreatology* 2017; **17**: 155-165 [PMID: 28159463 DOI: 10.1016/j.pan.2017.01.005]

28   **Zhu Y**, Pan X, Zeng H, He W, Xia L, Liu P, Zhu Y, Chen Y, Lv N. A Study on the Etiology, Severity, and Mortality of 3260 Patients With Acute Pancreatitis According to the Revised Atlanta Classification in Jiangxi, China Over an 8-Year Period. *Pancreas* 2017; **46**: 504-509 [PMID: 28196012 DOI: 10.1097/MPA.0000000000000776]

29   **Modrau IS**, Floyd AK, Thorlacius-Ussing O. The clinical value of procalcitonin in early assessment of acute pancreatitis. *Am J Gastroenterol* 2005; **100**: 1593-1597 [PMID: 15984987 DOI: 10.1111/j.1572-0241.2005.41456.x]

30   **Beger HG**, Bittner R, Block S, Büchler M. Bacterial contamination of pancreatic necrosis. A prospective clinical study. *Gastroenterology* 1986; **91**: 433-438 [PMID: 3522342 DOI: 10.1016/0016-5085(86)90579-2]

31   **Yu H**, Qi Z, Hang C, Fang Y, Shao R, Li C. Evaluating the value of dynamic procalcitonin and presepsin measurements for patients with severe sepsis. *Am J Emerg Med* 2017; **35**: 835-841 [PMID: 28153679 DOI: 10.1016/j.ajem.2017.01.037]

32   **Qi Z**, Zhang Q, Liu B, Shao F, Li C. Presepsin As a Biomarker for Evaluating Prognosis and Early Innate Immune Response of Out-of-Hospital Cardiac Arrest Patients After Return of Spontaneous Circulation. *Crit Care Med* 2019; **47**: e538-e546 [PMID: 30985453 DOI: 10.1097/CCM.0000000000003764]

ORIGINAL ARTICLE

Prospective Study

High prevalence of chronic viral hepatitis B and C in Minnesota Somalis contributes to rising hepatocellular carcinoma incidence

Essa A Mohamed, Nasra H Giama, Abubaker O Abdalla, Hassan M Shaleh, Abdul M Oseini, Hamdi A Ali, Fowsiyo Ahmed, Wesam Taha, Hager Ahmed Mohammed, Jessica Cvinar, Ibrahim A Waaeys, Hawa Ali, Loretta K Allotey, Abdiwahab O Ali, Safra A Mohamed, William S Harmsen, Eimad M Ahmmad, Numra A Bajwa, Mohamud D Afgarshe, Abdirashid M Shire, Joyce E Balls-Berry, Lewis R Roberts

Essa A Mohamed, Nasra H Giama, Hassan M Shaleh, Abdul M Oseini, Hamdi A Ali, Fowsiyo Ahmed, Wesam Taha, Hager Ahmed Mohammed, Jessica Cvinar, Hawa Ali, Loretta K Allotey, Eimad M Ahmmad, Numra A Bajwa, Abdirashid M Shire, Lewis R Roberts, Division of Gastroenterology and Hepatology, Mayo Clinic, Rochester, MN 55905, United States

Essa A Mohamed, Joyce E Balls-Berry, Center for Clinical and Translational Science, Mayo Clinic, Rochester, MN 55905, United States

Nasra H Giama, School of Nursing, University of Minnesota, Minneapolis, MN 55455, United States

Abubaker O Abdalla, Division of Digestive Diseases, Emory School of Medicine, Atlanta, GA 30322, United States

Hassan M Shaleh, Ibrahim A Waaeys, Abdiwahab O Ali, Safra A Mohamed, Department of Laboratory Medicine and Pathology, Mayo Clinic, Rochester, MN 55905, United States

Wesam Taha, Department of Internal Medicine, NewYork-Presbyterian Queens, Flushing, NY 11355, United States

Hager Ahmed Mohammed, Department of Pediatrics, University of Nevada Las Vegas, Las Vegas, NV 89154, United States

William S Harmsen, Department of Quantitative Health Sciences, Mayo Clinic, Rochester, MN 55905, United States

Mohamud D Afgarshe, Department of Medicine, Gargar Urgent Care and Clinic, Minneapolis, MN 55406, United States

Abdirashid M Shire, Office of the Director, Shire Scientific, Minneapolis, MN 55405, United States

Joyce E Balls-Berry, Department of Neurology, Washington University School of Medicine in St Louis, St Louis, MO 63130, United States

Joyce E Balls-Berry, Knight Alzheimer Disease Research Center, Washington University School of Medicine, St Louis, MO 63130, United States

Corresponding author: Lewis R Roberts, MBChB, PhD, Professor, Division of Gastroenterology and Hepatology, Mayo Clinic Rochester, 200 First Street SW, Rochester, MN 55905, United States. roberts.lewis@mayo.edu

Abstract

BACKGROUND

Chronic hepatitis B virus (HBV) and hepatitis C virus (HCV) infections are known risk factors for liver disease, cirrhosis and hepatocellular carcinoma (HCC). There is substantial global variation in HBV and HCV prevalence resulting in variations in cirrhosis and HCC. We previously reported high prevalence of HBV and HCV infections in Somali immigrants seen at an academic medical center in Minnesota.

AIM

To determine the prevalence of chronic viral hepatitis in Somali immigrants in Minnesota through a community-based screening program.

METHODS

We conducted a prospective community-based participatory research study in the Somali community in Minnesota in partnership with community advisory boards, community clinics and local mosques between November 2010 and December 2015 (data was analyzed in 2020). Serum was tested for hepatitis B surface antigen, hepatitis B core antibody, hepatitis B surface antibody and anti-HCV antibody.

RESULTS

Of 779 participants, 15.4% tested positive for chronic HBV infection, 50.2% for prior exposure to HBV and 7.6% for chronic HCV infection. Calculated age-adjusted frequencies in males and females for chronic HBV were 12.5% and 11.6%; for prior exposure to HBV were 44.8% and 41.3%; and for chronic HCV were 6.7% and 5.7%, respectively. Seven participants developed incident HCC during follow up.

CONCLUSION

Chronic HBV and HCV are major risk factors for liver disease and HCC among Somali immigrants, with prevalence of both infections substantially higher than in the general United States population. Community-based screening is essential for identifying and providing health education and linkage to care for diagnosed patients.

Key Words: Viral hepatitis; Liver disease; Community engagement; African; Immigrant health

Core Tip: This prospective community-based study evaluated the prevalence of chronic hepatitis B and C among the immigrant Somali community. Through community partnerships we were able to demonstrate a framework that can be used with other immigrant and/or minority communities at-risk for infectious diseases such as hepatitis B and C.

INTRODUCTION

Globally, liver cancer ranks 6th in cancer incidence and 4th in cancer mortality[1]. For many years, chronic hepatitis C virus (HCV) infection has been the most common risk factor for hepatocellular carcinoma (HCC) in the United States[2-6]. There is a high prevalence of chronic viral hepatitis in Asia and sub-Saharan Africa[7-11]. Partly due to immigration from high-prevalence countries in Africa and Asia,

hepatitis B virus (HBV) infection remains an important risk factor in the United States[12-15]. Consequently, HCC disproportionately affects individuals of African and Asian ancestry and Hispanic ethnicity[16,17]. Africa has the youngest median [interquartile range (IQR); range] age at HCC diagnosis worldwide [45 (35-57; 8-95)], increasing the burden of years of life lost from chronic viral hepatitis.

Minnesota's foreign-born population constitutes approximately 9% of the state population[18]. From 2008 to 2017, the Minnesota Department of Health reported an age-adjusted incidence rate of liver cancer of 22.4 per 100000 person-years among Black Minnesotans, a 4.3-fold higher rate than the rate of 5.2 per 100000 person-years among white, non-Hispanic Minnesotans[19]. A substantial proportion of Minnesota's Black population are recent African immigrants[18,20-22]. However, due to a general lack of awareness of viral hepatitis, Minnesota's most recent immigrants from Somalia have limited appreciation of their risk from chronic viral hepatitis and its associated complications[23].

To date, few studies have focused on chronic HBV and HCV infection and their sequelae among recent African immigrants to the United States. There is no population-based study of the rates of HBV and HCV infections among Somalis[20,24-28]. We previously conducted a clinic/hospital-based retrospective study of the rates of HBV and/or HCV infections in Somalis seen at Mayo Clinic from July 1996 to October 2009[29]. We found higher frequencies of chronic HBV (13.6%), prior exposure to HBV (55.5%), and chronic HCV (9.1%) in Somali Americans compared to 1.2%, 10.9%, and 2.2% respectively in non-Somali residents of Olmsted County (of whom 90% have European ancestry). Of 30 Somali HCC patients seen, 22 of 29 with available results (76%) were anti-HCV positive, while 5 of 28 with available results (18%) were hepatitis B surface antigen (HBsAg) positive. These results showed high rates of chronic HBV and HCV and revealed that HCV was a primary risk factor for HCC in Somalis[29]. Since clinic/hospital-based studies may overestimate true community disease prevalence, we tested for HBV and HCV in community-resident Somalis through a community-wide screening program.

MATERIALS AND METHODS

Study design
We performed a cross-sectional, community-wide screening study of Somali immigrant adults. Between November 2010 and December 2015, we used a community-based engagement research framework to offer free HBV and HCV screening to Somali immigrant adults living in Minnesota. Eligible individuals who self-identified as: (1) Of Somali descent; (2) ≥ 18 years of age; and (3) Resident in Minnesota received free HBV and HCV serological screening. Screening was provided for both foreign-born and United States-born participants. Study recruitment was carried out in the community. We partnered with three community-based health clinics with large Somali clienteles and faith-based establishments and charter schools, to which participants could come for enrollment and blood draws. In partnership with the Somali Health Advisory Committee (SHAC), a community advisory board based in Rochester and Minneapolis/St Paul, the research team provided educational seminars on viral hepatitis screening and liver disease. In addition, members of SHAC facilitated recruitment through word-of-mouth, advertisements, educational sessions and booths at various community events and health fairs in cities across Minnesota.

Study population
Individuals of Somali heritage who were at least 18 years of age were recruited to participate in the study. Participants provided written informed consent. At the completion of the study, participants received a $20 gift check (remuneration) mailed to their home address. Screening occurred at: (1) The Mayo Clinic Clinical Research and Trials Unit; (2) Community-based clinics; (3) A community-based health center; (4) Religious establishments (*i.e.* mosques); (5) Charter schools; or (6) At various community health-fairs. The study team consented and screened 779 participants aged 18 years to 91 years, of whom 49.9% (389) were male.

Ethical approval
The Mayo Clinic Institutional Review Board approved the study and study related materials including flyers and weekly community outreach program documentation. Study team members conducted outreach field recruitment to inform potential participants about the study in both English and Somali.

Serological tests
Blood samples were processed, stored at -80 °C, and tested for HBsAg, hepatitis B core antibody (HBcAb), hepatitis B surface antibody (HBsAb) and anti-HCV at the Mayo Clinic Department of Laboratory Medicine and Pathology. Participants were administered surveys either in English or in Somali, assessing their age, sex, country of birth, cultural practices and immigration patterns. The screening results were organized into 5 groups depending on the serological test results (Table 1). The first 4 groups defined the hepatitis B infection status, while the fifth reported hepatitis C antibody status. The chronic HBV infected group was defined as those who tested HBsAg positive, HBsAb

Table 1 Antibody and antigen biomarkers for hepatitis B and hepatitis C infections

	Chronic HBV	Resolved HBV	HBV vaccinated	HBV Susceptible	Chronic HCV
HBsAg	Pos	Neg	Neg	Neg	Pos/neg
HBcAb	Pos	Pos	Neg	Neg	Pos/neg
HBsAb	Neg	Pos/indeter/neg	Pos	Neg/indeter	Pos/neg
Anti-HCV	Neg/pos	Neg/pos	Neg/pos	Neg/pos	Pos

HBcAb: Hepatitis B core antibody; HBsAg: Hepatitis B surface antigen; HBsAb: Hepatitis B surface antibody; HBV: Hepatitis B virus; HCV: Hepatitis C virus; Indeter: Indeterminate; Neg: Negative; Pos: Positive.

negative, and HBcAb positive, regardless of anti-HCV status. The resolved HBV group, immune due to exposure to the live virus, was defined as participants who tested HBsAg negative, HBsAb positive and HBcAb positive, regardless of anti-HCV status. Combining the chronic HBV-infected group with the resolved HBV group gives the total number of persons exposed to live HBV infection. The vaccinated group was defined as those who tested HBsAg negative, HBsAb positive, and HBcAb negative, regardless of anti-HCV status. The HBV susceptible group was defined as those who tested HBsAg negative, HBsAb negative and HBcAb negative, regardless of anti-HCV status. Lastly, the chronic HCV infected group was defined as anyone who tested anti-HCV positive, regardless of HBsAg, HBcAb, or HBsAb status. We have previously shown that 93% of anti-HCV antibody-positive individuals in the Somali community also had measurable HCV RNA; thus, the rate of false positive anti-HCV antibody testing in this population is low[29]. Referrals for follow-up testing, health education, counseling, vaccination and treatment were provided to participants depending on their results.

Statistical methods

Descriptive statistics were computed to describe the study population. JMP (v.10; SAS Institute Inc., Cary, NC) was used for statistical analyses. Adjusted frequencies for viral hepatitis infection statuses were standardized using the 2010 United States Census and were stratified based on age and sex[30].

RESULTS

Characteristics of the study population

The study team consented and screened 779 participants aged 18 years to 91 years, of whom 49.9% (389) were male. This number represents 2.3% or 1 in 43 of the estimated 33208 Somalis aged 18 years to 84 years resident in Minnesota between 2013 and 2017[31]. The age distribution of the participants and the primary summary of rates are presented in Table 2.

Proportion of patients with HBV and HCV infections

The crude rates for each age and sex group are shown in Table 2, along with the age-adjusted rate for each group. Of the 779 Somali participants screened, 120 (15.4%) had chronic HBV (HBsAg+, HBcAb+, HBsAb-), and 271 (34.8%) were immune due to prior HBV infection (HBcAb+, HBsAg-, HBsAb+). In addition, a small subset of the patients had HBV and HCV co-infection (*n* = 5). The crude rates showed that, as is typical for HBV infection in Africa, many participants tested positive for chronic HBV infection by the age of 20. However, the converse was true for HCV, with most positive individuals being over 50 years. The age-adjusted rates for persons with chronic HBV were 12.5% and 11.6% for males and females, respectively. The age-adjusted rates for persons with resolved HBV, characteristic of prior exposure to HBV infection with spontaneous clearance, were 32.3% and 29.7% for males and females, respectively. For prior HBV exposure resulting in either chronic infection or spontaneous clearance, which measures all previous exposure to infectious HBV, the age-adjusted rates were 44.8% for males and 41.3% for females. Lastly, the age-adjusted positive rates for anti-HCV, the marker for HCV infection, were 6.7% for males and 5.7% for females. Of the 59 anti-HCV positive participants, 29 (49.2%) had follow-up testing for HCV RNA, and 28 (96.6%) of the 29 tested positive. This was consistent with the results of our previous retrospective study, in which 93% of anti-HCV-positive Somalis were HCV RNA positive. The most common HCV genotype was 4 (43%) followed by genotype 3 (14%).

Proportion of patients vaccinated or susceptible to HBV infections

Of the 779 Somali participants, 388 (49.8%) had not previously been exposed to HBV. Of these, 195 (25.0% of the total) tested positive for HBsAb only, consistent with immunity due to HBV vaccination. The remaining 193 (24.8%) tested negative for all HBV markers, indicating susceptibility to HBV

Table 2 Frequency of hepatitis B virus- and hepatitis C virus-positive test results in Community Recruited Minnesota Somali Residents

Age group (yr)	Chronic HBV infection		Previous HBV exposure including spontaneous clearance		Chronic HCV infection	
	HBsAg-positive/total males, *n*	HBsAg-positive/total females, *n*	HBcAb-positive/total males, *n*	HBcAb-positive/total females, *n*	Anti-HCV-positive/total males, *n*	Anti-HCV-positive/total females, *n*
≤ 20	0/8 (0)	0/9	1/8	2/9	0/8	0/9
21-30	10/89	6/74	29/89	12/74	3/89	0/74
31-40	20/92	12/92	24/92	29/92	3/92	2/92
41-50	12/72	5/82	32/72	27/82	5/72	1/82
51-60	12/50	10/64	23/50	24/64	3/50	3/64
61-70	6/35	11/40	20/35	16/40	5/35	10/40
> 70	6/43	10/29	20/43	12/29	17/43	7/29
Total	66/389	54/390	149/389	122/390	36/389	23/390
Age-adjusted frequency (per 1000 population)	125	116	323	297	67	57

HBcAb: Hepatitis B core antibody; HBsAg: Hepatitis B surface antigen; HBV: Hepatitis B virus; HCV: Hepatitis C virus.

(Table 3). Remarkably, of the 518 participants from this high prevalence community under age 50, 146 (28.2%) were unvaccinated and susceptible to HBV.

Age and sex group characteristics of HBV and HCV infections

Both age- and sex-specific rates showed differences. The highest proportion of HBsAg in Somalis was observed in females > 70 years of age (34.5%); in males, the highest proportion was in the 51-year-old to 60-year-old age group (24.0%) (Figure 1A). For HBcAb, the highest proportion of positivity for males was in the 61- year-old to 70-year-old age group (57.1%) and for females in the > 70-year-old group (41.4%) (Figure 1B). For anti-HCV, the highest proportion for males was > 70 years of age (39.5%), while the highest proportion for females was in the 61-year-old to 70-year-old age group (25.0%) (Figure 1C).

Follow-up and referral

After completing the serological tests, participants received screening results *via* telephone calls. Participants with positive HBsAg or anti-HCV were referred to their local medical care facility (University of Minnesota Gastroenterology Hepatology and Nutrition or Mayo Clinic Division of Gastroenterology and Hepatology) for subsequent management, surveillance and/or treatment. Participants who were HBsAg negative and anti-HBs negative were referred to their local primary care clinic (Gargar Clinic and Urgent Care or Axis Medical Center) to complete the HBV vaccination series.

Characteristics of participants who developed HCC

After serological tests confirmed positive HBV and/or HCV infection or susceptibility to HBV infection, patients were linked to care for treatment or monitoring of their viral hepatitis, as appropriate, or for HBV vaccination. They were encouraged to notify the study staff if they were diagnosed with advanced liver disease or HCC. Seven individuals were identified by review of the medical records or patient self-report to have HCC in follow-up after testing. Their ages ranged from 43 years to 83 years (mean 69.8 years; IQR 65.8, 76.8). Four were male (57%), and three (43%) were female. The most common etiology was HCV infection (*n* = 4; 57%); one patient had HBV infection (14%), one had non-alcoholic fatty liver disease without cirrhosis, and one had no known risk factor for HCC. Three of the 4 HCV HCC patients had cirrhosis (Table 4).

Due to the number of participants lost to follow-up, we do not have complete follow-up of the entire cohort of participants over the period and, therefore, were unable to calculate the exact incidence of HCC in the participants of this screening study. However, comparison to our previous retrospective hospital/clinic-based study, in which we found 30 Somali patients with HCC (2.5%) out of a total of 1218 patients tested for any chronic hepatitis markers, shows a lower incidence of 7 HCC cases (0.9%) of the 779 adults tested in this community-recruited cohort. This is not surprising, since the hospital/clinic-based cohort almost certainly had a selection bias for viral hepatitis or more severe chronic liver disease.

Table 3 Rates of hepatitis B virus vaccination and susceptibility in Community Recruited Minnesota Somali Residents				
	HBV vaccinated		**HBV susceptible**	
Age group (yr)	**HBV vaccinated[1]/total males, *n***	**HBV vaccinated[1]/total females, *n***	**HBV susceptible[2]/total males, *n***	**HBV susceptible[2]/total females, *n***
≤ 20	4/8	4/9	3/8	3/9
21-30	27/89	37/74	23/89	19/74
31-40	22/92	23/92	26/92	28/92
41-50	15/72	19/82	13/72	31/82
51-60	8/50	13/64	7/50	17/64
61-70	4/35	5/40	5/35	8/40
> 70	10/43	4/29	7/43	3/29
Total	90/389	105/390	84/389	109/390
Age-adjusted frequency (per 1000 population)	299	305	253	282

[1]Vaccinated: Hepatitis B surface antigen negative; anti-HBc negative; anti-HBs positive.
[2]Susceptible: Hepatitis B surface antigen negative; anti-HBc negative; anti-HBc negative.
HBV: Hepatitis B virus.

Table 4 Characteristics of 7 Somali participants who developed hepatocellular carcinoma									
Patient no.	**Age**	**Sex**	**Etiology**	**HCV genotype**	**Cirrhosis**	**MELD Score**	**Metastatic HCC**	**Portal hypertension**	**Fibrosis staging**
1	69	Male	NAFLD	-	No	8	No	No	NR
2	65	Female	HCV	3	Yes	7	No	Yes	NR
3	76	Female	Unknown	-	No	7	No	No	NR
4	75	Male	HCV	4	No	7	Yes	No	2 to 3/4
5	77	Male	HCV	UTG	Yes	11	No	No	4
6	43	Male	HBV	-	No	7	Yes	No	NR
7	83	Female	HCV	UTG	Yes	6	No	No	3 to 4

UTG: Unable to genotype; NR: Not reported; NAFLD: Non-alcoholic fatty liver disease; HCV: Hepatitis C virus; HBV: Hepatitis B virus; MELD: Model for end-stage liver disease; HCC: Hepatocellular carcinoma.

The observed incidence of 7 HCCs in the cohort of 779 adults prospectively tested in this study, albeit with incomplete follow-up over a median of approximately 8 years, is estimated to be 112 per 100000 person-years or 0.11% per year risk of HCC in the entire cohort. This is almost certainly an overestimate as some of the cases may have had unrecognized HCC at the time of initial testing.

DISCUSSION

The primary goal of our study was to examine the prevalence of HBV and HCV viral infections in the immigrant Somali community residing in Minnesota. As a secondary goal, we also ascertained any cases of HCC that developed in study participants by voluntary notification and review of available medical records. This study is the first of its kind to report the results of community-wide screening for HBV and HCV in this immigrant population. We found that 15.4% of participants had chronic HBV infection compared to the estimated United States general population prevalence of 0.4%[32]. HCV prevalence was 7.6%, also significantly higher than the general United States population prevalence of HCV which is less than 2%[33]. In comparison to our previously published results, this prospective study determined that chronic HBV rates are higher than the frequency reported in the 2012 clinic/hospital-based retrospective study[29].
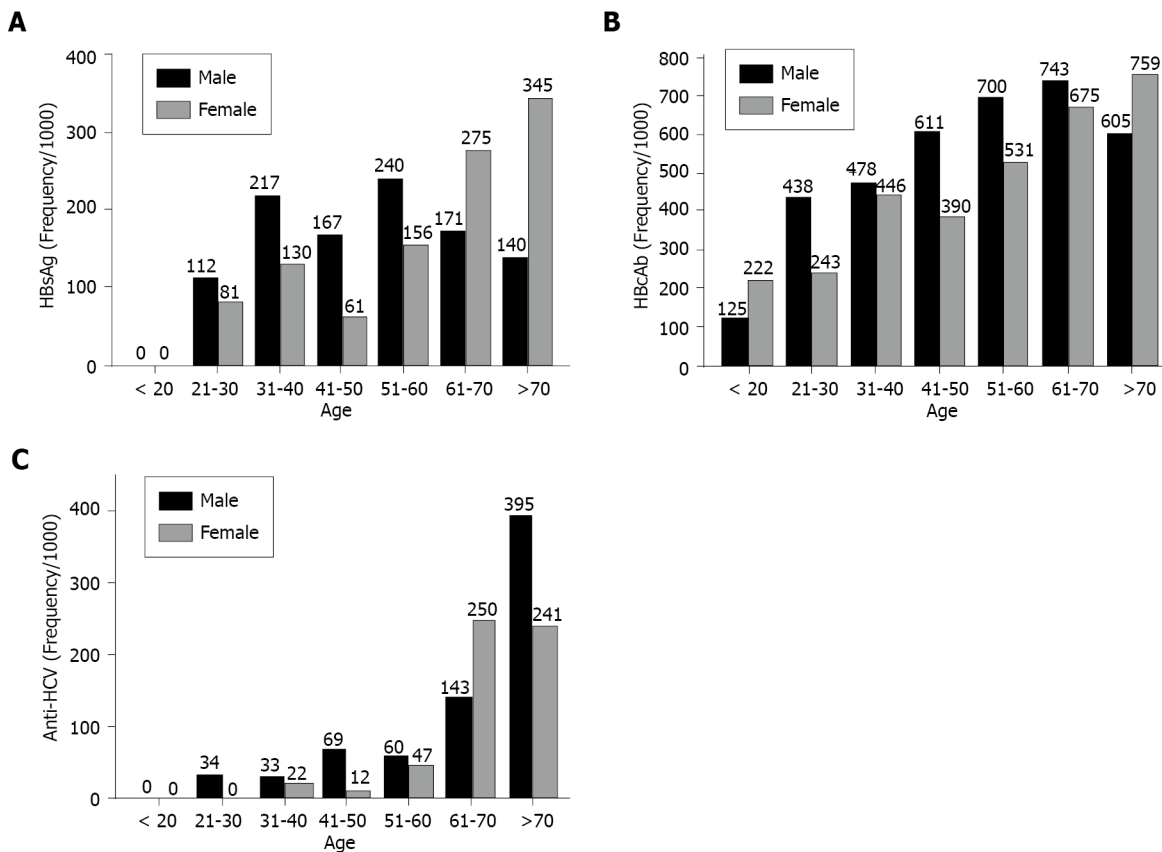
DOI: 10.3748/wjg.v28.i35.5217 **Copyright** ©The Author(s) 2022.

Figure 1 Frequency in Somali Patients Screening. A: Hepatitis B virus (HBV)-positive test results; B: Prior exposure of HBV test results; C: Hepatitis C virus-positive test results. HBcAb: Hepatitis B core antibody; HBsAg: Hepatitis B surface antigen; HCV: Hepatitis C virus.

Somalis in Minnesota are younger than the general population with a median age of 25 years compared to the general population median age of 37 years[34]. Therefore, surveillance for viral hepatitis is important for this community. Given the high prevalence of HBV and HCV infections in Somalia noted in prior studies, a significant number of Somali immigrants are likely to have chronic hepatitis and are at risk for HCC. Yang *et al*[35] reported that African-born individuals diagnosed with HCC in the United States, particularly those of West African ancestry, are diagnosed at a younger age. Most of these individuals have chronic HBV infection, which was acquired in the first few years of life, and it is recommended that HCC surveillance of this group begin at the age of 20 years[5]. The Somali immigrant community may be different; in addition to high rates of chronic HBV infection, there is also a high prevalence of chronic HCV infection, most likely acquired during adulthood. A multi-center, multi-national, retrospective observational cohort study that investigated the current clinical presentation of Africans with HCC showed that in Egypt, where chronic HCV is the major etiology of HCC, the median age of HCC onset was 58 years, compared to 46 years in eight other African countries with a predominance of HBV-induced HCC[6].

While the high level of chronic HBV infection in the immigrant Somali population suggests an elevated risk of maternal-to-child transmission and horizontal transmission of HBV between family members at an early age, it is important to note that about a third of all the individuals we screened had evidence of prior exposure to HBV infection that they had cleared spontaneously. This phenomenon occurs most commonly in adults exposed to HBV infection and suggests substantial transmission of HBV among adolescents and adults in the community. Risk factors associated with these infections need to be identified and addressed. Individuals from areas affected by conflict and displacement are at a greater risk of contracting infectious agents, such as viral hepatitis infections[36]. For instance, Khan *et al* [37] reported that internally displaced individuals have high levels of HBV and HCV infections. This may reflect the lack of basic health infrastructure and services in refugee camps and displaced communities.

Shire *et al*[29] showed an increased frequency of HBV and HCV among Somali patients seen in the hospital/clinic setting, which could potentially have been due to selection bias. However, our community-based screening study of Somali immigrants in Minnesota confirms high rates of chronic HBV and HCV infection rates among this population. The best outcomes for communities with high prevalence of chronic HBV and HCV infections have been shown in Japan and Taiwan, which have

comprehensive programs for screening all adults for chronic viral hepatitis and enrolling those at risk into surveillance programs for HCC. These programs have resulted in ≥ 70% of HCCs being detected at early stages when they are eligible for curative treatment. Consequently, the 5-year survival rate of patients diagnosed with HCC in these countries ranges from 50%-70%, substantially higher than the currently estimated rate of 15% in the United States[38]. Whether HCC surveillance decreases liver disease mortality is still controversial, but almost all international guidelines now recommend surveillance for HCC among high-risk patients using liver ultrasound performed every 6 mo with or without measurement of the serum alpha-fetoprotein[39-45]. There are active efforts underway to develop more sensitive and effective biomarker and imaging technologies for HCC surveillance. We are performing additional studies to assess the stage at diagnosis of HCC in the immigrant Somali community and discern any barriers or disparities in care related to chronic liver disease and HCC.

Furthermore, the observed incidence of 7 HCCs in the cohort of 779 adults prospectively tested in this study is estimated to be 112 per 100000 person-years or 0.11% per year risk of HCC in the entire cohort. This is almost certainly an overestimate as some of the cases may have had unrecognized HCC at the time of initial testing. By comparison, for the time period between 2012 and 2016, the age-standardized rates of liver cancer incidence in Minnesota were 5.7 per 100000 for Non-Hispanic Whites and 24.7 per 100000 for Blacks[46]. Since the total number of Somali adults aged 18-84 in Minnesota, estimated at 33208, represents approximately 23% of the 146020 adults of African descent aged 18-84 who are resident in Minnesota, the Somali immigrant community likely contributes substantially to the overall incidence of HCC in Minnesota[47,48].

The results of this study suggest a need to develop strategies to improve awareness of chronic hepatitis[49], increase screening for chronic HBV and HCV infections in the immigrant Somali community in the United States and promote hepatitis B vaccination in unvaccinated children and adults. These strategies could help prevent chronic liver disease and HCC, increase access to currently available treatments that suppress HBV viral load or cure HCV and substantially reduce the burden of hepatobiliary malignancies observed in Minnesota's non-Hispanic Black population[50-52]. Ahmed Mohammed *et al*[53] reported that visits to gastrointestinal/hepatologist specialists were linked to increased HCC surveillance in Minnesota residents, as compared to primary care practitioner visits. Given the limitations in access to specialist care, efforts to encourage HBV and HCV testing of immigrant Somalis in the primary care setting could improve the early diagnosis of chronic viral hepatitis and appropriate linkage to care.

Limitations
There are several limitations to this study. The first limitation is selection bias and this is due to the nature of the study design. However, through the use of community advisory boards, community-based organizations and clinics, we are confident that our data can be generalizable to the larger Somali community of Minnesota. Second, loss to follow-up was another limitation associated with this study, especially for those individuals who have developed liver cancer and associated co-morbidities. On the contrary, there are several strengths associated with this study. First, the implementation of community-engagement through health education and listening sessions have ensured participants are informed of the goals of the study in a culturally sensitive and responsive framework. Second, building strong partnerships with community-based organizations, charter schools and clinics were instrumental in the success of recruitment and dissemination of information.

CONCLUSION

Chronic HBV and HCV infections are prevalent among Somali immigrants in Minnesota and associated with high rates of HCC. Partnering with community stakeholders helped to improve recruitment rates and to spread awareness of the need for viral hepatitis screening. Community-wide screening is an effective way to identify and provide health education and linkage to care for individuals with or at risk for viral hepatitis. It is important to develop and implement culturally and linguistically acceptable viral hepatitis awareness programs in partnership with communities, in order to promote preventative vaccination, treatment of viral hepatitis and reduction of cancer risk.

ARTICLE HIGHLIGHTS

Research background
Somali immigrants come from regions of the world where viral hepatitis is endemic. Since the start of the Somali civil war in 1991, limited data is available on the impact of viral hepatitis in the community, especially those individuals in the diaspora.

Research motivation

The impetus of this project was communal outcry about community members succumbing to liver disease. In partnership with the community, our research team worked to assess the burden of viral hepatitis in Minnesota. Addressing this pressing communal matter, we were able to connect those who tested positive for hepatitis infections and/or were not vaccinated for hepatitis B virus (HBV) with the needed healthcare.

Research objectives

Our objective was to determine the prevalence of viral hepatitis infections within the community. This is significant because it laid the foundation to start conducting studies on host-viral interactions and the unique development of liver disease among this population. This is relevant to clinical practice because we can use this information to tailor screening practices and treatments for individuals from endemic regions which are historically under studied.

Research methods

In partnership with the community stakeholders, we conducted a prospective study using community-based participatory research from 2010 to 2015. We screened for viral hepatitis infections and reported the results back to the study participant. This is the first study of its kind to screen community based Somali immigrants in Minnesota at a large scale.

Research results

Viral hepatitis infections are a major under recognized disease within the Somali immigrant population. Age-adjusted prevalence rates are high and call for prioritizing responses from health agencies. This data will be used to lobby public health institutions to help address the unique needs of the Minnesota Somali population and for healthcare providers to implement programs to screen community members for both HBV and hepatitis C virus. Furthermore, the follow-up after the patients have enrolled into the study was quite difficult. We should consider effective methods to follow-up patients to assess the potential for development of liver disease sequelae.

Research conclusions

Although there were limitations to the study, we have learned that chronic viral hepatitis infection in the Somali community is high. Effective screening programs need to be implemented in order to prevent suffering and needless death. The use of community-based participatory research was a success and was the first of its kind with this community regarding a disease considered taboo. We will continue this partnership and expand research within this population historically under reported in clinical research.

Research perspectives

We will continue maintaining the partnership and will continue to understand the unique host-viral interactions. We have studies on immunoprofiling as well as examining the influence of the viral genome on liver disease progression. These studies will be used to improve the health of persons from this region of the world.

ACKNOWLEDGEMENTS

FOOTNOTES

ORCID number: Essa A Mohamed 0000-0002-0307-6241; Nasra H Giama 0000-0003-2764-866X; Abubaker O Abdalla 0000-0002-7022-1074; Hassan M Shaleh 0000-0002-4698-4610; Abdul M Oseini 0000-0003-4079-9825; Hamdi A Ali 0000-0002-2671-0532; Fowsiyo Ahmed 0000-0002-0201-6706; Wesam Taha 0000-0002-6737-3739; Hager Ahmed Mohammed 0000-0002-3731-4332; Jessica Cvinar 0000-0003-4855-6908; Ibrahim A Waaeys 0000-0003-2086-5477; Hawa Ali 0000-0003-4667-5233; Loretta K Allotey 0000-0002-5734-8839; Abdiwahab O Ali 0000-0003-1692-9829; Safra A Mohamed 0000-0001-8408-0017; William S Harmsen 0000-0001-7134-5362; Eimad M Ahmmad 0000-0002-1120-2631; Numra A Bajwa 0000-0002-2727-8710; Mohamud D Afgarshe 0000-0001-9066-0237; Abdirashid M Shire 0000-0002-8216-9971; Joyce E Balls-Berry 0000-0003-3497-1115; Lewis R Roberts 0000-0001-7885-8574.

REFERENCES

1   **Global Burden of Disease Cancer Collaboration**, Fitzmaurice C, Allen C, Barber RM, Barregard L, Bhutta ZA, Brenner H, Dicker DJ, Chimed-Orchir O, Dandona R, Dandona L, Fleming T, Forouzanfar MH, Hancock J, Hay RJ, Hunter-Merrill R, Huynh C, Hosgood HD, Johnson CO, Jonas JB, Khubchandani J, Kumar GA, Kutz M, Lan Q, Larson HJ, Liang X, Lim SS, Lopez AD, MacIntyre MF, Marczak L, Marquez N, Mokdad AH, Pinho C, Pourmalek F, Salomon JA, Sanabria JR, Sandar L, Sartorius B, Schwartz SM, Shackelford KA, Shibuya K, Stanaway J, Steiner C, Sun J, Takahashi K, Vollset SE, Vos T, Wagner JA, Wang H, Westerman R, Zeeb H, Zoeckler L, Abd-Allah F, Ahmed MB, Alabed S, Alam NK, Aldhahri SF, Alem G, Alemayohu MA, Ali R, Al-Raddadi R, Amare A, Amoako Y, Artaman A, Asayesh H, Atnafu N, Awasthi A, Saleem HB, Barac A, Bedi N, Bensenor I, Berhane A, Bernabé E, Betsu B, Binagwaho A, Boneya D, Campos-Nonato I, Castañeda-Orjuela C, Catalá-López F, Chiang P, Chibueze C, Chitheer A, Choi JY, Cowie B, Damtew S, das Neves J, Dey S, Dharmaratne S, Dhillon P, Ding E, Driscoll T, Ekwueme D, Endries AY, Farvid M, Farzadfar F, Fernandes J, Fischer F, G/Hiwot TT, Gebru A, Gopalani S, Hailu A, Horino M, Horita N, Husseini A, Huybrechts I, Inoue M, Islami F, Jakovljevic M, James S, Javanbakht M, Jee SH, Kasaeian A, Kedir MS, Khader YS, Khang YH, Kim D, Leigh J, Linn S, Lunevicius R, El Razek HMA, Malekzadeh R, Malta DC, Marcenes W, Markos D, Melaku YA, Meles KG, Mendoza W, Mengiste DT, Meretoja TJ, Miller TR, Mohammad KA, Mohammadi A, Mohammed S, Moradi-Lakeh M, Nagel G, Nand D, Le Nguyen Q, Nolte S, Ogbo FA, Oladimeji KE, Oren E, Pa M, Park EK, Pereira DM, Plass D, Qorbani M, Radfar A, Rafay A, Rahman M, Rana SM, Søreide K, Satpathy M, Sawhney M, Sepanlou SG, Shaikh MA, She J, Shiue I, Shore HR, Shrime MG, So S, Soneji S, Stathopoulou V, Stroumpoulis K, Sufiyan MB, Sykes BL, Tabarés-Seisdedos R, Tadese F, Tedla BA, Tessema GA, Thakur JS, Tran BX, Ukwaja KN, Uzochukwu BSC, Vlassov VV, Weiderpass E, Wubshet Terefe M, Yebyo HG, Yimam HH, Yonemoto N, Younis MZ, Yu C, Zaidi Z, Zaki MES, Zenebe ZM, Murray CJL, Naghavi M. Global, Regional, and National Cancer Incidence, Mortality, Years of Life Lost, Years Lived With Disability, and Disability-

Adjusted Life-years for 32 Cancer Groups, 1990 to 2015: A Systematic Analysis for the Global Burden of Disease Study. *JAMA Oncol* 2017; **3**: 524-548 [PMID: 27918777 DOI: 10.1001/jamaoncol.2016.5688]

2   **McGlynn KA**, Petrick JL, El-Serag HB. Epidemiology of Hepatocellular Carcinoma. *Hepatology* 2021; **73** Suppl 1: 4-13 [PMID: 32319693 DOI: 10.1002/hep.31288]

3   **Yang JD**, Kim WR, Coelho R, Mettler TA, Benson JT, Sanderson SO, Therneau TM, Kim B, Roberts LR. Cirrhosis is present in most patients with hepatitis B and hepatocellular carcinoma. *Clin Gastroenterol Hepatol* 2011; **9**: 64-70 [PMID: 20831903 DOI: 10.1016/j.cgh.2010.08.019]

4   **Razavi H**. Global Epidemiology of Viral Hepatitis. *Gastroenterol Clin North Am* 2020; **49**: 179-189 [PMID: 32389357 DOI: 10.1016/j.gtc.2020.01.001]

5   **Yang JD**, Gyedu A, Afihene MY, Duduyemi BM, Micah E, Kingham TP, Nyirenda M, Nkansah AA, Bandoh S, Duguru MJ, Okeke EN, Kouakou-Lohoues MJ, Abdo A, Awuku YA, Ajayi AO, Omonisi AE, Ocama P, Malu AO, Mustapha S, Okonkwo U, Kooffreh-Ada M, Debes JD, Onyekwere C, Ekere F, Rufina I, Roberts LR; Africa Network for Gastrointestinal and Liver Diseases. Hepatocellular Carcinoma Occurs at an Earlier Age in Africans, Particularly in Association With Chronic Hepatitis B. *Am J Gastroenterol* 2015; **110**: 1629-1631 [PMID: 26618430 DOI: 10.1038/ajg.2015.289]

6   **Yang JD**, Mohamed EA, Aziz AO, Shousha HI, Hashem MB, Nabeel MM, Abdelmaksoud AH, Elbaz TM, Afihene MY, Duduyemi BM, Ayawin JP, Gyedu A, Lohouès-Kouacou MJ, Ndam AW, Moustafa EF, Hassany SM, Moussa AM, Ugiagbe RA, Omuemu CE, Anthony R, Palmer D, Nyanga AF, Malu AO, Obekpa S, Abdo AE, Siddig AI, Mudawi HM, Okonkwo U, Kooffreh-Ada M, Awuku YA, Nartey YA, Abbew ET, Awuku NA, Otegbayo JA, Akande KO, Desalegn HM, Omonisi AE, Ajayi AO, Okeke EN, Duguru MJ, Davwar PM, Okorie MC, Mustapha S, Debes JD, Ocama P, Lesi OA, Odeghe E, Bello R, Onyekwere C, Ekere F, Igetei R, Mah'moud MA, Addissie B, Ali HM, Gores GJ, Topazian MD, Roberts LR; Africa Network for Gastrointestinal and Liver Diseases. Characteristics, management, and outcomes of patients with hepatocellular carcinoma in Africa: a multicountry observational study from the Africa Liver Cancer Consortium. *Lancet Gastroenterol Hepatol* 2017; **2**: 103-111 [PMID: 28403980 DOI: 10.1016/S2468-1253(16)30161-3]

7   **Hassan MA**, Kim WR, Li R, Smith CI, Fried MW, Sterling RK, Ghany MG, Wahed AS, Ganova-Raeva LM, Roberts LR, Lok ASF; Hepatitis B Research Network. Characteristics of US-Born Versus Foreign-Born Americans of African Descent With Chronic Hepatitis B. *Am J Epidemiol* 2017; **186**: 356-366 [PMID: 28525625 DOI: 10.1093/aje/kwx064]

8   **Sonderup MW**, Afihene M, Ally R, Apica B, Awuku Y, Cunha L, Dusheiko G, Gogela N, Lohouès-Kouacou MJ, Lam P, Lesi O, Mbaye PS, Musabeyezu E, Musau B, Ojo O, Rwegasha J, Scholz B, Shewaye AB, Tzeuton C, Kassianides C, Spearman CW; Gastroenterology and Hepatology Association of sub-Saharan Africa (GHASSA). Hepatitis C in sub-Saharan Africa: the current status and recommendations for achieving elimination by 2030. *Lancet Gastroenterol Hepatol* 2017; **2**: 910-919 [PMID: 29132760 DOI: 10.1016/S2468-1253(17)30249-2]

9   **Spearman CW**, Afihene M, Ally R, Apica B, Awuku Y, Cunha L, Dusheiko G, Gogela N, Kassianides C, Kew M, Lam P, Lesi O, Lohouès-Kouacou MJ, Mbaye PS, Musabeyezu E, Musau B, Ojo O, Rwegasha J, Scholz B, Shewaye AB, Tzeuton C, Sonderup MW; Gastroenterology and Hepatology Association of sub-Saharan Africa (GHASSA). Hepatitis B in sub-Saharan Africa: strategies to achieve the 2030 elimination targets. *Lancet Gastroenterol Hepatol* 2017; **2**: 900-909 [PMID: 29132759 DOI: 10.1016/S2468-1253(17)30295-9]

10 **Karuru JW**, Lule GN, Joshi M, Anzala O. Prevalence of HCV and HCV/HIV co-infection among in-patients at the Kenyatta National Hospital. *East Afr Med J* 2005; **82**: 170-172 [PMID: 16122083 DOI: 10.4314/eamj.v82i4.9276]

11 **Karuru JW**, Lule GN, Joshi M, Anzala O. Prevalence of HCV and HIV/HCV co-infection among volunteer blood donors and VCT clients. *East Afr Med J* 2005; **82**: 166-169 [PMID: 16122082 DOI: 10.4314/eamj.v82i4.9275]

12 **Tramuto F**, Maida CM, Colomba GM, Di Carlo P, Mazzola G, Li Vecchi V, Affronti M, Montalto G, Vitale F. Occult hepatitis B infection in the immigrant population of Sicily, Italy. *J Immigr Minor Health* 2013; **15**: 725-731 [PMID: 22875279 DOI: 10.1007/s10903-012-9699-y]

13 **Moore MS**, Bocour A, Tran OC, Qiao B, Schymura MJ, Laraque F, Winters A. Effect of Hepatocellular Carcinoma on Mortality Among Individuals With Hepatitis B or Hepatitis C Infection in New York City, 2001-2012. *Open Forum Infect Dis* 2018; **5**: ofy144 [PMID: 30019001 DOI: 10.1093/ofid/ofy144]

14 **Rossi C**, Shrier I, Marshall L, Cnossen S, Schwartzman K, Klein MB, Schwarzer G, Greenaway C. Seroprevalence of chronic hepatitis B virus infection and prior immunity in immigrants and refugees: a systematic review and meta-analysis. *PLoS One* 2012; **7**: e44611 [PMID: 22957088 DOI: 10.1371/journal.pone.0044611]

15 **Yang JD**, Hainaut P, Gores GJ, Amadou A, Plymoth A, Roberts LR. A global view of hepatocellular carcinoma: trends, risk, prevention and management. *Nat Rev Gastroenterol Hepatol* 2019; **16**: 589-604 [PMID: 31439937 DOI: 10.1038/s41575-019-0186-y]

16 **Ha J**, Yan M, Aguilar M, Bhuket T, Tana MM, Liu B, Gish RG, Wong RJ. Race/ethnicity-specific disparities in cancer incidence, burden of disease, and overall survival among patients with hepatocellular carcinoma in the United States. *Cancer* 2016; **122**: 2512-2523 [PMID: 27195481 DOI: 10.1002/cncr.30103]

17 **Roberts H**, Kruszon-Moran D, Ly KN, Hughes E, Iqbal K, Jiles RB, Holmberg SD. Prevalence of chronic hepatitis B virus (HBV) infection in U.S. households: National Health and Nutrition Examination Survey (NHANES), 1988-2012. *Hepatology* 2016; **63**: 388-397 [PMID: 26251317 DOI: 10.1002/hep.28109]

18 **American Immigration Council**. Immigrants in Minnesota. [cited 15 December 2021]. Available from: https://www.americanimmigrationcouncil.org/research/immigrants-in-minnesota

19 **Minnesota Department of Health**. Liver cancer is increasing in Minnesota. [cited 20 December 2021]. Available from: https://data.web.health.state.mn.us/cancer_liver

20 **Ugwu C**, Varkey P, Bagniewski S, Lesnick T. Sero-epidemiology of hepatitis B among new refugees to Minnesota. *J Immigr Minor Health* 2008; **10**: 469-474 [PMID: 18066661 DOI: 10.1007/s10903-007-9111-5]

21 **Adair R**, Nwaneri O. Communicable disease in African immigrants in Minneapolis. *Arch Intern Med* 1999; **159**: 83-85 [PMID: 9892335 DOI: 10.1001/archinte.159.1.83]

22 **Kim WR**, Benson JT, Therneau TM, Torgerson HA, Yawn BP, Melton LJ 3rd. Changing epidemiology of hepatitis B in a U.S. community. *Hepatology* 2004; **39**: 811-816 [PMID: 14999701 DOI: 10.1002/hep.20098]

23   **Mohamed EA**, Giama NH, Shaleh HM, Kerandi L, Oseini AM, Ahmed Mohammed H, Kerandi H, Allotey LK, Waaeys IA, Ali HA, Ali HM, Mohamed SA, Yang JD, Gaga WO, Tamire LL, Windissa A, Patten CA, Balls-Berry JE, Roberts LR. Knowledge, Attitudes, and Behaviors of Viral Hepatitis Among Recent African Immigrants in the United States: A Community Based Participatory Research Qualitative Study. *Front Public Health* 2020; **8**: 25 [PMID: 32211358 DOI: 10.3389/fpubh.2020.00025]

24   **Bile K**, Mohamud O, Aden C, Isse A, Norder H, Nilsson L, Magnius L. The risk for hepatitis A, B, and C at two institutions for children in Somalia with different socioeconomic conditions. *Am J Trop Med Hyg* 1992; **47**: 357-364 [PMID: 1524149 DOI: 10.4269/ajtmh.1992.47.357]

25   **Bile KM**, Abdirahman M, Aden C, Norder H, Magnius L, Lindberg G, Nilsson LH. Minor role of hepatitis B virus in the causation of chronic liver disease in Somalia indicated by a case-control study. *Trans R Soc Trop Med Hyg* 1991; **85**: 104-108 [PMID: 1712517 DOI: 10.1016/0035-9203(91)90177-z]

26   **Bile KM**, Aden A, Lindberg G, Nilsson L, Lidman K, Norder H, Magnius L. Epidemiology of hepatitis B in Somalia: inference from a cross-sectional survey of serological markers. *Trans R Soc Trop Med Hyg* 1987; **81**: 824-828 [PMID: 3502433 DOI: 10.1016/0035-9203(87)90043-5]

27   **Sebastiani A**, Aceti A, Paparo BS, Pennica A, Ilardi I, Bile K, Mohamud OM. Hepatitis B virus circulation in three different villages of Somalia. *Trans R Soc Trop Med Hyg* 1985; **79**: 162-164 [PMID: 4002285 DOI: 10.1016/0035-9203(85)90323-2]

28   **Hassan-Kadle MA**, Osman MS, Ogurtsov PP. Epidemiology of viral hepatitis in Somalia: Systematic review and meta-analysis study. *World J Gastroenterol* 2018; **24**: 3927-3957 [PMID: 30228786 DOI: 10.3748/wjg.v24.i34.3927]

29   **Shire AM**, Sandhu DS, Kaiya JK, Oseini AM, Yang JD, Chaiteerakij R, Mettler TA, Giama NH, Roberts RO, Therneau TM, Petersen GM, Knutson KL, Roberts LR. Viral hepatitis among Somali immigrants in Minnesota: association of hepatitis C with hepatocellular carcinoma. *Mayo Clin Proc* 2012; **87**: 17-24 [PMID: 22212964 DOI: 10.1016/j.mayocp.2011.08.001]

30   **Howden LM**, Meyer JA.   Age and Sex Composition: 2010. In: Bureau USC, editor. Economics and Statistics Administration. United States: Census Bureau, 2011

31   **Minnesota Compass**.   Cultural Communities Methodology. [cited 16 December 2021]. Available from: https://www.mncompass.org/topics/demographics/cultural-communities/methodology

32   **Kim WR**. Epidemiology of hepatitis B in the United States. *Hepatology* 2009; **49**: S28-34 [PMID: 19399791 DOI: 10.1002/hep.22975]

33   **Moosavy SH**, Davoodian P, Nazarnezhad MA, Nejatizaheh A, Eftekhar E, Mahboobi H. Epidemiology, transmission, diagnosis, and outcome of Hepatitis C virus infection. *Electron Physician* 2017; **9**: 5646-5656 [PMID: 29238510 DOI: 10.19082/5646]

34   US Department of Commerce. 2020. [cited 16 December 2021]. Available from: https://www.commerce.gov/

35   **Yang JD**, Altekruse SF, Nguyen MH, Gores GJ, Roberts LR. Impact of country of birth on age at the time of diagnosis of hepatocellular carcinoma in the United States. *Cancer* 2017; **123**: 81-89 [PMID: 27571320 DOI: 10.1002/cncr.30246]

36   **Ogunwobi OO**, Dibba O, Zhu L, Ilboudo A, Tan Y, Fraser MA, Ma GX. Hepatitis B Virus Screening and Vaccination in First-generation African Immigrants: A Pilot Study. *J Community Health* 2019; **44**: 1037-1043 [PMID: 31123877 DOI: 10.1007/s10900-019-00668-z]

37   **Khan A**, Qazi J. Risk factors and molecular epidemiology of HBV and HCV in internally displaced persons (IDPs) of North Waziristan Agency, Pakistan. *J Pak Med Assoc* 2018; **68**: 165-169 [PMID: 29479087]

38   **Park JW**, Chen M, Colombo M, Roberts LR, Schwartz M, Chen PJ, Kudo M, Johnson P, Wagner S, Orsini LS, Sherman M. Global patterns of hepatocellular carcinoma management from diagnosis to death: the BRIDGE Study. *Liver Int* 2015; **35**: 2155-2166 [PMID: 25752327 DOI: 10.1111/liv.12818]

39   **Omata M**, Cheng AL, Kokudo N, Kudo M, Lee JM, Jia J, Tateishi R, Han KH, Chawla YK, Shiina S, Jafri W, Payawal DA, Ohki T, Ogasawara S, Chen PJ, Lesmana CRA, Lesmana LA, Gani RA, Obi S, Dokmeci AK, Sarin SK. Asia-Pacific clinical practice guidelines on the management of hepatocellular carcinoma: a 2017 update. *Hepatol Int* 2017; **11**: 317-370 [PMID: 28620797 DOI: 10.1007/s12072-017-9799-9]

40   **Bruix J**, Sherman M; American Association for the Study of Liver Diseases. Management of hepatocellular carcinoma: an update. *Hepatology* 2011; **53**: 1020-1022 [PMID: 21374666 DOI: 10.1002/hep.24199]

41   **Song P**, Tobe RG, Inagaki Y, Kokudo N, Hasegawa K, Sugawara Y, Tang W. The management of hepatocellular carcinoma around the world: a comparison of guidelines from 2001 to 2011. *Liver Int* 2012; **32**: 1053-1063 [PMID: 22432445 DOI: 10.1111/j.1478-3231.2012.02792.x]

42   **European Association for the Study of the Liver**. ; European Association for the Study of the Liver. EASL Clinical Practice Guidelines: Management of hepatocellular carcinoma. *J Hepatol* 2018; **69**: 182-236 [PMID: 29628281 DOI: 10.1016/j.jhep.2018.03.019]

43   **Johnson P**, Berhane S, Kagebayashi C, Satomura S, Teng M, Fox R, Yeo W, Mo F, Lai P, Chan SL, Tada T, Toyoda H, Kumada T. Impact of disease stage and aetiology on survival in hepatocellular carcinoma: implications for surveillance. *Br J Cancer* 2017; **116**: 441-447 [PMID: 28081537 DOI: 10.1038/bjc.2016.422]

44   **Zhang BH**, Yang BH, Tang ZY. Randomized controlled trial of screening for hepatocellular carcinoma. *J Cancer Res Clin Oncol* 2004; **130**: 417-422 [PMID: 15042359 DOI: 10.1007/s00432-004-0552-0]

45   **Mittal S**, Kanwal F, Ying J, Chung R, Sada YH, Temple S, Davila JA, El-Serag HB. Effectiveness of surveillance for hepatocellular carcinoma in clinical practice: A United States cohort. *J Hepatol* 2016; **65**: 1148-1154 [PMID: 27476765 DOI: 10.1016/j.jhep.2016.07.025]

46   **Minnesota Department of Health**.   Liver and Intrahepatic Bile Duct Cancer. [cited 20 December 2021]. Available from: https://www.health.state.mn.us/data/mcrs/docs/livercancerffff.pdf

47   **Minnesota Compass**.   Somali population. 2020. [cited 20 December 2021]. Available from: https://www.mncompass.org/topics/demographics/cultural-communities/somali

48   **Minnesota Compass**.   African American population. 2020. [cited 20 December 2021]. Available from: https://www.mncompass.org/topics/demographics/cultural-communities/african-american

49   **Emeasoba EU**, Omarufilo F, Bosah JN, Sigal SH. Breaking down barriers for hepatitis B screening in the Bronx West African community through education in collaboration with faith-based organizations: A cohort study. *Lancet Regional Health - Americas* 2022; **7**: 100120 [DOI: 10.1016/j.lana.2021.100120]

50   **Minnesota Department of Health**.   Cancer in Minnesota 1988-2017. [cited 16 December 2021]. Available from: https://www.health.state.mn.us/data/mcrs/docs/2021bienrpt.pdf

51   **Cohen C**, Moraras K, Jackson M, Kamischke M, Gish RG, Brosgart CL, Toy M, Hutton D, Block TM, Wang S, So S. Letter to the editor: Importance of universal screening for chronic hepatitis B infection in adults in the United States. *Hepatology* 2022; **75**: 1062-1063 [PMID: 34951931 DOI: 10.1002/hep.32304]

52   **Ramrakhiani NS**, Chen VL, Le M, Yeo YH, Barnett SD, Waljee AK, Zhu J, Nguyen MH. Optimizing hepatitis B virus screening in the United States using a simple demographics-based model. *Hepatology* 2022; **75**: 430-437 [PMID: 34496066 DOI: 10.1002/hep.32142]

53   **Ahmed Mohammed HA**, Yang JD, Giama NH, Choi J, Ali HM, Mara KC, Harmsen WS, Wiesner RH, Leise MD, Therneau TM, Roberts LR. Factors Influencing Surveillance for Hepatocellular Carcinoma in Patients with Liver Cirrhosis. *Liver Cancer* 2017; **6**: 126-136 [PMID: 28275579 DOI: 10.1159/000450833]

LETTER TO THE EDITOR

Urotensin II level is elevated in inflammatory bowel disease patients

Yan Zhang, Guo-Xun Chen

Yan Zhang, Department of Gastroenterology, Affiliated Puren Hospital of Wuhan University of Science and Technology, Wuhan 430081, Hubei Province, China

Guo-Xun Chen, Department of Nutrition, The University of Tennessee, Knoxville, TN 37996, United States

Corresponding author: Guo-Xun Chen, PhD, Associate Professor, Research Scientist, Department of Nutrition, The University of Tennessee, Room 229, Jessie Harris Building, 1512 West Cumberland Avenue, Knoxville, TN 37996, United States. gchen6@utk.edu

Abstract

It was reported that the urotensin II (U-II) level in inflammatory bowel disease (IBD) patients are significantly higher than in controls. To provide future guidance for the management of cardiovascular risk factors in IBD patients, the sample size of the current study appears to be limited, and more clinical samples to compare U-II levels in IBD patients and controls are needed. This will clarify the possible roles of inflammation factors and related signaling pathways (like EPK1/2, NF-κB and Rho/ROCK) in the pathophysiology of IBD. Therefore, large multicenter studies should be done to confirm the findings and underlying mechanisms in the future.

Key Words: Inflammatory bowel disease; Urotensin II; Inflammatory factors; High sensitivity C reactive peptide

Core Tip: An observational report showed that the level of urotensin II (U-II) in inflammatory bowel disease (IBD) patients was significantly increased compared with that in controls. The authors also reported that blood U-II level was positively correlated with high-sensitivity C-reactive protein, and severe endoscopic features of the disease. This study provides us with a new role of U-II in IBD, which warrants larger, multicenter clinical and basic studies to determine the mechanisms by which U-II triggers inflammatory responses and activates signaling pathways (EPK1/2, NF-κB and Rho/ROCK).

TO THE EDITOR

We read the observational study reported by Alicic *et al*[1], who have convincingly shown the role of elevated urotensin II (U-II) level in patients with inflammatory bowel disease (IBD). IBD comprising Crohn's disease (CD) and ulcerative colitis (UC) is a multifactorial condition of relapsing chronic inflammation in the gastrointestinal tract with an unpredictable course[2]. In addition, extraintestinal manifestations of IBD cardiovascular risk factors occur frequently and contribute to morbidity and reduced quality of life[3-5].

U-II is a peptide ligand that acts as a potent vasoconstrictor, which was originally discovered four decades ago. The vasoconstriction activity of U-II is 10-fold more potent than that of endothelin-1[6]. Most studies of U-II have been conducted to understand its role in the development of cardiovascular diseases[7]. A growing number of scholars have recognized the links of U-II levels with malignant lesions associated with the liver, pancreas and gut[8]. Whether U-II participates in the initiation and progress of IBD has always intrigued contemporary gastroenterologists. This observational study reported the potential relationship of U-II and IBD, which provides the field with new knowledge and attracted our attention.

Alicic *et al*[1] compared the blood level of U-II in IBD patients and healthy controls, and investigated the association of U-II levels with the anthropometric, clinical and biochemical parameters. The study included 50 adult patients with prediagnosed IBD (24 with UC and 26 with CD) and 50 healthy, age- and gender-matched controls. IBD patients had significantly higher U-II level than control subjects had. Significant positive correlations between serum U-II level and high-sensitivity C-reactive protein (hsCRP) level, UC Endoscopic Index of Severity and Simple Endoscopic Score for CD were observed. Whether these clinical data imply the involvement of U-II in the inflammatory responses and disease outcomes of IBD patients remains to be confirmed.

The action of U-II is mediated by U-II receptor (UTR). UTR is also called GPR14, which is a G-protein-linked receptor[9]. Both U-II and UTR can be found in various cells of the cardiovascular, pulmonary and central nervous systems, kidneys, and other metabolic organs and tissues. The biding of U-II as a ligand activates UTR, which mobilizes calcium in the cytoplasm, induces proliferation of smooth myocytes, and triggers inflammation[10,11]. As expected, the level of inflammatory factor hsCRP in IBD patients is significantly higher than that in healthy controls.

The study by Alicic *et al*[1] is the first clinical study to investigate blood UII level in both UC and CD patients. However, limitations can be seen, which could bolster the authors' conclusions if resolved: (1) This single center study only had 50 subjects each in the IBD and control groups. If more institutions were included in a multicenter investigation and more patients were recruited, the conclusions would become more convincing and relevant. Therefore, large multicenter studies are anticipated in the future; and (2) the results showed that elevation of blood U-II level was associated with disease development and progression, and attributed to the inflammation mediated by hsCRP. However, the levels of other inflammatory factors were not measured (*e.g.*, interleukin-6, interleukin-8, and tumor necrosis factor-α). Their level and involvement in the elevated U-II concentration and inflammatory responses in those patients should be clarified. Regarding the mechanisms, it is possible that U-II as a ligand activates pathways that stimulate the release of inflammatory effectors, such as the cytokines listed above. These cytokines may potently activate signaling pathways consisting of EPK1/2, NF-κB and Rho/ROCK, which regulate a variety of downstream inflammatory responses[12-14]. Whether those cytokines and U-II act against each other or in concert to form a system influencing the host inflammation status remains to be answered. In the future, gastroenterologists should investigate how U-II interacts with other inflammatory mediators, and how U-II modifies those signaling pathways to potentiate IBD severity in various *in vivo* and *in vitro* systems. In so doing, more results could be collected and analyzed, which are needed to form theoretical and practical evidence to guide prevention and treatment of cardiovascular complications in IBD. Additionally, antagonists to the UTR activation system could also be developed, which may counteract any detrimental effects due to increased level of U-II in patients with IBD.

FOOTNOTES

REFERENCES

1   **Alicic D**, Martinovic D, Rusic D, Zivkovic PM, Tadin Hadjina I, Vilovic M, Kumric M, Tokic D, Supe-Domic D, Lupi-Ferandin S, Bozic J. Urotensin II levels in patients with inflammatory bowel disease. *World J Gastroenterol* 2021; **27**: 6142-6153 [PMID: 34629825 DOI: 10.3748/wjg.v27.i36.6142]

2   **Zhang YZ**, Li YY. Inflammatory bowel disease: pathogenesis. *World J Gastroenterol* 2014; **20**: 91-99 [PMID: 24415861 DOI: 10.3748/wjg.v20.i1.91]

3   **Bigeh A**, Sanchez A, Maestas C, Gulati M. Inflammatory bowel disease and the risk for cardiovascular disease: Does all inflammation lead to heart disease? *Trends Cardiovasc Med* 2020; **30**: 463-469 [PMID: 31653485 DOI: 10.1016/j.tcm.2019.10.001]

4   **Singh S**, Kullo IJ, Pardi DS, Loftus EV Jr. Epidemiology, risk factors and management of cardiovascular diseases in IBD. *Nat Rev Gastroenterol Hepatol* 2015; **12**: 26-35 [PMID: 25446727 DOI: 10.1038/nrgastro.2014.202]

5   **Zivkovic PM**, Matetic A, Tadin Hadjina I, Rusic D, Vilovic M, Supe-Domic D, Borovac JA, Mudnic I, Tonkic A, Bozic J. Serum Catestatin Levels and Arterial Stiffness Parameters Are Increased in Patients with Inflammatory Bowel Disease. *J Clin Med* 2020; **9** [PMID: 32110996 DOI: 10.3390/jcm9030628]

6   **Svistunov AA**, Tarasov VV, Shakhmardanova SA, Sologova SS, Bagaturiya ET, Chubarev VN, Galenko-Yaroshevsky PA, Avila-Rodriguez MF, Barreto GE, Aliev G. Urotensin II: Molecular Mechanisms of Biological Activity. *Curr Protein Pept Sci* 2018; **19**: 924-934 [PMID: 28875851 DOI: 10.2174/1389203718666170829162335]

7   **Pereira-Castro J**, Brás-Silva C, Fontes-Sousa AP. Novel insights into the role of urotensin II in cardiovascular disease. *Drug Discov Today* 2019; **24**: 2170-2180 [PMID: 31430542 DOI: 10.1016/j.drudis.2019.08.005]

8   **Zappavigna S**, Abate M, Cossu AM, Lusa S, Campani V, Scotti L, Luce A, Yousif AM, Merlino F, Grieco P, De Rosa G, Caraglia M. Urotensin-II-Targeted Liposomes as a New Drug Delivery System towards Prostate and Colon Cancer Cells. *J Oncol* 2019; **2019**: 9293560 [PMID: 31929800 DOI: 10.1155/2019/9293560]

9   **Ross B**, McKendy K, Giaid A. Role of urotensin II in health and disease. *Am J Physiol Regul Integr Comp Physiol* 2010; **298**: R1156-R1172 [PMID: 20421634 DOI: 10.1152/ajpregu.00706.2009]

10   **Sun SL**, Liu LM. Urotensin II: an inflammatory cytokine. *J Endocrinol* 2019 [PMID: 30601760 DOI: 10.1530/joe-18-0505]

11   **Liang DY**, Liu LM, Ye CG, Zhao L, Yu FP, Gao DY, Wang YY, Yang ZW. Inhibition of UII/UTR system relieves acute inflammation of liver through preventing activation of NF-κB pathway in ALF mice. *PLoS One* 2014; **8**: e64895 [PMID: 23755157 DOI: 10.1371/journal.pone.0064895]

12   **Yang Y**, Zhang J, Chen X, Wu T, Xu X, Cao G, Li H, Li Y. UII/GPR14 is involved in NF-κB-mediated colonic inflammation *in vivo* and in vitro. *Oncol Rep* 2016; **36**: 2800-2806 [PMID: 27600191 DOI: 10.3892/or.2016.5069]

13   **Li J**, Zhao PP, Hao T, Wang D, Wang Y, Zhu YZ, Wu YQ, Zhou CH. Urotensin II inhibitor eases neuropathic pain by suppressing the JNK/NF-κB pathway. *J Endocrinol* 2017; **232**: 165-174 [PMID: 27895138 DOI: 10.1530/JOE-16-0255]

14   **Lu D**, Peng F, Li J, Zhao J, Ye X, Li B, Ding W. Urotensin II promotes secretion of LTB_4 through 5-lipoxygenase *via* the UT-ROS-Akt pathway in RAW264.7 macrophages. *Arch Med Sci* 2019; **15**: 1065-1072 [PMID: 31360201 DOI: 10.5114/aoms.2019.85197]

LETTER TO THE EDITOR

Hepatitis B viral infection and role of alcohol

Manuel Muro, Aurelia Collados-Ros, Isabel Legaz

Manuel Muro, Department of Immunology, Clinical University Hospital ́Virgen de la Arrixaca-IMIB (Murcian Institute of Biomedical Investigation), Murcia 30120, Spain

Aurelia Collados-Ros, Isabel Legaz, Department of Legal and Forensic Medicine, Biomedical Research Institute (IMIB), Regional Campus of International Excellence "Campus Mare Nostrum", Faculty of Medicine, University of Murcia (Spain), Universidad de Murcia, Espinardo 30100, Murcia, Spain

Corresponding author: Isabel Legaz, PhD, Senior Lecturer, Department of Legal and Forensic Medicine, Biomedical Research Institute (IMIB), Regional Campus of International Excellence "Campus Mare Nostrum", Faculty of Medicine, University of Murcia (Spain), Universidad de Murcia, Campus de Espinardo, Facultad de Medicina, Espinardo 30100, Murcia, Spain. isalegaz@um.es

Abstract

End-stage liver disease is frequently caused by hepatitis B virus (HBV) and alcohol consumption. Notably, the mechanism by which alcohol affects the course of HBV-associated liver disease is unknown, and additional research is needed in this area. A reduced immunological response, oxidative stress, endoplasmic reticulum stress, Golgi apparatus stress, and enhanced HBV replication are a few potential causes.

Key Words: Hepatitis B virus; Alcohol; Hepatocarcinoma; Immunity; Liver disease

Core Tip: In this letter to the editor, we comment on and discuss the combined effects of alcohol consumption and hepatitis B virus (HBV) infection in the progression of liver diseases. In the worst evolution of end-stage liver pathologies, a concordant clinical relationship between alcohol consumption and HBV infection starts to be revealed. There are many potential causes, but some might include increased viral replication, oxidative stress on cellular organelles, and weakened immune responses. Understanding these precepts will open new avenues in managing and treating these patients.

TO THE EDITOR

We have read with great attention and special interest the review by Ganesan and collaborators entitled "Role of alcohol in the pathogenesis of hepatitis B virus (HBV) infection"[1]. The authors examine the potential mechanisms by which alcohol results in an increased risk of HBV-associated liver disease. HBV infection combined with alcohol usage accelerates the progression of liver damage[2,3], primarily hepatocellular carcinoma, the fifth most common type of cancer. The mechanisms behind these adverse effects of alcohol in HBV-positive patients are unknown. Chronic alcohol consumption changes the architecture of the liver and reduces its functional capability.

The effects of alcohol metabolism on protein function, DNA, immune system changes, and oxidative stress impact both hepatocytes and other liver cells. Because the liver is the central location for the replication of hepatotropic viruses (HCV and HBV), ethanol metabolism is linked to viral hepatitis[4,5].

Regarding the immune system, the early stages of viral infections result in the generation of interferon (IFN) type 1 and the activation of natural killer (NK) cells. IFN type 1 and other antiviral cytokines, which HBV induces, are not particularly efficient. According to various investigations of persistent HBV infection, NK cells exhibit varying alterations in quantity, phenotype, and/or function. HBV-infected hepatocytes are cleared more quickly when activated NK cells are present. However, when chronic infection progresses, the tolerogenic actions of liver ligands and cytokines can inhibit both NK and T cells, limiting their antiviral activity[6,7]. According to reports, alcohol has an impact on NK cell antiviral activity during acute HBV infection[8].

The large, medium, and small forms of HBsAg, as well as the hepatitis B virus core antigen (HBcAg) and hepatitis B e antigen (HBeAg), can all be targeted by polyclonal antibodies produced by B cells in chronic HBV-infected patients[9]. During acute HBV infection, distinct antibodies are produced against the HBV surface antigen and the HBV core antigen. Anti-HBc is a marker for current or past infection, whereas anti-HBs signifies sickness remission[10]. Alcohol may reduce the number of B cells, decreasing HBV antibodies by weakening B cell immunological responses[11].

The B cell response to acute HBV infection is less well understood, but HBV-specific CD4+ and CD8+ T cell-mediated responses usually become detectable as HBV replication increases exponentially[12,13]. Numerous studies have demonstrated a substantial correlation and link between acute hepatitis, CD4+ T cell response, and viral shedding[14-16].

Cytotoxic T lymphocytes (CTLs) that express particular T cell receptors are in charge of eliminating HBV-infected hepatocytes in HBV infection. CTL activation may be diminished, which thus prevents clearance of HBV-infected hepatocytes when the viral peptide/MHC class I complex display in HBV-infected hepatocytes is compromised[17]. The body's capacity to eliminate HBV may be diminished due to ethanol consumption, allowing the virus to persist and eventually produce end-stage liver disorders such as cirrhosis and hepatocellular carcinoma.

The immune response in the liver is meticulously regulated by signals from the commensal microbiota in the gut. Additionally, drinking alcohol causes the close connections between intestinal epithelial cells to weaken, allowing germs to enter the bloodstream and cause an infection[18-20].

However, hepatic metabolism of ethanol may increase the production of reactive oxygen species (ROS), principally hydrogen peroxide and superoxide anion[21].

Recent studies have shown that the ethanol metabolite acetaldehyde can suppress proteasome activity, which is essential for producing antigenic peptides for MHC class I-restricted antigen presentation and can also cause lipid peroxidation, the formation of protein adducts with 4-hydroxynonenal and malonaldehydes (oxidative stress markers). This reduces the HBV-MHC peptide class I complex exposure to CTL identification and restricts the removal of infected cells[1], which causes HBV persistence and ensuing end-stage liver disease. HBV and alcohol addiction stresses the endoplasmic reticulum (ER), and these two stresses may have additive or synergistic effects. Alcohol has been shown to synergistically cause ER stress when other substances, the environment, or a viral illness are present [22]. The increase in HBV DNA, HbsAg, and HBx protein caused by alcohol may be the mechanism by which alcohol induces ER stress in HBV infection. A strained Golgi apparatus frequently matches a stressed ER.

Further study in this area is required since the interaction of alcohol misuse and HBV infection can be harmful. Future research should examine how alcohol metabolism affects innate IFN responses and IFN-stimulated gene activation throughout the pathogenesis of HBV infection, as well as if IFN therapy might be an effective treatment option for alcoholics with HBV infection.

Additionally, there is a significant gap between the role of alcohol in controlling B cell function and its contribution to the pathogenesis of HBV, necessitating further research in this area. To fully comprehend the processes of alcohol-induced impairment and investigate the effects of ethanol on MHC class II presentation, which is mainly catalyzed by effector cells, additional studies examining the relationship between alcohol and HBV adaptive immune response are required.

FOOTNOTES

REFERENCES

1 **Ganesan M**, Eikenberry A, Poluektova LY, Kharbanda KK, Osna NA. Role of alcohol in pathogenesis of hepatitis B virus infection. *World J Gastroenterol* 2020; **26**: 883-903 [PMID: 32206001 DOI: 10.3748/wjg.v26.i9.883]

2 **El-Serag HB**. Hepatocellular carcinoma. *N Engl J Med* 2011; **365**: 1118-1127 [PMID: 21992124 DOI: 10.1056/NEJMra1001683]

3 **Sayiner M**, Golabi P, Younossi ZM. Disease Burden of Hepatocellular Carcinoma: A Global Perspective. *Dig Dis Sci* 2019; **64**: 910-917 [PMID: 30835028 DOI: 10.1007/s10620-019-05537-2]

4 **Novo-Veleiro I**, Alvela-Suárez L, Chamorro AJ, González-Sarmiento R, Laso FJ, Marcos M. Alcoholic liver disease and hepatitis C virus infection. *World J Gastroenterol* 2016; **22**: 1411-1420 [PMID: 26819510 DOI: 10.3748/wjg.v22.i4.141]

5 **Shoreibah M**, Anand BS, Singal AK. Alcoholic hepatitis and concomitant hepatitis C virus infection. *World J Gastroenterol* 2014; **20**: 11929-11934 [PMID: 25232227 DOI: 10.3748/wjg.v20.i34.11929]

6 **Maini MK**, Peppa D. NK cells: a double-edged sword in chronic hepatitis B virus infection. *Front Immunol* 2013; **4**: 57 [PMID: 23459859 DOI: 10.3389/fimmu.2013.00057]

7 **Peppa D**, Micco L, Javaid A, Kennedy PT, Schurich A, Dunn C, Pallant C, Ellis G, Khanna P, Dusheiko G, Gilson RJ, Maini MK. Blockade of immunosuppressive cytokines restores NK cell antiviral function in chronic hepatitis B virus infection. *PLoS Pathog* 2010; **6**: e1001227 [PMID: 21187913 DOI: 10.1371/journal.ppat.1001227]

8 **Zhang P**, Bagby GJ, Happel KI, Raasch CE, Nelson S. Alcohol abuse, immunosuppression, and pulmonary infection. *Curr Drug Abuse Rev* 2008; **1**: 56-67 [PMID: 19630706 DOI: 10.2174/1874473710801010056]

9 **Gerlich WH**. Medical virology of hepatitis B: how it began and where we are now. *Virol J* 2013; **10**: 239 [PMID: 23870415 DOI: 10.1186/1743-422X-10-239]

10 **Hoofnagle JH**, Gerety RJ, Barker LF. Antibody to hepatitis-B-virus core in man. *Lancet* 1973; **2**: 869-873 [PMID: 4126916 DOI: 10.1016/s0140-6736(73)92004-7]

11 **Pasala S**, Barr T, Messaoudi I. Impact of Alcohol Abuse on the Adaptive Immune System. *Alcohol Res* 2015; **37**: 185-197 [PMID: 26695744]

12 **Fisicaro P**, Valdatta C, Boni C, Massari M, Mori C, Zerbini A, Orlandini A, Sacchelli L, Missale G, Ferrari C. Early kinetics of innate and adaptive immune responses during hepatitis B virus infection. *Gut* 2009; **58**: 974-982 [PMID: 19201769 DOI: 10.1136/gut.2008.163600]

13 **Webster GJ**, Reignat S, Maini MK, Whalley SA, Ogg GS, King A, Brown D, Amlot PL, Williams R, Vergani D, Dusheiko GM, Bertoletti A. Incubation phase of acute hepatitis B in man: dynamic of cellular immune mechanisms. *Hepatology* 2000; **32**: 1117-1124 [PMID: 11050064 DOI: 10.1053/jhep.2000.19324]

14 **Ferrari C**, Penna A, Bertoletti A, Valli A, Antoni AD, Giuberti T, Cavalli A, Petit MA, Fiaccadori F. Cellular immune response to hepatitis B virus-encoded antigens in acute and chronic hepatitis B virus infection. *J Immunol* 1990; **145**: 3442-3449 [PMID: 2230128]

15 **Jung MC**, Spengler U, Schraut W, Hoffmann R, Zachoval R, Eisenburg J, Eichenlaub D, Riethmüller G, Paumgartner G, Ziegler-Heitbrock HW. Hepatitis B virus antigen-specific T-cell activation in patients with acute and chronic hepatitis B. *J Hepatol* 1991; **13**: 310-317 [PMID: 1808224 DOI: 10.1016/0168-8278(91)90074-l]

16   **Tsui LV**, Guidotti LG, Ishikawa T, Chisari FV. Posttranscriptional clearance of hepatitis B virus RNA by cytotoxic T lymphocyte-activated hepatocytes. *Proc Natl Acad Sci U S A* 1995; **92**: 12398-12402 [PMID: 8618909 DOI: 10.1073/pnas.92.26.12398]

17   **Ganesan M**, Krutik VM, Makarov E, Mathews S, Kharbanda KK, Poluektova LY, Casey CA, Osna NA. Acetaldehyde suppresses the display of HBV-MHC class I complexes on HBV-expressing hepatocytes. *Am J Physiol Gastrointest Liver Physiol* 2019; **317**: G127-G140 [PMID: 31141391 DOI: 10.1152/ajpgi.00064.2019]

18   **Bishehsari F**, Magno E, Swanson G, Desai V, Voigt RM, Forsyth CB, Keshavarzian A. Alcohol and Gut-Derived Inflammation. *Alcohol Res* 2017; **38**: 163-171 [PMID: 28988571]

19   **Lowe PP**, Gyongyosi B, Satishchandran A, Iracheta-Vellve A, Cho Y, Ambade A, Szabo G. Reduced gut microbiome protects from alcohol-induced neuroinflammation and alters intestinal and brain inflammasome expression. *J Neuroinflammation* 2018; **15**: 298 [PMID: 30368255 DOI: 10.1186/s12974-018-1328-9]

20   **Meroni M**, Longo M, Dongiovanni P. Alcohol or Gut Microbiota: Who Is the Guilty? *Int J Mol Sci* 2019; **20** [PMID: 31540133 DOI: 10.3390/ijms20184568]

21   **Iida-Ueno A**, Enomoto M, Tamori A, Kawada N. Hepatitis B virus infection and alcohol consumption. *World J Gastroenterol* 2017; **23**: 2651-2659 [PMID: 28487602 DOI: 10.3748/wjg.v23.i15.2651]

22   **Ji C**. Mechanisms of alcohol-induced endoplasmic reticulum stress and organ injuries. *Biochem Res Int* 2012; **2012**: 216450 [PMID: 22110961 DOI: 10.1155/2012/216450]

CORRECTION

Correction to "Inhibiting heme oxygenase-1 attenuates rat liver fibrosis by removing iron accumulation"

Qiu-Ming Wang, Jian-Ling Du, Zhi-Jun Duan, Shi-Bin Guo, Xiao-Yu Sun, Zhen Liu

Qiu-Ming Wang, Zhi-Jun Duan, Shi-Bin Guo, Xiao-Yu Sun, Zhen Liu, Department of Gastroenterology, The First Affiliated Hospital of Dalian Medical University, Dalian 116011, Liaoning Province, China

Jian-Ling Du, Department of Endocrinology, The First Affiliated Hospital of Dalian Medical University, Dalian 116011, Liaoning Province, China

Corresponding author: Zhi-Jun Duan, MD, Chief Doctor, Department of Gastroenterology, The First Affiliated Hospital of Dalian Medical University, Dalian 116011, Liaoning Province, China. cathydoctor@sina.com

Abstract

We found a mistake in Figure 6. Panels A (Sham group) and F (DFX group) (180 degrees rotated) is same images. We have replaced the incorrect images (Panels F) with the correct Figure. This error does not change the meaning of the picture or the conclusion of the manuscript. We apologize for our unintentional mistakes, which caused great inconvenience.

Key Words: Heme oxygenase-1; Hepcidin; Iron accumulation; Oxidative stress; Portal vein pressure; Carboxyhemoglobin; Bile duct ligation

Core Tip: We found a mistake in Figure 6. Panels A (Sham group) and F (DFX group) (180 degrees rotated) is same images. We have replaced the incorrect images (Panels F) with the correct Figure. This error does not change the meaning of the picture or the conclusion of the manuscript. We apologize for our unintentional mistakes, which caused great inconvenience.

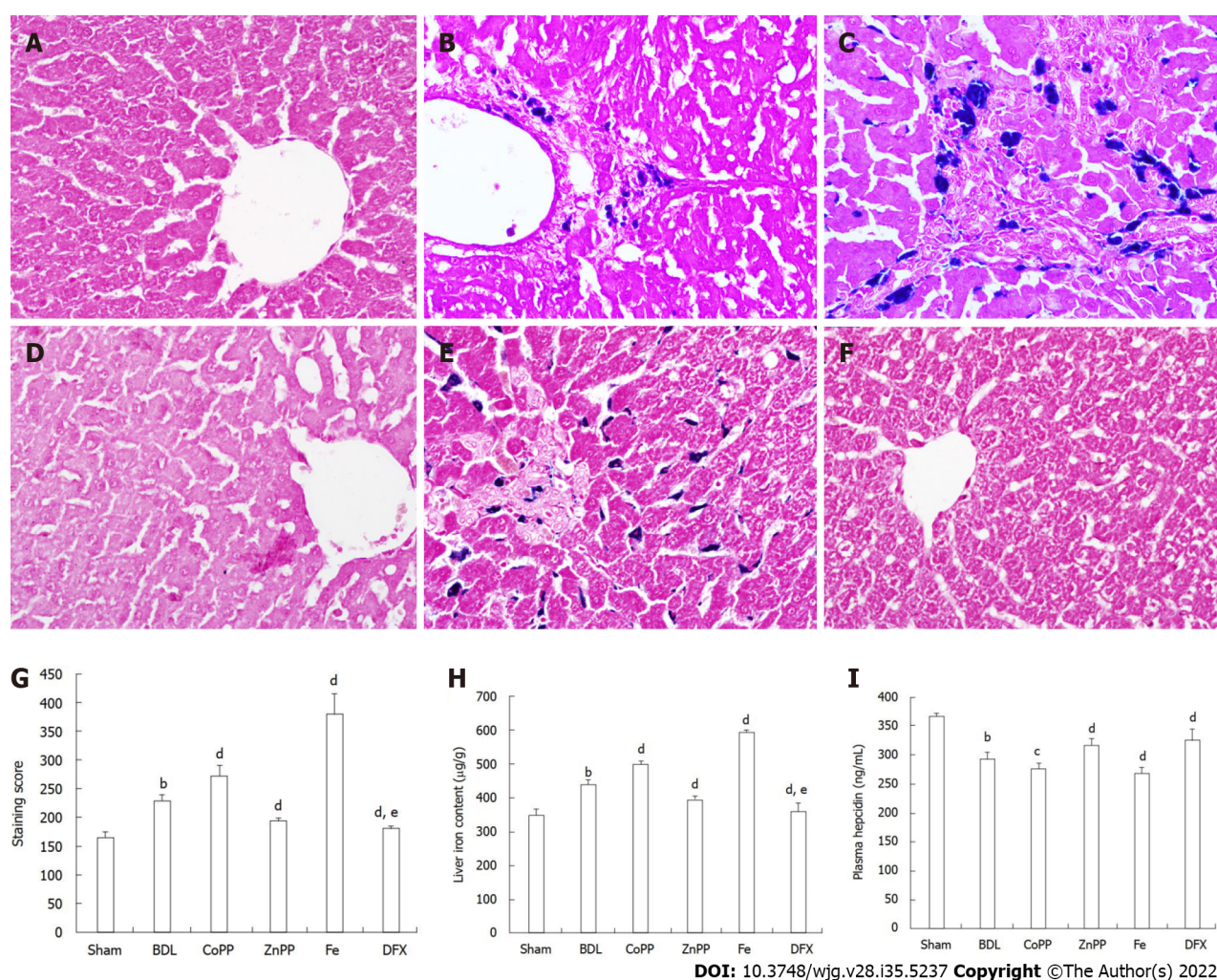DOI: 10.3748/wjg.v28.i35.5237 **Copyright** ©The Author(s) 2022.

Figure 1 erl's Prussian blue staining, levels of hepcidin, serum and liver iron. A: No iron accumulated in the Sham group; B: A small amount of iron mainly accumulated on Kupffer cells in the bile duct ligation (BDL) group; C: Much more iron accumulation was found in interlobular and macrophagocytes in the cobalt protoporphyrin (CoPP) group; D and F: Almost no iron accumulation was detected in the zinc protoporphyrin (ZnPP) group and deferoxamine (DFX) group; E: Massive iron accumulation was observed in the Fe group; G and H: There were no differences in the hepatic and serum iron content of these six groups; I: Plasma hepcidin also was measured by enzyme-linked immuno sorbent assay (magnification × 400). Values are expressed as mean ± SE (n = 6). [b]$P < 0.01$ *vs* Sham group; [c] $P < 0.05$, [d]$P < 0.01$ *vs* BDL group; [e]$P < 0.05$ *vs* ZnPP group.

TO THE EDITOR

We found a mistake in Figure 6. Panels A (Sham group) and F (DFX group) (180 degrees rotated) is same images. We have replaced the incorrect images (Panels F) with the correct Figure 1. We only revised the incorrect figure, and the Manuscript NO: 75978 don't need to revise[1].

FOOTNOTES

Author contributions: Wang QM and Du JL performed the experiments, analyzed the data and wrote the manuscript; Duan ZJ and Wang QM designed the experiments; Wang QM performed the experiments, analyzed the data and wrote the manuscript; Duan ZJ and Guo SB revised the manuscript.

Conflict-of-interest statement: We declare that we have no conflict of interest.

Country/Territory of origin: China

ORCID number: Qiu-Ming Wang 0000-0003-1262-6361; Jian-Ling Du 0000-0003-4782-1052; Zhi-Jun Duan 0000-0001-7976-4959; Shi-Bin Guo 0000-0003-2971-3859; Xiao-Yu Sun 0000-0002-4138-6005; Zhen Liu 0000-0002-9899-8184.

REFERENCES

1   **Wang QM**, Du JL, Duan ZJ, Guo SB, Sun XY, Liu Z. Inhibiting heme oxygenase-1 attenuates rat liver fibrosis by removing iron accumulation. *World J Gastroenterol* 2013; **19**: 2921-2934 [PMID: 23704825 DOI: 10.3748/wjg.v19.i19.2921]

Published by **Baishideng Publishing Group Inc**
7041 Koll Center Parkway, Suite 160, Pleasanton, CA 94566, USA
Telephone: +1-925-3991568
E-mail: bpgoffice@wjgnet.com
Help Desk: https://www.f6publishing.com/helpdesk
https://www.wjgnet.com